Investigations of Age- and Plaque-related Learning Deficits in PDAPP Mice and Evaluations of Anti-amyloidosis Strategies on Amyloid Precursor Protein Transgenic Mice.

Guiquan Chen

PhD Thesis

Submitted in satisfaction of the requirements for the degree of PhD in the University of Edinburgh, 2004.

Declaration

In accordance with the University of Edinburgh postgraduate regulation 3.8.7, I declare that the work described in this thesis is my own, except where otherwise indicated, and that this thesis was composed by myself.

Guiquan Chen (陈贵泉)

Acknowledgement

First of all, I thank my wife, Xiaoyan Zou (邹小燕) for her invaluable emotional support of my PhD study during the past five year.

I would like to thank my supervisor, Professor Richard Morris, for giving me the opportunity to work on the PDAPP projects in his lab and for his constant advice throughout. I thank our collaborators, Dr. Stephen Freedman, Dr. Karen Chen at Elan Pharmaceuticals for supplying the PDAPP mice, AN-1792 and ELN44989; and Dione Kobayashi at Elan Pharmaceuticals for doing the ELISAs for ELN44989 study. I also thank our collaborators, Dr. Jie Shen and Dr. Carlos Saura at Harvard University for supplying the PS1cKO;APP mice.

I am indebted to Jane Knox for conducting the 3D6 immunohistology; Richard Watson and Larraine Wells for doing the dosing for ELN44989. Thanks also to Andrew Bernard and Ann Paterson for technical help, Patrick Spooner for helping with his superior EPS program of electrophysiology. Finally, I would thank other members of the lab – Drs. Jennifer Inglis, Stephen Martin, Urania Coumis and Colin O'Carroll for their constant advice, encouragement and technical help.

Finally, my thanks also go to the Medical Research Council (MRC, UK) for supporting all studies described in this thesis, and to Elan Pharmaceuticals for paying part of my overseas PhD student fees.

Contents.

List of figures and tables.

List of abbreviations:

3×Tg-AD	triple Tg mouse model for AD
5-HT	serotonin
Aβ	beta-amyloid
AChE	acetylcholinesterase
AChEIs	acetylcholinesterase inhibitors
ACSF	artificial cerebrospinal fluid
AD	Alzheimer's disease
ADAM	a disintegrin and metalloprotease
ADAS-Cog	Alzheimer disease assessment scale-cognitive
AICD	amyloid intracellular domain
AIDS	acquired immune deficiency syndrome
AMPA	α-amino-3-hydroxy-5-methyl-4-isoxazolepropionic acid
ANOVA	analysis of variance
AP5	2-amino-5-phosphopentanoate
APLP	amyloid precursor-like proteins
ApoE	apolipoprotein E
APP	amyloid precursor protein
Arg (R)	arginine
Asn (N)	asparagine
BACE	beta-site APP cleaving enzyme
BEHAVE-AD	behavioural pathology in Alzheimer's disease rating scale
BSA	bovine serum albumin
CAATase	chloramphenicol acetyltransferase
CaMKII	Ca2+/calmodulin-dependent protein kinase II
cAMP	cyclic adenosine monoposphate
CANTAB	cambridge neuropsychological test automated battery
CAT	choline acetyltransferase
CDT	clock draw test
CERAD	consortium to establish a registry for Alzheimer's disease
CHO	Chinese hamster ovary
CNQX	6-cyano-7-nitroquinoxaline-2,3-dione
CPB	carboxypeptidase B
CTF	c-terminal fragment
DA	dopamine
DAB	diaminobenzidine
DG	dentate gyrus

DMP	delayed-matching-to-place
Egb	extract of Ginkgo biloba
ELISA	enzyme linked immunosorbent assay
FAD	familial Alzheimer's disease
fEPSPs	field excitatory postsynaptic potentials
FTDP-17	frontotemporal dementia with Parkinsonism linked to chromosome 17
GFAP	glial fibrillary acidic protein
Gln (Q)	glutamine
Glu (E)	glutamic acid
Gly (G)	glycine
HDL	high density lipoproteins
HE	hydroxyethylene
HIV	human immunodeficiency virus
HMG-CR	3-hydroxy-methyl-glutaryl CoA reductase
HPLC	high performance liquid chromatography
I/O curve	input/output curve
Ile (I)	isoleucine
IPIs	inter-pulse intervals
ISI	inter-stimulus interval
ITI	inter-trial interval
KI	knockin
KPI	Kunitz-type protease inhibitor
LDL	low density lipoprotein
Leu (L)	leucine
LTD	long-term depression
LTP	long-term potentiation
Lys (K)	lysine
mAb	monoclonal antibody
MAP	microtubule associated protein
ME	microelectrode
Met (M)	methionine
mg	milligram
ml	millilitre
MMSE	mini mental state exam
mRNA	messenger ribonucleic acid
MT	microtubule
NA	noradrenaline

NaCI	sodium chloride
Nct	nicastrin
NFTs	neurofibrillary tangles
NMDA	*N*-methyl-D-aspartate
NS	not significant
NSAIDs	nonsteroidal anti-inflammatory drugs
NTF	N-terminal fragment
OA	okadaic acid
PBS	phosphate buffered saline
PDGF	platelet-derived growth factor
pg	pico-gram
Phe (F)	phenylalanine
PHFs	paired helical filaments
PI	preference index
PIP2	phosphatidylinositol bisphosphate
PKC	protein kinase C
PPF	paired-pulse facilitation
Pro (P)	proline
PrP	prion promoter
PS	presenilin
PS1cKO	presenilin1 conditional knockout
PTP	post-tetanic potentiation
SAD	sporadic Alzheimer's disease
SAMP	senescence-accelerated- prone
SDS	sodium dodecyl sulphate
Ser (S)	serine
SMON	subacute myelo-optico-neuropathy
SREBPs	sterol regulatory element binding proteins
TACE	tumor necrosis factor converting enzyme
TBS	theta-burst stimulation
Tg	transgenic
Thr (T)	threonine
TM	transmembrane
TNF	tumor necrosis factor
Val (V)	valine
VLDL	very low density lipoproteins
Trp (W)	tryptophan
μl	microlitre

Abstract.

Alzheimer's disease (AD) is a neurodegenerative disease, characterised by the presence of amyloid plaques and neurofibrillary tangles, and is associated with a progressive memory loss. It has been hypothesized that beta-amyloid (Aβ) accumulation and deposition play the central role in the pathogenesis of AD. However, recent evidence suggests that the contribution of Aβ plaques to cognitive impairment of AD is very controversial. Genetic studies showed that mutations of amyloid precursor protein (APP), presenilins (PS1 and PS2) and apolipoprotein ε4 (apoE4) genes in familial forms of autosomal AD (FAD) resulted in increased amyloid plaques in the brain. PDAPP and other APP transgenic mice have previously been shown to exhibit age-related deposition of amyloid plaques, other AD-like neuropathology and age-independent learning deficits prior to any plaque deposition.

A cross-sectional and a longitudinal design were employed to address whether PDAPP mice exhibit any plaque-related learning deficit. First, the cross-sectional study indicated that PDAPP mice simultaneously displayed an early (plaque-independent) and age-related learning impairment. Further analysis showed that the age-related learning deficit was highly correlated with plaque burden in the hippocampus of aged PDAPP mice, suggesting that amyloid plaques play a very important role in memory loss of AD. Second, the longitudinal study showed that the same PDAPP mice exhibited significant age-related learning deficits in trials to criterion and learning capacity tasks when they aged. Interestingly, cued navigation and object recognition in both cross-sectional and longitudinal studies were unaffected, indicating normal sensorimotor function and recognition memory of PDAPP mice. The longitudinal study further showed that the age-related learning impairment was significantly correlated with significantly reduced size of field potentials, suggesting important roles of amyloid plaques in disturbing synaptic transmission and cognitive function.

Preclinical data indicated that Aβ immunotherapy is very effective to improve both AD-like neuropathology and cognitive impairment in APP transgenic mice. Using active Aβ immunisation, long-term (9 months: prevention study) and short-term (5

months: treatment study) effects of Aβ vaccines (AN-1792) on synaptic transmission and spatial learning of PDAPP mice were investigated. Although neither of the two studies showed that Aβ vaccines had significant improvement on either synaptic transmission or spatial learning of PDAPP mice, both long-term and short-term Aβ vaccinations effectively reduced the levels of total Aβ. Thus, these two studies indicated that active Aβ immunotherapy might be very effective to improve AD-like pathology, but ineffective to rescue the learning impairment in APP mice.

The γ- and β-secretases have become the prime targets for pharmaceutical intervention of AD. In this thesis, it was investigated, using a genetic and a pharmacological method, whether inhibition of the γ-secretase has any effects on synaptic transmission and spatial learning of APP transgenic mice. First, using genetically modified APP mice, PS1cKO;APP mice, in which the PS1 gene is conditionally inactivated in the forebrain, their spatial learning was studied. Interestingly, young PS1cKO;APP mice exhibited normal spatial learning in the trials to criterion and learning capacity tasks, whereas young APP transgenic mice were impaired, suggesting a significant rescue effect of PS1 inactivation on spatial learning at young age. However, although old PS1cKO;APP mice displayed normal learning in the trials to criterion task, they exhibited significant impairment on a cuetask and a learning capacity task, suggesting that long-term PS1 inactivation may only partially rescue impaired learning in old APP animals. Thus, these findings raise the possibility that massive accumulation of APP CTFs can cause learning deficits. Secondly, a potent functional γ-secretase inhibitor, ELN 44989 was administered to PDAPP mice to investigate its chronic *in vivo* effects on AD-like pathology and spatial learning. This study showed that ELN 44989 had no significant effect on Aβ levels in the brain and also showed no effect on impaired spatial learning of PDAPP mice. Future work needs to examine whether more potent and selective γ-secretase inhibitor will show any effect on improvement of neuropathology and memory loss in APP mice.

Chapter 1: General Introduction.

The main purposes of this chapter are to present a general overview of the background, molecular mechanisms and animal models for Alzheimer's disease (AD). As the contribution of transgenic animal models to the research of the pathogenesis of AD is so huge, a big effort has been made to review transgenic mouse models of AD. AD remains one of the biggest challenges to modern medicine, so current and potential novel treatment strategies of AD are also reviewed. The aims of the present experiments of this thesis are briefly described in the last section. Following this introduction chapter, a more specific and/or detailed introduction to the issue addressed will be presented in each subsequent chapter.

1.1 The background of Alzheimer's disease.

1.1.1 Dementia and the prevalence of Alzheimer's disease.

Dementia is defined as memory loss accompanied by one or more of the following symptoms: aphasia, apraxia, agnosia and impaired executive functioning (American Psychiatric Association, 1994). Dementia is present in up to 50% of elderly people aged 85 years or over (Evans et al., 1989). There are various subtypes, including Alzheimer's disease (AD), vascular dementia, Lewy body dementia, frontotemporal dementia, Parkinson's disease dementia, Pick's disease dementia, HIV infection and AIDS dementia, etc. (Delacourte et al., 1998). Among these subtypes, AD and vascular dementia are the most common causes, as AD accounts for more than 55% of all dementia cases and vascular dementia accounts for about 15% (Dugu et al., 2003).

The first AD case of a 51 years old woman, Auguste D., was reported by Alois Alzheimer in an abstract in which no morphology of the disease was presented (Alzheimer, 1907). The detailed pathological data of amyloid plaques of AD were later reported by Alzheimer and were actually from his second patient named Johann F. (Alzheimer, 1911). The disease was named after him by Emil Kraeplin in 1910 (Moller and Graeber, 1998). Very interestingly, it has recently been argued that the dementia of Auguste D is not caused by AD but by arteriosclerosis of the brain (O'Brien, 1996).

As the most common cause of dementia, AD is an irreversible neurodegenerative disorder. In addition to progressive memory loss, AD patients have developed other typical symptoms, such as depression, anxiety, irritability, sleep disorder, hyper-vulnerability to stress, delusions, hallucinations and hyperactivity. While the majority of AD is sporadic Alzheimer's disease (SAD), being 90-95% of all cases, the remaining (5-10%) is autosomal familial Alzheimer's disease (FAD) (Harman, 2002).

The prevalence of AD rises exponentially as the worldwide population ages. Approximately 7% of the population older than 65 years has AD, but this figure doubles every 5 years, so the prevalence of AD is more than 40% at age 85 or above (Small et al., 1997). It is estimated that there are more than 15 million AD patients worldwide. In the USA, there were 4.5 million in 2000 and this number will increase to 13.2 million by 2050 (Hebert et al., 2003; Helmuth, 2003). There are currently 400,000 AD people in the UK and the occurrence of AD is 4.4% of people over 65 in Europe (Lobo et al., 2000). As the country with the largest population in the world, China had about 4-5 million AD cases in 1999 and will have more than 15 million by 2050 (Chen, 1999; Zhang, 2003). One recent study has shown that annual costs for all AD individuals are about 100 billion dollars in the USA (Ernst and Hay, 1994). As the total number of AD people will reach more than 30 million worldwide in 2050, it may bring a tremendous economic burden and an even larger public health problem if we do not have an effective treatment for this devastating disease by that time.

1.1.2 Clinical diagnostic methods for Alzheimer's disease.

It is believed that AD can be definitively confirmed at autopsy by examining amyloid plaques and neurofibrillary tangles from the brain of AD patients. The current clinical diagnosis of AD is made by some informant interviews and several neuropsychological tests, and it can reach an accuracy of up to 90 percent (Rasmusson et al., 1996; Pearl, 1997). The neuropsychological tests used in the diagnosis of AD include the Blessed Test (Blessed et al., 1968), Mini Mental State Exam (MMSE) (Folstein et al., 1975), Alzheimer Disease Assessment Scale-Cognitive (ADAS-Cog) (Rosen et al., 1984), Behavioural Pathology in Alzheimer's Disease Rating Scale (BEHAVE-AD) (Reisberg et al., 1987), the Consortium to Establish a Registry for Alzheimer's Disease (CERAD) (Morris et al., 1988), the Clock Draw Test (CDT)

(Sunderland et al., 1989) and Cambridge Neuropsychological Test Automated Battery (CANTAB) (Robbins et al., 1994).

The MMSE is most commonly used for medical diagnosis of cognitive status (Folstein et al., 1975). ADAS-Cog is widely accepted for assessment of language and memory of AD patients, and has been called a golden method for the diagnosis of AD (Rosen et al., 1984). The CERAD includes Verbal Fluency Test, Boston Naming Test, MMSE, ten-item word recall and delayed recall of praxis items (Morris et al., 1988; Morris et al., 1989), and it is very effective in diagnosing cognitive decline in AD. CDT has been proposed as a useful neuropsychological screening instrument for dementia of Alzheimer type (DAT). As dementia may arise from more than one disease, a brain autopsy is recommended to confirm a diagnosis of AD (The National Institute on Aging and Reagan Institute Working Group on Diagnostic Criteria for the Neuropathological Assessment of Alzheimer's, 1997).

1.1.3 Neuropathological features of Alzheimer's disease.

Although progressive cognitive impairment is the main clinical symptom of AD, amyloid plaques, neurofibrillary tangles (NFTs) and neuronal loss are the major pathological hallmarks of AD (Wilkins and Brody, 1969).

Amyloid plaques, the major lesion in AD, are extracellular deposits in the brain. Amyloid plaques are composed of β-amyloid peptides, which are 39-43 amino acids in length and are derived from a larger integral membrane protein called amyloid precursor protein (APP) (Kang et al., 1987). There are two major Aβ peptides found in amyloid plaques, Aβ40 and Aβ42 (Masters et al., 1985). Amyloid plaques observed in the brain of AD can be divided into two different types: neuritic plaques, the minority of β-amyloid deposits, and diffuse plaques, the majority (Allsop et al., 1989; Ikeda et al., 1989b). A typical neuritic plaque consists of a central spherical core of radiating amyloid fibrils surrounded by microglia, astrocytes as well as dystrophic neuritis (Mann et al., 1989). These amyloid fibrils are straight, 6-10 nm in diameter, and are of Congo red birefringence (Hardy and Allsop, 1991). The astrocytes and microglia surrounding the neuritic plaques are highly activated (Wisniewski and Wegiel, 1994). Both dystrophic and degenerating neurites are also observed in

neuritic plaques (Hardy and Allsop, 1991). The dystrophic and degenerating neuritis contain degenerating mitochondria, electron-dense bodies, neurofilaments and paired helical filaments (PHFs). Like neuritic plaques, diffuse plaques are spherical but are less dense (Ikeda et al., 1989a), however, diffuse plaques do not contain dystrophic neurites and are not associated with astrocytosis and microgliosis.

As the second major pathological hallmark of AD, neurofibrillary tangles (NFTs) are abundant in the brain of AD. Interestingly, large amount of NFTs are also observed in other neurodegenerative diseases such as Pick's disease and frontotemporal dementia with Parkinsonism linked to chromosome 17 (FTDP-17) (Hutton et al., 1998). Electron microscopy reveals that the main constituents of NFTs are pairs of twisted filaments arranged in a helix (PHFs), 25nm across at its widest point and constricting every 80nm (Kidd, 1963; Terry, 1963). Nukina et al first demonstrated that the actual component of PHFs is microtubule associated protein tau (Nukina and Ihara, 1985, 1986). As monoclonal antibody against tau protein completely recognizes the de-phosphorylated PHF of NFTs *in vitro*, this suggests that tau in NFTs is abnormally phosphorylated (Grundke-Iqbal et al., 1986). The hyper-phosphorylated tau binds poorly to microtubules, so it disturbs the stability of microtubule and other cytoskeletal constituents, and affects intracellular transport (Lee et al., 2001).

Other neuropathological features of AD have also been widely documented. Davies and Maloney first observed that there is a selective loss of cholinergic neurons in AD (Davies and Maloney, 1976). AD patients display substantial neuronal loss particularly in the nucleus basalis of Meynert (Whitehouse et al., 1981). The loss of hippocampal neurons has also been found in AD with CA1 area displaying the most prominent loss (West and Gundersen, 1990). An extensive synaptic loss (50% of decrease) in the density of the granular neuropil immunoreaction in the parietal, temporal and midfrontal cortex has been found in AD (Masliah et al., 1989). Dekosky et al reported that the number of synapses in lamina III of Brodmann's area 9 is significantly decreased (DeKosky and Scheff, 1990). Interestingly, synapse loss in AD has been shown to be the major correlate of cognitive impairment (Terry et al., 1991). Impaired neurotransmitter deficits have also been observed in AD patients. Noradrenaline (NA), dopamine (DA) and serotonin (5-HT) are significantly reduced in most sub-regions of the brain of AD patients (Cross et al., 1983; Arai et al., 1984).

Glutamatergic neurotransmission abnormalities are found in AD (Cowburn et al., 1990). Choline acetyltransferase activity is markedly decreased in the specimens of AD (Arendt, 2001). The frontal cortex of AD patients display highly active astrocytic reaction, suggesting an astrocytosis in AD (Jorgensen et al., 1990). Overall, synaptic loss, deficits in the cholinergic system and other neurotransmitters, as well as microgliosis and astrocytosis constitute the other neuropathological features of AD.

1.2 Aetiology of Alzheimer's disease.

The causes and mechanisms of AD are not clear. For the past two decades, many hypotheses have been proposed to explain the pathogenesis of AD. This section reviews three major theories which have made significant impacts in this field. These include the cholinergic hypothesis, the tau hypothesis and the amyloid cascade hypothesis.

1.2.1 The cholinergic hypothesis.

The cholinergic system is one of the most important neurotransmitter systems in the brain and is believed to control activities underlying conscious awareness (Perry and Perry, 1995). Evidence from human study suggests that the cholinergic pathways of the basal forebrain play important roles in conscious awareness, attention and several mnemonic processes (Perry et al., 1999). It is established that there is a profound impairment in the cholinergic system of AD. For example, Bowen et al provided the first evidence showing a markedly reduced activity of choline acetyltransferase (CAT) in the cerebral cortex of AD patients (Bowen et al., 1976). A selective loss of central cholinergic neurons is observed in AD (Davies and Maloney, 1976). The acetylcholine synthesis in AD is less than that in controls (Powen et al., 1981).

The cholinergic hypothesis was first suggested by Davis and Berger when they were investigating the cholinergic dysfunctions in Huntington's disease (HD) and schizophrenia (Davis and Berger, 1978). In one of their early studies, choline chloride and physostigmine, an acetylcholinesterase (AChE) inhibitor, were found to improve the symptoms of HD (Davis and Berger, 1978). Physostigmine can also significantly improve the recognition memory of AD subjects (Davis et al., 1978; Davis et al., 1979). Interestingly, it is Bartus who has systematically proposed the cholinergic

hypothesis, asserting that the loss of cholinergic function in the central nervous system contributes significantly to the cognitive decline in the elderly (Bartus et al., 1982).

Since the time of its inception (Davis and Berger, 1978; Bartus et al., 1982), this hypothesis has stimulated widespread research interests and debates (Fibiger, 1991). More importantly, ever since the first attempt to use physostigmine in clinical trials for the treatment of AD (Davis et al., 1978), this hypothesis has become one of the main rationales for the treatment strategy and drug development for AD. Thal and colleagues were the first to investigate the clinical effects of physostigmine in AD. They observed that physostigmine improves memory in AD patients. However, they also found that progressive dementia ensues despite physostigmine therapy (Thal et al., 1986). Long-term effects of physostigmine on patients with probable AD were examined by a second group, who reported that memory test scores of AD patients are significantly better during the drug-treatment period (Stern et al., 1988). More recently, four AChE inhibitors, including tacrine, donepezil, galantamine and rivastigmine, have been developed for the treatment of AD (Bartus, 2000).

1.2.2 The tau hypothesis.

NFTs are one of the major neuropathological features of AD. NFTs are intraneuronal aggregations of highly phosphorylated microtubule-associated tau proteins. The tau hypothesis, initially suggested by Braak and Braak, is also called the neuronal cytoskeletal degeneration hypothesis, which emphasizes the central role of tau and associated neurofibrillary tangles in neurodegeneration and dementia of AD (Braak and Braak, 1991; Braak et al., 1994). In addition to emphasizing the most important role of NFTs in the pathogenesis of AD, this hypothesis further implies that, although deposition of extracellular Aβ is almost an invariant event in AD, it is not the central cause of dementia, but a by-product during neurodegeneration.

Early evidence that led to this theory came from a quantitative study by Wilcock and Esiri who found a highly significant correlation between the severity of dementia and the number of NFTs in the cerebral cortex (Wilcock and Esiri, 1982). Hyman and his colleagues also demonstrated that NFTs but not amyloid plaques parallel the severity of AD (Arriagada et al., 1992), and that the degree of dementia is better correlated

with the density of cerebral NFTs (Hyman and Tanzi, 1992). Gomez-Isla and colleagues have found that both NFTs and neuronal loss increase in parallel with the severity of AD, and that plaques are not related to the duration of disease (Gomez-Isla et al., 1997).

1.2.3 The amyloid cascade hypothesis.

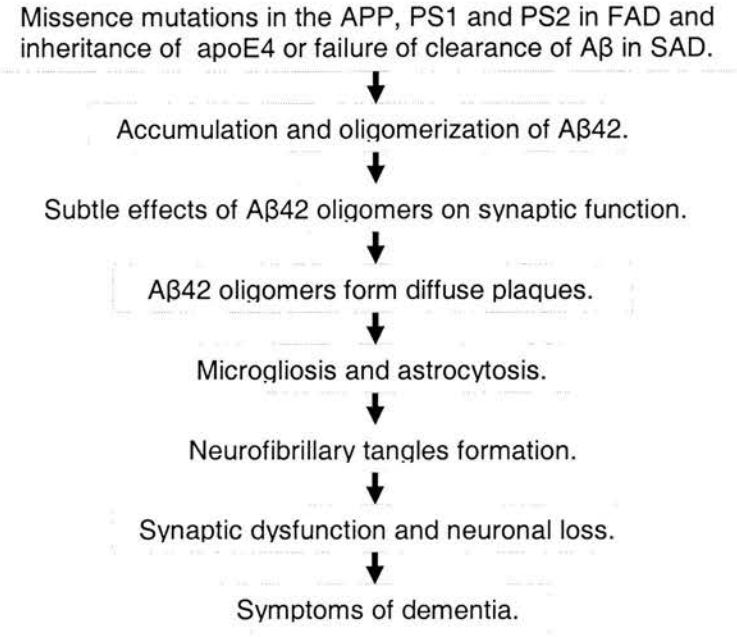

Figure1. **The Amyloid Cascade Hypothesis**. Adopted from Selkoe (2002).

During the last decade, the amyloid cascade hypothesis has become the most popular hypothesis for the aetiology of AD. This theory basically states that the neurodegenerative process of AD is a series of events triggered by the abnormal processing of APP and amyloid deposition (Hardy and Allsop, 1991; Hardy and Higgins, 1992; Selkoe, 1994). As shown in Figure 1, it has been proposed that accumulation of the 42-residue form of Aβ triggers synaptic dysfunction, causes microgliosis and astrocytosis and finally leads to dementia in AD (Selkoe, 2002).

Despite several arguments, a large body of quantitative studies support this theory. Earliest evidence has shown the correlation between quantitative measures of amyloid plaques and dementia in the cerebral grey matter of AD patients (Roth et al., 1966; Blessed et al., 1968). Wilcock and Esiri also demonstrated a significant correlation between the severity of dementia and amyloid plaques (Wilcock and Esiri, 1982). Cummings et al found that the strongest predictor of premortem cognitive impairment

is the relative area of entorhinal cortex occupied by amyloid deposition (Cummings and Cotman, 1995; Cummings et al., 1996a). It has been demonstrated that the mean Aβ plaque burden in the hippocampus correlates with severity and psychological test scores of AD (Bartoo et al., 1997). Naslund et al also reported that the levels of Aβ40 and Aβ42 are elevated early in dementia and are strongly correlated with cognitive decline (Naslund et al., 2000). Furthermore, in the frontal cortex, Aβ is elevated before the occurrence of significant tau pathology (Naslund et al., 2000). Interestingly, some AD cases are a plaque-only disease and do not develop neocortical NFTs at all (Terry et al., 1987; Graeber et al., 1997; Moller and Graeber, 1998). By contrast, there are fewer studies showing the positive correlation between the level of cognitive impairment and NFTs in AD, so the amyloid cascade hypothesis has gained more evidence than the tau hypothesis.

Another line of strong support for the amyloid cascade hypothesis comes from genetic studies. It has been long found that mutations on APP, presenilin-1 (PS1) and presenilin-2 (PS2) are closely linked with the inherited FAD, and that apolipoprotein E ε4 (APOE4) is a risk factor for late-onset SAD (Price and Sisodia, 1998). All mutations on APP (Citron and Oltersdorf T, 1992; Cai et al., 1993; Citron et al., 1994; Haass et al., 1994; Suzuki et al., 1994), PS1 and PS2 (Duff et al., 1996; Scheuner et al., 1996; Thinakaran et al., 1996; Citron et al., 1997) produce increased Aβ levels or Aβ deposition. The APOE4 gene dose increases Aβ deposition as well (Schmechel et al., 1993; Greenberg et al., 1995). Studies on Down's syndrome have also shown that patients who develop AD pathology before the age of 50 produce huge amount of Aβ from birth, often beginning to display amyloid plaques as early as 20 years old, long before they develop NFTs (Querfurth et al., 1995; Lemere et al., 1996).

1.3 Molecular basis of Alzheimer's disease.

Genes, age and environmental factors can influence the development of AD. Age is one of the main risk factors for AD while gene mutations account for all early-onset autosomal FAD. Until now, more than 100 mutations on APP, PS1 and PS2, have been identified, and they are linked with FAD. In late-onset SAD, mutations on these three genes are quite rare, instead, a polymorphic variant of the APOE gene on

chromosome 19 has been found to be a risk factor for SAD. The genes involved in FAD and SAD are reviewed in the following sections.

1.3.1 APP mutations and early onset of AD.

Glenner and Wong first isolated and purified Aβ peptide, the major constituent of amyloid, from the blood vessels of AD patients (Glenner and Wong, 1984). Using the amino acid information of Aβ by Glenner and Wong, several different groups successfully cloned the APP gene (Goldgaber et al., 1987; Kang et al., 1987; Robakis et al., 1987). The APP gene is mapped to chromosome 21 (St George-Hyslop et al., 1987). Levy and colleagues were the first to report a mutation on the APP gene, the Dutch mutation, which is a missense substitution (Glu for Gln) at codon 693 of APP770 (Levy et al., 1990). The London mutation at residue 717 (Ile for Val) was discovered by Goate and colleagues (Goate et al., 1991). Murrell et al reported the Indiana mutation at 717 (Phe for Val) (Murrell et al., 1991). Mullan and colleagues identified the Swedish double mutations in two large early-onset AD families from Sweden, and these mutations at codons 670 and 671 result in the substitution of Lys-Met by Asn-Leu (Mullan et al., 1992). There are several other AD-linked APP mutations (Chartier-Harlin et al., 1991; Hendriks et al., 1992; Mullan et al., 1992). Interestingly, APP gene mutations account for a very small portion of FAD (Tanzi et al., 1992).

1.3.1.1 The structure of APP.

The APP gene is a ~400 kb DNA, contains 18 exons, and encodes several alternatively spliced APP mRNAs. APP is a big transmembrane protein including an N-terminal signal peptide, a large ectodomain with sites for N-glycosylation, a Kunitz-type protease inhibitor (KPI) domain, an Aβ region, a single transmembrane helix and a short cytoplasmic domain for endocytic signalling pathways (Hardy, 1997; Price and Sisodia, 1998). Due to alternative mRNA splicing, three different isoforms of APP, APP695, APP751 and APP770 are produced in neurons. APP695 is the dominant isoform in both central and peripheral neurons (Sisodia et al., 1993). APP695 differs from APP751 and APP770 in that it does not contain the KPI domain located near the N-terminus of the protein (Tanzi et al., 1988). APP belongs to a larger gene family including amyloid precursor-like proteins (APLP), APLP1 and APLP2 (Wasco et al., 1992; von Koch et al., 1995). APLP1 and APLP2 share much

sequence homology with APP, except that APLPs lack the Aβ domain (Wasco et al., 1992).

1.3.1.2 Processing of APP.

APP is cleaved by three different proteases, designated the α-, β- and γ-secretases (Price and Sisodia, 1998). In the CNS, APP is processed by two different cleavage pathways, non-amyloidogenic and amyloidogenic pathway.

In the non-amyloidogenic pathway, the α-secretase first cleaves the site between amino acid 612 and 613 and produces a soluble N-terminal ectodomain of APP called sAPPα and an 83-residue C-terminal fragment called C83 (Esch et al., 1990). The C83 is further processed by the γ-secretase to release a 3-kDa peptide called p3 and C57–59 fragment called amyloid intracellular domain (AICD). The physiological functions of the AICD and p3 are unknown, but the sAPPα can promote neurite outgrowth in PC12 cells and is neuroprotective in cultured neurons from excitotoxic stimulations (Mattson et al., 1993).

In the amyloidogenic pathway, the β-secretase first cleaves between amino acid 596 and 597 of APP. A soluble N-terminal APP fragment called sAPPβ and a 99-residue C-terminal fragment, C99, are produced after the β-secretase cleavage. The C99 remains membrane-bound but is a substrate of the γ-secretase. As the γ-secretase makes proteolyses the C99 within neuron membrane, the C99 is cut to release a 4-kDa peptide called Aβ and C57–59 (Haass et al., 1993). Cleavage of the C99 by the γ-secretase is heterogeneous: most of the full-length Aβ species produced comprise 40-residue peptide (Aβ40), whereas a small proportion comprise 42-residue fragment (Aβ42). Aβ42 is more hydrophobic and is much more prone to form fibril than Aβ40 (Jarrett et al., 1993). Aβ42 is the major Aβ species in amyloid plaques.

1.3.1.3 Proteases for APP cleavage.

1) α-Secretase.

The α-secretase cleaves APP at the α-site to release the C83 and sAPPα. This enzyme displays characteristics of metalloproteases (Esch et al., 1990). It has been reported that trans-Golgi might be the sites for the α-cleavage (Kuentzel et al., 1993). Three

members from a disintegrin and metalloprotease (ADAM) family, tumor necrosis factor-α (TNF-α)-converting enzyme (TACE or ADAM-17), ADAM-10 and ADAM-9, are candidates for the α-secretase.

TACE cleaves pro-TNFα, releasing the extracellular domain (TNF-α) in a manner similar to that of APP. TACE processes a spectrum of type 1 membrane glycoproteins, including TNF-α, the p75 TNF receptor, L-selectin adhesion molecule and TGF-α. TACE also processes Notch receptors. Gene knockout of TACE in cell culture reduces the release of the sAPPα, but still produces a residual α-secretase activity (Buxbaum et al., 1998). ADAM-10 also processes APP (Lopez-Perez et al., 1999). Overexpression of ADAM-10 increases the α-secretase activity in a phorbol ester-inducible manner. A dominant-negative form of ADAM-10 with a point mutation in the zinc-binding site has been found to inhibit the constitutive and PKC-regulated α-secretase activity, but it does not totally abolish the sAPPα production (Lammich et al., 1999). As a member of the ADAM family, ADAM9 (MDC9 or meltrin-γ) plays important roles in cell–cell fusion, intracellular signaling and other cellular functions (Hotoda et al., 2002). ADAM9 also displays an α-secretase activity which is activated by phorbol ester (Koike et al., 1999).

2) β-Secretase.

Using genetic screening or direct enzyme purification, several different labs have identified the β-secretase (beta-site APP cleaving enzyme, or BACE) (Hussain et al., 1999; Sinha et al., 1999; Vassar et al., 1999). This enzyme is also called Asp2 or memapsin 2 (Yan et al., 1999; Lin et al., 2000). The β-secretase RNA is highly expressed in the brain and in a variety of human tissues. The β-secretase belongs to aspartyl proteases of the pepsin family and is an integral membrane protein. In addition to its transmembrane domain near the C-terminus, the β-secretase also contains a cytosolic domain, a connecting strand and a protease domain at the N-terminus.

There are two homologues for the β-secretase: BACE (or BACE1) and BACE2 (Bennett et al., 2000). BACE mRNA is highly expressed in the brain and is the dominant form of the β-secretase (Vassar et al., 1999). By contrast, BACE2 mRNA is highly expressed in peripheral tissues, such as heart, kidney, pancreas, placenta,

prostate, stomach and trachea (Bennett et al., 2000). The intracellular localization of the β-secretase is primarily in the Golgi and endosomes (Vassar et al., 1999). The BACE gene is located on chromosome 11, and no AD-causing mutation on this gene has been found. BACE2 gene is mapped on chromosome 21, and this raises a possibility that BACE2 contributes to Down's syndrome (Saunders et al., 1999). There is a third candidate for the β-secretase, which has been identified as a novel protease belonging to the carboxypeptidase B (CPB) family. In contrast to BACE and BACE2, this enzyme lacks a transmembrane domain and is a soluble enzyme (Matsumoto et al., 2000).

3) γ-Secretase.

The γ-secretase was first recognized because of its role in the production of Aβ (Selkoe, 2001). However, APP is not the only substrate for the γ-secretase and the other substrates include Notch, ErbB-4 (Ni et al., 2001), sterol regulatory element binding proteins (SREBPs) (Brown et al., 2000) and numerous type I transmembrane receptors.

It has been suspected that presenilins (PSs) are the long-sought γ-secretase (Nunan and Small, 2000). PSs can be cleaved into two heterodimers, N-terminal and C-terminal fragments (NTF and CTF), which remain associated. These heterodimers are the biologically active form of the protein (Thinakaran et al., 1996). Each piece of the two heterodimers contains one of the two aspartate residues important for γ-secretase activity. Presenilins do not act alone to carry out the proteolysis of the CTF of APP. The levels of PS heterodimers are regulated by other limiting cellular factors (Thinakaran et al., 1997). Nicastrin (Nct) is one of the factors. Recent evidence suggests that maturation of Nct depends on PS (Edbauer et al., 2002) and is directly associated with the γ-secretase (Esler et al., 2002). Other limiting factors are Aph1 and Pen2. Aph1 is a transmembrane protein and displays similar functions to PS in *C. elegans* (Levitan et al., 2001). Both Aph1 and Pen2 are required for PS endoproteolysis in *C. elegans* (Francis et al., 2002). Kimberly et al have found that Aph1 and Pen2 proteins are also the integral components of the γ-secretase complex (Kimberly et al., 2003). Overall, the γ-secretase is a large multimeric transmembrane protein complex which is composed of PSs, Nct, Aph1 and Pen2.

1.3.1.4 Neurotrophic and neurotoxic properties of Aβ.

Aβ is normally generated by healthy cells and circulates in extracellular fluids in humans throughout life, so both Aβ40 and Aβ42 are normal metabolic products of intracellular APP processing. However, the normal physiological role of Aβ is still unknown. It has been very controversial whether Aβ is neurotrophic, neurotoxic, or without effects on neurons.

It has been shown that Aβ1–28 enhances survival of cultured hippocampal neurons (Whitson et al., 1989). Synthetic Aβ42 increases cell survival (Whitson et al., 1990). Aβ at low concentrations is also neurotrophic to undifferentiated hippocampal neurons (Yankner et al., 1990). By contrast, a high level of Aβ is neurotoxic. A considerable neuronal loss in the hippocampus has been found after SDS-isolated amyloid cores were injected into the cortex and hippocampus of the rats (Frautschy et al., 1991). Injections of Aβ40 peptides into rat or monkey cerebral cortex can induce localized neuronal loss and gliosis (Kowall et al., 1992). Controversially, there is much evidence showing no effects of Aβ either *in vivo* or *in vitro*. Games et al reported that a number of synthetic Aβ peptides (Aβ40, Aβ38, and Aβ25–35) over a wide range of concentrations were injected into the hippocampus and cortex of adult rats, and that no significant morphological changes were produced (Games et al., 1992). Clemens et al also observed that Aβ40 and Aβ42 injected into the brain of 3-month-old and 18-month-old rats failed to induce pathological characteristic of AD (Clemens and Stephenson, 1992).

To explain the discrepancy stated above, it has been suggested that the aggregation properties of Aβ are critical to its neurotoxicity *in vitro* and *in vivo* (Pike et al., 1993). In general, large amounts of Aβ can readily generate neurotoxicity *in vitro* and *in vivo*, but a small amount of Aβ injection does not induce neurotoxicity.

1.3.2 Presenilins and early onset of AD.

The PS1 gene, mapped on chromosome 14 (St George-Hyslop et al., 1992; Van Broeckhoven et al., 1992), was identified by a positional cloning strategy (Sherrington et al., 1995). The PS2 gene, mapped to chromosome 1, was isolated and identified by two different groups (Levy-Lahad et al., 1995a; Rogaev et al., 1995). Mutations on

PS1 are responsible for 25-30% of all FAD cases (Schellenberg, 1995), while PS2 mutations in AD are very rare (Sherrington et al., 1996).

The PS1 gene spans more than 50 to 75 kb and contains 12 exons (Alzheimer's disease collaborative group, 1995). The longest open reading frame, from exons 3 to 12, encodes a 463-amino acid protein. The localization of PS1 mRNAs is found very similar in healthy and SAD brains (Nishiyama et al., 1996). More than 70 missense mutations have been identified (Hardy, 1997) and some of them can cause AD before the age of 30 (Campion et al., 1996). The number of mutations identified on the PS1 gene is still increasing. The gene structure of PS2 is very similar to that of PS1, with 12 exons corresponding to a 24-kb genomic region. Exons 3 to 12 give rise to an open reading frame encoding a 448-amino acid protein (Levy-Lahad et al., 1996). 6 mutations on PS2 have been characterized (Hardy and Gwinn-Hardy, 1998).

1.3.2.1 The biology of presenilins.

PS1 and PS2 are highly homologous proteins and share 67% amino acid identity. They are 463 and 448 amino acids in length, respectively. PS1 contains seven transmembrane domains, including a hydrophilic acidic loop encompassing amino acids 263-407, in which most of the missense mutations have occurred (Sherrington et al., 1995). Topology studies show that the N-terminus, loop, and C-terminus of PS1 are cytoplasmic (Doan et al., 1996). PS1 immunoreactivity is mainly found in perikarya and dendrites, but very weakly in axons (Elder et al., 1996). PS2 differs from PS1 mainly in the N-terminus and the large hydrophilic loop between TM6 and TM7 (Levy-Lahad et al., 1995b). Although PS2 is co-localized with PS1 in the brain, PS2 immunoreactivity is mainly present in the cell body of neurons (Blanchard et al., 1997). Several studies have shown that the subcellular localization of PS1 and PS2 is in the endoplasmic reticulum (ER), Golgi apparatus (Cook et al., 1996; Kovacs et al., 1996), plasma and nuclear membranes (Takashima et al., 1996; Li et al., 1997).

The metabolism of PS1 has been investigated in cell cultures and *in vivo*. PS1 is synthesized as a ~43 kDa polypeptide and is cleaved within a region encompassing amino acids 260-407. Interestingly, PS1-related species which accumulate in cell culture, in animal or human brains are a 27 kDa N-terminal fragment (NTF) and a 17 kDa C-terminal fragment (CTF). The ratio of NTF to CTF is about 1:1 (Lee et al.,

1996). The NTF of PS1 could be co-precipitated along with the CTF after the detergent solubilization, and thus form a larger complex of ~100 kDa in cell cultures. There is little information on the identity of the enzyme for PS1/PS2 cleavage.

1.3.2.2 The physiological roles of presenilins.

As PSs are the active site of the γ-secretase, one of the main functions of PS is to cleave APP. Several studies indicate that elevated Aβ and Aβ42 levels are found in the secreted medium of fibroblasts derived from patients bearing FAD-linked PS1 and PS2 mutations (Scheuner et al., 1996). Overexpression of mutant human form of PS leads to overproduction of Aβ42 in either stably transfected cells (Ancolio et al., 1997) or APP/PS1 Tg mice (Duff et al., 1996). The mechanism by which mutant PS regulates APP processing is possibly through reducing the activity of the γ-secretase, meanwhile increasing that of the β-secretase.

PS1 has very important role in somitic development. Wong et al reported that embryos of PS1 knockout mice exhibit abnormal patterning of the axial skeleton and spinal ganglia, suggesting defects in somitic segmentation and differentiation (Wong et al., 1997). Shen and colleagues found that PS1 homozyous knockouts die shortly after birth and the skeleton of the homozygote is grossly deformed. Haemorrhages occur in the CNS of PS1 knockouts with varying location and severity (Shen et al., 1997). Interestingly, PS1-/- mice can be rescued for viability by both wild-type and FAD-linked PS1 (Davis et al., 1998; Qian et al., 1998), suggesting a very important role of PS during development.

The involvement of PS1 in learning and memory has recently been reported (Yu et al., 2001). Using the newly developed conditional gene knockout techniques, PS1 conditional knockout mice (PS1cKO), in which PS1 inactivation is restricted to the postnatal forebrain, were generated. Interestingly, these mice display normal hippocampal basal synaptic transmission, long-term potentiation (LTP) and long-term depression (LTD), but exhibit long-term spatial memory deficit in a watermaze reference memory task, suggesting a potential role of PS1 in long-term learning and memory (Yu et al., 2001).

1.3.3 Apolipoprotein E and late onset of AD.

The genetic association between apolipoprotein E (APOE) ε4 and the risk of AD was first reported in 1993 (Saunders et al., 1993; Strittmatter et al., 1993a). These findings mark a major breakthrough in understanding the etiology of AD. Subsequent studies have established APOE gene as the most important genetic determinant of susceptibility to SAD and late-onset FAD (Corder et al., 1993; Mayeux et al., 1993; Poirier et al., 1993). It appears that APOE4 accounts for ~50% of the genetic risk for AD.

APOE genotyping is considered a prototype of genetic risk factor assessment for common and late-onset AD. APOE4 genotyping is not used as a predictive test for AD and it is not recommended by the US National Institute on Aging/Alzheimer's Association Working Group, as the usefulness of APOE4 genotyping for predicting risk of AD in asymptomatic individuals has not been established in longitudinal population studies. However, APOE genotyping has been proposed as a possible adjunctive diagnostic test for AD, because it can improve specificity of the diagnosis (Mayeux et al., 1998).

1.3.3.1 The biology of apolipoprotein E.

The APOE4 allele is a common polymorphism in ~25-33% of the population (Corder et al., 1993). The APOE gene is mapped on chromosome 19 and has three allelic forms, APOE-ε2, APOE-ε3 and APOE-ε4. APOE-ε3 is the most common allele, while the APOE-ε4 allele only has a frequency of 15% in general population. The APOE-ε4 allele is about three times more frequent among AD patients than age-matched controls, while APOE-ε2 is lowly expressed in AD (Price et al., 1998).

ApoE (protein) exists mainly in plasma and is also produced in astrocytes of the brain. Antibodies to apoE are immunoreactive in plaques and NFTs in the brain sections of AD patients (Strittmatter et al., 1993b). Patients with homozygous APOE-ε4 show larger and denser Aβ immunoreactivity in the brain than those with homozygous APOE-ε3 (Schmechel et al., 1993). ApoE contains 299 amino acids in a single polypeptide chain (Strittmatter et al., 1994). Three isoforms of apoE differ from each other by cysteine-arginine interchanges at positions 112 and 158. At these

polymorphic sites, apoE3 contains cysteine and arginine, apoE4 contains arginine and apoE2 contains cysteine at both sites (Weisgraber et al., 1981).

Structural analysis indicates that apoE contains two independent domains: an N-terminal domain and a C-terminal domain. The N-terminal domain has five α-helices and contains the region that binds to lipoprotein receptors. The C-terminus contains the major lipid binding elements of apoE. ApoE3 and apoE4 show high affinity to the low density lipoprotein (LDL) receptor, but apoE2 has low affinity (Dong et al., 1994). Due to the cysteine-arginine difference at position 112 at the N-terminus, apoE4 preferentially associates with large, triglyceride-rich very low density lipoproteins (VLDL) and apoE3 with small, cholesterol-rich high density lipoproteins (HDL).

1.3.3.2 The interaction between apoE and Aβ.

It has been suggested that apoE isoforms differentially affect amyloid deposition, NFTs formation, neuronal plasticity, cholinergic function and other pathophysiology of AD (Horsburgh et al., 2000). ApoE can bind to Aβ peptide, and the residues 244-272 in the C-terminal domain are required for the interaction (Strittmatter et al., 1993b). It has been shown that long-term incubation of both apoE3 and apoE4 with Aβ peptide forms aggregates that precipitate from solution and further forms monofibrillar structures, but apoE4 is more effective (Wisniewski et al., 1995).

1.3.3.3 The interaction between apoE and tau.

ApoE3 could form a sodium dodecyl sulphate (SDS)-stable complex with normal tau, not the phosphorylated tau. It is suggested that the interaction between the apoE3 and tau has protective role (Strittmatter et al., 1994). The binding site between the apoE3 and tau is in the vicinity of the polymorphic site at position 112, and cysteine/arginine-112 or arginine-61 may be the key residues for the interaction. The binding of the apoE3 to tau stabilizes microtubules and cytoskeleton, and thus helps maintain the structure of neurons. This binding might also inhibit the phosphorylation of tau and therefore prevent the PHF formation in NFTs. However, apoE4 does not display any protection like that by apoE3.

1.3.3.4 Brain injury and apoE.

ApoE plays important roles in the response to acute brain injury, neuronal protection and repair. It has recently been found that the cortical levels of apoE do not change 30 minutes after the haematoma induction but are significantly elevated 4 hours after (Horsburgh et al., 1997). However, apoE isoforms may have different effects on neuronal repair within the CNS, as impaired neuronal plasticity has been observed in apoE4 transgenic (Tg) mice but not in apoE3 transgenics (White et al., 2001).

1.3.4 Tau and AD.

Tau proteins are one of the microtubule-associated proteins (MAPs) and are abundant in the CNS. The mutations in the tau gene have been reported to cause neurodegeneration, AD and dementia (Hutton et al., 1998; Poorkaj et al., 1998; Spillantini et al., 1998).

1.3.4.1 Microtubules and tau.

Cytoskeletal microtubules (MTs), along with actin and intermediate filaments, establish the overall architecture of the cytoplasm. As the primary component of the mitotic spindle, microtubules are mainly consisted of heterodimers of MAPs, α- and β-tubulin. It is believed that the oriented microtubule arrays in axons serve as the tracks for vesicles and cell organelles to be translocated from the center part to the distal end and back again by several different proteins such as members from the kinesin and dynein families (Allen et al., 1985; Nangaku et al., 1994; Trinczek et al., 1999). About 80% of microtubule components are tubulins, while the remaining 20% are MAPs, including MAP1 (>250 kDa), MAP2 (~200 kDa) and tau proteins (50–70 kDa). MAP2 and tau, the two major MAPs in neurons, are localized to different subcellular compartments. The MAP2 is largely expressed in dendrites, but the tau is mainly in axons. Astrocytes and oligodendrocytes also express low levels of tau.

The TAU gene contains 16 exons and major tau protein isoforms in the CNS are encoded by 11 exons (Andreadis et al., 1992). By alternative mRNA splicing of exons E2, E3, and E10, six tau isoforms named 4R2N, 4R1N, 4R0N, 3R2N, 3R1N, and 3R0N are expressed in adult human brain (Lee et al., 2001). Interestingly, only three isoforms including the 4R0N, 4R1N and 4R2N are expressed in rodents (Goedert and Jakes, 1990). They differ by the presence of one or two short fragments or absence of

any fragment in the N-terminus (1N, 2N and 0N), and by the presence of either three or four microtubule-binding repeat motives in the C-terminus (3R and 4R).

1.3.4.2 Physiological functions of MAPs and tau.

One major physiological function of MAPs and tau is to promote microtubule (MT) polymerization, bind to and stabilize microtubules (MTs) (Cleveland et al., 1977; Lee and Rook, 1992). The polymerization of tubulin into MTs is regulated by the state of phosphorylation of tau proteins. Hypophosphorylated tau induces tubulin polymerization and microtubule stabilization. The MT binding domains of the tau are localized to the C-terminus of the molecule within the four MT binding motives. These motives are composed of highly conserved 18–amino–acid–long binding elements separated by flexible, but less conserved, inter-repeat sequences that are 13–14–amino–acid–long (Himmler et al., 1989; Lee et al., 1989). Among the 80 Ser/Thr residues on the tau, at least 30 phosphorylation sites have been described, most of which occur on Ser–Pro and Thr–Pro motives. In fact, phosphorylation of Ser262, located in the first MT-binding domain, dramatically reduces the affinity of tau for MTs *in vitro* (Buee et al., 2000).

The normal physiological function of tau has been investigated. Harada et al reported that the nervous system of tau knockout mice appears to be normal and that axonal elongation is not affected. However, MT stability is decreased and MT organization is significantly changed in the tau knockouts, suggesting that tau is crucial in the stabilization and organization of MTs in certain types of axon (Harada et al., 1994). Tau also acts as a phosphatidylinositol bisphosphate (PIP2) binding protein and regulates activities of several actin binding proteins (Flanagan et al., 1997).

1.3.4.3 Tau mutations and dementia.

All tau mutations identified so far are in the carboxyl-terminal side of the tau protein. Hutton et al first reported three missense mutations in exons 9, 10, and 13 (G272V, P301L and R406W) (Hutton et al., 1998). A V279M mutation was identified from FTDP-17 family (Poorkaj et al., 1998). The G to A mutation in the intron following the exon 10 of tau was found in a familial multiple system tauopathy with presenile dementia (MSTD) (Spillantini et al., 1998). Mutations in exon 9 (K257T and G272V), exon 12 (V337M and E342V) and exon 13 (G389R and R406W) affect all six tau

isoforms, however, mutations in exon 10 (N279K, ΔK280, ΔN296, P301L, P301S and S305N) only affect tau isoforms with the 4R (Clark et al., 1998; Goedert et al., 1999; Pastor et al., 2001; Ferrer et al., 2003). Tau mutations can cause changes in MT binding, MT polymerization, rapid axonal transport and the abnormal aggregation of tau in various neurodegenerative diseases (Jicha et al., 1999). Missense mutations of tau have also been found to affect the integrity of the MT system and to initiate the formation of tau inclusions in FTDP-17 (DeTure et al., 2000).

1.4 Modelling Alzheimer's disease.

The lack of good animal model of AD has been a big problem for the pathological study of AD and to the development of novel therapeutics for AD. Animal models displaying neuronal degeneration, plaque formation and neurofibrillary lesions are certainly very powerful to facilitate understanding the mechanisms of the disease. Generally, an ideal animal model should develop most or all aspects of a disease in a reproducible way. Animal models of AD are dramatically advancing with lesions in large animals such as primates and canines and the development of transgenic animals.

Researchers in the field of AD have spent several decades trying to discover better animal models. Historically, the development of AD animal models can be divided into two phases: non-transgenic era, in which traditional lesion techniques have been utilised to create non-transgenic models, and transgenic era, in which the modern molecular biology technology has been used to produce transgenic (Tg) animals. Due to great efforts devoted to the generation of Tg animal model of AD, during the past decade, numerous Tg models have been published. This section (section 1.4) will only focus on reviewing non-transgenic animal models of AD and discussing their setbacks. The next three sections will review the APP (section 1.5), tau (section 1.6) and plaque/tangle (section 1.7) Tg mouse models, separately.

1.4.1 Primate models of AD.

Aged monkeys develop plaques, manifest behavioural impairments (Wisniewski et al., 1973) and display neurotransmitter deficits (Goldman-Rakic and Brown, 1981). Plaque loads are highest in the prefrontal and temporal cortices and lowest in the

occipital cortex of aged macaques (Struble et al., 1984; Struble et al., 1985). Nonhuman primates seem to be a feasible model for the study of human AD.

1.4.2 Mouse models of AD.

It was generally believed that normal aged rodents do not develop any human AD pathology, however, this view has been changed since the senescence-accelerated-prone (SAMP) mouse was reported in early 1970s (Takeda et al., 1981). It has been reported that the SAMP8 line exhibits an age-dependent plaque formation in the hippocampus (Morley et al., 2000) and displays age-related learning impairments in several behavioural tasks (Miyamoto et al., 1986; Flood and E. Morley, 1997; Ohta et al., 2001). The SAMP mouse is a useful animal model of senescence and AD.

1.4.3 Bear models of AD.

Plaques, cytoskeletal abnormalities and NFTs have been identified in aged bears (Cork et al., 1988), so aged bears could be used as an animal model of AD.

1.4.4 Canine models of AD.

Aged beagles have been found to develop diffuse plaques (Cummings et al., 1993). Aged dogs also display behavioural deficits on discrimination, reversal and spatial learning. It has been reported that behavioural deficits in dogs are significantly correlated with the increased Aβ deposition (Cummings et al., 1996b).

1.4.5 Aluminium injection model of AD.

Injection of aluminium chloride into the CNS of rabbits has been found to produce neurofibrillary changes and learning impairment (Wisniewski et al., 1980). However, the structure of the neurofibrillary changes induced by aluminum is different from the NFTs seen in AD.

1.4.6 Lesion models of AD.

Monkeys, injected with cholinergic receptor blocker (scopolamine), display striking memory impairments (Bartus et al., 1982). Chronic infusion of okadaic acid (OA), a specific inhibitor of the serine/threonine protein phosphatases 1 and 2A, into rat brain ventricles has been found to produce a severe memory impairment, a PHF-like phosphorylation of tau protein and the formation of plaque-like structures in grey and

white matter areas (Arendt et al., 1995). Another specific inhibitor of PP1 and PP2A, calyculin A, can also induce tau hyperphosphorylation and a deficit in spatial learning in rats (Sun et al., 2003). Collectively, the OA- or calyculinA-induced neurodegeneration may be a useful model for AD.

1.4.7 Cholesterol-fed rat model of AD.

It has been suggested that cholesterol is involved in the pathophysiology of AD (Wolozin et al., 2000). A cholesterol diet was used to feed rats for 4-6 months and immunohistochemical staining reveals amyloid plaques in the hippocampus and cortex of the rats. Impaired hippocampal LTP is also observed (Koudinov and Koudinova, 2001). No NFTs have been produced in the cholesterol-fed rats.

1.4.8 Aβ infusion models of AD.

In vitro studies have shown that aggregated synthetic Aβ42 induces toxicity in neurons (Pike et al., 1991). Kowall and colleagues also found that infusion of Aβ into rats induces focal plaque deposition and profound neurodegeneration in the cortex (Kowall et al., 1991). Hippocampal LTP is impaired in Aβ-infused rats (Itoh et al., 1999). One recent study has shown that rats injected with Aβ40 and Aβ43 display both impaired hippocampal LTP and working memory (Stephan et al., 2001). Aβ infusion models are very useful to investigate the mechanisms of AD.

1.4.9 Summary for non-transgenic animal models of AD.

Nonhuman primate, dog, bear and SAMP mouse have been useful models for the research on AD. However, there are many drawbacks to these models. First, the availability of some of these models is restricted. Monkeys, bears and dog live 20 years or longer, so the process of developing diffuse plaques is very time-consuming. Second, only very limited AD-like pathology, such as diffuse plaques, has been observed in those models, but no NFTs, no neuronal or synaptic loss, no microgliosis and no astrocytosis. Obviously, the big animal models like monkey and bear are not applicable to any general laboratory. Third, OA lesion or Aβ infusion models seem more promising than nonhuman primates, because they produce more AD-like pathology both acutely and focally. However, one big problem about lesion or infusion models is that AD is not an acute disease and its pathology develops

progressively and chronically throughout the whole nervous system. Another problem is that lesions or Aβ infusions can be quite variable and it is difficult to reproduce the same results across different laboratories (Greenberg et al., 1996). Fourth, the SAMP8 mouse displays diffuse plaques and learning deficits at old ages, but they should be viewed as a model for aging brain rather than AD.

The various weaknesses of the non-transgenic animal models have prevented them from being used more widely. Although they have been in use for about four decades in the research of AD, our understanding of AD remains very poor. Transgenic technology has brought a new optimism, as it represents a unique and powerful tool for *in vitro* and *in vivo* study of the pathophysiology of a gene of interest. As genetic mutations on APP and tau in FAD and FTDP-17 have been identified, using transgenic approaches, one can directly examine whether the overexpression of human mutant APP or tau genes in the brain of animals leads to AD-like pathology and thus provide extremely important information on the molecular mechanisms of the disease. For the past decade, a very large number of research groups have been attempting to generate rodent models of AD using both cDNA- and genomic-based approaches. While the failure of early attempts to generate Tg AD models had been very discouraging to the field, the advent of mouse models generated by overexpression of human mutant APP (Games et al., 1995) and tau (Lewis et al., 2000) has marked great breakthroughs and has been proven extremely important to this field.

1.5 APP transgenic mouse models for Alzheimer's disease.

The overall goal of APP transgenic efforts is to get high levels of mutant APP expression in the nervous system in order to produce partial or complete AD-like pathology in animals. Ideally, the AD-like neuropathology should be developed in an age-dependent manner in the animal so that it, at least partially, mimics the disease progression in human AD. Interestingly, early efforts to generate plaque-producing Tg mice using either full-length or fragment of wildtype APP were unsuccessful (Quon et al., 1991; Yamaguchi et al., 1991). Since the mutated human APP gene was first introduced into the mouse in 1995, numerous APP Tg mouse models have been

created by a large number of different laboratories so far. This section will review the representatives of APP Tg mouse models.

1.5.1 The APP751 (SciosNova) mouse.

The APP751 mice express the full-length wildtype human 751-amino acid isoform of APP cDNA under the control of a rat neuron-specific enolase promoter (Quon et al., 1991; Higgins et al., 1994; Higgins and Cordell, 1995). The APP751 mice display more abundant transgene mRNA than endogeous APP mRNA, elevated Aβ and full-length APP in the brain. Immunostaining with antibodies to Aβ and to the C-terminus of Aβ42 reveals diffuse Aβ deposits. Histology was examined in mice at 2 and 22 months of age. At 2 months, 27% of brain sections of the APP751 mouse have at least one deposit. At 22 months, 42% of sections have deposits. Increased tau protein immunoreactivity is also found in the hippocampus, cortex and amygdala at old age (Higgins et al., 1994; Higgins and Cordell, 1995). But there is no evidence showing neuritic plaques, synaptic and neuronal loss.

Two cohorts of these mice, one at 5–6 months and the other at 9–12 months of age, were first tested with several general sensorimotor tasks such as string test, rotarod, general activity, elevated plus-maze and behavioural despair test (Moran et al., 1995). The Tg mice do not differ from non-Tg controls at either 6 or 12 months in muscle strength, motor coordination, level of anxiety or behavioural despair (Moran et al., 1995). Tgs and non-Tgs display similar circadian activity at both ages. Cognitive behaviour was then evaluated in a Y-maze for spontaneous alternation and in a water maze for spatial reference memory and cued learning. Although the Tg mice do not differ from the non-Tg in the spontaneous alternation at 6 months, they show lower alternation rates than non-Tg littermates at 12 moths. During the watermaze reference memory testing, The Tg mice display significantly longer average escape latency than that by the controls at both 6 and 12 months. Interestingly, the Tg mice also constantly display longer latencies in the cued learning. In three probe tests, the 12-month Tg mice display significant impairment in searching for the target quadrant in which platform was previously present during the acquisition training (Moran et al., 1995).

As the APP751 mouse is the first mouse model to overexpress the full-length wildtype human APP gene, it might be a good model for Down's syndrome. However, the weakness of this model is that it only develops diffuse plaques.

1.5.2 The PDAPP mouse.

The PDAPP mouse, overexpressing a mutated human APP gene harbouring the Indiana mutation under the control of a β-chain promoter of platelet-derived growth factor (PDGF), was first described by neuroscientists at Athena Neurosciences (Games et al., 1995). The introns 6-8 of APP gene are included in the construct which allows alternative splicing of exon 7 and 8, leading to very high expression of all three human APP isoforms in the brain. Probably the PDGF promoter and use of the introns from the APP gene in the construct result in the expression of high level of both APP and Aβ (Duff and Hardy, 1995). Levels of human APP mRNA and APP proteins are approximately 4-5 times higher than that of endogenous APP (Games et al., 1995).

The PDAPP mouse displays an age-dependent AD-like pathology. At young age (<6 months), no diffuse Aβ deposits can be detected (Games et al., 1995). Between 6-9 months, the Tg mice start to display Aβ deposits and mature plaques in the hippocampus and cerebral cortex. The deposition of Aβ becomes more abundant as the animals get older (Johnson-Wood et al., 1997). At 18 months, the level of Aβ deposits is higher than that in human AD brain (Irizarry et al., 1997). At >22 months, the whole hippocampus and cortex are covered by huge amount of Aβ plaques. The nature of the plaques in PDAPP mice is very similar to that in human AD (Masliah et al., 1996). Besides diffuse and neuritic plaques, in which the amyloid core is surrounded by massive clusters of dystrophic neuritis, PDAPP mice also display an age-dependent astrocytosis and microgliosis similar to that in human AD brain; no activated astrocytes are found at less than 6 months but begin to be apparent at 10 months. Astrocytosis lags the formation of Aβ plaque formation by about 2 months. Microgliosis is also found at about 8 months and increases with aging.

Although there is no overt neuronal loss in PDAPP mice at even 24 months, about 20% of synaptic loss has been found in young Tg mice (Hyman et al., 1997). Dodart et al also reported a hippocampal dystrophy at 3 months (Dodart et al., 2000). The PDAPP mouse develops early neurofibrillary pathology, for example, Masliah et al

(2001) observed phosphorylated neurofilament-immunoreactive dystrophic neurites in plaques at 10- 12 months, phosphorylated tau-immunoreactive dystrophic neurites after 14 months, but no paired helical filaments at even 20 months.

A clear weakness of this model is that the expression of APP and Aβ is much higher than that in human AD. High levels of APP751 and APP770, which are believed to be non-neuronal APP isoforms, have been found in the brain as well. It is reasonable to argue that PDAPP mice may represent a model for the Aβ plaques of human AD rather than a complete model. Nevertheless, as Aβ accumulation and deposition plays the central role in the pathogenesis of AD (Hardy and Allsop, 1991), these mice have been very helpful in understanding the mechanisms of Aβ accumulation and in testing agents that may reduce or remove Aβ plaque formation. Because PDAPP mice have been the main subjects for my whole PhD study, the behavioural studies on this model will be reviewed and discussed in two subsequent chapters (Chapters 3 and 4). Two pharmacological studies using PDAPP mice, Aβ vaccines and γ-secretase inhibitors are discussed in Chapters 5 and 7.

1.5.3 The Tg2576 mouse.

Two lines of APP transgenic mouse expressing both human wildtype and mutated forms of APP695 have been generated by Karen Hsiao (Hsiao et al., 1995; Hsiao et al., 1996). The first line, which express human APP695 driven by a prion promoter (PrP) in the FVB strain background, display neophobia and seizures, die before 6 months of age and display no amyloid plaques (Hsiao et al., 1995). The second line, named as the Tg2576 mouse, overexpress a mutant human APP695 gene with the Swedish double mutations under the same prion promoter in the C57B6/SJL strain background. Tg2576 mice express 3-5 times the level of endogenous APP in human brain and display age-dependent Aβ accumulation and deposition in the amygdala, hippocampus and cortex (Hsiao et al., 1996). Tg2576 mice produce a 4-5 times increase in the concentration of Aβ40 and a 14-fold increase of Aβ42 between 2-13 months of age. Tg2576 mice also display astrocytosis and microgliosis surrounding the plaques (Hsiao, 1996).

In the initial paper by Hsiao et al, two behavioural tests have been performed in Tg2576 mice aged from 3 to 14 months (Hsiao, 1996). First, two cohorts of Tg2576

mice at 3 and 10 months were tested in Y-maze alternation; second, three groups of mice at 3, 6 and 9 months, were evaluated by cuetask and reference memory task in a watermaze. In the Y-maze task, 3-month Tg mice do not show any difference from controls, however, 10-month Tg mice display much less alternations, suggesting an age-dependent alternation in Tg2576 mice. In the reference memory task, 2-month Tg mice are not different from the controls in terms of escape latency to the hidden platform, 6-month Tg mice are also relatively unimpaired compared to the controls, however, 9-10 months Tg2576 mice display significant impairment. A probe test, in which 60s was given to allow animals to search for the hidden platform which was previously available but not present during this trial, was conducted at the end of training. In the probe trial, the percentage time spent in the target quadrant and the total crossings of the previous platform were analysed. Young groups (3- and 6-month) do not differ from the aged-matched controls and only old Tg mice show much less time spent in the target quadrant and much less crossings of the platform than that by the controls. The above results were interpreted as plaque-related memory deficits (Hsiao et al., 1996), however, this claim was strongly criticized (Routtenberg et al., 1997). First, the data presented in the initial paper (i.e. the graphs for spatial learning in the water maze) clearly indicate that old Tg2576 mice display a striking impairment in the visible cuetask (Hsiao et al., 1996), so these results at least suggest an impairment related to locomotor component in Tg animals. Second, there seems no evidence showing that three cohorts of Tg mice (2-, 6- and 9-10-month) display any plaque-related impairment of memory, as the performance of the three groups of Tg mice seems quite comparable. By contrast, the three cohorts of control mice might display an age-related memory improvement, for example, the old non-Tg mice (47% of target quadrant time) show much better performance than the young ones (38% and 35% at 3- and 6-month, respectively) (Hsiao et al., 1996). Indeed, the initial claim by Hsiao et al (1996), in which the deficit in spatial learning and memory of Tg2576 mice is age- and plaque-related, is even weakened by a later study from King and colleagues (King et al., 1999).

Using a comprehensive behavioural test battery, King et al re-examined sensorimotor and cognitive performance of Tg2576 mice. Mice at 3 and 9 months of age were tested with open-field, beam crossing, forepaw grip, Y-maze alternation, cuetask, reference memory, Barnes maze, and passive and active avoidance tasks. In contrast

to the findings by Hsiao et al (1996), King and colleagues found that Tg2576 mice do not differ from the controls at both 3- and 9-month in the Y-maze alternation and acquisition of reference memory in the water maze. However, Tg2576 mice display significant impairment in a visible cuetask in the water maze, and this impairment is progressively worsening with age. More interestingly, very old Tg2576 (14- and 19-month) mice also exhibit no impairment in the reference memory in the water maze but only show impairment in the visible cuetask (King and Arendash, 2002). It seems very difficult to explain the difference between the findings by these two laboratories (Hsiao et al., 1996; King et al., 1999). Procedural differences, such as animals being singly housed during the experiment or animals being tested using a battery of behavioural tests (King et al., 1999), may partially explain this discrepancy. It has been suggested that different genetic background of mouse strains may yield different results, but it is unclear whether these two laboratories bred or backcrossed their Tg2576 mice to different strain, such as C57B/6.

Chapman et al (1999) later employed a different behavioural paradigm, a forced choice T-maze alternation task to test Tg2576 mice. Analysis of the performance in the T-maze between 2- and 10-month Tg mice and the controls indicated that, 2- and 10-month non-Tg mice perform this task comparably, but the 10-month Tg2576 mice display a significantly lower rate of learning during training. Electrophysiological studies on the same mice have shown that both young and aged Tg2576 mice exhibit normal basal synaptic transmission and short term synaptic plasticity such as paired-pulse facilitation (PPF), but only old Tg2576 mice display severely impaired *in vitro* and *in vivo* LTP in both the CA1 and dentate gyrus regions of the hippocampus (Chapman et al., 1999). The correlation study further demonstrated that LTP deficits are significantly correlated with the impaired T-maze performance in old Tg mice (Chapman et al., 1999).

In contrast to the electrophysiological findings from Chapman et al (1999), another group of neuroscientists in the University of Bristol reported different results using Tg2576 mice. In the study by Fitzjohn et al (2001), synaptic transmission, short- and long-term synaptic plasticity in the hippocampus of Tg2576 mice were investigated. Interestingly, an age-related deficit in basal synaptic transmission but no impairment of LTP in the hippocampus was observed. Hippocampal slices from 12-month

Tg2576 mice display reduced levels of synaptic transmission in the CA1 region compared with the controls. The application of an ionotropic glutamate receptor antagonist, kynurenate during the preparation of brain slices abolished this deficit. At 18 months, a selective deficit in basal synaptic transmission was again observed in the CA1 region of the hippocampus with or without treatment of kynurenate during the slice preparation. However, hippocampal LTP is normal in Tg2576 mice at both 12 and 18 months.

In conclusion, Tg2576 mice develop both diffuse and neuritic plaques, astrocytosis and microgliosis in an age-dependent manner. Tg2576 mice also display age-related cognitive impairment. As Tg2576 mice do not develop NFTs and neuronal loss, they could serve as a good mouse model for the amyloidosis of AD. Although they are not the first plaque-producing mouse model, Tg2576 mice have been much more widely used by different laboratories throughout the world due to its unlimited commercial distribution than PDAPP mice, the first plaque-producing model, which are not commercially available.

1.5.4 The Scripps, H6 and J9 mice.

Scripps mice express wildtype or Indiana mutated form of APP695 and APP751 (Mucke et al., 1994). The promoter is the rat neuron-specific enolase promoter plus the SV40 polyA signal. It has been reported that levels of human APP in Tg mice are 30-50% higher than these of endogenous murine APP. Interestingly, a synaptotrophic effect in the cortex has been observed. No evidence indicates that Scripps mice develop plaques or other AD-like pathology at age up to 24 months (Mucke et al., 1994).

Although the Scripps mouse was unsuccessful in developing AD-like pathology, Mucke's group subsequently generated other two lines, H6 and J9, both of which display several aspects of AD-like neuropathology (Rockenstein et al., 1995; Wyss-Coray et al., 1997; Hsia et al., 1999). The H6 line overexpresses the Indiana form of mutated APP gene (V717F) under the control of a PDGF promoter. The J9 line overexpresses both the Swedish (K670N, M671L) and Indiana (V717F) mutated forms of APP gene, driven by the same PDGF promoter. The expression level of APP in the brain of H6 mice is similar to that of PDAPP mice, but much higher than that of

the J9 (Mucke et al., 2000). There is a widespread expression of human APP in the brain of both H6 and J9 mice with maximal levels found in the neocortex and hippocampus. Interestingly, hippocampal levels of human APP and Aβ increase in an age-dependent manner and the deposition of Aβ plaques is age-dependent. Amyloid plaques have been found in H6 and J9 mice at 8-10 months, but the J9 exhibit more plaques than the H6 at this age. J9 mice display plaques at 5-7 months, but no plaques have been found at 2-5 months in both lines. J9 mice also display much higher levels of total Aβ and Aβ42 in the hippocampus than H6 (Mucke et al., 2000). The densities of synaptophysin-immunoreactive presynaptic terminals and MAP2-positive neurons in the CA1 region are significantly lower in 2-3-month H6 and J9 mice than in the controls. More interestingly, neuronal loss was observed in the CA3 region of old H6 animals (Hsia et al., 1999).

Using extracellular slice recording techniques, Hsia et al (1999) investigated synaptic transmission and plasticity in H6 and J9 mice. Basal synaptic transmission in the Schaeffer-collateral pathway was examined by recording field EPSPs. In 1-4-month H6 mice, a ~40% decrease in the slope of input-output curves was observed, suggesting a significant deficit in hippocampal synaptic transmission. At 8-10 months, a >80% impairment in basal synaptic transmission was again observed in H6 mice, suggesting a progressive decline of the strength of synaptic transmission. The deficit in hippocampal synaptic transmission in J9 mice is almost twice as large as that in the H6. This might be due to the J9 expressing much higher level of Aβ and Aβ42 than the H6. Moreover, no amyloid plaques were detected in H6 and J9 mice at 2-4 months, indicating that the deficits in basal synaptic transmission in the H6 and J9 are not related to extracellular deposition of Aβ and thus are plaque-independent (Hsia et al., 1999). Finally, hippocampal LTP in the CA1 region of the two lines is not impaired (Hsia et al., 1999). No behavioural study was conducted on the same mice examined electrophysiologically.

1.5.5 The C-terminus (C-104) APP Tg mouse.

The C-104 model was reported in 1997. It is a line of Tg mice containing APP cDNA encoding residues 591-695 (C104 APP) being cloned into the first exon of the human neurofilament NF-L gene and under transcriptional control of its regulatory elements (Nalbantoglu et al., 1997). With aging, C-104 mice exhibit more prevalent

extracellular Aβ immunoreactivity, which is present as dense structures in the cortex and hippocampus but absent in control animals which are transgenic for chloramphenicol acetyltransferase (CAATase) under the control of the same NF-L sequences. This immunoreactivity is accompanied by a generalised gliosis which increases with aging. Glial fibrillary acidic protein (GFAP)-positive reactive astrocytes were found as early as 4-5 months in C-104 mice, but not in controls. Apparent microgliosis was also observed. Interestingly, analysis in hippocampal CA1 cell counting in old C-104 animals reveals a decrease in both cell number (about 10%) and density (about 20%) (Nalbantoglu et al., 1997).

Spatial memory of 8-month-old C104 mice was studied using a water maze task (Nalbantoglu et al., 1997). The mice were first trained for 8 trials per day for 7 days. After this, the platform was moved to the opposite quadrant and all animals were trained 8 trials per day for 7 days again. Probably at the end of this stage, or the next day, a probe test was given (the methods are unclear). Following this, a visible cuetask was conducted for the next 7 days. A final 7-day training of hidden platform, 8 trials per day, was performed. The main behavioural finding of this study is that the C104 mice take longer to find the platform than the CAATase Tg mice on all 3 phases of hidden platform testing. In the visible cuetask, the overall performance of both groups is comparable. The reversal transfer test reveals a strong spatial memory of the new platform position in the CAATase Tg mice but not in the C104 group. Interestingly, analysis of swim speed reveals that the C104 mice swam faster and over longer distances than the controls. No thigmotaxis data on these animals at three different phases of testing are presented, but it is likely that C104 mice are more thigmotaxic than the controls.

The C104 mouse was the first APP Tg model to be analyzed electrophysiologically (Nalbantoglu et al., 1997). Hippocampal CA1 LTP was induced by theta-burst stimulation (TBS) and recorded for at least 60 min after the tetanus. Although there is no difference in post-tetanic potentiation (PTP), C104 mice exhibit significantly impaired hippocampal LTP as compared to the control group. Both PPF and LTD were also studied, but there is no difference. After the electrophysiology, a binding study was conducted to test whether the impairment of hippocampal LTP in C104

mice might be due to deficits in NMDA receptor function. The amount of binding of 100nM ^{3}H-glutamate was assayed in several different regions of the brain, but no differences were found. Second, in the presence of a low Mg^{2+} concentration and DNQX (the AMPA antagonist), the NMDA response was further studied and it is normal in C104 mice. So the impairment of LTP is due to other mechanism rather than the NMDA receptor function (Nalbantoglu et al., 1997).

Overall, the C104 Tg mice display several aspects of AD-like neuropathology in the brain, and they also display neuronal and synaptic loss (Nalbantoglu et al., 1997). More interestingly, C104 mice show striking impairment in both spatial learning and hippocampal synaptic plasticity. Worthy of mention, unlike previous studies in which non-Tg (or wildtype) mice always served as the control group (Games et al., 1995; Hsiao et al., 1996), Nalbantoglu et al first employed a control transgene, i.e. the CAATase gene, driven by the same promoter used in the C104 mice. This CAATase Tg line may be a better control group than the wildtype controls in previous studies. For example, the deficits in spatial learning and synaptic plasticity shown in the C104 mice can be concluded to be specifically due to the expression of the C-terminus of APP in the brain, but not any other protein or promoter effects.

1.5.6 The TgAPP22 and TgAPP23 mice.

TgAPP22 and TgAPP23 mice were reported by neuroscientists in Novartis Pharma, Inc. (Sturchler-Pierrat et al., 1997). Transgenic constructs used contain murine Thy-1 expression cassettes and human mutant APP751 cDNAs. TgAPP22 mice overexpress an APP transgene harbouring the Swedish (K670N, M671L) and London (V717I) mutations, while the TgAPP23 only have the Swedish mutations.

Different patterns for plaque development were found in these two lines. TgAPP22 mice show a 2-fold overexpression of APP over endogenous human APP and display Aβ deposits in the cortex and hippocampus at 18 months of age. However, TgAPP23 mice exhibit a 7-fold overexpression of APP and display Aβ plaques as early as 6 months. TgAPP22 and TgAPP23 mice develop different types of plaques in the brain. The major form of amyloid deposits found in TgAPP22 mice is the diffuse plaque, but almost all amyloid deposits in TgAPP23 mice are the neuritic ones which are Congo red-positive. Vascular amyloid is also present and occurs most frequently in the

meningeal, neocortical and thalamic vessels (Calhoun et al., 1998). Using unbiased stereological methods of cell counting, Calhoun et al demonstrated that, in hippocampal CA1 area of 14–18-month TgAPP23 mice, neuronal loss is 14% and much higher in mice with high Aβ load, but no neuronal loss was found in the neocortex (Calhoun et al., 1998).

Although the overt AD-like neuropathology in TgAPP23 mice was reported several years ago, until very recently, the behavioural testing of this Tg line has been conducted by two different groups. First, using a passive avoidance and a water maze protocols, Kelly et al (2003) completed a cross-sectional study using three cohorts of APP23 mice aged at 3, 18 and 25 months. In the passive avoidance task, although no main genotype effects were observed, the 25-month group shows an impaired retention compared to age-matched non-Tgs, suggesting an age-related deficit (Kelly et al., 2003). These mice were further evaluated in two water mazes with different sizes, one being 60 cm in diameter and the other 133 cm. Results from the smaller water maze indicate significant main genotype and age effects, suggesting an age- and plaque-related impairment in spatial learning (Kelly et al., 2003). However, in the bigger pool, it was found that APP23 mice at all ages are impaired in acquisition training, suggesting an age-independent learning deficit. As 18-month APP23 and controls display identical performance in a visible cuetask, the spatial learning deficit in APP23 mice is therefore not due to sensorimotor problem. The interesting finding from the two studies is that, using two different sizes of water maze, both age-dependent and age-independent deficits in spatial learning are observed and can be dissociated in APP23 mice (Kelly et al., 2003). This conclusion is similar to that from a PDAPP study by us (Chen et al., 2000). Second, Van Dam and colleagues (2003) focused on exploring activity, learning and cognition only in young heterozygous APP23 mice aged at 6-8 weeks, 3 and 6 months. The pool used in this study is 150 cm in diameter. Consistent with the finding by Kelly et al (2003) from their large pool, Van Dam et al (2003) also observed a learning deficit in APP23 mice as early as 6-8 weeks. More interestingly, APP23 mice further display an age-dependent decline (Van Dam et al., 2003). Performance in the probe trial was found to be negatively correlated with soluble Aβ level in 3-month APP23 mutants, suggesting that the learning deficit in young APP23 mice is due to soluble Aβ, but not amyloid burden (Van Dam et al., 2003).

1.5.7 The TgCRND8 Mouse.

TgCRND8 mice were reported by Janus et al (2000) in a vaccine study. TgCRND8 mice encode a double mutant form of APP695, including the Swedish (K670N, M671L) and Indiana mutation (V717F), under the control of a PrP promoter. Both human Aβ40 and Aβ42 are present in the brain of TgCRND8 mice and their levels increase with age. Aβ40 keeps stable between 4 and 10 weeks, but Aβ42 increases slowly between 4 and 8 weeks and shows a sharp increase at 10 weeks (Chishti et al., 2001). Amyloid plaques increase with age and spread to more regions of the brain at 65-90 days of age. 11-35 and 22-43 plaques are present in the cortex at 90 and 150 days, but there are 127-416 and 528-1024 at 240 and 350 days. In the hippocampus, 1-5 and 11-12 plaques are found at 90 and 150 days, but 39-65 and 123-147 plaques at 240 and 360 days. By 243 days, the cerebellum and brain stem are also fully filled by plaques (Chishti et al., 2001).

Spatial learning of these mice was assessed (Janus et al., 2000). In a visible cuetask of water maze, 10.5-week TgCRND8 mice use equivalent time to learn it to the control. However, TgCRND8 mice display a significant impairment in both acquisition and retention training of water maze, taking significantly longer latencies to find the hidden platform and spending markedly less time in the target quadrant during the probe test than the control (Janus et al., 2000; Chishti et al., 2001). This finding suggests a plaque-independent deficit in spatial learning of TgCRND8 mice.

1.5.8 The TgAPP/Ld, APP/Sw and APP/Wt mice.

Moechars et al reported two lines of mice expressing the London mutation (V717I), TgAPP/Ld/-2 and -6, two lines expressing the Swedish mutation (K670N, M671L), TgAPP/Sw-1 and -3, and two lines expressing wildtype human APP, TgAPP/Wt-2 and -4 (Moechars et al., 1999). In a behaviour study, TgAPP/Ld/2 and TgAPP/Wt/4, were chosen to undergo spatial memory testing in a water maze at 3 to 6 months. Both of them display much longer escape latencies to find the hidden platform than control animals. The performance of TgAPP/Ld/2 and TgAPP/Wt/4 mice is equivalent. In the probe trial (24 h after training), control mice show preferential search of the target quadrant, however, the two APP lines only display a chance performance (25% searching time). While they display early-onset learning impairment, the two APP lines also show a decreased hippocampal LTP (Moechars et al., 1999). These results

indicate that the overexpression of human mutant or wildtype APP gene in the mice disrupt spatial learning and memory either long before the formation of amyloid plaques, which start to be apparent at 13–18 months in TgAPP/Ld/2 mice, or in the absence of amyloid deposits in APP/Wt mice (Moechars et al., 1999).

1.5.9 The Tg2576/PS1 mice.

Presenilins are integral components of the γ-secretase complex (Kimberly et al., 2003). Using a PDGF promoter, Duff et al (1996) generated transgenic mice expressing human wildtype PS1 and mutant PS1 (M146L or M146V). Expression of mutant or wildtype PS1 has no effect on brain Aβ40, but expression of mutant but not wildtype PS1 increases brain Aβ42 (Duff et al., 1996). PS1 Tg lines do not display any AD-like pathology by two years of age (Duff et al., 1996; Citron et al., 1997). The advent of APP and PS1 Tg mice has prompted a number of studies on mice expressing both the human presenilins and APP. Doubly transgenic line, Tg2576/PS1, from a cross between Tg2576 mice and TgPS1 mice has been reported by Mayo Clinics (Holcomb et al., 1998). The double mutant Tg2576/PS1 model displays accelerated AD-type phenotype relatively to the Tg2576 animals. Tg2576/PS1 mice develop detectable amyloid deposits in hippocampus and cerebral cortex at an earlier age than their single Tg2576 littermates (Holcomb et al., 1998). Tg2576/PS1 double Tg mice also display a selective increase in Aβ42 in the brain, and exhibit massive amyloid deposits in the hippocampus and cortex by 6 months of age (McGowan et al., 1999).

The Tg2576/PS1 mice were tested in a Y-maze spontaneous alternation task at 3 months of age. Both Tg2576/PS1 and Tg2576 mice show significantly lower spontaneous alternation than control groups (Holcomb et al., 1998). In a follow-up study by the same investigators, 6- and 9-month Tg2576/PS1, Tg2576, TgPS1 and non-Tg littermate mice were tested using a Y-maze alternation and a water maze reference memory task. At 6 months, both Tg2576/PS1 and Tg2576 mice show significantly lower alternation rate compared to TgPS1 and non-Tgs. At 9 months, only Tg2576/PS1 mice are significantly impaired compared to non-Tg mice. At 6 months, no differences have been found in acquisition training of the water maze between four genotypes. The performance during the probe trial is comparable

between four different genotypes. Similarly, no significant genotype effect was found during the acquisition training at 9 months. The probe test also reveals a comparable performance between four genotypes (Holcomb et al., 1999). This study seems to indicate that plenty of amyloid plaques are not sufficient to produce cognitive impairment in a triple genetic background that includes Swiss Webster, C57BL/6//SJL and DBA/2 strains.

Recently, Arendash et al (2001) have re-investigated Tg2576/PS1 mice using a behavioural testing battery including a Y-maze alternation, a water maze reference memory and a radial-arm watermaze task. Progressive cognitive impairment was found in Tg2576/PS1 mice in the water maze acquisition and radial arm water maze working memory (Arendash et al., 2001). However, Tg2576/PS1 mice do not display impairments in the Y-maze alternation, water maze retention or visible cuetask at 5-7 and 15-17 months of age (Arendash et al., 2001). In summary, the Tg2576/PS1 mouse is an ideal transgenic model to develop therapeutics for the treatment and prevention of Alzheimer's disease.

1.5.10 Concluding remarks

The main purpose of using transgenic animals is to examine the function of genes implicated in AD *in vivo*. It is generally believed that a valid animal model for AD should exhibit progressive AD-like neuropathology and ideally, age- and/or plaque-related cognitive deficits. All APP Tg models reviewed above display most AD-like pathology, age-related and/or plaque-independent learning deficits. Because none of them recapitulates all AD features, the APP Tg mouse should be viewed as a partial model for AD. However, APP transgenics are indeed good rodent models for the amyloidosis of AD. Despite some limitations, they have greatly helped us not only to understand the molecular and cellular mechanisms of the pathophysiology of human AD since the advent of the first APP Tg mouse in 1991, but also to answer questions for therapeutic intervention of AD, such as whether the pathology and the progression can be reversed or prevented.

1.6 Tau transgenic mouse models of Alzheimer's disease.

Although all APP Tg models replicate most AD-like neuropathology, their major drawback is that they do not produce any neurofibrillary tangles (NFTs). Great efforts have been made by neuroscientists during the last decade in order to create the NFTs-producing mouse model. Using wildtype human tau gene, one group led by Gotz (1995) tried their first attempt to make NFTs-producing mice. However, this tau model fails to display any pretangles or NFTs in the brain (Goedert et al., 1995; Gotz et al., 1995). Shortly after the FTDP-17 tau mutation was discovered (Hutton et al., 1998), the first NFTs-producing mouse (JNPL3) has eventually been generated at Mayo Clinic (Lewis et al., 2000). Several different groups have later published other NFTs-producing mice (Gotz et al., 2001a; Higuchi et al., 2002). As tau models are not the main focus of this thesis, this section will briefly review several tau Tg mice available to the field.

1.6.1 The ALZ7 mouse.

The ALZ7 mouse, the first tau model of AD, expresses the longest human four-repeat (4R) tau isoform, htau40, under the control of a human Thy1 promoter in the B6D2F1 background. This line expresses human tau at 10% of endogenous murine tau level and no NFTs were observed (Gotz et al., 1995).

1.6.2 The Tg23 mouse.

The Tg23 tau mice express the shortest human tau, htau44, using a murine 3-hydroxy-methyl-glutaryl CoA reductase (HMG-CR) promoter. The human tau protein is widely produced in the CNS, but no NFTs were found (Brion et al., 1999).

1.6.3 The Tau 7, 27 and 43 mice.

A murine PrP promoter was used to drive the expression of a htau44 in three lines, 7, 27 and 43. About 20% of axon degeneration was observed in the brain and spinal cord (Ishihara et al., 1999). Very old mice (18-24 months) display NFTs in the hippocampus, entorhinal cortex, amygdala and neocortex (Ishihara et al., 2001).

1.6.4 The Tau40-1 and -5 mice.

In tau40-1 and -5 mice, a murine Thy1.2 promoter was used to express a htau40 in the FVB genetic background. The expression level of human tau protein in transgenic mice is 1.5-fold and 4-fold, respectively, higher than that of endogenous tau in the brain. Both lines do not show any NFTs (Spittaels et al., 1999).

1.6.5 The ALZ17 mouse.

Using a murine Thy1.2 promoter and a htau40 in the B6D2F1 background, Gotz's group generated the ALZ17 mouse. The level of human tau in ALZ17 mice is much higher than that of endogenous tau. However, the ALZ17 mouse shows no evidence of NFTs up to 17- to 20-month of age (Probst et al., 2000).

1.6.6 The Tau P301L (JNPL3) mouse.

The JNPL3 mouse is the first tau mouse model to display true NFTs. A human 4R tau isoform lacking the two N-terminus inserts, htau43 with a mutation of P301L, is expressed under the control of a mouse PrP promoter (Lewis et al., 2000). Heterozygous JNPL3 mice express the mutant human tau at levels equivalent to that of endogenous tau. In the brain, the tau-positive NFTs, including flame- and globe-shaped NFTs, are similar to those found in FTDP-17. Neurons with NFTs in the brainstem and spinal cord have filamentous aggregates in the perikarya and proximal dendrites. Most filaments are straight and about 10–30 nm in diameter, but others have a twisted ribbon appearance. Reactive astrocytes with abundant glial filaments, but not tau inclusions, are found to be around NFTs (Lewis et al., 2000).

1.6.7 The Tau40 P301L (pR5-183) mouse.

In the tau40 P301L mouse, a mutant htau40 with a P301L mutation is expressed in the pR5 background under the control of a neuron-specific mouse Thy1.2 promoter. NFTs are detectable in the spinal cord, brain stem, and cortical layers 5 and 6 by thioflavin-S and Gallyas silver staining. The activated astrocytes can be found in the amygdala and cortical areas. Astrocytosis is positively correlated with the number of tau expressing neurons, but there is no astrocytosis in the hippocampus. No neuronal loss was observed (Gotz et al., 2001b).

1.6.8 The Tau40 V337M (Tg214) mouse.

A mouse PDGF-β promoter was used to drive a htau40 with a mutation of V337M (Val-Met) in Tg214 mice. Mutant tau is observed in the hippocampus at 11 months. The irregularly shaped NFT-bearing neurons are also observed. No deficits were found in a spatial learning task in the water maze, suggesting a normal spatial learning in Tg214 mice (Tanemura et al., 2001).

1.6.9 The Tau40 R406W mouse.

A htau40 gene with a mutation of R406W, driven by an alpha-calcium–calmodulin-dependent kinase-II (αCaMKII) promoter is used to generate the tau40 R406W mouse. Aged mice (>18 months) display a selective expression of mutant tau in the brain. The irregularly shaped NFT-bearing neurons are detectable. Behavioural studies have shown no significant differences between tau R406W Tg mice and non-Tg controls regarding to sensorimotor reflexes, motor coordination and locomotor activity. However, tau40 R406W mice display significant impairment in both contextual and cued fear conditioning, suggesting an impaired associative learning (Tatebayashi et al., 2002).

1.6.10 Summary.

In early attempt to create tau Tg mice, Gotz and colleagues used wildtype human tau and generated two lines, Alz7 and Alz17 mice, which display some changes associated with NFTs but fail to develop any NFTs-like neuropathology. In later efforts to develop tau mice, several other groups have realized that similar strategies to those adopted in the generation of APP mice, i.e. stronger promoters and mutant human tau isoforms, might be needed in order to successfully generate NFTs-producing models. Overall, the most recent NFTs-producing Tg mice, such as the JNPL3 and tau40 P301L, have marked a further breakthrough in modelling AD to APP Tg models.

1.7 Plaque/Tangle transgenic mouse models for Alzheimer's disease.

All tau Tg models reviewed in section 1.6 develop neither amyloid plaque nor massive neuronal loss, although the JNPL3 mouse displays motor neuron loss in the spinal cord (Lewis et al., 2000). Plaques, tangles and neurodegeneration may be

reproduced by combining transgenic strains that express different disease-associated genes in brain. By inter-crossing the current tau Tg mice with APP transgenics, it will allow us to examine the relationship between Aβ production and neurofibrillary tangles. In this section, two latest transgenic mouse models displaying both amyloid plaques and neurofibrillary tangles are reviewed.

1.7.1 The TAPP mouse.

The TAPP mouse is made by Lewis and colleagues (2001) who crossed the JNPL3 line with the Tg2576 mouse. The brain and spinal cord of TAPP mice aged at 2.5-3.5 months, 6-7 months and 8.5-15 months were examined. Plaques can be detected as early as 6 months of age and become numerous in the olfactory cortex, cingulate gyrus, amygdala, entorhinal cortex and hippocampus of 8.5-15-month TAPP and Tg2576 mice. NFTs become numerous in 8.5-15-month TAPP and JNPL3 mice. All NFTs are positive for Gallyas silver stain and immunoreactive with tau antibodies. Ultrastructurally, NFTs, composed of straight filaments, 17 to 22 nm in diameter, in TAPP mice are similar to those in JNPL3 mice (Lewis et al., 2001).

Interestingly, 9-11 month female TAPP mice display a marked increase in NFTs in limbic areas, such as the olfactory cortex, entorhinal cortex and amygdala, compared to JNPL3 mice. The density of NFTs in these regions is much greater in 9-11 month female TAPP mice than age-matched female JNPL3 mice. The increase of NFTs occurs as early as 6 months in TAPP mice. NFTs are also found in the subiculum, hippocampus and isocortex of TAPP mice, but have never been found in the same areas of JNPL3 mice. By contrast, no increase in the density of NFTs is found in the diencephalon, hindbrain and spinal cord of TAPP mice. Increased astrocytosis is also found in limbic areas of TAPP mice, but gliosis is equally severe in the ventral diencephalon, hindbrain and spinal cord of both lines. Interestingly, the distribution and density of amyloid plaques is similar in TAPP and Tg2576 mice (Lewis et al., 2001). In addition to increased NFTs, granulovacuolar degeneration was observed in neurons in the amygdala, entorhinal cortex and subiculum of female TAPP mice. By contrast, JNPL3 mice show rare granulovacuolar degeneration in the amygdala.

TAPP mice develop similar motor disturbances to those in JNPL3 mice, showing progressive hindlimb weakness, hunched posture, eye irritations, reduced vocalization

and decreased grooming. It was found that the motor phenotype is associated with spinal and neuromuscular pathology in both TAPP and JNPL3 mice (Lewis et al., 2001).

1.7.2 The triple Tg mouse model for AD (3×Tg-AD).

Instead of crossing independent Tg lines, two independent transgenes, encoding human APP with the Swedish mutation and human tau (P301L) under the control of mouse Thy1.2 regulatory element, were co-microinjected into single-cell embryos from homozygous mutant PS1(M146V) knockin (KI) mice (Oddo et al., 2003). Six founder lines were identified, five of which harbour all three transgenes. Southern blotting analysis indicated that tau and APP transgenes are integrated at the same locus in the majority of founder lines.

As the mouse Thy1.2 promoter drives transgene expression predominantly in the CNS, tau and APP are exclusively found there. The hippocampus and cerebral cortex show the highest levels of human tau and APP. A progressive increase in Aβ formation can be observed in 3×Tg-AD mice as they get older. Intracellular Aβ immunoreactivity is present in the neocortex of 3×Tg-AD mice at 3-4 months, and in CA1 region of the hippocampus by 6 months. Extracellular Aβ deposits first appear in the frontal cortex at 6 months and become evident in other cortical regions, including the hippocampus by 12 months, suggesting that Aβ deposition develops first in the neocortex and progresses to the hippocampus. Although extracellular Aβ deposits are first seen in the cortex by 6 months of age, no tau alterations are observed at this age. It has been found that, at about 12 months, extensive human tau immunoreactivity is first evident in CA1 neurons of the hippocampus, and later progresses to other cortical areas. These findings indicate that Aβ pathology develops much earlier than tau pathology in 3×Tg-AD mice, consistent with the amyloid cascade hypothesis.

Two cohorts of mice at 1- and 6-month were used to investigate synaptic transmission and synaptic plasticity in the hippocampus of 3×Tg-AD mice. The I-O curves of 1-month PS1-KI and 3×Tg-AD mice are not different from those of non-Tg mice. By contrast, both 6-month PS1-KI and 3×Tg-AD mice exhibit significantly smaller fEPSP slopes and amplitudes than non-Tg mice. These results suggest an age-related

impairment of basal synaptic transmission in both PS1-KI and 3×Tg-AD mice. Although 3×Tg-AD mice do not show any impairment in PPF compared to non-Tg mice, an age-related impairment of hippocampal LTP was observed. As there are no Aβ deposits in the hippocampus of 3×Tg-AD mice at 6-month, synaptic dysfunction might be due to intraneuronal accumulation of Aβ (Oddo et al., 2003).

1.8 The treatment of Alzheimer's disease.

Although much has been learned about AD since last century, there is still not a cure. Five drugs have recently been approved by the FDA of the USA for the treatment of AD, but they provide only symptomatic effects. Several novel treatment strategies have been in the process of development. This section reviews the currently available and potentially novel treatment strategies for AD.

1.8.1 Current treatment strategies for AD.

The cholinergic hypothesis has historically shown its massive impacts on the field of AD (Bartus et al., 1982). From early 1980s to late 1990s, many acetylcholinesterase inhibitors (AChEIs), which can pharmacologically enhance cholinergic neurotransmission and maintain ACh levels in the brain, have been tested and found to improve learning and memory. The FDA first approved tacrine for the treatment of AD in 1993. Since then, donepezil, galantamine and rivastigmine have also been approved. These four drugs are the well-known AChEIs. However, memantine, the fifth drug approved by the FDA, is an N-methyl-D-aspartate (NMDA) receptor antagonist.

1.8.1.1 Tacrine (Cognex).

Tacrine can inhibit AChE reversibly in a noncompetitive manner (Hardegg and Heilbronn, 1961). Recently, a 30-week randomized controlled trial of tacrine (40-160 mg/day) has been conducted in patients with AD. Tacrine produces significant improvements on objective performance-based tests, clinician- and caregiver-rated global evaluations, and measures of quality of life. However, tacrine-treated patients frequently show hepatotoxicity, such as highly elevated alanine aminotransferase level, nausea, vomiting, diarrhea, anorexia, dyspepsia and abdominal pain (Knapp et al., 1994). These side effects have limited its clinical use.

1.8.1.2 Donepezil (Aricept).

Donepezil, approved by the FDA in 1999, is a piperidine-based reversible inhibitor of AChE and has a long plasma half-life of approximately 70 h (Snape et al., 1999). Unlike tacrine, donepezil does not induce hepatotoxicity. In a short-term, double-blind, placebo-controlled clinical study, mild-to-moderate AD patients were randomly assigned to daily receive a single dose of placebo or 5 or 10 mg donepezil hydrochloride for 24 weeks and the cognitive ability is significantly improved by donepezil (Rogers et al., 1998). The side effects by donepezil are much less than those by tacrine and can be controlled.

1.8.1.3 Galantamine (Reminyl).

Galantamine is a selective competitive AChEI and has a serum half-life of 4-6 h. In a clinical study, galantamine (8, 16, or 24 mg/day) or placebo was given to 978 patients for 5 months. The cognitive ability of the galantamine group is significantly improved at dose levels of 16 or 24 mg/day compared to the placebo group (Tariot et al., 2000). The long-term (2 years) effects of galantamine on cognition of AD patients were also reported (Doody, 2003). ADAS-cog scores for the galantamine group are about 4 points below their initial baseline after 2 years of treatment, but are 12-14 points below the original baseline for the placebo group (Doody, 2003). The major side effects of galantamine are nausea, vomiting, diarrhea and headache, but there is no evidence of hepatotoxicity.

1.8.1.4 Rivastigmine (Exelon).

Rivastigmine tartrate is a reversible AchE inhibitor and has been approved in more than 40 countries. It can be well-absorbed and has a plasma half-life of 2 h (Spencer and Noble, 1998). In a randomised, double blind, placebo controlled, 26-week trial, 725 patients with mild-to-moderate AD in Europe and America received placebo, 1-4 mg/day (lower dose) or 6-12 mg/day (higher dose) rivastigmine. At the end of the study, the placebo group show deteriorated cognitive function, however, and the higher dose rivastigmine group display significant improvement in cognition as compared to the placebo group (Rosler et al., 1999).

In conclusion, tacrine , donepezil, galantamine and rivastigmine show positive effects on the treatment of AD and they are effective for mild-to-moderate AD. Limitations

of the AChEIs are related to their modest effects on baseline and their side effects. The modest improvements do not sustain indefinitely, as the disease still progresses while patients are receiving their treatment. Moreover, the adverse effects such as vomiting and weight loss sometimes make patients discontinue the treatment.

1.8.1.5 Memantine.

As clinical studies indicated deficits of glutamatergic function in AD, the glutamatergic neurotransmitter pathway has been hypothesized as a target for therapeutic intervention of AD. Memantine is a low affinity, uncompetitive NMDA receptor antagonist. Memantine can rapidly cross the blood-brain barrier and exhibits a long half-life of 60-80 hours. In a recent randomised, double blind, placebo controlled clinical study, 252 patients from 32 US AD centres have participated. Patients receiving memantine showed a better outcome than those receiving placebo (Reisberg et al., 2003). Importantly, memantine is not associated with a significant frequency of adverse events (Reisberg et al., 2003). Memantine has been approved for the treatment of moderately severe to severe AD in the European Union and Australia, but it was not approved by the FDA in the US until late last year.

1.8.2 Potential treatment strategies for AD.

At the present time, cholinergic-based therapy is still the most important clinical approach for improving cognitive deficits in AD. However, several novel treatment strategies have also been in the process of development.

1.8.2.1 Agents that increase neuroprotective sAPPα.

APPα, the soluble N-terminus fragment of APP, is derived from the α-secretase cleavage pathway. The sAPPα protects neurons from ischemic injury or enhances recovery from ischemic injury in rats (Bowes et al., 1994). Many acetylcholine receptor agonists such as acetylcholine, nicotine and carbacol were found to increase the release of the sAPPα and reduce the accumulation of toxic Aβ (Mattson et al., 1993). Evidence suggested that stimulation of the nicotinic receptor improves amyloidosis in animal models of AD (Nordberg et al., 2002). In a double-blind study, three doses (6, 12, and 23 mg) of a novel selective nicotinic agonist, ABT-418 were acutely administered over 6 h in AD patients. Subjects receiving ABT-418 displayed significant improvements in total recall, spatial learning and memory, and repeated

acquisition (Potter et al., 1999). However, long-term clinical effects of nicotinic agonists need to be assessed in a larger population.

1.8.2.2 Metal chelators inhibiting aggregation of plaques.

It is long believed that some bio-metals such as aluminium, iron, zinc and copper promote Aβ aggregation and neurotoxicity in the brain of AD (Suh and Checler, 2002). Clioquinol is a metal chelator for copper and zinc and can solubilize Aβ from postmortem AD brain (Cherny et al., 1999). In a recent animal study, a significant decrease in Aβ deposits but a highly elevated level of soluble Aβ were found in the brain of Tg2576 mice treated with clioquinol for 9 weeks (Cherny et al., 2001). However, it remains unclear whether clioquinol also improves cognitive deficits in the same APP mice.

Clioquinol causes severe adverse effects, such as vitamin B-12 deficiency and subacute myelo-optico-neuropathy (SMON), in human or dogs, so the use of clioquinol was banned in Japan (Tabira et al., 2001). In the US, a randomized pilot clinical study has recently been conducted. Patients with moderately severe AD were assigned to receive either clioquinol or placebo. The clioquinol group show minimal deterioration in cognitive tests, but the placebo group show a substantial worsening of scores, suggesting that clioquinol might slow down the progression of AD (Ritchie et al., 2003). Further study on clioquinol with a much larger size of samples is needed to test its potential use in the treatment of AD.

1.8.2.3 Antioxidants.

Ginkgo biloba, an antioxidant, has been used in traditional Chinese medicine for thousand years. Ginkgo biloba extract can protect neurons from hydrogen peroxide-induced oxidative stress (Oyama et al., 1996). A double-blind, randomized, placebo-controlled, one-year clinical study of Egb761, an extract of Ginkgo biloba (Egb) was conducted. 236 AD patients were assigned randomly to receive Egb (120 mg/d) or placebo. Interestingly, the Egb group show no significant change in the ADAS-Cog test before and after treatment. However, the placebo group show a significant worse effect in the ADAS-Cog (Le Bars et al., 1997).

Studies on animal models have shown that cognitive impairments can be attenuated by treatment of either vitamin E or idebenone, an antioxidant and free-radical scavenger (Behl et al., 1992; Yamada et al., 1999). Idebenone was examined in 450 mild-to-moderate AD patients in a 2-year randomized, double-blind clinical study. During the first year of treatment, idebenone produces significant dose-dependent improvement on ADAS cognitive test. A further improvement was also found in the second year (Gutzmann and Hadler, 1998). A follow-up clinical study indicated that patients who received idebenone show a better benefit than those with tacrine (Gutzmann et al., 2002). In conclusion, antioxidants have beneficial effects on the prevention and treatment of AD, but the improvement observed in clinical studies is small or only marginal (Thal et al., 2003). More studies are needed to draw a conclusion on the efficacy of antioxidants.

1.8.2.4 Anti-inflammatory drugs.

Much clinical evidence has shown that the sustained use of nonsteroidal anti-inflammatory drugs (NSAIDs) delays the progression of AD (McGeer et al., 1990; Rich et al., 1995; Stewart et al., 1997). Several clinical trials on the effects of NSAIDs on the treatment of AD have recently been reported. In two double-blind, placebo-controlled, randomized, 26-week trials, concurrent use of anti-inflammatory agents and estrogen in AD patients produced superior cognitive performance (Doraiswamy et al., 1997). Another study showed that the risk of AD is significantly lower in those with long-term use of NSAIDs than those with short-term or intermediate-term use (in 't Veld et al., 2001; Landi et al., 2003). Interestingly, chronic treatment of Tg2576 mice with 375 ppm ibuprofen from 10 months of age for 6 months significantly reduces astrogliosis, microgliosis and amyloid deposits (Lim et al., 2000; Yan et al., 2003).

1.8.2.5 Estrogen.

Estrogen, one member of a family of sex hormones, is closely associated with AD (Tang et al., 1996). It is suggested that the risk of AD is lower in women receiving estrogen-replacement therapy (ERT) during the postmenopausal period, and that estrogen replacement improves cognitive performance (Tang et al., 1996). Estrogen may serve as an antioxidant or stimulate α-secretase activities (Behl et al., 1994; Jaffe

et al., 1994). Estrogen can also enhance synaptic transmission and synaptic plasticity (Foy et al., 1999).

1.8.2.6 Aβ vaccines.

The vaccine concept for the treatment of AD first appeared after a novel Aβ vaccination study on PDAPP mice (Schenk et al., 1999). Schenk and colleagues injected synthetic Aβ42 (AN-1792) into PDAPP mice for several months either prior to (prevention study) or after (treatment study) plaque formation. Plaques are completely prevented in PDAPP mice in the prevention study, and are significantly reduced in the treatment study. These results raise a hope that Aβ vaccine is possibly a novel therapy for AD (Schenk et al., 1999).

Weiner et al (2000) extended the initial finding by the Schenk group. They orally or nasally administered Aβ peptide to immunize the PDAPP mouse and have found a 50 to 60% reduction of plaque burden in the brain of mice, which were immunized intranasally by a high dose of Aβ (25 μg) (Weiner et al., 2000). There are no significant effects in mice immunized intranasally by a lower dose (5 μg) or in mice immunized orally. Lower Aβ load is associated with decreased local microglial and astrocytic activation. These results suggest a novel mucosal immunological approach for the treatment or prevention of AD (Weiner et al., 2000). In another study, a soluble nonamyloidogenic, nontoxic Aβ homologous peptide was used to immunize Tg2576 mice for 7 months. Immunisation has reduced cortical and hippocampal brain amyloid burden by 89% and 81%, respectively. The brain levels of soluble Aβ42 are reduced by 57% (Sigurdsson et al., 2001).

Two separate behavioural studies using Aβ vaccine were conducted and reported by two different research groups. In one of them, a reference memory task in the water maze was used. Aβ vaccination on 3-4-month CRND8 Tg mice significantly improves learning deficits in acquisition training, although the vaccinated CRND8 mice are still significantly worse than the controls (Janus et al., 2000). A significant reduction of Aβ deposits is also observed in the vaccinated CRND8 mice. The other one used Tg2576/PS1 Tg mice and a radial-arm water maze to test the effects of Aβ vaccines on spatial learning (Morgan et al., 2000). Vaccinated Tg2576/PS1 mice perform significantly better than non-immunized Tg mice, but worse than non-Tg controls.

However, Aβ vaccines do not produce a significant decrease in plaque burden (Morgan et al., 2000).

The above two preclinical behavioural studies provided strong evidence to support a novel Aβ immunotherapy. However, as Janus et al (2000) tested only very young mice, it remains unknown whether Aβ vaccines can also rescue learning deficit of old APP mice. Secondly, as the novel radial-arm water maze used by Morgan et al (2000) is not sensitive to reveal any soluble Aβ-dependent learning deficit in PS1/APP mice, it is difficult to explain why Aβ vaccines fail to reduce plaque burden but only reverse learning impairment. In the same time that Janus et al and Morgan et al published their findings, our own Aβ vaccine study was in the progress. These findings are described in Chapter 5.

1.8.2.7 β-secretase inhibitors.

Because Aβ and its accumulation seem to play a central role in the pathogenesis of AD, two proteases, directly responsible for the production of Aβ, have become the most interesting targets for therapeutic intervention of AD. As BACE (β-secretase) is the dominant form of β-secretase in the brain (Sinha et al., 1999; Vassar et al., 1999; Yan et al., 1999), blockage of this enzyme will certainly reduce the production of Aβ. As a homolog to BACE, BACE-2 is the main β-secretase in peripheral organs of human and rodents (Hussain et al., 1999). As several reports have shown that BACE homozygous knockout mice do not produce any detectable Aβ in the brain and are healthy and viable, inhibition of BACE may not produce severe side effects (Cai et al., 2001; Luo et al., 2001; Roberds et al., 2001).

Recently, several different structure-based BACE inhibitors have been published. The first β-secretase inhibitor is substrate-based analogue and contains a critical statine residue and has an IC50 of about 30 nM (Sinha et al., 1999). Based on the β-secretase cleavage site (VNL-DA) of the Swedish mutant APP, Abbenante et al developed a series of β-secretase inhibitors, which display very low potency (IC50 = 700 nM) (Abbenante et al., 2000).

The structural analysis of memapsin 2 (BACE), co-crystallized with an active-site-directed BACE inhibitor indicated that BACE is more open and less hydrophobic than

other human aspartic proteases (Hong et al., 2000). Due to its resemblance to other aspartic proteases such as Renin and HIV-1 protease, the structure-based design has been used to search for more potent and selective BACE inhibitors. Using this design, a group led by Tang in Oklahoma generated two inhibitors for BACE, OM99-1 and OM99-2, displaying very potent inhibitory activity against recombinant BACE (Ghosh et al., 2000). Later, the same group generated a third BACE inhibitor, OM00-3, which is the most potent inhibitor for memapsin 2 (K_i = 0.3 nM), about three times more potent than OM99-2 (Turner et al., 2001). The molecular size of OM00-3 is only 722 Da, but it can not freely penetrate the blood brain barrier. Moreover, OM00-3 equally inhibits both BACE and memapsin 1 (BACE2) (Hong et al., 2002).

Since publishing the first BACE inhibitor, Elan has recently reported two potent cell-permeable BACE inhibitors, Compound 38 (John et al., 2003) and Compound 20 (Hom et al., 2004). Compound 38 selectively inhibits Aβ secretion in human embryonic kidney cells (John et al., 2003). Compound 20 is a hydroxyethylene (HE) transition state isostere-based BACE inhibitor. Compound 20 is very potent (IC50=30nM) and has an enhanced cell penetration (Hom et al., 2004). The inhibitory specificity of either Compound 38 or Compound 20 is unclear. As BACE1/BACE2 double knockout mice display no gross phenotypic defects (Harper et al., 2003), itself a puzzling observation given the importance of APP processing in normal brain function, the specificity of either OM00-3 or BACE inhibitor 20 may not be a big problem for *in vivo* study. Recently, scientists at LG Life Science have reported three peptidomimetic BACE inhibitors, LB83190, LB83192 and LB83202. Using a cell-based assay, LB83190, LB83192 but not LB83202 were found to effectively inhibit BACE activity in a dose-dependent manner (Oh et al., 2003).

In 2001, Takeda disclosed the first non-peptide BACE inhibitor, aminoethyl-substituted tetralin inhibitor 7, identified as the most potent inhibitor of BACE with an IC50 of 0.35 μM (John et al., 2003). However, *in vivo* data have not been reported for this low molecular weight BACE inhibitor. Neurologic has disclosed piperazine-substituted phosphinyl- and phosphorylmethyl succinic acid derivatives as inhibitors of BACE, showing a dose-dependent release on sAPPα (John et al., 2003).

In summary, as recent genetic and behavioural studies on BACE knockouts are extremely encouraging (Cai et al., 2001; Luo et al., 2001; Ohno et al., 2004), β-secretase inhibitors are believed to be very promising as a potential candidate for the treatment of AD. However, caution also needs to be taken. A recent study has indicated that homozygous BACE1 KO mice display learning deficits in a novel training to criterion task in the water maze at all ages tested (3, 13 and 18 months). Furthermore, BACE1(-/-)APP mice are also impaired in learning this task at all ages tested (Kobayashi et al., 2003). Thus, this study has raised a possibility that BACE1 inhibition may not be effective in rescuing memory loss in AD patients.

1.8.2.8 γ-secretase inhibitors.

Gamma-secretase is an important enzyme for processing both APP and Notch. Due to being a complex of integral membrane proteins including presenilin, nicastrin, Aph-1, and Pen-2, the γ-secretase is more complex than the β-secretase (Kimberly et al., 2003). However, searching for cell-permeable γ-secretase inhibitors seems much easier than for the β-secretase ones. Great progress has been made in developing γ-secretase inhibitors. The currently available γ-secretase inhibitors can be classified as peptidic and non-peptidic.

The peptidic γ-secretase inhibitors are structure-based and many of them have been synthesized. MDL28170 (Z-VF-CHO) is the first published γ-secretase inhibitor, and also is a calpain proteinase inhibitor. MDL28170 (>50 μM) significantly inhibits the production of Aβ40, but not Aβ42 in CHO cultures stably transfected with APP695 (Higaki et al., 1995; Citron et al., 1996). MG132 (Z-LLL) reduces the production of Aβ40, but not Aβ42 production (Klafki et al., 1996; Skovronsky and Lee, 2000). Difluoroketone peptidomimetic 1 (MW167), a selective γ-secretase inhibitor (IC_{50}=13 μM), inhibits both Aβ40 and Aβ42 production in human APP-transfected CHO cells, reduces the NICD production as well (IC_{50}=10-30 μM) (Wolfe et al., 1998; De Strooper et al., 1999). 2-Naphthoyl-VF-CHO and Z-LF-CHO are cell-permeable and inhibit the release of Aβ40 and Aβ42 in HEK293 cells transfected with the Swedish mutant APP (Sinha and Lieberburg, 1999). Compound *t*-3,5-DMC-IL-CHO, a potent cell-permeable and reversible γ-secretase inhibitor, mainly inhibits the secretion of Aβ40 in CHO cells stably transfected with the cDNA encoding APP695 (Higaki et al., 1999). Z-LL-CHO and Z-VL-CHO are cell-permeable and reversible γ-

secretase inhibitors which inhibit the secretion of both Aβ40 and Aβ42 in APP-transfected cell cultures (Figueiredo-Pereira et al., 1999). Boc-GVV-CHO can preferentially inhibit Aβ40 production in HEK293 cells transiently transfected with APP695NL, but has no effect on Aβ42 (Murphy et al., 2000).

The nonpeptidic γ-secretase inhibitors are normally the transition-state analogues. The first nonpeptidic γ-secretase inhibitor is Compound L-685,458 (Shearman et al., 2000). L-685,458 dose-dependently inhibits Aβ production in both Neuro2A and CHO cell lines overexpressing human APP695. L-685,458 reduces both Aβ40 and Aβ42 production in these cells and is not neurotoxic at concentrations up to 10μM (Shearman et al., 2000). As a potent transition-state analogue γ-secretase inhibitor, WPE-III-31C inhibits the cleavage of both APP and Notch (Esler et al., 2000). The third one is called as DAPT (*N*-[*N*-(3,5-difluorophenacetyl)-L-alanyl]-*S*-phenglycine *t*-butyl ester), which is very potent. The DAPT reduces the production of Aβ40 and Aβ42 in HEK293 cells overexpressing human APP751 and in human primary neuronal cultures. It was reported that oral administration of DAPT to PDAPP mice reduces levels of Aβ in the brain within 3 h (Dovey et al., 2001). LY411575, which is 100 times more potent than DAPT, was used to treat PDAPP mice (6.5-7 months) for 90 days and this chronic treatment resulted in 70-90% reduction of brain Aβ levels (May et al., 2001).

It remains very interesting whether inhibition of γ-secretase rescues learning and memory impairment in APP Tg mice. An answer for this question is pivotal to clinical use of γ-secretase inhibitors as a novel treatment strategy of AD. To address this question, a genetic and a pharmacological study have been designed and conducted in this thesis. First, using PS1cKO;APP mice, I have investigated whether selective inactivation of PS1 in the forebrain has any effects on spatial learning and memory. Second, using ELN44989, a potent compound like LY411575 (May et al., 2001), I have examined its *in vivo* efficacy and its effects on spatial learning and memory of PDAPP mice. These two studies are described in Chapters 6 and 7.

1.9 Aims of this thesis.

1) The first aim of this thesis was to use a cross-sectional design, in which three different cohorts of naïve PDAPP mice were utilised, and a behavioural test battery to investigate whether PDAPP mice display an age- and plaque-related learning deficit;
2) The second purpose of this thesis was to use a longitudinal design, in which the same PDAPP mice were tested repeatedly at three different ages, and a behavioural test battery to investigate whether the same PDAPP mice also display an age- and plaque-related learning deficit;
3) The third objective of this thesis was to use aged PDAPP mice behaviourally tested to investigate whether they display altered synaptic transmission, and whether there is any relationship between altered synaptic transmission and impaired spatial learning in the same mice;
4) The fourth aim of this thesis was to use our novel serial spatial learning task to investigate whether Aβ immunisation has any effects on altered synaptic transmission and impaired spatial learning in PDAPP mice;
5) As the γ-secretase in one of the prime targets for novel therapeutics for AD, the fifth aim of this thesis was to use a genetically modified PS1cKO;APP mouse and the serial spatial learning task to investigate whether inactivation of PS1 in APP mice could improve the impaired synaptic transmission and spatial learning;
6) The sixth aim of this thesis was to use a functional γ-secretase inhibitor, ELN44989, and the serial spatial learning task to test the amyloid cascade hypothesis and to examine whether ELN44989 can rescue the impaired spatial learning in PDAPP mice.

Chapter 2: Materials and Methods.

2.1 Behavioural tests in the watermaze.

The watermaze was first developed to investigate spatial learning and memory in rats and to test its dependence on the hippocampus (Morris, 1981; Morris et al., 1982). Since then, the watermaze has become a powerful and widely used tool in behavioural neuroscience for the examination of learning and memory in rodents. It has been estimated that the watermaze has been utilized in more than 2000 original research publications between 1989 and 2001 (D'Hooge and De Deyn, 2001).

The watermaze is an open-field navigation task that is very sensitive to lesions of the hippocampus in rats (Morris et al., 1982). In practice, a variety of different tasks can be scheduled such that it is valuable to distinguish between the watermaze as an 'apparatus'and the watermaze as a set of 'protocols'. The hidden platform task of the watermaze is most commonly used to train the rodent to swim through the open-field and search for the platform. As there are no local cues for the hidden platform, the animal has to learn the extra-maze cues and needs to figure out the relation between the cues and the platform location.

2.1.1 The watermaze apparatus.

The watermaze (Fig.2.1.1) is 2m (in diameter) and 60cm (in height). It is made of fibreglass with the interior wall being painted white. It is about 60cm above the floor of the testing room enriched with extra-maze cues such as posters, black curtains, metal racks and doors. The water level is about 40cm above the bottom of the maze. Escape platform is 20cm in diameter and is about 1.5 cm below the water surface. The water is made opaque by adding 800 ml of cempolatex liquid (Cementone-Beaver Ltd., UK), so the escape platform is not visible to a swimming mouse. The swimming path of a mouse is monitored by a video camera sitting far right above the pool (on the ceiling of the room) and the video signal is recorded by a video recorder (Fig.2.1.2). This signal is fed to an image analyser (HVS VP112). The co-ordinates of the mouse are sampled at 10Hz by an Acorn computer running the Watermaze software (Roger Spooner) or a PC running the PC version of Watermaze program (Actimetrics). The software calculates several measures such as the escape latency taken on a training

Figure 2.1.1 Watermaze Apparatus.

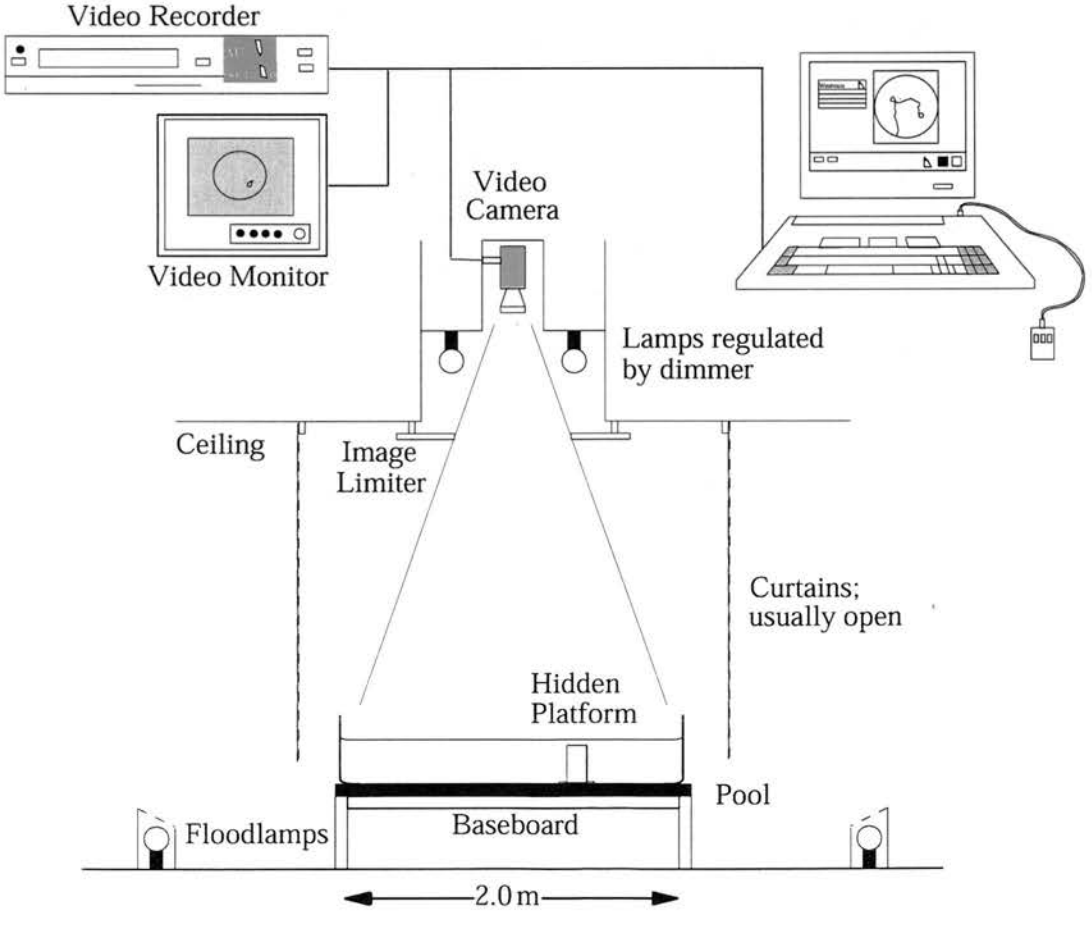

Figure 2.1.2 Watermaze Setup. (See texts for description)

trial, the swim path length, the swim speed, the percentage time spent near the side-walls (thigomataxis) and the percentage time spent in each quadrant of the pool during probe tests.

2.1.2 The general protocol.

Each training trial consists of the following sequence of events. The mouse is placed and released into the water by hand facing the wall at one of the four pre-planned start positions (North, South, East and West). The mouse swims until it finds the platform. If it fails to find the platform after 90 sec has elapsed, the mouse is guided to it by hand. Once on the platform, which is a metal cylinder (20cm in diameter) with its top surface 1.5 cm below the water, the mouse is allowed to remain on it for 30 s to look around the extra maze cues and so learn the platform position. After 30 s, the mouse is taken away from the platform using a small paint roller and placed back into a drying cage. This cage is placed under an infra-red heat lamp in a small animal room next to the watermaze room. The mouse is given about 10 min before the next trial starts, as this interval can allow the animal to dry itself and avoid hypothermia. Each animal receives 3 to 8 trials per day in different tasks (see below).

2.1.3 The cuetask.

In this task, curtains are drawn round the pool to occlude the extra-maze cues. The platform, submerged below the water, is made visible by putting a 15 cm high bronze cylinder on it that can be easily seen. The purpose of this task is to habituate the animals to the watermaze, to ensure that they can see, swim and climb onto the platform normally, and to establish that they are motivated to escape. Animals with serious sensorimotor abnormalities would display a deficit in this task. There were 4 trials per day for 5 days and the platform position was changed across trials. The water during testing was kept at 25±1°C.

2.1.4 The reference memory task.

In this task, the hidden platform remains fixed throughout training in the centre of one of four quadrants (North East, South West, North West or South East). This task consisted of 4-day acquisition training and two probe trials (or transfer tests). There were 4 trials per day. The inter-trial interval (ITI) was 10 min, the same as in the cuetask. At the end of training, or one week after the acquisition training, the mice

were given two probe trials. In the probe trial, the platform was removed from the maze and the mouse was allowed to swim in the pool for 60 s and was removed by the painter roller after 60 s has elapsed. By analyzing the swim paths, the time spent in different quadrants of the maze by each mouse could be further analyzed. These two probe tests can determine either the short-term (1 day after training) or long-term (7 days) memory for the location of the platform within the maze for each animal.

2.1.5 The delayed-match-to-place (DMP) task.

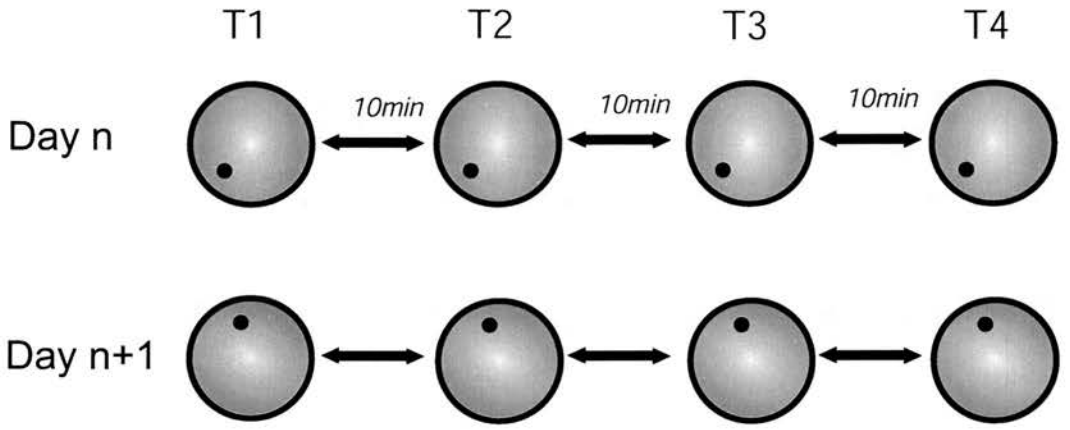

Figure 2.1.3 The Delayed-match-to-place (DMP) Task. Animals are given 4 trials/day. The platform location is changed between days.

Although this task was never used in the experiments of this thesis, the novel spatial learning task described in the next two sections is a modified version of the DMP task. The method is introduced here in order that readers can compare and better understand the other two modified versions of the DMP task. The DMP task (Fig.2.1.3) in watermaze was initially developed by Steele & Morris (Steele and Morris, 1999). The platform position is changed randomly from day to day and the animal receives 4 trials per day to learn its position. In other words, the platform position remains in the same position within each day, but is different between days. So, on the first trial (T1) of any day (Day n), the mouse has no information about where the platform is present, but in subsequent trials (T2-T4), the location of the platform remains the same as that on T1 of that day. On the next day (Day n+1), the platform moves on T1, and remains fixed in that position for the remaining trials. On

T1 of any day, the mouse does not know the platform location, but on T2 to T4, it can 'match to place'.

2.1.6 The trials-to-criterion version of DMP.

In this task, the platform is always hidden under water and is not marked by any local cues within the pool. All animals are trained on 5 consecutive different problems (i.e. platform locations). The platform location was changed only after a mouse reached a strict performance criterion for any particular location, so each mouse needed to reach the performance criterion five times in order to complete this task (Fig.2.1.4). The performance criterion for learning each problem was an average escape latency for three trials in a row being less than 20 s. On each day, all mice received up to 8 trials, and this depended on the performance by individual animal. Overall, the total number of trials on each day (after day 1) for each mouse could vary from 1 to 8, because a mouse was stopped swimming and taken back to its original home cage in the animal house on any given day once it reached the performance criterion. So, on the first trial of the next day, this mouse started searching for a new platform location and continuously learned the same new position in the subsequent trials of that day until it reached the criterion. After all animals finished this task, the number of trials taken by each animal for each problem was calculated, rather than escape latency as used in the standard watermaze task.

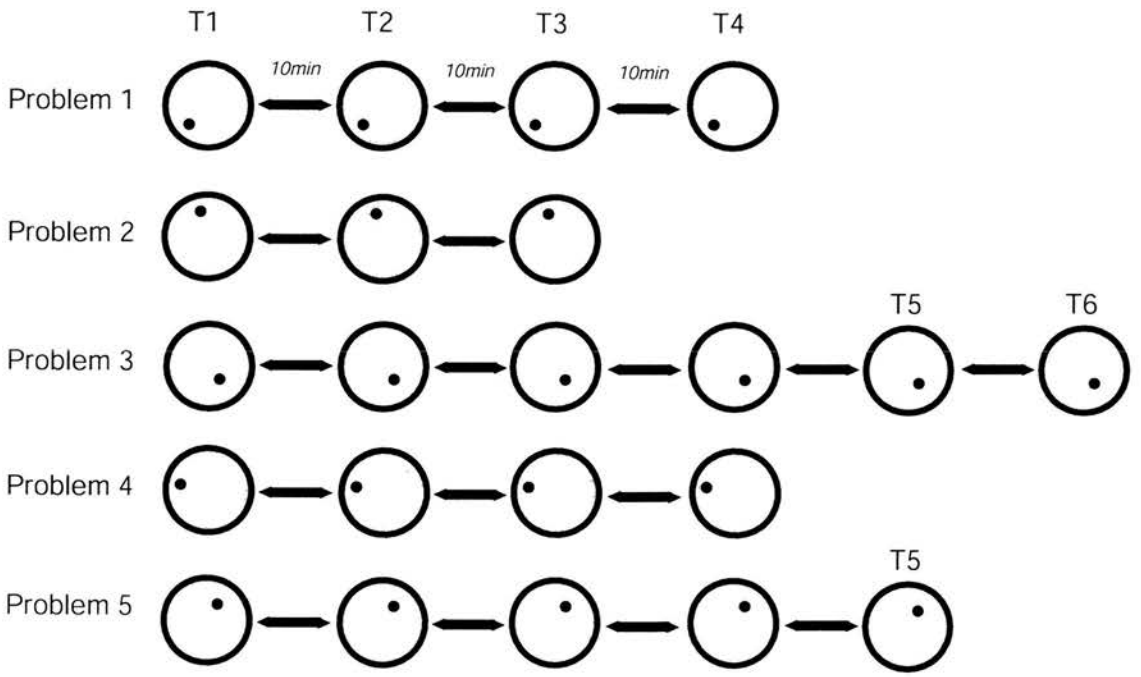

Figure 2.1.4 **Trials-to-criterion Task**. See details from the texts.

The learning rate of this novel watermaze task by each animal reflects the speed with which it acquires new information in successive problems and how fast it forgets old information for previous locations. Accordingly, this task requires animals to change their memory representation in order to solve all the problems. As the learning rate is different in each animal, it is possible to calculate a mean and a variance for a group of mice learning this task. Sometimes, learning failed. Accordingly, an additional criterion was that if a mouse could not reach the criterion for any problem by 32 trials (4 days), it was stopped by Trial 32 on this problem and started learning a new location the next day. In this case, 32 trials would be used as the number of trials to reach criterion for this problem in calculating the mean.

2.1.7 The learning capacity version of DMP.

The form 'learning capacity' is used to capture a measure of how much the mice could learn in a given time. Strictly speaking, it is not a measure of absolute capacity but only of capacity per unit of time. The design for this task is slightly different from the trials-to-criterion, in which all 5 consecutive problems had to be learned by all animals, no matter how many days to be taken. In this task, the mice were given 10 days to learn as many platforms as they could, so the duration of this task was 10 days (Fig.2.1.5). Procedurally, the task is identical with respect to what happens in the watermaze. The platform location was changed only after a mouse reached the performance criterion (average escape latency for three trials in a row being less than 20 s). The maximum number of trials of every day for each mouse was again 8, and this number also varied from 1 to 8 from mouse to mouse. The maximum number of trials for any mouse to learn any problem was 32. The ITI was always 10 min. At the end of day 10, the number of problems learned by each animal was calculated as learning capacity. As there were a maximum of 10 different problems (locations) to be learned in this task, the total number of problems learned by each mouse varied as a function of the individual learning ability of such mouse.

The trials-to-criterion and learning capacity versions of DMP are not totally independent tasks, and they should be viewed as part of the serial spatial learning task. However, as they have been conducted separately in Chapters 3 and 4, the names of the trials to criterion task (for the **trials to criterion version of DMP**) and learning

capacity task (for the **learning capacity version of DMP**) were used throughout the thesis.

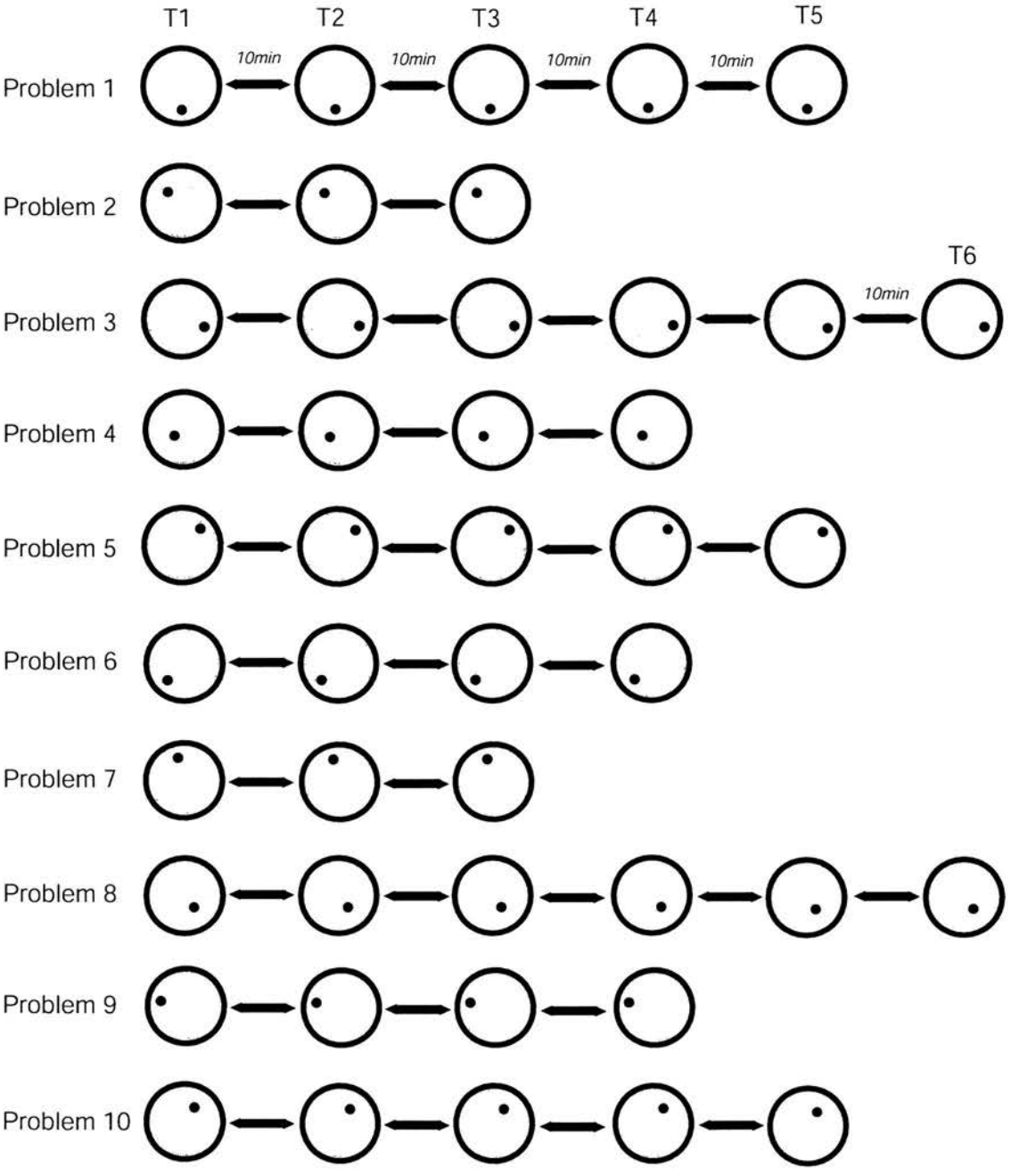

Figure 2.1.5 Learning Capacity Task. 10 different platform locations are set. The animals use 10 days to learn as many locations as they can.

2.2 Spontaneous object recognition test.

2.2.1 The object recognition arena.

The object recognition task was first introduced by Enaceur et al in 1988 (Ennaceur and Delacour, 1988; Ennaceur et al., 1989). Due to its simple methodology, it has

been widely accepted since its first introduction (Tang et al., 1999; Chen et al., 2000; Malleret et al., 2001; Dodart et al., 2002). It is sometimes called spontaneous object recognition as no training is involved.

The object recognition arena with sloping walls is 50 cm long, 50 cm in wide and 40 cm high. The floor of the arena is covered by 1 cm of sawdust. It is made of plywood and painted white. The arena is placed 60cm above the floor of the laboratory room and is enclosed with white curtains. Exploratory behaviour is monitored via a video camera 1.5 m above the arena with the video signal recorded by a video recorder. Exploration time for each object is calculated using a Labview-based program for timing (written by Patrick Spooner on a PC). This PC timer software can calculate time spent in each object by a mouse and the preference index (PI = time spent in exploring the novel object/total exploration time*100).

2.2.2 The habituation in the arena.

The object recognition task consists of habituation and two test phases. For habituation, each mouse was placed in the empty arena (Fig. 2.2.1) for 5 min/day for 5 days, or 10 min/session, two sessions/day for 2 days. For the latter case, the inter-session interval was 3 hours. The bedding of sawdust was changed every day.

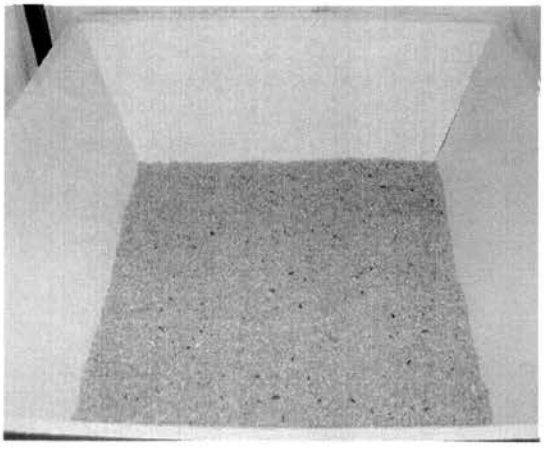

Figure 2.2.1 The Arena

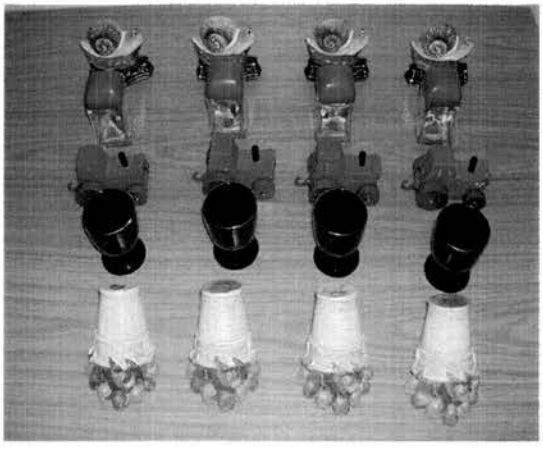

Figure 2.2.2 Five Sets of Objects

2.2.3 The sample phase of the task.

After 1 week or 2 days of habituation (used in different procedures), all mice received object recognition tests for five days. Five different retention intervals were chosen to test immediate, short-term and long-term object recognition memory. There were five

sets of different objects available for this task (Fig.2.2.2). On every testing day, the object recognition test consisted of a sample phase and a choice phase. In the sample phase (Fig.2.2.3), two identical objects, 10-15 cm in height were first placed into the arena at two fixed locations, about 10 cm away from the corner of the arena. A mouse was then released facing the opposite wall of the objects and allowed to explore these two objects until it had accumulated 30 s of total exploration time. The exploration was scored only when the mouse was within 1 cm of the object and was sniffing, licking, touching, pushing or even biting the objects. Staying or sitting on the objects without moving was not considered as active exploration. Once the 30 sec of exploration time was reached, the mouse and the objects were removed from the arena immediately. The objects were then cleaned with 90% alcohol.

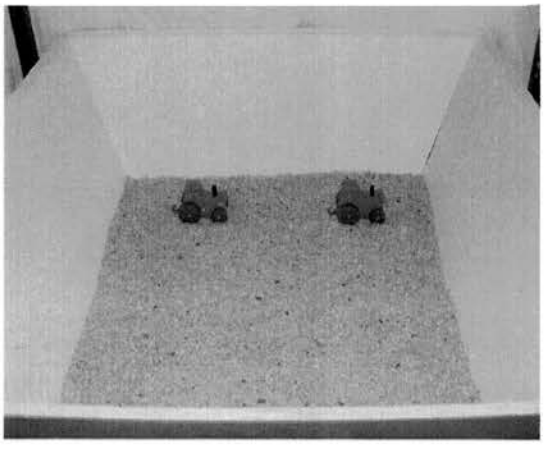

Figure 2.2.3 Sample Phase

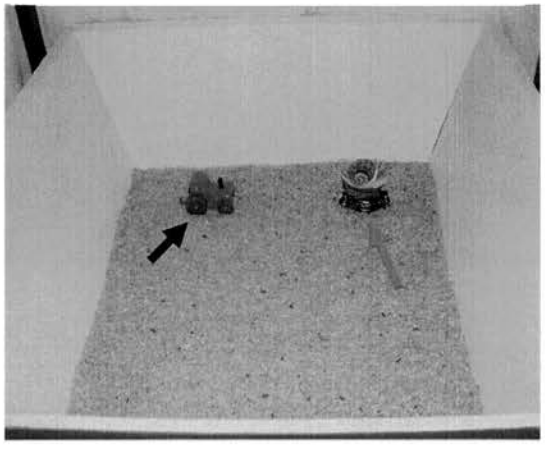

Figure 2.2.4 Choice Phase

2.2.4 The choice phase in the arena.

After any one of 5 different intervals (10s, 1min, 10min, 1h or 4h) from sample phase, a third copy of the earlier familiar objects (the TRACTOR as shown by black arrow in Fig.2.2.4) used in sample phase was placed into the arena at one location and a novel object, which did not appear in the sample phase, like the SNAIL as shown by red arrow in Fig.2.2.4, at the other position. Once the interval elapsed, the mouse was then taken back to the arena from its home cage and released again facing the opposite wall. The choice phase was stopped once 30s of exploration time had again accumulated. After the choice phase was completed, the objects and the animal were taken away from the arena and the objects were cleaned with 90% alcohol. Finally, a

preference index (PI) was calculated using the formula PI = 100 x (Novel Object Exploration Time)/30.

2.3 Electrophysiology.

2.3.1 The in vitro hippocampal slice.

The brain slice *in vitro* electrophysiology has become a standard tool to investigate the physiological or pharmacological features of neurons as well as neuronal circuits since it was first developed in 1966 (Yamamoto and McIlwain, 1966; Yamamoto and Kawai, 1967; Bliss and Richards, 1971). The *in vitro* slice electrophysiology technique provides several attractive advantages: first, the recording environment, such as the incubating solution and temperature, is very easy to control; second, even with low-power microscope, the anatomical structures of hippocampal slices are visibly clear to experimenters; third, one single animal can provide many slices to the experimenters, and so on. Within the hippocampus (Fig.2.3.1 & Fig.2.3.2), there are several distinct cellular areas, such as CA1, CA2, CA3 and dentate gyrus (DG). The entorhinal cortex provides the DG with input via the perforant pathway. The DG sends its projections by mossy fibres to pyramidal cells in the CA3 area. CA3 pyramidal cells project the CA1 pyramidal cells via the Schaffer collaterals pathway in the hippocampus.

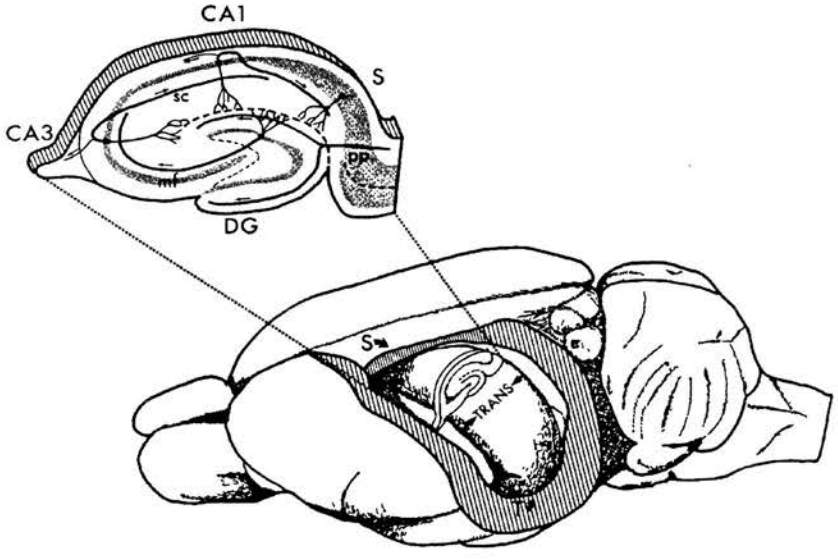

Figure 2.3.1 Hippocampal Slice, Brain and Hippocampus.

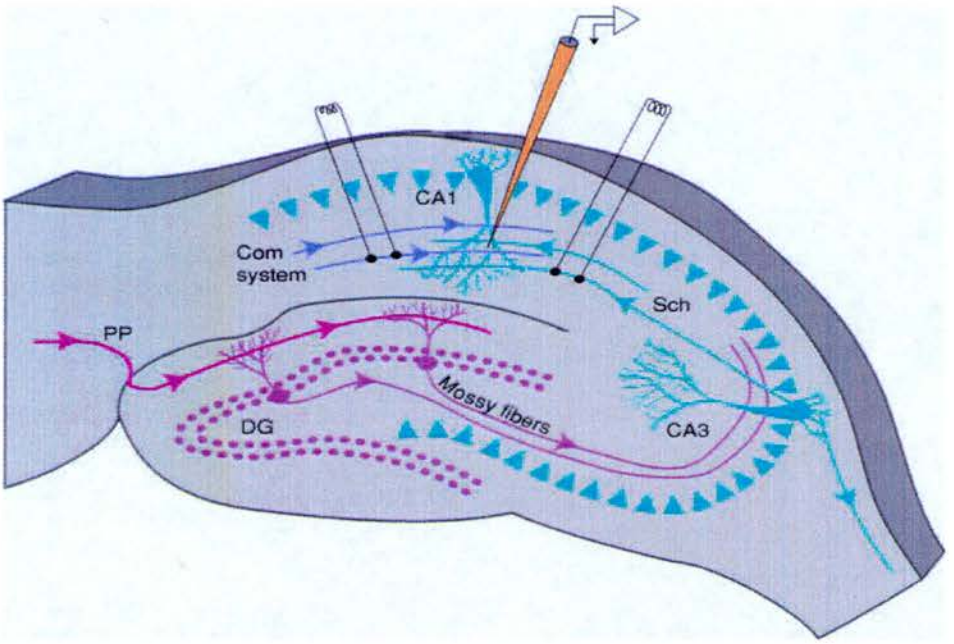

Figure 2.3.2 *In vitro* Technique in Transverse Hippocampal Slice.

2.3.2 Preparation of slices.

For all the electrophysiological experiments, transverse hippocampal slices were prepared by a vibrotome slicer (Campden Instruments, Loughborough, UK) from APP Tg or non-Tg mice at different ages. All animals were singly housed, and were maintained on a 12:12h light: dark cycle, with lights on at 0800 hours. Food and water was supplied ad libitum. Most had participated in behavioural experiments. The artificial cerebrospinal fluid (ACSF) was made up using distilled water filtered (10–18 MΩ/Cm) by the Millipore Milli-Q filter system (Millipore; Molsheim, France). The standard ACSF comprised (in mM): NaCl, 124; KCl, 3; $NaHCO_3$, 26; NaH_2PO_4, 1.25; $CaCl_2$, 2; $MgSO_4$, 1; D-glucose, 10; and was bubbled with 95% 0_2/5% CO_2 (BOC Medical Gasses, UK) to maintain a pH of 7.4–7.5. All chemicals were ordered from BDH Chemicals Ltd., Poole, UK. The ×10 stock medium, from which the fresh ACSF was made, was stored in the fridge, which did not contain either $NaHCO_3$ or D-Glucose, both of which were freshly prepared before experiments. Stock solutions were made every 2 weeks.

The mice were killed by cervical dislocation followed by decapitation in accordance with UK Home Office guidelines (Schedule 1). The brain was rapidly taken out with a

spatula and immediately put into ice cold (0–4°C) ACSF bubbled with 95% O_2/5% CO_2 for at least 10 minutes. In order to keep the temperature of the ACSF in a 400 ml Petri beaker at 0-4°C throughout the dissection process, an aluminium cooling block, which had been kept in the freezer at -20°C for at least several hours, was placed beneath the Petri beaker. After removal of the cerebellum on one piece of filter paper which was placed in a small Petri dish and moistened by the addition of cold ACSF, a big cut was carefully made in the sagittal plane of the brain without the cerebellum, along the midline, to separate the two hemispheres. The right hemisphere of the brain was immediately placed back in ice cold ACSF bubbled with 95% O_2/5% CO_2 for further immunohistological analysis. Using superglue, the left hemisphere was then fixed to a polypropylene block for the subsequent sectioning of 400 μm thick transverse coronal slices by a vibroslicer. The position of the blade in the slicer was adjusted before dissection so that the longitudinal axis of the hippocampus was oriented at 20-30° to the blade. The blade was always submerged in the cold ACSF during dissection. Slices were cut by either manual or automatic regulation of the movement and the position of the blade. Approximately 5-6 transverse slices were cut from the ventral brain. Throughout the whole process of dissection, the chamber, which contained the brain and slices, was fulfilled with ice cold ACSF, so that the slices were always maintained cold and oxygenated. After dissection, the first 2-3 slices were discarded, and the others, from which the cortical and midbrain parts were cut away, were transferred to incubation wells in a plastic beaker containing cold, and oxgenated ACSF at room temperature (18–24 °C).

2.3.3 The recording chambers.

Fig. 2.3.3 shows the set-up for recording chamber. Two different types of recording chambers have been widely used for LTP experiments in different laboratories, the submerged and the interface chamber. They have constituted the standard recording methods for in vitro electrophysiology. The main difference between the submerged and interface chamber was that nylon mesh was taken out from the central compartment for the submerged recording (Fig. 2.3.3). Without the nylon mesh, slice was sitting at the bottom of the recording chamber and was held by two silver grids, so it was completely covered by the oxygenated ACSF, which flowed at 1ml/min. There are several advantages in submerged recording. For example, the ACSF flows

completely through the slice and can allow pharmacological molecules to enter the slice thoroughly and therefore interact with their targets very fast and easily. As the temperature for this chamber is easier to control and can be maintained constantly, this makes the recording more stable, especially for the recording of late-phase LTP (>3hr) or late LTP (>6hr). The condensation problem, which happens very often in the interface recording, does not occur in this case, as the recording electrode is already deeply in the ACSF medium. However, the major problem found for the submerged recording was that the size of the evoked fEPSP was very small for either PDAPP or non-Tg mice (PhD thesis by Urania Coumis, the University of Edinburgh). The possible reason is that the surrounding solution of the recording electrode shunted the current and also magnified stimulus artefacts. It was also found that, the surface of the slice was not easy to see when placing the electrodes (pilot study by myself).

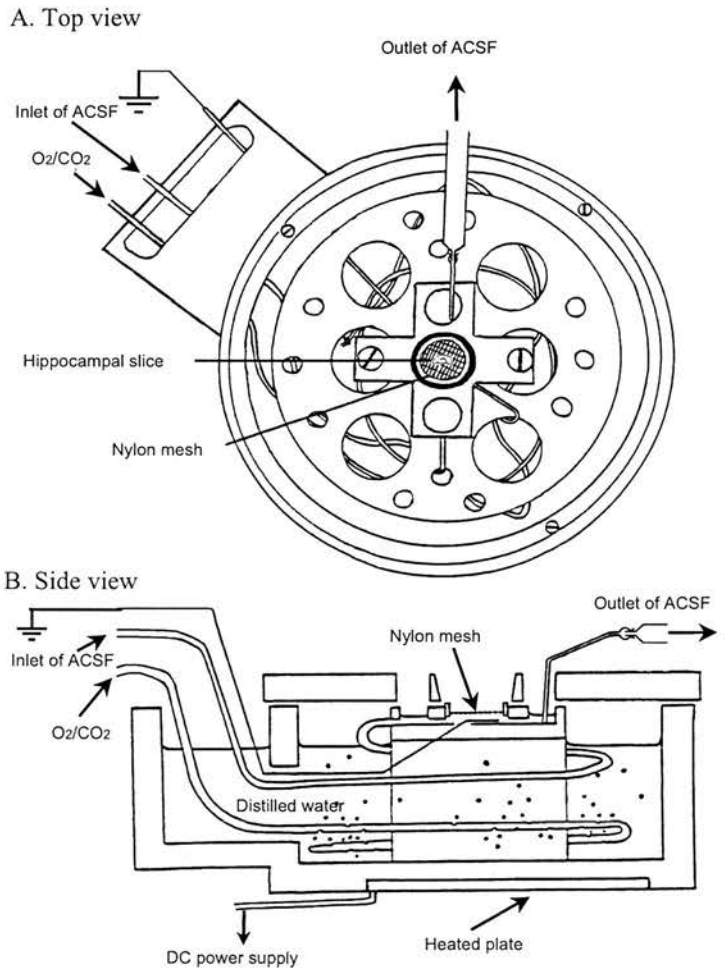

Figure 2.3.3 Design of The Interface Recording Chamber.
Schematic representations of the recording chamber as viewed from above (A) and from the side (B).

Due to these problems, the submerged chamber was modified to the interface one (Spencer et al., 1976). In this case, the nylon mesh was fixed tightly in the small recording chamber, so the slices sat on the mesh. The top surface of the ACSF medium in the recording chamber was just slightly above the level of the mesh, so the ACSF (1ml/min) can only flow slowly through the slices, which were maintained at the interface between a layer of slow flowing ACSF and a layer of humidified 95% O_2 / 5% CO_2 gas. This type of chamber was found to be very advantageous especially in conducting electrophysiology in Tg animals. For example, the surface of the slice was very visible under the low-resolution microscope when placing electrodes. More importantly, this design produced much bigger responses after delivering stimuli. Although the condensation was observed during the recording, it did not become a disaster as no long-term experiments were performed.

The whole recording system, supplied by Scientific Systems Design Inc., UK, consisted of an outer water bath with two tightly fixed thick platforms on which the tri-compartmental recording chamber was securely mounted (Fig.2.3.3 and Fig.2.3.4). The outer water bath was normally about 70% filled with distilled water. Using a peristaltic pump (Watson-Marlow, England), the oxygenated ACSF was pumped into the first compartment (or well) of the recording chamber at a constant flow rate of 2 ml/min. The ACSF then flowed around the circumference of this well and slowly entered the recording chamber through a small hole between these two compartments. In this compartment, the ACSF flowed underneath the nylon mesh and also through the slices, finally entering the third well through another hole between the second and the third compartments. In the last well, there was hypodermic suction needle which was connected to pump which finally removed the ACSF from the recording chamber. The peristaltic pump from Watson-Marlow has multi channels. One channel of this pump served as the inflow to drive the ACSF into the recording chamber and another one or two were used as outflow channels to remove the ACSF from the recording chamber. By changing the magnitude of the outlet suction (for example, two outflow channels of the pump could be connected suction tubing), the level of ACSF in the recording chamber could be in balance such that it paralleled with the mesh but would not fully cover the slices later. Using the artists brush, two slices were then transferred from the incubation chamber to the interface recording chamber, where they needed to be maintained for 1h at 32°C. As these two slices were already

incubated for about 30 min in the incubation chamber at room temperature after dissection, the total incubation time was approximately 90 min. The remaining slices kept in the plastic incubation chamber were still viable for at least several hours. If either of the first two slices got damaged by the brush or the quality of recordings from either of them looked bad, it could be replaced at a later time. As the perfusion ACSF was bubbled by 95% O_2 / 5% CO_2 gas, the slices could get the oxygen supply from the solution. But, as ACSF is a poor carrier of dissolved oxygen, the slices needed to obtain extra oxygen from the environment within the recording chamber. This was achieved through the following mechanism. In the base of the outer water bath filled with water, there was a ceramic bubbler which passed the 95% O_2/ 5% CO_2 gas into water. By carefully adjusting the height of the covering lid of the outer bath, it could allow an oxygenated and humidified atmosphere to fulfill the entire recording chamber.

Figure 2.3.4 Incubation of Hippocampal Slices

(two hippocampal slices are incubated in the recording chamber)

2.3.4 Recording in hippocampal slices.

In hippocampal slices, field potentials can be elicited and recorded postsynaptically when a stimulus is applied to presynaptic fibres. The responses come from a

population of neurons within the area recorded. Normally, the recording position is within the dendritic regions of CA1 pyramidal neurons, i.e. *stratum radiatum*, with stimulations applied to the Schaffer-collateral pathway. The responses from the dendritic region are called the field excitatory postsynaptic potential (fEPSP). Sometimes, action potentials can also be found and recorded from the dendritic areas. The action potentials, also called population spikes, are recorded simultaneously and are superimposed each other. From the stratum radiatum of CA1 neurons, the fEPSP is always negative, when a stimulus is applied to the Schaffer-collateral pathway, suggesting an inward current associated with dendritic synaptic activity.

All electrodes were mounted on mechanical manipulators (MB-K, Narishige, Japan) which allowed three-dimensional movement in the *x*, *y* and *z* axes. For the recording electrode, an additional hydraulic manipulator (MB-K, Narishige, Japan), which can do fine movement, was used to allow increased sensitivity when moving the electrode into slice. In order to make fine placement of electrodes into the slice, an overhead dissecting angle microscope (M3C, Leica, England) and a cold light source which was projected from above onto the slices were used to view the slice. All the recording and stimulating electrodes were placed, at about a 45° to the vertical, in *stratum radiatum* (CA1 pyramidal cell apical dendritic layer) of the hippocampal slice.

The Schaffer collateral-commissural fiber input to CA1 pyramidal neurons were orthodromically stimulated using bipolar stimulating electrodes which were placed on the surface of the slice in *stratum radiatum*. The stimulating electrodes consisted of two 50 μm diameter Formvar insulated nickel-chromium (80%:20%) wires (Advent Research Materials Ltd., England) twisted together and cut at the end to provide a focal stimulation. Stimuli were produced by constant voltage isolated stimulator boxes (DS2A, Digitimer, England) (for the longitudinal and vaccination studies described in this thesis) and constant current isolated stimulator boxes (NL800, Digitimer, England) (for the PS1 and γ-secretase studies described in this thesis). The timing and duration of test stimuli (biphasic square-wave pulse, pulse half-width 0.1 ms, ranging from 0-100V for DS2A or 0-100μA for NL800) were controlled by Neurolog. The stimuli were delivered homosynaptically at a fixed intensity every 30 sec.

For the longitudinal and vaccination studies, recording electrodes were made from thick walled (internal diameter: 0.69 mm; outer diameter: 1.2 mm) borosillicate glass capillaries with an inner filament (120F-10, Clark Electromedical Instruments, England), by a horizontal Flaming-Brown P-97 micropipette puller (Sutter Instruments Co., USA). The recording electrode was filled with 3M sodium chloride (NaCI) with resistance ranging from 1 to 5 MΩ. Before recording, this electrode was mounted into electrode holder (Clark Electrochemical Instruments, England) in which a silver chloride coated silver wire made a tight contact with the NaCI solution within the recording electrode. This holder was then inserted into the head stage (current gain x 0.1 or x 1.0: Axon Instruments, CA, USA) and connected to an Axoclamp-2B amplifier through the microelectrode 1 (ME1) port for use in "bridge balance" mode. The reference electrode, a silver wire, submerged in the recording chamber, was also connected to the head stage and grounded through the Axoclamp amplifier. Synaptic potentials recorded through the ME1 port on the Axoclamp-2B amplifier were amplified 10 fold by an in-built gain. In DCC mode the amplifier set the sample rate (3–5 kHz switching frequency). Signals above 1–3 kHz were filtered, using a low-pass filter, which did not noticeably affect the waveform of the synaptic potentials. Secondary amplification of synaptic responses was provided by variable gain DC amplifiers (Neurolog, Digitimer, England). The output signals were then digitally filtered through a Digidata 1200 interface (Axon Instruments Ltd.) connected to a PC (Dell, Texas, USA) (Fig. 2.3). In LTP experiments, a program called LTP (Version 1.14J) was used to record and analyze data (written by William Anderson, University of Bristol, http://www.ltp-program.com/Ltp114j).

For the PS1cKO;APP and ELN44989 studies, due to an upgrade of the recording system in the lab, the old recording system was replaced by a new AM recording system. The old LTP recording software, LTP114J, was based on a DOS interface, so it was also upgraded by new labview-based LTP software. After upgrade, field EPSPs were recorded with a monopolar stainless steel electrode with a 250 μm tip diameter, tapered at 12°, with a resistance of 5MΩ (AM Systems Inc. USA). The reference electrode in the recording chamber was connected to the ground wire. Field EPSPs were amplified, filtered at 5k Hz (1700, AM Systems), sampled at 10k Hz, and then

stored onto a PC computer. The waveform and amplitude of the fEPSP (mV) was monitored by labview-based LTP software written by Patrick Spooner (Division of Neuroscience, the University of Edinburgh). On-line or off-line analysis of the fEPSP slope (mV/ms) was made by the same software. The slope of fEPSP was measured by linear regression between the 10% and the 90% of the peak response of fEPSP curve. Two stimulating electrodes were placed in the Schaffer-collateral pathway of the *stratum radiatum*. Each stimulating electrode was approximately 200μm distant from the recording electrode, so they stimulate independent synaptic populations in Schaffer-collateral pathway. The maximum fEPSP response was judged after measuring the input/output curve (I/O curve). Single biphasic pulses (0.2 ms in width) were applied to the slice by each stimulating electrode, once every 30 sec, at intensities ranging from 10-100μA (10μA, 20μA, 30μA, 40μA, 50μA, 60μA, 70μA, 80μA, 90μA and 100μA). The maximum response was induced by a pulse at an intensity of 70-100μA. In all the electrophysiology experiments, the intensity of test stimulation was set to evoke a response, the amplitude of which was ~50% of the maximum response found from the I/O curves. Normally, the half size of the maximum fEPSPs was between 0.8 and 1.5mV. To measure paired-pulse facilitation (PPF), four different inter-pulse intervals (IPIs), such as 25ms, 50ms, 100ms, and 200ms, were used.

For long-term potentiation (LTP) experiments (the longitudinal study), stimuli were delivered by alternating between 2 independent Schaeffer collateral-CA1 pathways, one being the test and the other being the control pathway. Each pathway received a stimulus once every minute, so the stimulus interval between the two pathways was 30 s. During a baseline period (30 minutes duration), if the slope of the fEPSP for both pathways increased or decreased by >20%, the recording was stopped and the stimulus intensity was adjusted by either reducing or increasing the value of intensity which elicited a half size of maximal response. In any experiment for LTP, if the time taken to get a stable baseline of LTP exceeded 2 hours, the slice was discarded and, another slice from the incubation chamber was used to get a new LTP recording. LTP was induced in the testing pathway by theta-burst stimulation (TBS) of 3 trains (2min intertrain interval), each consisting of 15 [200ms inter-stimulus interval (ISI)]×4 pulses (100 Hz). Data were collected by LTP114J and stored on a computer. The

initial slope of field EPSP evoked by stimulation of the Schaeffer collateral-CA1 pathway was analyzed online. Responses in each experiment were normalized to baseline, which was defined as the mean value obtained in at least 20-minute responses before TBS. A 20-minute stable baseline comprised of successive field EPSP slopes that differed no more than 15 %. At this point, TBS was delivered to the slice and the recording of EPSPs was continued for 1–4 h depending on the LTP induction protocol employed.

2.3.5 Analysis of data.

In the I-O curves, at each stimulus intensity, the synaptic responses were averaged from three successive responses; In the LTP experiments, 6 fEPSPs were averaged in a two-minute period. Averaging six responses could reduce noise (variance of response). Pooled data were presented as means ± standard error of the mean (SEM.) and statistical significance was assessed using Students *t*-test. $P < 0.05$ indicates statistical significance.

2.4 Immunohistology and Enzyme Linked ImmunoSorbent Assay (ELISA).

2.4.1 Brain tissue preparation for quantitating APP and Aβ.

After the brain was removed during hippocampal slice preparation, the first 6 brain slices from one hemisphere were prepared for in vitro slice electrophysiology. The remaining brain tissue from this hemisphere was used for immunohistochemical analysis. In the mean time, from the other hemisphere of the same brain, three brain areas, including the cerebellum, hippocampus and cortex, were dissected and used for Aβ ELISA measurements.

The procedures of tissue preparation consisted of: 1) the dissections for three brain regions mentioned above were performed on a piece of filter paper (Whatman 3 mm) dampened with ACSF placed on top of an ice-cold aluminum block (an upside-down micro test tube stand from Micro-Metric Instrument Co., FL, USA); 2) each region was placed into a pre-weighed homogenization tube (Kontes Microtubes, Fisher, USA) and kept on ice; 3) the tubes were weighed with the tissue on a balance after wiping off any excess moisture from the ice on the outside of the tube prior to

weighing; 4) the volume of 5M guanidine buffer (5.97g guanidine; 7.5ml sterile water; 0.625ml Tris; more sterile water was added to 12.5ml) to add to each tube was determined by subtracting (tissue+tube) from (tube alone) and multiplying the tissue weight (mg) by 10 to obtain the volume of guanidine buffer in microlitre (μl) to be added to the tube; 5) 200 μl of guanidine buffer or less was added to each tube. If the tissue weight was less than 20 mg, the appropriate volume of 5M guanidine buffer was added to each tube for homogenization; 6) the tissue was completely homogenized with a hand-held homogenizer (Kontes motorized pestle, Fisher, USA); 7) the remainder of 5M guanidine buffer was added to each tube. For the cortical samples, it was always best to add another 200 μl as cortical tissue is often heavier than 20 mg, and the homogenization procedure repeated, and finally the remainder of the 5M guanidine buffer was added; 8) once all the samples were processed, the tubes were gently agitated on a Nutator (Adams Nutator, Fisher, USA) for 3-4 hrs at room temperature and stored at -20 °C until assayed for APP and Aβ levels.

2.4.2 3D6 immunohistology.

The tissue was prepared during slice dissection for electrophysiology. One hemisphere of the brain for each mouse was dropped into 4% formaldehyde and post-fixed for about one week. After 1-week fixation, the following immunohistological procedures were all carried out by Ms. Jane Knox. The tissue was mounted coronally and cut at 30μm sections using a vibratome. Every fifth section from the posterior cortex through the hippocampus was collected in multiwells filled with antifreeze solution (30% glycerol/30% ethylene glycol in 40 mM NaPO4) and stored at -20°C in freezer before immunostaining. On day 1 for staining, 1) wash sections for twice, 10 minutes each, using phosphate buffer saline (PBS); 2) put sections in 4.5 ml PBS with 30%H_2O_2 and 50 μl Triton-X-100 for 20 minutes; 3) wash sections in PBS for twice, 10 minutes/each; 4) make up 1% horse serum in PBS; 5) add primary antibody 3D6 at 1:500; 6) incubate sections in fridge overnight. On day 2, 1) make up AB kit (horseradish peroxidase-avidin-biotin complex (Vector Laboratories)) with two drops of A + 5 ml TBS + two drops of B. This was done 30 minutes before use; 2) wash sections for twice, 10 minutes/each, in PBS; 3) incubate sections for 30 minutes with AB at room temperature; 4) wash sections in PBS for twice, 10 minutes/each; 5) make up diaminobenzidine (DAB) kit using 5 ml distilled water. 6) develop the sections in

DAB for 40 seconds; 7) wash sections in distilled water; 8) mount sections on Superfrost charged slides; 8) dry, dehydrate, clear and mount sections with Fluoromount.

2.4.3 Aβ load quantification.

This part of work was conducted by Dr. Jennifer Inglis and Ms. Jane Knox. Amyloid deposition was quantified automatically using a Leica Q-Win image analysis system. Video images of the brain were captured, and the area of the hippocampus was outlined and a threshold optical density was obtained that discriminated staining from background. The amyloid `plaque burden' was defined as the average percentage of hippocampal area covered by amyloid depositions over six sections.

2.4.4 ELISA measurements for Aβ.

The ELISAs were carried out by our collaborators, Karen Chen and Dione Kobiyashi, in Elan Pharmaceuticals, but the methods are described as follows. The brain homogenates were further diluted 1:10 with ice-cold casein buffer (0.25% casein/0.05% sodium azide/20 μg/ml aprotinin/5 mM EDTA, pH 8.0/10 μg/ml leupeptin in PBS) before centrifugation (16,000 × *g* for 20 min at 4°C). The Aβ standards (40 or 42) were prepared such that the final composition included 0.5 M guanidine in the presence of 0.1% bovine serum albumin (BSA).

The total Aβ sandwich ELISA consisted of the capture antibody 266, which was specific to amino acids 13-28 of Aβ, and the biotinylated reporter antibody 3D6, which was specific to amino acids 1-5 of Aβ. The 3D6 antibody did not recognize secreted APP or APP-FL but detected only Aβ species with amino-terminal aspartic acid. The assay had a lower limit of sensitivity of ~50 pg/ml (11 pM) and showed no crossreactivity to the endogenous murine Aβ peptide at concentrations up to 1 ng/ml.

The Aβ42-specific sandwich ELISA used the capture antibody mAb 21F12 ($A\beta_{33\text{-}42}$). Biotinylated 3D6 was the reporter antibody in this assay, which had a lower limit of sensitivity of ~125 pg/ml (28 pM). An $A\beta_{x\text{-}42}$ sandwich ELISA, using 266 as the capture antibody and biotinylated 21F12 as the reporter antibody, was used on a subset of brain homogenates. The low end sensitivity of this assay is ~250 pg/ml (56 pM). The 266 and 21F12 mAbs were coated at 10 μg/ml into 96-well immunoassay plates

(Costar) overnight at room temperature. The plates were then aspirated and blocked with 0.25% human serum albumin in PBS buffer for at least 1 hr at room temperature, then stored dessicated at 4°C until use. The plates were rehydrated with wash buffer (0.05% Tween 20 in tris-buffered saline) before use. The samples and standards were added to the plates and incubated at room temperature for 1 hr. The plates were washed three or more times with wash buffer between each step of the assay.

The biotinylated 3D6, diluted to 0.5 μg/ml in casein assay buffer (0.25% casein/ 0.05% Tween 20, pH 7.4, in PBS), was incubated in the wells for 1 hr at room temperature. Avidin-horseradish peroxidase (Vector Laboratories), diluted 1:4000 in casein assay buffer, was added to the wells for 1 hr at room temperature. The colorimetric substrate, Slow TMB-ELISA (Pierce), was added and allowed to react for 15 min, after which the enzymatic reaction was stopped with addition of 1 M H_2SO_4. Reaction product was quantified using a Molecular Devices Vmax spectrophotometer measuring the difference in absorbance at 450 nm and 650 nm.

Chapter 3: A Cross-sectional Investigation of Age- and Plaque-related Learning Deficits in PDAPP Mice.

3.1 Introduction.

The purpose of this first experiment was to use three cohorts of naïve PDAPP mice at three different ages to investigate plaque- and age-related cognitive impairment.

3.1.1. Early studies on APP Tg mice failed to reveal plaque-related learning deficit.

The APP751 (or SciosNova) mouse was the first APP Tg model of AD (Quon et al., 1991). Created in 1991, immunohistological and behavioural analysis was not conducted until 1995, revealing the age-related formation of diffuse plaques, but not neuritic plaques (Higgins et al., 1995), and an age-related behavioural deficit in spontaneous Y-maze alternation and an age-independent deficit in spatial learning (Moran et al., 1995). These findings indicated that overexpression of wildtype (WT) human APP could impair learning.

Historically, a learning deficit in APP Tg mice was first reported as early as 1991. This was found using the so-called Cambridge mouse, in which a mouse metallothionein II promoter was used to overexpress human WT APP695 (Yamaguchi et al., 1991). Although no mRNA and protein expression data were published, a cohort of animals aged 8-20 weeks were tested in the watermaze. Only a subtle deficit in the initial performance of Tg mice was observed, but no difference from non-Tg mice during the later days of reference memory training. No pathological changes, such as amyloid deposition, were reported in the same mice used for the behavioural test. It is difficult to know what to make of these findings, but a possible link between overexpression of WT human APP and a subtle impairment of spatial learning in APP Tg mice was hinted.

Between 1991 and 1995, several different APP Tg mouse lines, all of which overexpress either full-length or C-terminus of APP using different promoters, were reported. They all expressed WT human APP at a level equivalent to the endogenous mouse APP but did not develop any neuritic plaques in the brain (Kawabata et al., 1991; Kammesheidt et al., 1992; Kawabata et al., 1992; Fukuchi et al., 1993; Lamb et

al., 1993; Fukuchi et al., 1994; Greenberg et al., 1996). Behavioural studies indicated that most of these Tg lines display early learning deficits prior to plaque deposition, suggesting that APP metabolites, such as APP CTF and Aβ, may be responsible (Nalbantoglu et al., 1997; Sato et al., 1997; Berger-Sweeney et al., 1999).

3.1.2. A standard reference memory task in the watermaze may not be sufficiently sensitive to reveal plaque-related learning deficit in APP Tg mice.

Using a β-chain promoter of PDGF and a human APP gene containing the Indiana mutation, Games et al reported the first plaque-producing Tg rodent, the PDAPP mouse (Games et al., 1995). Importantly, the PDAPP mouse displays AD-like pathology such as Aβ accumulation, diffuse and neuritic plaques, microgliosis and astrocytosis in an age-dependent manner (Games et al., 1995; Irizarry et al., 1997; Johnson-Wood et al., 1997). Preliminary behavioural characterization of PDAPP mice was conducted by Justice et al (former Athena Neuroscience) and Ramsay (MSc thesis, Edinburgh University). Using a standard reference memory task in the watermaze, Justice et al observed an age-independent learning deficit, unrelated to plaque deposition (Justice and Motter, 1997). Ramsay et al employed a DMP task in the watermaze (Steele and Morris, 1999) to test PDAPP mice using a longitudinal design. This longitudinal study also revealed an age-independent learning deficit in PDAPP mice (Ramsay and Morris, 1998). Both findings were surprising and raised issues of task sensitivity.

Shortly after Games et al (1995) reported the PDAPP mouse, a second group successfully generated a plaque-producing Tg mouse line, the Tg2576 mouse, which overexpresses a mutant human APP695 gene with the double Swedish mutations under the control of a prion promoter (Hsiao et al., 1996). The Tg2576 mouse starts the formation of neuritic plaques from 8-10 months of age. It has been reported that Tg2576 mice display both age- and plaque-related learning deficits in a Y-maze alternation and a watermaze reference memory task. In the watermaze, two young groups (2- and 6-month) of Tg2576 mice were found to be unimpaired in acquisition training and the probe test of reference memory. However, older Tg2576 mice (9-10-month) were impaired (Hsiao et al., 1996). The claim of an age- or plaque-related memory deficit in Tg2576 mice has been criticised (Routtenberg et al., 1997), as inspection of the data indicates that the age-related memory deficit was primarily due

to improved spatial memory in old non-Tg mice. Indeed, using Tg2576 mice and a watermaze reference memory protocol, a second group have failed to observe any deficit in spatial learning and memory even at very old ages (14- and 19-month) (King and Arendash, 2002). Recently, Hsiao's group have re-investigated learning and memory of Tg2576 mice and reported a detergent insoluble Aβ-related learning deficit in Tg2576 mice (Westerman et al., 2002). However, due to performance incompetence, about 16-32% of Tg2576 mice were excluded from their final data analysis. The fact that so many mice were excluded in a behavioural study raises questions about the adequacy of the behavioural protocol.

3.1.3. Novel behavioural task to investigate plaque-related learning deficits in APP Tg mice.

The studies discussed above imply that the standard reference memory task in the watermaze might not be sensitive enough to detect a plaque-related learning deficit in APP Tg animals. Chapman et al were the first to report a different behavioural paradigm, a forced choice T-maze alternation task to test the plaque-related learning deficit in Tg2576 mice (Chapman et al., 1999). 2- and 10-month mice were tested in this study. Only the 10-month Tg2576 mice displayed a significantly lower rate of performance than age-matched non-Tgs. This finding suggests that novel behavioural paradigms may be able to dissociate age-related and age-independent learning deficits in Tg animal models of AD.

Dodart et al (1999) tested three different cohorts of PDAPP mice on C57BL/6, DBA/2 and Swiss Webster genetic background at 3, 6, and 9–10 months of age (Dodart et al., 1999). The testing protocols included an object-recognition task, an eight-arm radial-maze spatial discrimination task and a bar-press learning task. In the radial maze task, PDAPP mice displayed a robust age-independent memory deficit. They also showed age-independent deficit in the barpress learning task. However, in the object recognition task, PDAPP mice showed an age-dependent decrease in performance, which was more severe at the age at which amyloid deposition started (Dodart et al., 1999). The same investigators also analyzed neuroanatomical abnormalities in the same mice behaviourally tested (Dodart et al., 2000). An unexpected observation was a 20–40% of hippocampal atrophy in PDAPP mice as young as 3 months. A correlation analysis indicated that the deficit in object recognition was significantly

correlated with the number of plaques in the cingulate cortex, and in CA1, CA3, and dentate gyrus of the hippocampus. However, the deficits in radial-maze spatial learning were unrelated to plaque deposition, but did correlate with the marked atrophy of the hippocampal formation. These results further suggest that novel behavioural tasks may reveal different components of learning deficits in APP Tg mice.

It is believed that brain areas, which are affected at the early stage of AD, are the entorhinal cortex and hippocampus. Studies on the function of the hippocampus have suggested that the hippocampus is implicated in learning and memory (Squire, 1992), or the hippocampus mediates a neuronal representation of space or a cognitive map (O'Keefe and Nadel, 1978). Two seminal studies demonstrated that watermaze spatial training is a task very sensitive to hippocampal lesions in rats (Morris et al., 1982; Morris et al., 1986). More evidence further indicated that hippocampus-lesioned rats are severely impaired when learning new place problems, i.e. reversal locations in watermaze (Morris et al., 1986; Whishaw and Tomie, 1997; Steele and Morris, 1999). A novel delayed matching-to-place (DMP) protocol in the watermaze was first introduced by Morris in 1983 and has been developed later (Steele and Morris, 1999). In the DMP task, there are 4 trials each day at a 10-min ITI. On each trial, once the mice find the escape platform, they are allowed to stay there for 30 s before being taken away from the pool to have a 10 min rest. Normally, the mice exhibit a striking reduction in escape latency between trial 1 of the day and subsequent trials. Once the mice have learned the general strategy of this task, new spatial problems can be tested repeatedly.

In the present study, I modified the general DMP protocol by introducing a performance criterion. Two novel behavioural protocols in the watermaze, 'trials to criterion' and 'learning capacity' were developed. Generally speaking, once the mice were escaping quickly onto the hidden platform at one location and had reliably learned this location by reaching the performance criterion, the platform was moved to a new location. Five successive platform locations were learned by the mice in the trials to criterion task. In the learning capacity task, but only the total number of problems learned by the mice in a 10-day period is counted as a measure of learning capacity. In these two modified DMP protocols, the learning of earlier platform

locations is encoded into long-term memory, which can potentially cause interference with the learning of later problems. In order to perform this task reliably, memory retrieval must be restricted to the most recently encoded information, i.e. the new location. This property of these tasks gives them the character of being ''episodic''. Interestingly, the PDAPP mouse first forms the highest density of plaques in the outer molecular layer of the dentate gyrus and other regions of the hippocampus. So, like AD in humans, the hippocampus is possibly the first brain area to be affected by amyloid plaques in PDAPP mice. As human AD subjects develop impairment in episodic memory, the ''episodic memory-like'' character of the DMP tasks may be particularly suitable for revealing plaque-related cognitive impairment.

3.2 Methods.

3.2.1. The subjects.

All PDAPP mice used in this study were non-white heterozygous males, on a DBA/C57BL/6 double strain background. They were shipped from the former Athena Neurosciences, USA. Three different ages of mice were tested. Young, middle-aged and old groups were 6-9 months (n=50, PDAPP=25, non-Tg=25), 13-15 months (n=29, PDAPP=15, non-Tg=14), and 18-21 months (n=20, PDAPP=9, non-Tg=11) of age. The mice were group-housed (2-4 mice each cage) and had different ear marks so that the experimenter could recognize any individual without problem. The mice were given *ad libitum* access to food and water. The animal room was kept at a temperature of 25 °C and on a 12:12 light dark cycle.

3.2.2. The watermaze.

The watermaze used is 2 m in diameter. The temperature was kept at 25 ± 1°C. The escape platform is 20 cm in diameter and its top surface is 1.5 cm below the water surface. In all testing trials, the animals were placed into the pool by hand but removed by them climbing onto a small paint roller from the platform. During the ITI, the animals were singly housed in an experimental cage with dry paper. The running sequence was organized by Dr. Stephen Martin, so the experimenter was blind to the genotype of the mice throughout the whole duration of the study. The mice were run in squads of 6 mice (3 non-Tg and 3 Tg per squad).

3.2.3. Experimental design.

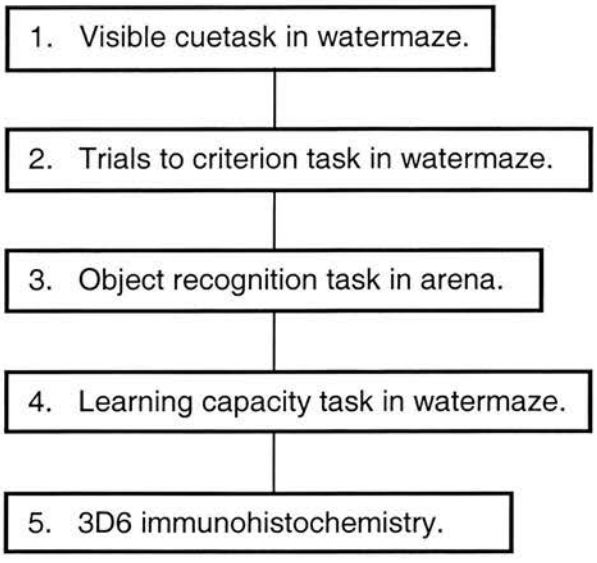

Figure 3.2.1 Experimental Design.

The experimental design is shown in Fig. 3.2.1. PDAPP and control mice were tested on a battery of 4 different behavioural tasks, consisting of (1) cuetask for 5 days, (2) trials to criterion task for 1 to 4 weeks, depending on performance of individual animal, (3) object recognition task for 10 days, and (4) learning capacity task for 10 days. After the behavioural testing was completed, the mice were immunohistologically analyzed for Aβ plaques.

3.2.4. Visible cuetask.

There were 4 trials per day for 5 days and platform location was changed across trials. If any individual mouse failed to learn the cuetask, it was excluded from the study.

3.2.5. Trials to criterion task.

The trials to criterion task consisted of learning 5 successive different hidden platform locations to the strict performance criterion. Once this criterion was met, the mouse was stopped on that day and only started to learn the next platform location on the following day. The mice were trained for up to 8 trials per day and trained for as many days as necessary to learn all 5 different problems. As several animals failed to reach the criterion when learning some of the five locations, the maximum trial number was set to 40 for problem 1 and 32 for problems 2 to 5. For counterbalancing reasons, two different sets of platform locations were arrayed. In these, Problem 1 in

Set A was close to the centre of the pool, but Problem 1 in Set B was close to the wall, and so on. Half of the mice were assigned to receive training using platform locations in Set A and the other half using locations in Set B. Fig. 3.2.2 shows the 2 sets of 5 consecutive platform locations used in this task.

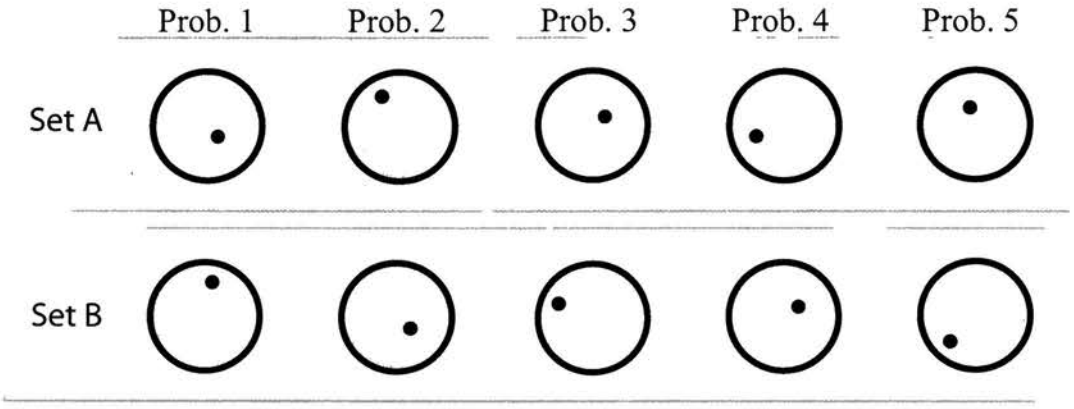

Figure 3.2.2 Two Sets of Five Different Problems. All mice at three different ages were divided into two groups. One group were trained by the platform locations shown on Set A, and the other group were tested by Set B.

3.2.6. Object recognition.

The floor of the object recognition arena was covered by 1 cm of sawdust. Habituation consisted of 5-min period for 5 days in the arena without any object presented. Following 5 days habituation, object recognition test consisting of a sample phase, a retention interval, and a choice phase was given to the mice. In order to examine short- and long-term object recognition memory in the mice, five different retention intervals were used, 10 s, 1 min, 10 min, 1h and 4h. During the interval, the animal stayed in its home cage, and the objects were cleaned with 95% alcohol.

3.2.7. Learning capacity task.

For counterbalancing reasons, two different sets of 10 platform locations were used in the learning capacity task. All mice at 3 different ages were assigned into 2 different groups by Dr. Stephen Martin, so one group received the Set C platform locations and the other one received the Set D. For any individual mouse, the platform position was changed only after the performance criterion was met. Each mouse was trained for up to 8 trials per day. At the end of 10-day training, each mouse was regarded as having a ''learning capacity'' defined as the total number of platform locations learned.

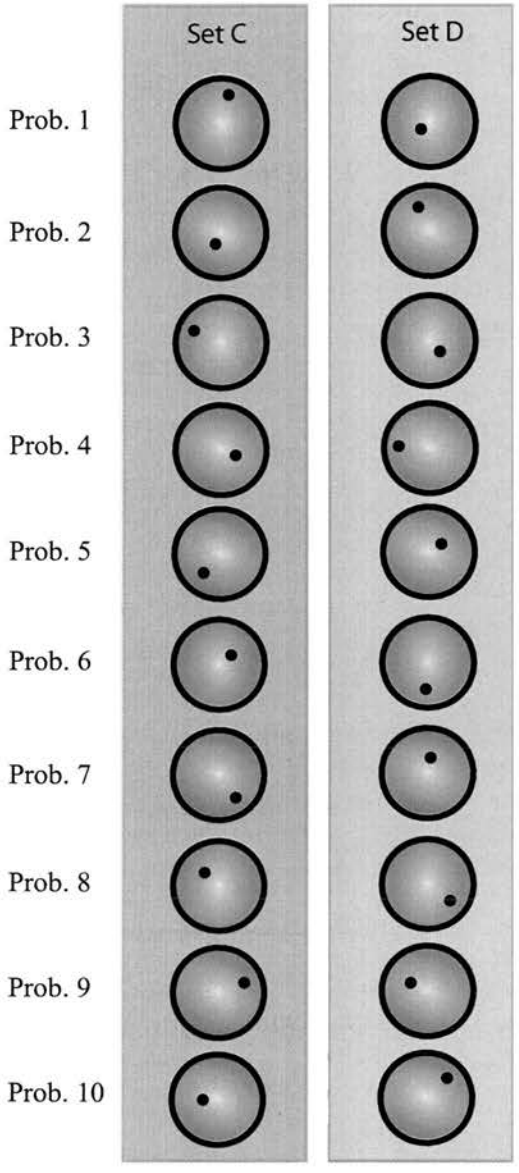

Figure 3.2.3 Two Sets of Ten Different Problems for Learning Capacity Task. All mice at three different ages were divided into two groups. One group were trained by the 10 platform locations shown on Set C, and the other one by Set D.

3.2.8. Immunocytochemistry and plaque load quantification.

After all behavioural training was completed, all middle-aged and old mice, and a subset of young mice (n=12, 6 Tg and 6 non-Tg) were sacrificed to examine the extent of amyloid plaque deposition. The methods for immunocytochemistry and plaque load quantification are given in Chapter 2. The immunocytochemistry was conducted by Ms. Jane Knox and the quantification of plaque burden was done by Dr. Jenniffer Inglis.

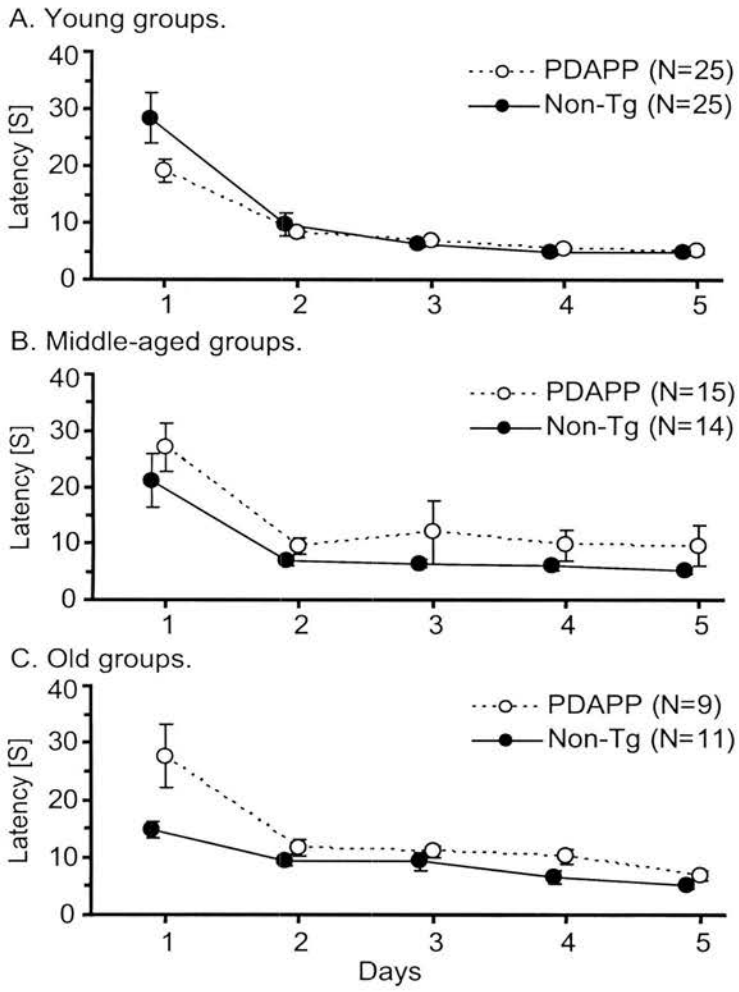

Figure 3.3.1 Cuetask Performance in PDAPP and non-Tg Mice. There was no significant difference between Tg and non-Tg mice at 3 different ages. Cuetask performance in 6-9-month mice (A), in 13-15-month mice (B) and in 18-21-month mice (C).

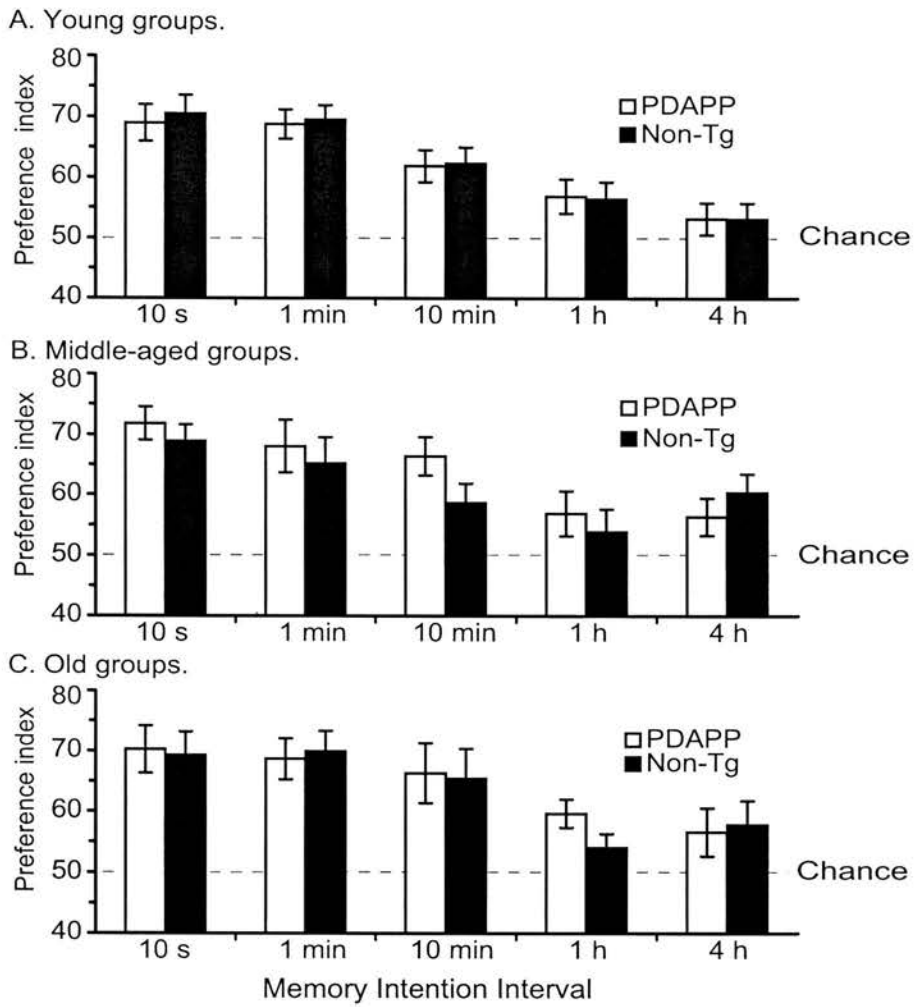

Figure 3.3.2 Normal Object Recognition Memory in PDAPP Mice. Preference index for recognition of a novel object. Chance performance = 50%. PDAPP and non-Tg mice displayed equivalent above-chance performance at 6-9 months (A), 13-15 months (B) and 18-21 months of age (C).

3.3 Results.

1. Normal cuetask learning in PDAPP mice.

The results of cuetask training are shown in Fig. 3.3.1. Statistical analysis revealed no significant genotype effect for all 3 different ages of mice (6-9, 13-15 and 18-21 months) ($F=3.31$, $df1/93$, $p>0.07$). Interestingly, in the old age group (18-21-month), although no significant genotype effect was found ($F<1$), old PDAPP mice displayed a significant impairment on day 1 ($p<0.05$, two-tailed student t-test) as compared to non-Tg mice, suggesting a transient deficit. Overall, old PDAPP mice swam as well as the controls from day 2 to day 5. The mean escape latency was less than 10 s in both non-Tg and PDAPP mice for all 3 age groups after day 1, indicating that PDAPP mice did not display any significant sensorimotor abnormalities.

2. Normal object recognition memory in PDAPP mice.

It has previously been reported that PDAPP mice can display a plaque-related deficit in long-term object recognition memory (Dodart et al., 1999). However, Dodart et al tested their PDAPP mice with a 4 h retention interval only, leaving the presence of short-term object recognition deficits unknown. In this study, several different memory retention intervals were used to investigate both short- and long-term object recognition memory in PDAPP mice. As shown in Fig. 3.3.2, in contrast to the findings by Dodart et al, it seems that PDAPP mice did not display any age-related or age-independent deficits in this task at any memory retention delay. Both PDAPP and non-Tg mice were found to explore the novel object preferentially (Fig. 3.3.2). The analysis of variance revealed gradual forgetting over 4 h ($F=20.8$, $df4/352$, $p<0.001$) but no difference between PDAPP and non-Tg mice at any age (Fig. 3.3.2: $F<1$). Memory for novel objects in both genotypes decayed normally over time (Fig. 3.3.2). The mean performance of both groups was significantly above chance at all retention intervals ($p<0.05$, independent t-test), indicating that PDAPP mice displayed normal short- and long-term object recognition memory.

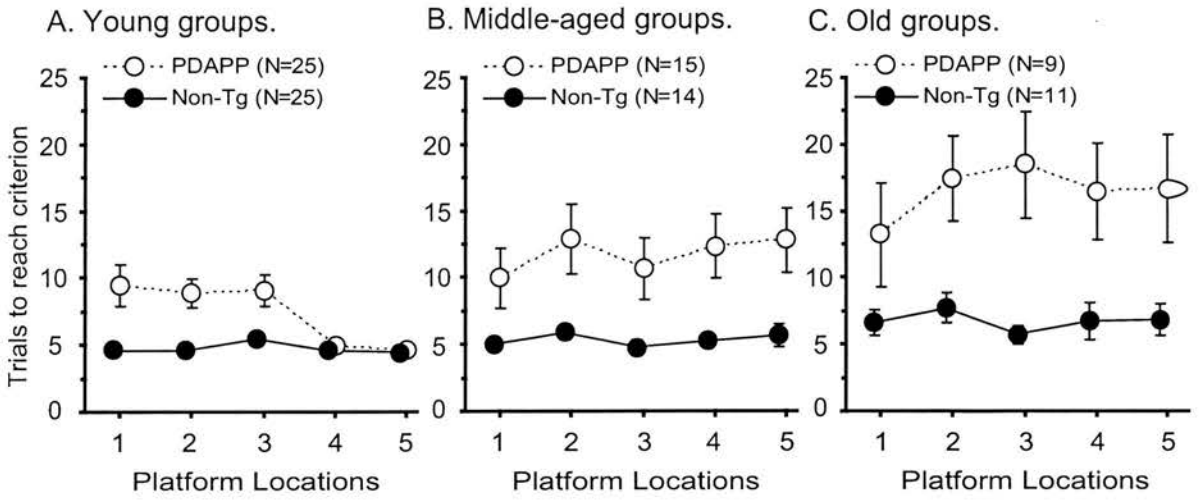

Figure 3.3.3 Early Deficits in Spatial Learning of PDAPP Mice Getting Progressively Worse. Five different platform locations needed to be learned in trials to criterion task. Performance of PDAPP and non-Tg mice at 6-9 months (A), 13-15 months (B), and 18-21 months (C).

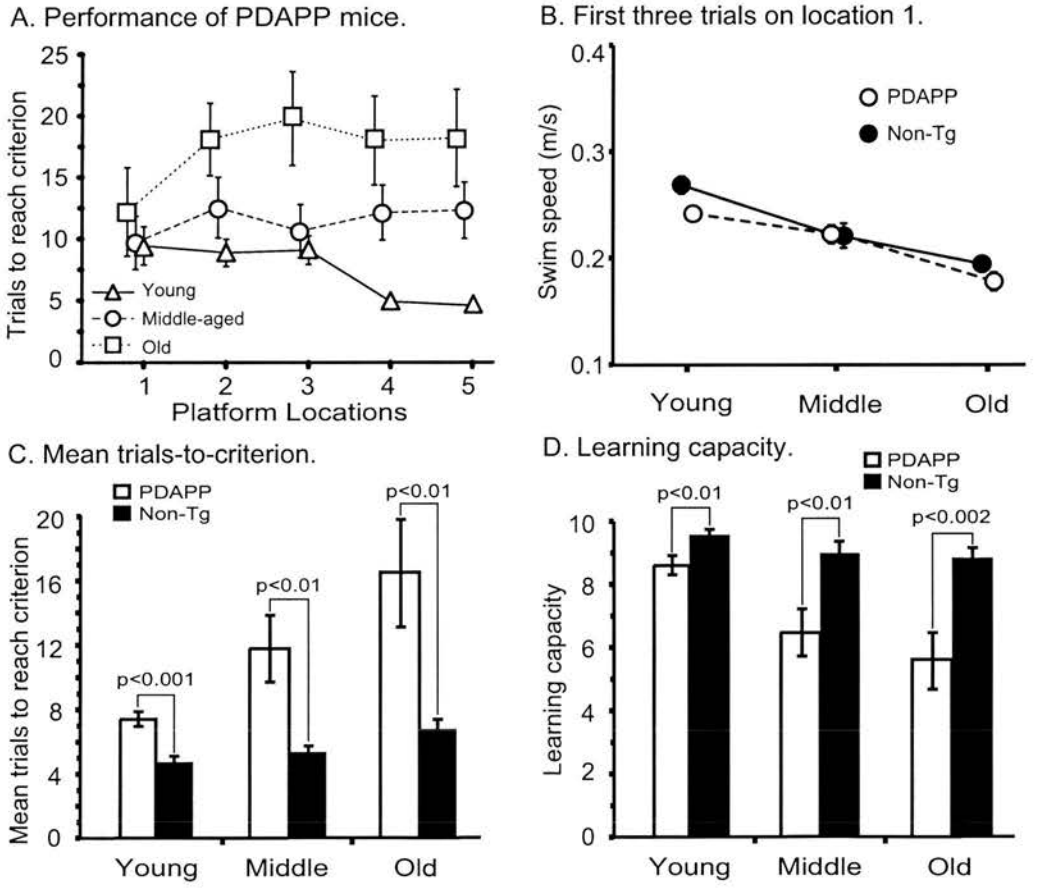

Figure 3.3.4 Age-related Learning Deficit in PDAPP Mice. A. Performance on trials to criterion task by PDAPP mice only. There was a highly significant aging effect. B. There was no significant genotype effect observed in swim speed of PDAPP mice. C. PDAPP mice displayed a significant aging effect as a function of mean performance across five platform locations in trials to criterion task. D. PDAPP mice displayed a significant aging effect in learning capacity task.

3. Early impairment of spatial learning in PDAPP mice getting worse with age.

Figure 3.3.3 shows the performance of both PDAPP and non-Tg mice at 6-9, 13-15 and 18-21 months of age on trials to criterion task. Analysis of variance (Fig. 3.3.3A) showed that young PDAPP mice displayed a significant learning deficit in the trials to criterion task ($F=26.28$, $df1/48$, $p<0.001$), although they could have only developed few plaques in the brain at this age point (Johnson-Wood et al., 1997). Interestingly, the other two groups of older PDAPP mice also displayed severe deficits (Fig. 3.3.3B: $F=10.25$, $df1/27$, $p<0.01$, at 13-15-month; Fig. 3.3.3C: $F=10.97$, $df1/18$, $p<0.01$, at 18-21-month). The observation of early spatial learning deficit in young PDAPP mice was further confirmed when measuring the mean trials to criterion across the five successive platform locations, which represents an overall performance of the mice in this task (Fig. 3.3.4C: $p<0.001$, at 6-9-month). Very consistently, an early learning deficit was also observed in the learning capacity task in young PDAPP mice (Figure 3.3.4D: $F=7.88$, $df1/48$, $p<0.01$), further indicating that young PDAPP mice had already displayed early deficit in spatial learning. Older PDAPP mice also showed significant impairment in the learning capacity (Figure 3.3.4D: $F=9.27$, $df1/27$, $p<0.01$, at 13-15-month; $F=14.36$, $df1/18$, $p<0.002$, at 18-21-month).

However, the analysis above is somewhat deceptive because the overall statistical analysis of variance for the trials to criterion not only revealed a significant genotype ($F=45.61$, $df1/93$, $p<0.001$) and age ($F=12.20$, $df2/93$, $p<0.001$) effect, but also a significant genotype x age interaction ($F=5.26$, $df2/93$, $p<0.01$), which allowed a further separate analysis of the performance by PDAPP and non-Tg mice. Across all 5 successive spatial problems, PDAPP mice displayed a significant aging effect on their performance (Figure 3.3.4A+C: $F=8.32$, $df2/46$, $p<0.002$); the controls did also although, in absolute terms, the aging effect in controls is much more modest (Figure 3.3.4C: $F=7.24$, $df2/47$, $p<0.005$). Figure 3.3.4A clearly shows that young PDAPP mice performed significantly better than both middle-aged and old PDAPP mice. Consistently, in terms of the mean trials to criterion, PDAPP mice again displayed significant aging effects (Fig. 3.3.4C).

Similarly, the learning deficit of PDAPP mice in the learning capacity progressively got worse with age (Fig. 3.3.4D). Statistical analysis of the learning capacity showed a significant genotype effect ($F=37.36$, $df1/93$, $p<0.001$), an age effect ($F=11.92$,

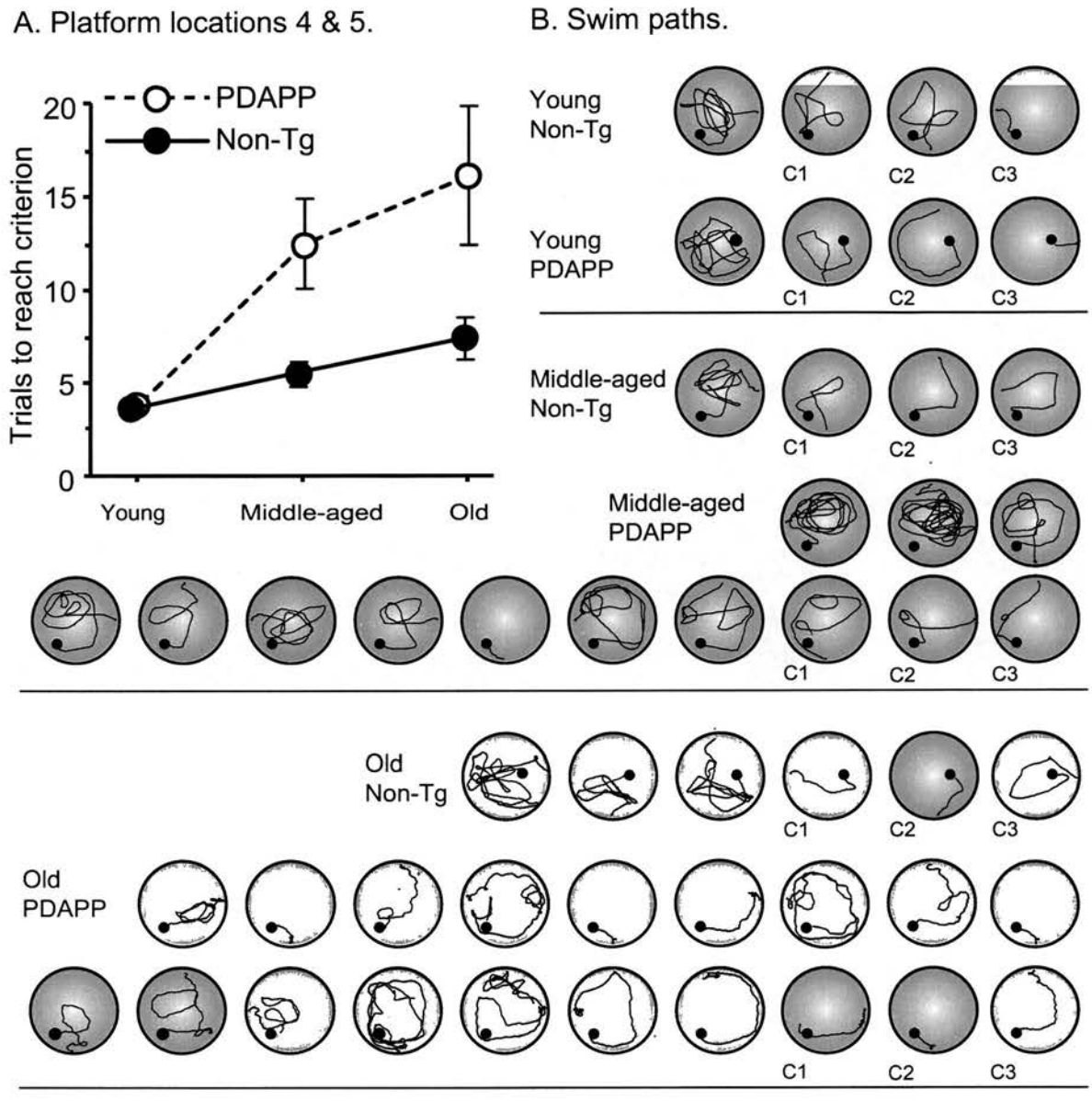

Figure 3.3.5 Age-related Learning Deficits in PDAPP Mice.

A. Age-related learning deficit of PDAPP mice in learning platform locations 4 and 5.

B. Representative swim paths taken from 1 non-Tg and 1 PDAPP mouse at 6-9 (young), 13-15 (midde-aged) and 18-21 (old) months of age on problem 5.

df2/93, p<0.001) and, importantly, a genotype × age interaction (F=4.04, df 2/93, p< 0.05). Separate analysis of each genotype group revealed a trend but not significant age-related decline in non-Tg mice (F = 2.94, df 2/47, 0.10 >p> 0.05), however, a highly significant performance decline in PDAPP mice (F = 8.84, df 2/46, p < 0.002), further confirming that PDAPP mice displayed a deficit in spatial learning at young age, but this deficit progressively got worse with age. It seems that this age-related deficit may be specific to spatial learning in my test battery. First, a swim speed analysis revealed no difference between PDAPP and non-Tg mice on the first three trials of training (Fig. 3.3.4B, p>0.05), although the swim speed of both groups was significantly reduced with age (F=27.46, df2/93, p<0.001). Second, as shown above, there is no impairment in object recognition memory

Very interestingly, ANOVA of the trials to criterion further revealed a significant location × age interaction (F=2.275, df7.03/327.00, p<0.05; Greenhouse-Geisser correction), suggesting an age-related deficit in learning individual platform locations of this task. This further justified separate analysis of age-related and age-independent learning deficits in PDAPP mice, and these findings are discussed in the following two sections.

4. Age-dependent component of learning impairment in PDAPP mice.

Statistical analysis restricted to the PDAPP mice only revealed a significant locations × age interaction (F=2.17, 6.59/151.7, p<0.05; Greenhouse-Geisser correction; Fig. 3.3.4A). Very interestingly, young PDAPP mice were indistinguishable from age-matched controls on platforms 4 and 5 of this task, by contrast, middle-aged and old PDAPP mice took much longer to learn these two platform locations than the controls (Fig. 3.3.5A). This suggests that PDAPP mice display an age-dependent component of their learning deficit. In contrast, all three non-Tg control groups learned the last two platform locations at an equivalent rate (Fig. 3.3.5A). As shown in Fig. 3.3.5A., analysis of performance on platform locations 4 and 5 revealed not only significant genotype and age effects, but also a genotype x age interaction (F=6.82, df2/93, p<0.005). Separate analyses of these two locations averaged together indicated that PDAPP mice performed progressively worse with age (F=11.3, df2/46, p<0.001), whereas non-Tg mice displayed only a trend towards a significant age effect (F=2.58, df2/47, 0.10>p>0.05) (Fig. 3.3.5A).

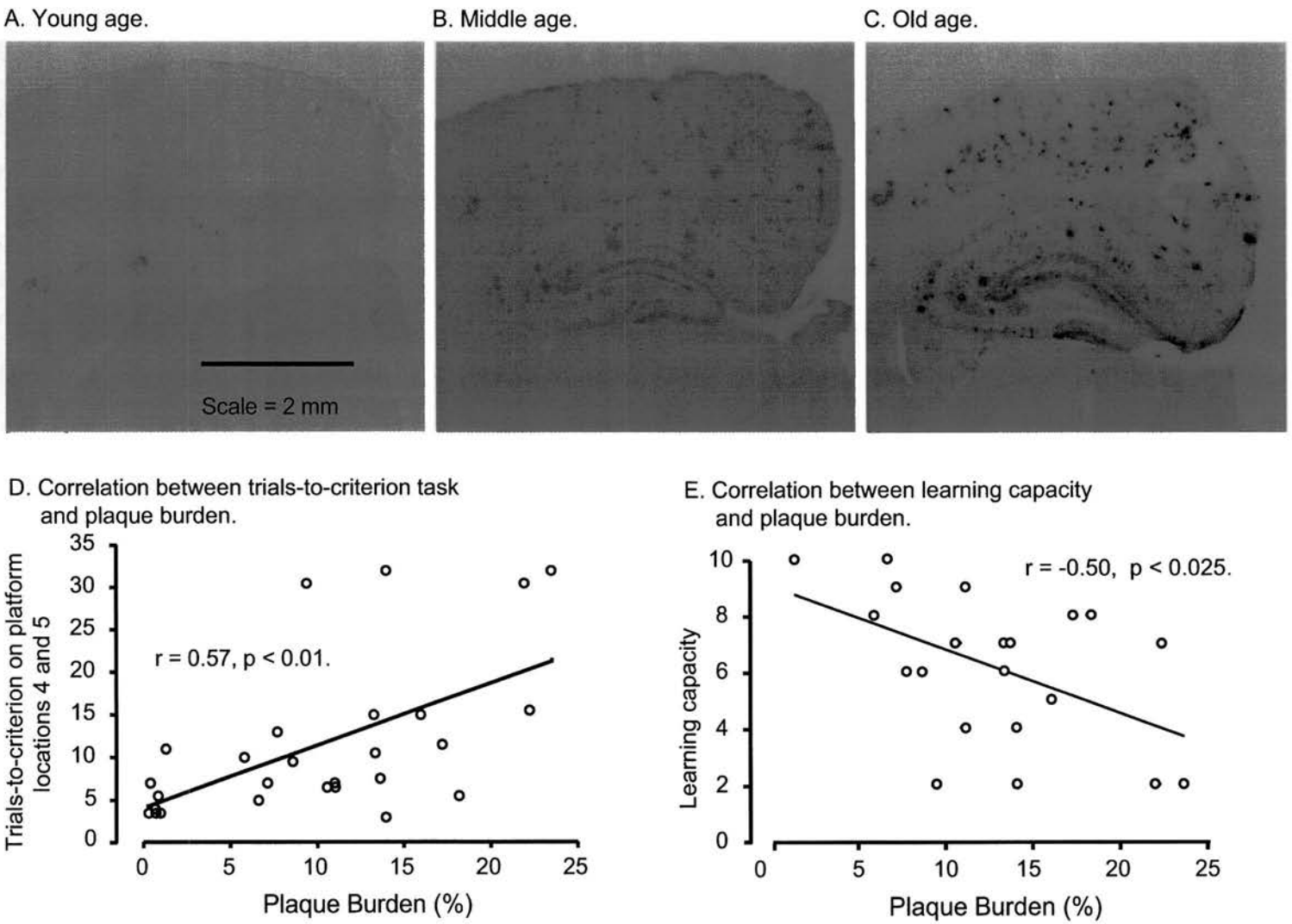

Figure 3.3.6 Relationship between Amyloid Plaque Deposition and Behavioural Performance. Representative amyloid plaques in PDAPP mice at 9 months (A), 16 months (B) and 22 months (C). D. Trials to criterion on locations 4 and 5 as a function of plaque burden. The correlation is significant. E. Learning capacity as a function of plaque burden. The correlation is significant.

It remains unknown why young PDAPP mice performed much better on the later problems in a series of 5. However, analysis of swim paths of these mice may give us some clues. Fig. 3.3.5B shows swim paths for all trials taken to learn platform location 5 of trials to criterion task from a representative control and PDAPP mouse at three ages (6-9-month; 13-15-month; 18-21-month). Interestingly, young PDAPP mouse reached the performance criterion (the criterion trials being named as C1, C2 and C3) as quickly as its age-matched non-Tg animal did, as both of them took 4 trials. By contrast, middle-aged PDAPP mouse finished this problem with 13 trials whereas the control did it with 4 trials, and old PDAPP mouse took 19 trials to learn this problem whereas the control littermate made it with 6 trials (Fig. 3.3.5B). Fig. 3.3.5B also shows that the older PDAPP mice displayed more circuitous searching behaviour than that of the young one, and it seems that they could not maintain accurate swim paths constantly from trial to trial until they finally reached criterion. This inconsistency may explain why older PDAPP mice could not improve their performance on later problems.

5. Significant correlation between plaque burden and behavioural performance.

The immunocytochemical analyses (Jane Knox) confirmed an age-dependent deposition of amyloid plaques in PDAPP mice. There were few plaques in the hippocampus of PDAPP mice at 9 months (Fig. 3.3.6A). At 16 months, plaques became much denser, particularly in the dentate gyrus, hippocampus and entorhinal cortex (Fig. 3.3.6B). At 22 months, amyloid plaques showed the highest level of density throughout the hippocampus and cortex (Fig. 3.3.6C). Quantification analysis of plaque burdens in the hippocampus revealed these were 0.6%, 11.8% and 14.5% across three ages.

In order to investigate possible relationship between plaque burden and behavioural performance of PDAPP mice, two correlation studies between plaque burden and performance on both tasks were conducted (Fig. 3.3.6D and E). As middle-aged and old PDAPP mice developed statistically indistinguishable levels of amyloid plaques, they were pooled together. First, an overall analysis of all PDAPP mice aged at 16-22 month revealed a significant positive correlation between trials to criterion on locations 4 and 5 and plaque burden ($r=0.57$; $p<0.01$).

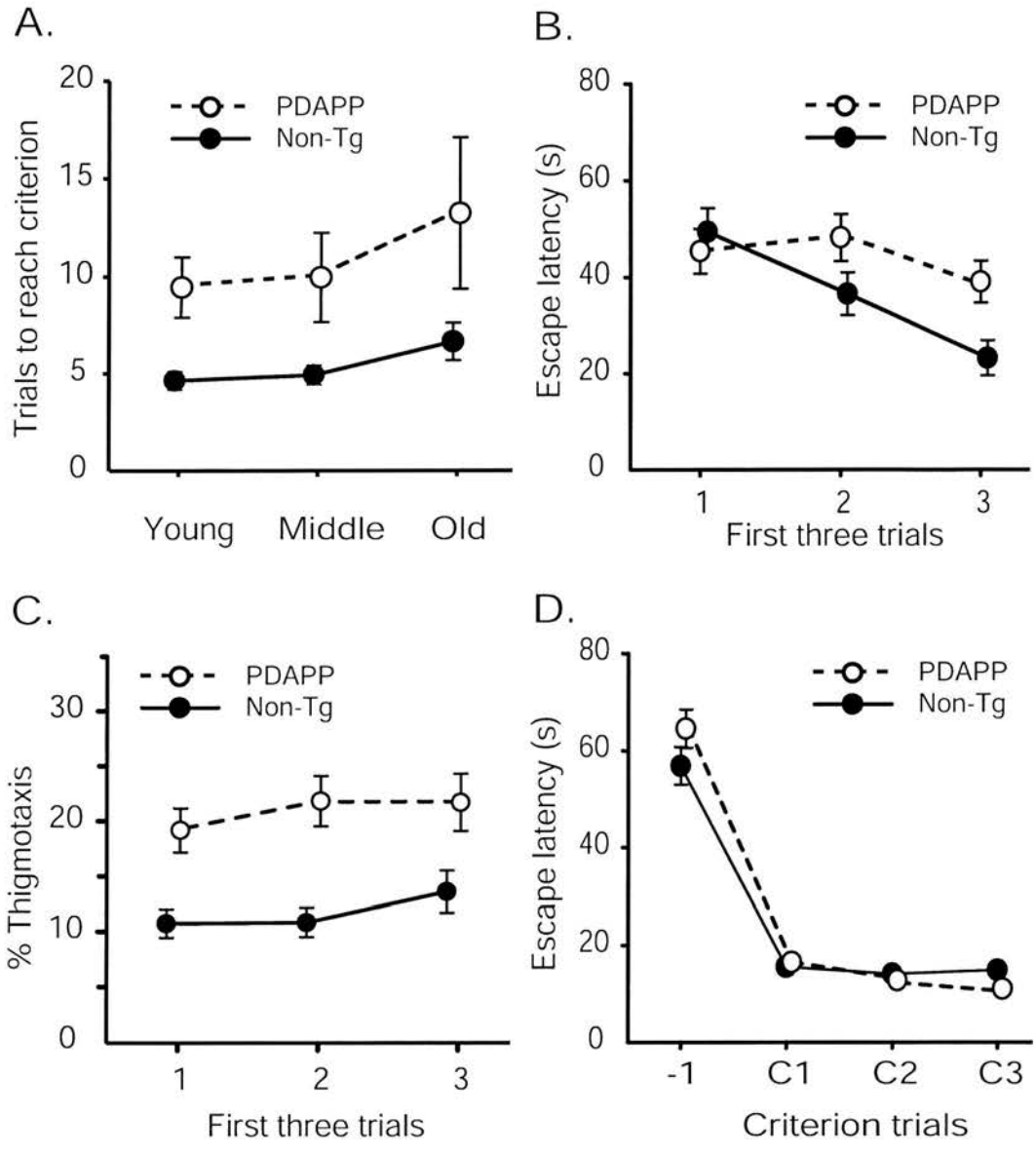

Figure 3.3.7. Analysis of Performance on Platform Location 1.

A. Age-independent learning deficit of PDAPP mice on platform location 1 as a function of age.

B. Escape latency on the first 3 trials of problem 1 (averaged all 3 age groups).

C. Thigmataxis of the mice. Percentage time spent within 15cm of the watermaze walls over the first 3 trials on problem 1 (averaged all 3 age groups).

D. Backward learning curves show escape latency for three criterion trials (C1-C3) plus the preceding trial immediately to the first criterion trial (C1) on problem 1.

(Fig. 3.3.6D). Second, a significant negative correlation between learning capacity and plaque burden of PDAPP mice was also observed ($r=-0.50$, $p<0.05$) (Fig. 3.3.6E). As the correlation between plaque burden and behavioural performance is significant, it suggests that amyloid plaques play a very important role in disrupting spatial learning of PDAPP mice.

6. Age-independent deficit in spatial learning of PDAPP mice.

Comparisons of the performance of PDAPP mice at all three ages on problem 1 (Fig. 3.3.3) showed that the spatial deficit in PDAPP mice was equivalent at all ages. Performance of both PDAPP and non-Tg mice on location 1 is plotted and shown in Fig. 3.3.7A. ANOVA of problem 1 revealed only a significant genotype effect ($F=15.2$, $df1/93$, $p<0.001$), but neither an age effect ($F<1$) nor any interaction. It is likely that learning problem 1 in the trials to criterion task is no different from learning a standard spatial reference memory task in the watermaze, so this age-independent learning impairment of PDAPP mice is consistent with previous findings using a reference memory task (Justice and Motter, 1997).

The slower learning rate of PDAPP mice was also analysed in relation to escape latency on platform location 1. As some mice, including both non-Tg and PDAPP, only took three trials to learn the first location, the analysis had to focus on only the first three trials to include all animals. Figure 3.3.7B shows that the escape latency for the first three trials of PDAPP mice decreased more slowly than that of non-Tg mice. Thus PDAPP mice have a slower learning rate on problem 1 compared to non-Tg controls.

Increased thigmotaxis in PDAPP mice was observed on these same first three trials of location 1, compared with non-Tg controls (Fig. 3.3.7C). This might contribute to or be due to the impaired learning of PDAPP mice. It is not an impairment of swimming ability, as there was no significant difference in swim speed between PDAPP and non-Tg mice (Fig. 3.3.4C). Finally, the so-called backward learning curves, in which the escape latency on all three criterion trials for all animals on platform location 1 plus one preceding trial immediately to the first criterion trial was averaged for both genotype groups, are shown in Fig. 3.3.7D. Analysis of these learning curves revealed no genotype difference ($F=2.33$, $df1/94$, $p>0.1$) and no genotype $\times$ trials interaction

($F=1.18$, df 2/188, $p > 0.3$), suggesting that, once PDAPP mice learned problem 1 by using more trials than the controls, they showed no difficulty in finding the platform. Thus they were not different from the controls after reaching the performance criterion. Collectively, these findings indicated that PDAPP mice could eventually learn (or encode) and remember the hidden platform location, although their learning rate was relatively slow.

3.4 Discussion.

In early 1999, when this research project initially started, no evidence showing age-related or more specifically, plaque-related learning deficit in the PDAPP mouse had been reported. Although Hsiao et al's report (1996) had suggested an age- and plaque-related memory deficit in Tg2576 mice using the standard watermaze reference memory task, this claim was contested (Routtenberg et al., 1997). Indeed, early studies on either plaque-free APP transgenics or PDAPP mice had failed to reveal any plaque- or age-related learning deficits. I therefore claim that the findings of this study are the first convincing demonstration of an age- and plaque-associated learning deficit. They were published in Chen et al (2000).

Interestingly, since it was proposed in 1991, the amyloid cascade hypothesis, which emphasizes the central role of plaque deposition in AD, has become the dominant one in the field. Although much genetic evidence supports this hypothesis, there is much less clinical or pre-clinical support. As human AD subjects display progressive memory loss with age, it has been important to establish whether overexpression of mutant really does play a central role in cognitive impairment of AD. The initial purpose of this cross-sectional study was to investigate plaque- and age-related learning deficits in APP Tg animals, and it seems to have succeeded in revealing these.

Consistent with previous reports (Justice and Motter, 1997; Ramsay and Morris, 1998), a learning deficit in young PDAPP mice was also found using this novel DMP task. However, the deficit in young PDAPP mice also got progressively worse with age, suggesting that there is an additional spatial learning deficit that is age-dependent. As significant correlation between plaque burden and behavioural

performance on the trials to criterion and learning capacity tasks was observed in PDAPP mice, the age-related learning deficit is plaque-related as well.

It is possible that the learning deficit in PDAPP mice is due to high levels of APP, total Aβ or APP CTFs. First, studies on human wildtype APP Tg mice have indicated that overexpression of human APP disrupts spatial learning and memory in Tg mice even in the absence of plaques (Yamaguchi et al., 1991; Moran et al., 1995). Second, several other plaque-free APP Tg mice, who produce high levels of Aβ and APP CTFs in the brain, also display severe deficit in spatial learning and memory (Nalbantoglu et al., 1997; Berger-Sweeney et al., 1999), strongly suggesting that abnormal accumulation of Aβ, APP CTFs or both has significant deleterious effect on spatial learning and memory. As PDAPP mice express very high levels of soluble and insoluble Aβ (40 and 42) but few plaques at 6-9 months of age (Johnson-Wood et al., 1997), these might account for the impaired spatial learning of PDAPP mice at early age. However, the cellular mechanisms by which they do so are unclear.

The claim of a separate age-related learning deficit of PDAPP mice rests on three lines of evidence. First, the deficit in PDAPP mice got progressively worse with age; second, young PDAPP mice improved their performance on later problems 4 and 5 of a series of 5 in the trials to criterion task to a point where they were not different from age-matched non-Tg controls, whereas two older groups displayed consistent severe deficits on problems 4 and 5; third, correlation studies revealed an association with plaque deposition which clearly can not be a factor in the deficit by young PDAPP mice. These findings are consistent with the idea that deposition of plaques plays a very important role in causing spatial learning or memory loss in PDAPP mice, but one must also consider the possibility that plaques are a surrogate marker for some other upstream events including elevated Aβ levels.

The successful demonstration of a component of age-related learning deficit in PDAPP mice in this study indicates that a behavioural task sensitive to the integrity of the hippocampus, entorhinal, cingulate and cerebral cortex is sufficient and may even be required to achieve this goal. A key factor seems to be the constantly changing platform location requiring the animal to keep updating his memory representation. In contrast, previous studies have indicated that the watermaze reference memory task is

sufficiently sensitive to reveal plaque-independent impairment of spatial learning in APP Tg mice (Justice and Motter, 1997; Moechars et al., 1999). But interestingly, this task has consistently failed to reveal an age-independent learning deficit in Tg2576 mice (Hsiao et al., 1996; King and Arendash, 2002; Westerman et al., 2002). However, plaque-independent learning deficits have been commonly observed in all other APP Tg lines, PDAPP, WT human APP transgenics, APP104 and CRND8 Tg mice (Yamaguchi et al., 1991; Moran et al., 1995; Justice and Motter, 1997; Nalbantoglu et al., 1997; Moechars et al., 1999; Janus et al., 2000; Van Dam et al., 2003).

In contrast to Dodart et al's (1999) finding of age-related deficit in object recognition memory of PDAPP mice, unimpaired object recognition memory was observed here. It is difficult to explain this discrepancy. Differences of methodology may partly account for it. First, Dodart et al (1999) have only tested a 4h retention interval with their cohort of PDAPP mice. In this study, PDAPP mice were repeatedly tested with 5 different intervals ranging from short-term (10 s) to long-term (4 h). It is possible that repeated exposure to the range of objects used in this study might reduce exploration initiatives and activities for novel objects, or simply produce a carry-over (practice) effect in the mice. For example, the object memory index (~70%) at 10 s interval in both PDAPP and non-Tg mice of this study was equivalent to that at 4 h delay in Dodart et al's report (1999). Second, it is unclear whether using two identical objects in the sample phase of this task and using 30 s of total active exploration time as the duration of each phase affected the overall performance of the mice. Third, and probably most importantly, the two studies used different genetic background of PDAPP mice. Although the original PDAPP mouse was produced in a DBA/C57BL6/Swiss Webster triple strain background, the colony of PDAPP mice used by Dodart et al (1999) were the same as the original one, but the colony of PDAPP mice used in this study was the DBA/C57BL6 double strain background (personal discussion with Dione Kobayashi). Recently, Mathis' group in Strasbourg have tested performance difference between WT C57/BL/6 and Swiss Webster mice. What they have found was that Swiss Webster mice display above 70% memory index of object recognition at 4 h interval, similar to that for the control group in their original report, but very interestingly, C57BL/6 mice only display chance performance (scientific communications with J.C Dodart and C. Mathis). It is

observed that the color of the mice used for this cross-sectional and following longitudinal study from the former Athena Neuroscience, was black, agouti or brown, but many Dodart's mice were white (personal discussion with J.C. Dodart). This, however, raises a problem about Dodart et al's methodology. Their use of only one retention interval makes it very unlikely to distinguish between a perceptual and a memory deficit. Albino mice are thought to have poorer vision and the PDAPP phenotype may interact to influence perceptual abilities in the Lilly but not the Elan (or Athena) line of mice. Finally, it is unclear whether gender differences between our studies may also make difference in the results, as all mice in this study were male, but Dodart et al used both genders (personal discussion with J.C. Dodart). To summarise, it is inappropriate to draw a firm conclusion about the presence or absence of recognition memory deficits in PDAPP mice.

In conclusion, PDAPP mice were found to display both age-related and age-independent spatial learning deficits. These were significantly correlated with plaque burden in old PDAPP mice. Furthermore, our line of PDAPP mice showed normal swimming ability, normal learning in the visible cuetask, and normal object recognition memory, suggesting that the age-related learning deficit of PDAPP mice is not due to sensorimotor problems or motivation to learn.

Chapter 4: A Longitudinal Investigation of Age-related Learning Deficits in PDAPP Mice.

4.1 Introduction.

4.1.1. The advantages of a longitudinal design for the study of age-related changes in cognition on APP mice.

Cross-sectional designs have most commonly been used in behavioural explorations of age-related cognitive deficits in APP Tg mice. Most cross-sectional studies have been carried out at limited selection of different age points (i.e. 2 to 3 different ages). For example, Hsiao et al's (1996) study was on Tg2576 mice at 3, 6 and 9-10 months of age using Y-maze alternation and watermaze reference memory. More recently, Tg2576 mice were tested at 2 and 9-10 months using a forced choice T-maze task (Chapman et al., 1999). Likewise, object recognition, bar press and radial 8-arm maze tasks were used to test PDAPP mice at 3, 6 and 9-10 months (Dodart et al., 1999).

It seems that no longitudinal studies on APP Tg mice had been published before 1998. Although the progression of severity of AD can be evaluated from several cross-sectional studies of different groups of patients, cross-sectional methods are not the usual way to study progressive disorders. Clinical trials to evaluate the therapeutic efficacy of a prospective anti-AD drug are necessarily dependent on longitudinal studies, as one major setback of the cross-sectional method is that the variance of individual differences is sometimes huge. A longitudinal study on APP Tg mice could allow us to test the same mice repeatedly at different stages of development, such that individual differences have less impact than in a cross-sectional study. It should provide more reliable information on changes of cognitive performance. Overall, longitudinal studies on APP Tg mice are essential to the field to validate the transgene effect on disease progression.

4.1.2. Longitudinal studies on APP Tg mice.

To our knowledge, our group was the first to apply longitudinal methodology to the study of APP Tg mice (Ramsay and Morris, 1998). Using a longitudinal design, Ramsay and Morris used a 4 trials/day DMP task in the watermaze to investigate whether PDAPP mice display an age- or plaque-related learning deficit. PDAPP mice

were initially tested using a visible cuetask at 4-5 months of age, and then repeatedly tested by a DMP task at 6 different age points from 5-6 to 19-20 months. The performance of PDAPP mice in the cuetask was normal. In the DMP task, 5-6-month PDAPP mice displayed a significant deficit which persisted throughout the whole testing period in the same mice (Ramsay and Morris, 1998). These findings indicated that the early deficit seen in spatial learning of PDAPP mice did not progress with age when the same mice performed the same task. So these findings are consistent with those observed in PDAPP mice using a cross-sectional design (Justice and Motter, 1997). However, the study was conclusive as the PDAPP mice were severely impaired. The lack of an age effect may have been due to a ceiling effect.

After our group's first attempts to longitudinally examine PDAPP mice, several longitudinal studies have been reported on other APP Tg lines later. For example, Janus et al have reported an age-independent early deficit in TgCRND8 mice using the standard watermaze reference memory task in an Aβ vaccine study (Janus et al., 2000). In another Aβ vaccine study, using a longitudinal design and a radial-arm watermaze task, Morgan et al have reported that the same APP/PS1 doubly Tg mice display normal spatial learning at 11 months of age but impaired learning at 15 months (Morgan et al., 2000). Paradoxically, it is possible that age-related learning deficits of APP/PS1 mice in the radial-arm watermaze are not plaque-dependent, as 11-month mice, which are plaque-rich, are cognitively normal. Using a forced choice T-maze alternation task, another longitudinal study has been reported on Tg2576 mice (Barnes et al., 2001). The same male Tg2576 mice were tested at three different ages. At four months of age, Tg2576 mice exhibited normal acquisition of the forced-choice alternation. At 8 months, the same animals displayed a deficit when performing the same task. This deficit increased in severity at 12 months (Barnes et al., 2001). Consistent with previous findings from the same group (Chapman et al., 1999), these results established an age-dependent learning impairment in the Tg2576 mouse model of AD. However, no data on amyloid plaques were reported.

4.1.3. Purposes of this longitudinal study on PDAPP mice.

As reported in Chapter 3 of this thesis, both age-related and age-independent learning deficits were simultaneously observed in PDAPP mice in a cross-sectional study using a modified DMP task. It seemed very interesting to us whether a longitudinal design

would reveal a similar finding by using the same PDAPP mice. To answer this question, PDAPP mice were first tested at 6-9 months using several different behavioural paradigms including cuetask, trials to criterion, object recognition and learning capacity task. 6-9 months was chosen as the earliest testing age, because it is a crucial stage for PDAPP mice to first display the formation of amyloid plaques in the dentate gyrus and hippocampus of the brain (Johnson-Wood et al., 1997). The same mice were then repeatedly tested using the same behavioural protocols at 14-15 and 21-22 months. In order to avoid as much as the carry-over (practice) effect on the same mice due to repeated testing, 7-8 months was used as the interval between different testing phases. At the end stage of this study, synaptic transmission, synaptic plasticity of the hippocampus and plaque burden of the brain were further examined.

Overall, a longitudinal design allows a direct comparison of performance among young, middle-aged and old mice while the plaque pathology develops with age, and also allows a direct correlation study to examine relationships between behavioural performance, synaptic strength in the hippocampus and amyloid plaques.

4.2 Methods.

4.2.1. The subjects.

PDAPP and non-Tg control mice used in this study were the same 50 young animals (6-9 months) used in the cross-sectional study of Chapter 3. Tg mice were heterzygous on a DBA/C57BL/6 double strain background. The mice (PDAPP =25, non-Tg=25) were first tested at 6-9 months, and later, repeatedly at 14-15 and 21-22 months. The mice were group-housed (2-4 mice each cage). The running sequence was assigned by Dr. Stephen Martin.

During the long duration of this longitudinal testing (18 months), some animals died. 12 of them (PDAPP=6; non-Tg=6) were sacrificed at 9 months to examine the pathology for the young groups of the cross-sectional study in Chapter 3. The following table (Table 1) shows how many mice were alive at three different stages of testing. Final data analyses were only carried out on 25 mice who completed the whole behavioural and electrophysiological study (PDAPP =12, non-Tg=13) at 22 months. The mortality of PDAPP and non-Tg mice was 36.84% and 31.58%,

respectively, during the 18-month testing period. Under the same experimental conditions, there was no difference of mortality between PDAPP and non-Tg mice ($\chi 2$=0.117; df=1; p>0.5; chi-square test).

Age of the Mice	Number of the PDAPP Mice	Number of the non-Tg Mice
6--9 months	25	25
14--15 months	18	19
21--22 months	12	13

Table 4.1 The Number of the Mice Completing the Study.

4.2.2. The experimental design.

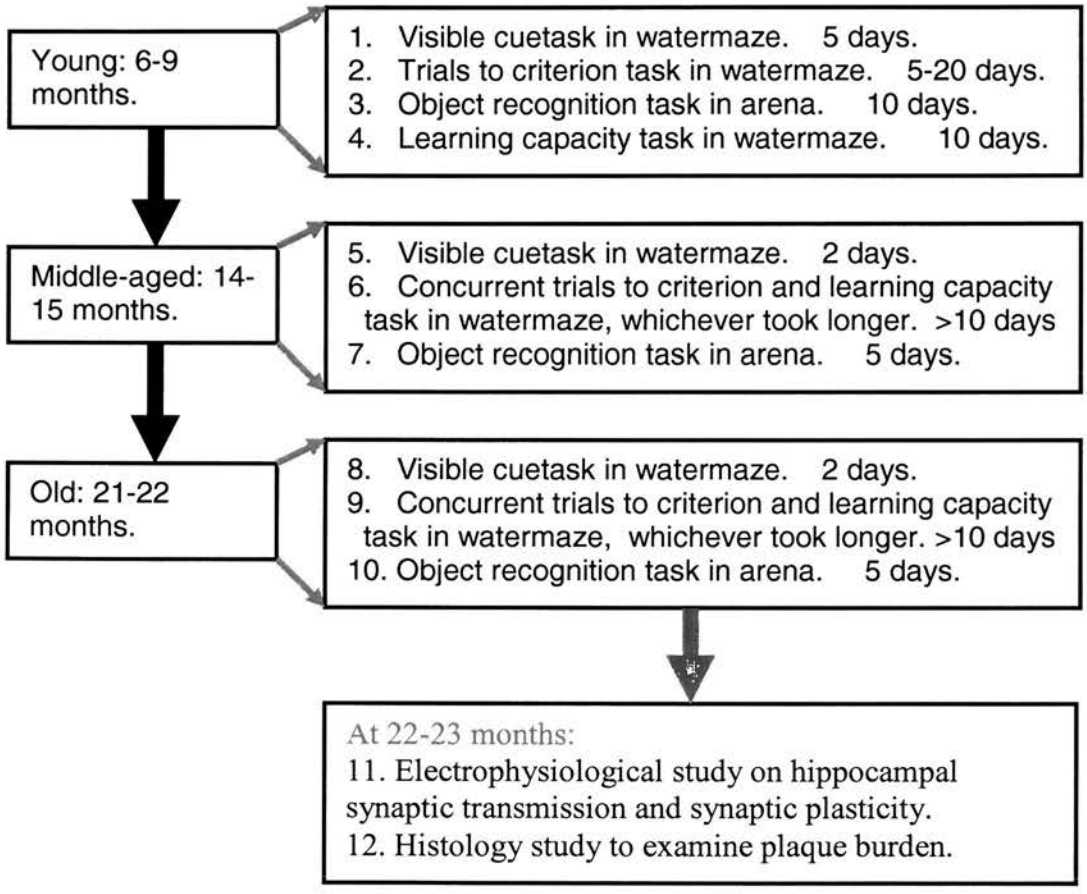

Figure 4.2.1 Experimental Design.

The experimental design for this longitudinal study is shown in Fig. 4.2.1. PDAPP and control mice were tested with a battery of 4 different behavioural tasks, including cuetask, trials-to-criterion, object recognition and learning capacity task at 6-9 months. About six months later, the same mice were tested again with the same tasks, but the trials to criterion task and learning capacity task were run concurrently, and

continued for whichever took longer. Old mice were tested at 21-22 months and the testing protocols were exactly the same as those used for 14-15 months of mice. Finally, hippocampal synaptic transmission, synaptic plasticity and Aβ plaques of the mice were investigated at 22-23 months.

4.2.3. The watermaze.

The same watermaze and associated equipment was used as described in Chapters 2 and 3.

4.2.4. Visible cuetask.

For young mice, there were 4 trials/day for 5 days. At two older ages, the duration of the cuetask was reduced to two days.

4.2.5. Trials to criterion and learning capacity task.

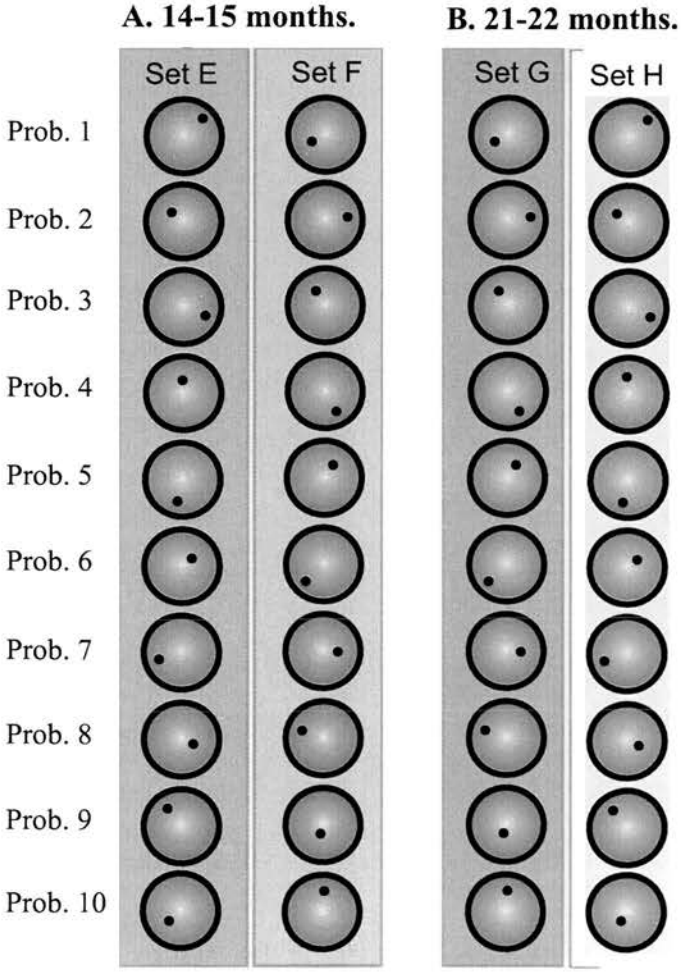

Figure 4.2.2 Two Sets of Ten Different Platform Locations.
A. Two sets (E and F) for the middle-aged groups.
B. Two sets (G and F) for the old groups.

For young groups, the trials to criterion and learning capacity tasks were run separately (see Chapter 3). For two older ages, the trials to criterion and learning capacity tasks were run concurrently. Fig. 4.2.2 shows four sets of 10 different locations for middle-aged (Sets E and F) and old (Sets G and H) animals. At 14-15 or 21-22 months, the animals were required to learn as many problems as they could in 10 days. But if any of them had not learned the first five platform locations within 10 days, they were allowed to take as long as they needed to complete the first five, which constituted the trials to criterion task. The learning capacity for the animals was the total number of problems learned in 10 days. A maximum trial number of 32 was allowed for each animal to learn any one of the first five problems.

4.2.6. Object recognition.

For young animals, five ITIs were used, as described in Chapter 3. For middle-aged and old groups, only three ITIs were chosen to explore immediate (10 s), short-term (10 min) and long-term (4 h) object recognition memory.

4.2.7. Slice preparation.

Briefly, 400 μm thick standard transverse coronal slices were prepared using a vibroslicer and collected into an incubation chamber (see Chapter 3). About 10 minutes later, two slices were then transferred to the recording chamber.

4.2.8. Electrophysiology.

Slices were allowed to recover in the recording chamber for 80 min. Recording was performed at 32 ± 1°C. Field EPSPs of CA1 apical dendrites were recorded extracellularly with a glass electrode filled with 3M NaCl. Two bipolar stimulating electrodes were placed on either side of the recording electrode. Input-output (I-O) curves were recorded using 11 different intensities of stimulation (0.2 V, 0.3 V, 0.4 V, 0.5 V, 0.6 V, 0.8 V, 1.0 V, 1.2 V, 1.4 V, 1.6 V and 1.8 V). At each stimulus intensity, 3 fEPSPs were elicited with the mean value of fEPSP slope used for final data analysis. To measure paired-pulse facilitation (PPF), 4 different interpulse-intervals (IPIs), 25ms, 50ms, 100ms and 200ms, were exploited. For long-term potentiation (LTP) experiments, stimuli were delivered by alternating between 2 independent Schaeffer collateral-CA1 pathways, one being the tetanized and the other one being

the control pathway, at a frequency of 0.067 Hz to each pathway. Stimulation was set to induce a fEPSP with amplitude of ~50% of maximum response. LTP was induced in the testing pathway by theta-burst stimulation (TBS) of 3 trains (2min intertrain interval), each consisting of 15 (200ms interstimulus interval (ISI))×4 pulses (100 Hz). Data were collected by software called LTP114J© and stored into a computer. The initial slope of fEPSP evoked by stimulation of the Schaeffer collateral-CA1 pathway was analyzed online. Responses in each experiment were normalized to baseline, which was defined as the mean value obtained in at least 20-minute responses before TBS, and shown as mean±SEM.

4.2.9. Immunocytochemistry and plaque load quantification.

The right hemispheres of 25 mice were fixed in formalin for at least one week. Ms. Jane Knox then did all immunohistology experiments.

4.3 Results.

4.3.1. PDAPP mice showed normal cuetask learning at all ages tested.

Results for the longitudinal cuetask testing are shown in Fig. 4.3.1. Statistical analysis revealed no significant genotype or age effect for the same mice ($F=0.27$, $df1/23$, $p>0.6$). All PDAPP mice swam as well as the controls at different testing ages, suggesting that they were normal in cuetask learning.

4.3.2. PDAPP mice displayed normal object recognition memory.

Similar to the findings of Chapter 3, Fig. 4.3.2 shows that both PDAPP and non-Tg mice displayed comparable performance in this task at all ages tested ($F<1$). They explored the novel objects preferentially. The ANOVA revealed gradual forgetting over 4 h ($F = 21.21$, df 1.97/23.65, $p < 0.001$, Greenhouse-Geisser correction), but no difference between PDAPP and non-Tg mice at any age ($F<1$). Overall, the mean performance of both groups was significantly above chance at all retention intervals ($p<0.05$, one sample t-test). This indicates that PDAPP mice displayed normal short- and long-term object recognition memory.

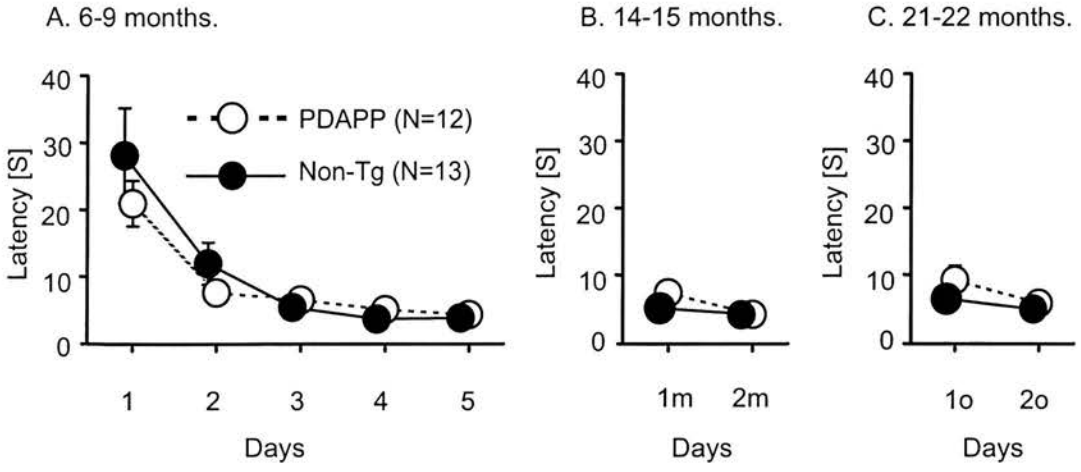

Figure 4.3.1 Cuetask Performance in PDAPP and non-Tg Mice. There was no significant difference between the same PDAPP and non-Tg mice at 3 different ages. A. 6-9 months. B. 14-15 months. C. 21-22 months.

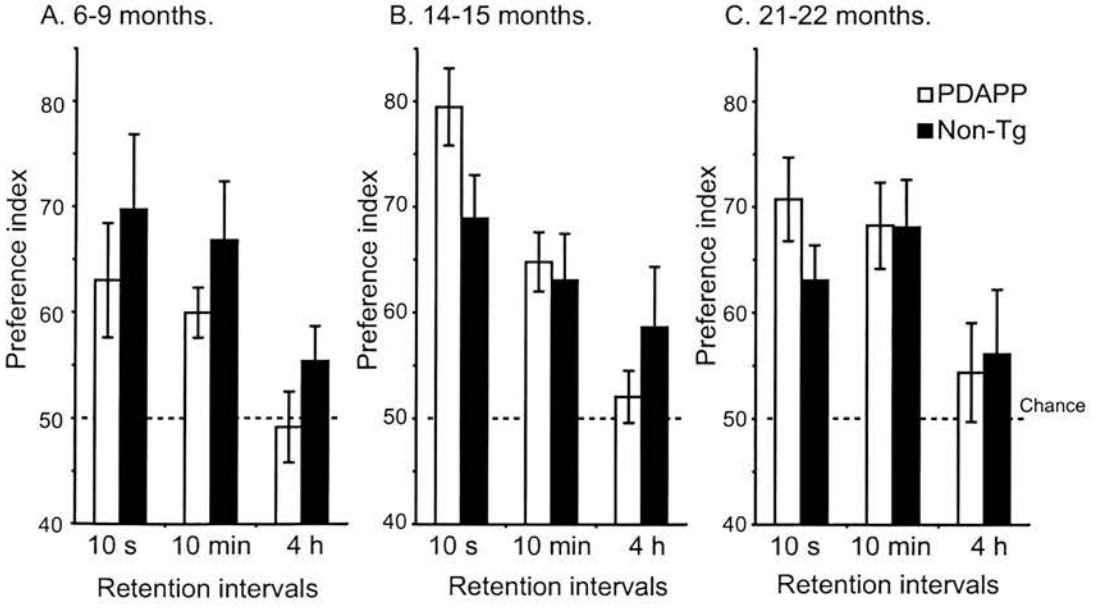

Figure 4.3.2 Normal Object Recognition Memory in PDAPP Mice. PDAPP and non-Tg mice showed equivalent performance for three age groups ($F < 1$). A. 6-9 months. B. 14-15 months. C. 21-22 months.

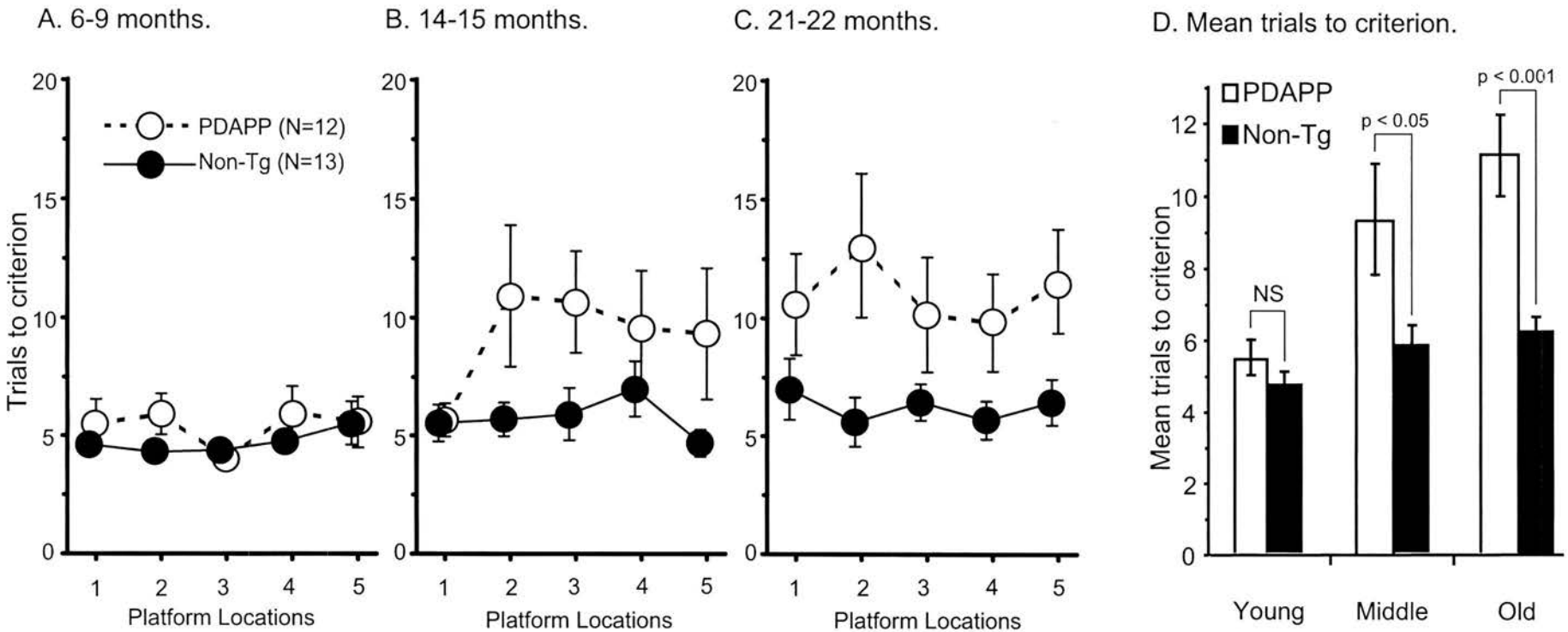

Figure 4.3.3 Age-related Deficits in Spatial Learning of PDAPP Mice. The same mice were tested in trials to criterion task repeatedly.

A. Performance of PDAPP and non-Tg mice at 6-9 months.

B. Performance of PDAPP and non-Tg mice at 14-15 months.

C. Performance of PDAPP and non-Tg mice at 21-22 months.

D. Mean trials to criterion of PDAPP and non-Tg mice across five platform locations in trials to criterion task. There was a significant age-related impairment of learning in PDAPP mice. The same PDAPP mice did not differ from the age-matched controls at 6-9 months, but showed significant deficits at both 14-15 and 21-22 months.

4.3.3. PDAPP mice displayed age-related deficits in spatial learning.

I. Age-related learning deficit of PDAPP mice in trials to criterion task.

Fig. 4.3.3 shows the performance by the same PDAPP and non-Tg mice at different ages. Analysis of variance first revealed a significant main transgene effect in this longitudinal study ($F=10.36$, $df1/23$, $p<0.005$), indicating that PDAPP mice were impaired in this trials to criterion task. The ANOVA further revealed a significant genotype × age effect ($F=8.86$, $df1.48/34.01$, $p<0.003$), reflecting the age-related impairment of spatial learning in PDAPP mice. Moreover, separate analyses of variance for both PDAPP and non-Tg mice showed significant age-related worsening of performance in PDAPP groups (Fig. 4.3.3 D: $F=20.02$, $df1.39/15.3$, $p<0.001$) and, though smaller in non-Tgs as well (Fig. 4.3.3 D: $F=5.59$, $df1.73/20.72$, $p<0.05$). In contrast to the finding of a small but a detectable deficit in learning in young PDAPP mice from my previous cross-sectional study (Chapter 3), the subset of 12 PDAPP mice, who successfully survived and completed the longitudinal study of the original 25, were unimpaired at 6-9 months (Fig. 4.3.3A and Fig. 4.3.3D: $F=1.53$, $df1/23$, $p>0.2$). However, these same PDAPP mice did significantly differ from the age-matched non-Tgs at the two older age points (for 14-15 months: Figs. 4.3.3B and 4.3.3D: $F=5.79$, $df1/23$, $p<0.05$; for 21-22 months: Figs. 4.3.3C and 4.3.3D: $F=19.16$, $df1/23$, $p<0.001$, respectively).

In contrast with what I have observed in the middle-aged PDAPP mice of the cross-sectional study (Fig. 3.3.3B, Chapter 3), Figure 4.3.3B shows that the middle-aged PDAPP mice did not display deficit in learning the first platform location. The longitudinal set of animals had been trained with 15 different locations in the watermaze at 6-9 months of age and had learned the procedural aspects of the task. The findings which they displayed deficit on platforms 2 to 5 at 14-15 months but not on platform 1 suggest that changing a memory representation is particularly difficult in middle-aged PDAPP mice.

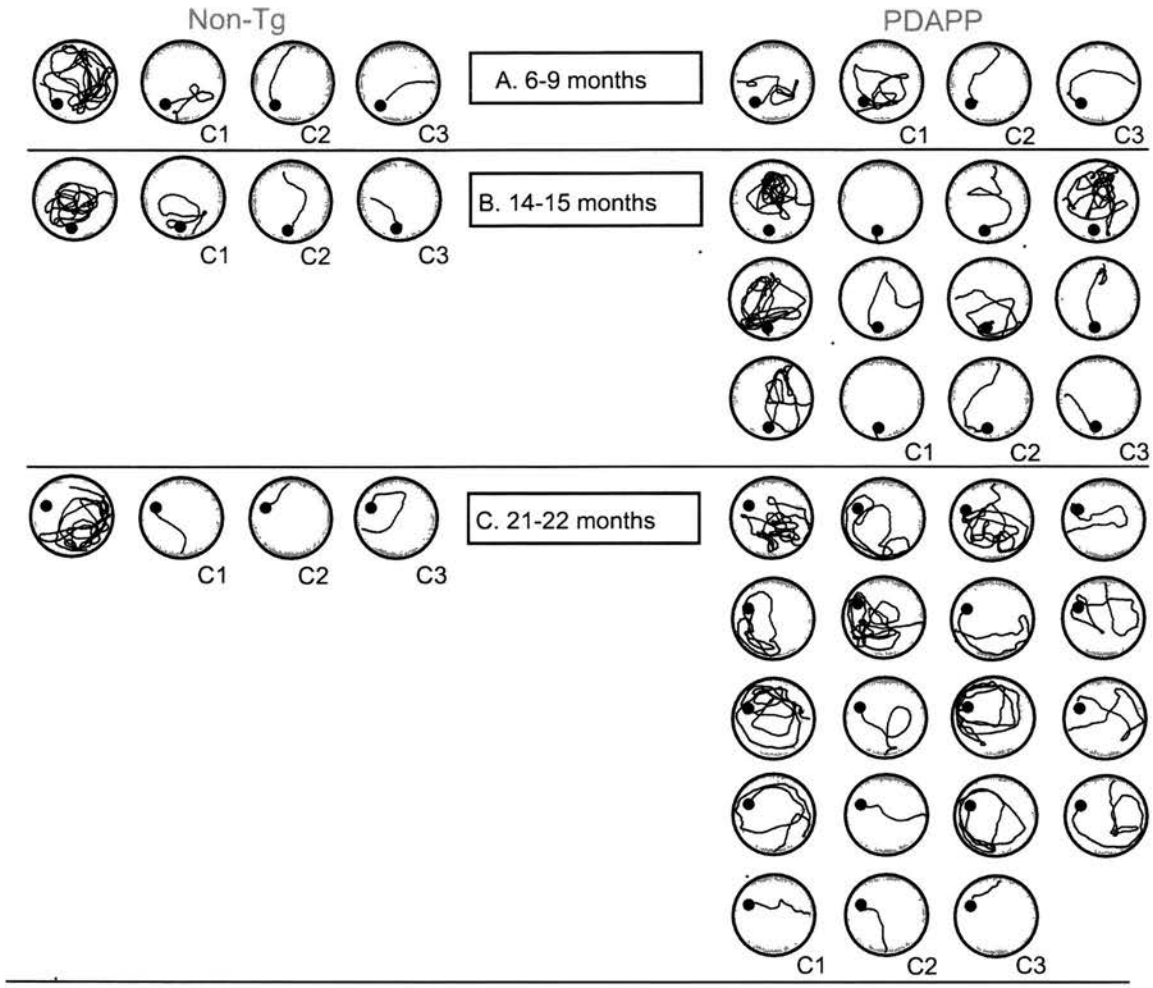

Figure 4.3.4 Representative Swim Paths. Representative swim paths taken from a non-Tg and PDAPP mouse at 6-9, 14-15 and 21-22 months of age on problem 5 (the same mice). A. 6-9 months. B. 14-15 months. C. 21-22 months.

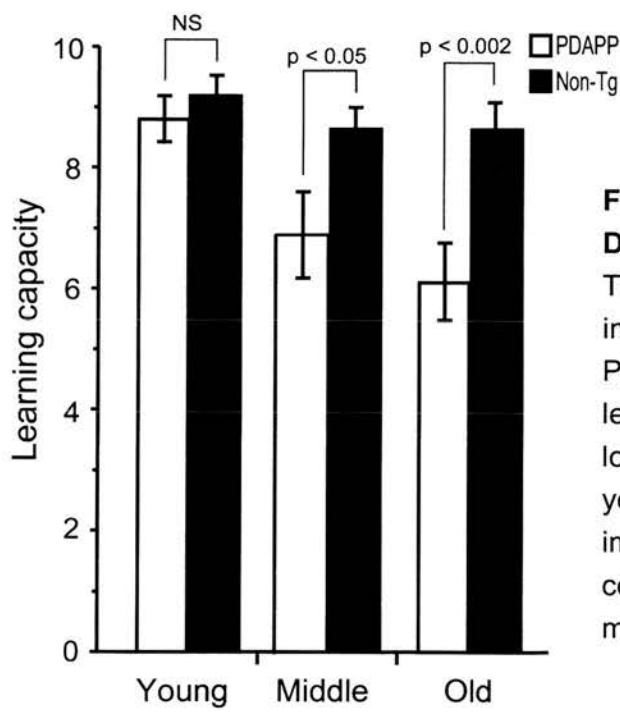

Figure 4.3.5 Age-related Learning Deficits in PDAPP Mice.
There was a significant age-related impairment of learning capacity in PDAPP mice. The same PDAPP mice learned equivalent number of platform locations to that by the controls at young age, but showed significant impairment from the age-matched controls at both 14-15 and 21-22 months.

Figure 4.3.4 shows the swim paths taken by two representative animals (1 non-Tg, 1 Tg) in the longitudinal study on learning location 5 at all ages. The same PDAPP mouse reached the performance criterion (the criterion trials were labelled C1 to C3) as quickly as the control (4 trials) at young age. As these two mice got older, the same PDAPP mouse displayed more circuitous paths and took 12 and 19 trials to learn the fifth problem at 14-15 and 21-22 months, but the same non-Tg mouse learned the same problem using 4 and 6 trials at 14-15 and 21-22 months. Figure 4.3.4 also shows that the PDAPP mouse occasionally displayed short paths (i.e. trials 4, 10 and 14), but was unable to do a series of short paths easily. Interestingly, the swim paths taken by this old PDAPP mouse were comparable to those by old PDAPP mice described in Chapter 3 for the cross-sectional study.

II. Age-related learning deficit of PDAPP mice in learning capacity task.

Although the learning capacity task is similar to the trials to criterion, it measures a slightly different aspect of learning ability of the mice. An age-related learning deficit in PDAPP mice was again observed using this task (Fig. 4.3.5). First, the ANOVA revealed a significant main effect of genotype ($F=8.84$, df1/23, $p<0.01$). Second, it also revealed a significant genptype × age interaction ($F=6.83$, df1.75/40.32, $p<0.01$; Greenhouse-Geisser correction). This interaction allowed a separate analysis of two different groups. In non-Tg groups, no significant age-related decline was observed (Fig. 4.3.5: $F=1.66$, df1.67/20.01, $p>0.2$), by contrast, in PDAPP groups, a significant decline of learning capacity was found (Fig. 4.3.5: $F=18.30$, df1.80/19.79, $p<0.001$). The results on learning capacity strongly suggested that the decline of learning capacity of PDAPP mice progressed significantly with age whereas that of non-Tg mice showed only a trend.

Three further ANOVAs were conducted at the separate ages. At 6-9 months, no significant difference of learning capacity between PDAPP and non-Tg mice was found (Fig. 4.3.5: $F<1$). The same PDAPP mice did differ from the same non-Tgs at 14-15 months of age (Fig. 4.3.5: $F=5.57$, df1/23, $p<0.05$). At the oldest age (21-22 months), a highly significant difference was found between PDAPP and control mice (Fig. 4.3.5: $F=13.94$, df1/23, $p<0.002$).

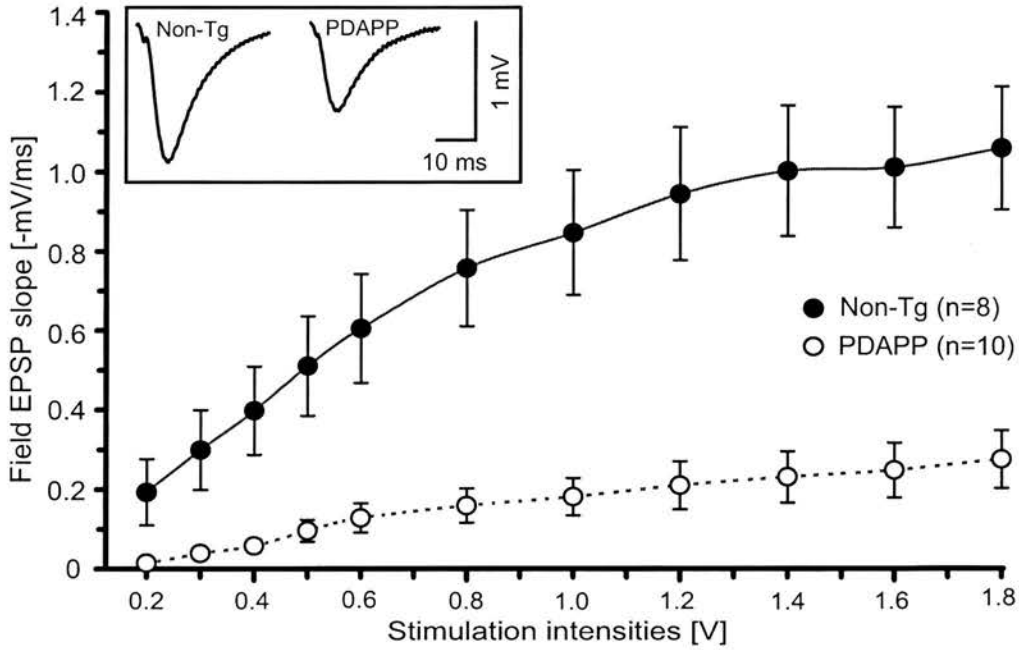

Figure 4.3.6 Impaired Basal Synaptic Transmission in PDAPP Mice. Input-output curves for aged PDAPP and non-Tg mice (22-23 months). There was a significant main genotype effect ($p<0.001$). Inset: Two responses (waveforms) from a PDAPP and Non-Tg hippocampal slice (about half maximum size of fEPSP by 1.0 V stimulation intensity).

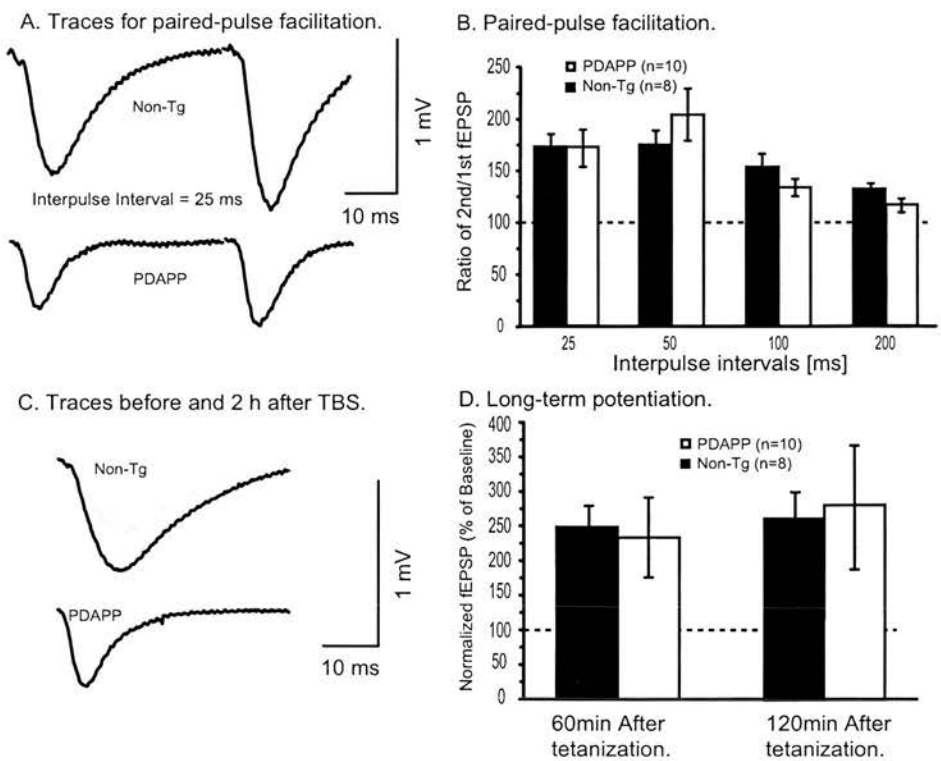

Figure 4.3.7 Normal Synaptic Plasticity in 22-23 Months PDAPP Mice. A. Waveforms of fEPSPs for paired-pulse facilitation (PPF) in PDAPP and non-Tg mice. B. There was no difference on PPF between PDAPP and non-Tg mice. C. Waveforms of fEPSPs before (light curves) and 2 h after (solid curves) tetanization in PDAPP and non-Tg mice. D. Normal hippocampal long-term potentiation (LTP) in PDAPP mice 1 or 2 h after tetanization.

4.3.4. Old PDAPP mice exhibited an altered synaptic transmission.

Hippocampal slices were taken from the mice longitudinally tested to investigate basal synaptic transmission and synaptic plasticity of the Schaeffer collateral CA1 area. First, the input-output curves were recorded using several different intensities of stimuli. Aged PDAPP mice displayed much smaller field EPSPs in area CA1 than non-Tg controls (Fig. 4.3.6: $F=29.93$, $df1/17$, $p<0.001$).

Two different forms of synaptic plasticity, short- and long-term, were further investigated in aged PDAPP mice. Paired-pulse facilitation (PPF) belongs to a short-term form of synaptic plasticity. Using several different interstimulus intervals, including 25, 50, 100 and 200 ms, PPFs were induced and shown in Figure 4.3.7. The representative responses (fEPSPs) from non-Tg and PDAPP mice are shown in Figure 4.3.7A. No significant difference of PPF between non-Tg and PDAPP mice was found ($F<1$; Fig. 4.3.7B). PPF at 50 ms ITI showed the biggest ratio among all tested ITIs in both PDAPP and non-Tg groups (Fig. 4.3.7B).

Early- and mid-phase of hippocampal LTP was also investigated in slices from aged PDAPP mice (Fig. 4.3.7C+D). Figure 4.3.7C shows representative traces from both PDAPP and non-Tg mice. Interestingly, there was no significant difference of hippocampal LTP between these two groups (Fig. 4.3.7D: $ps > 0.8$, student's T-test, at 1 h and 2 h post-tetanization).

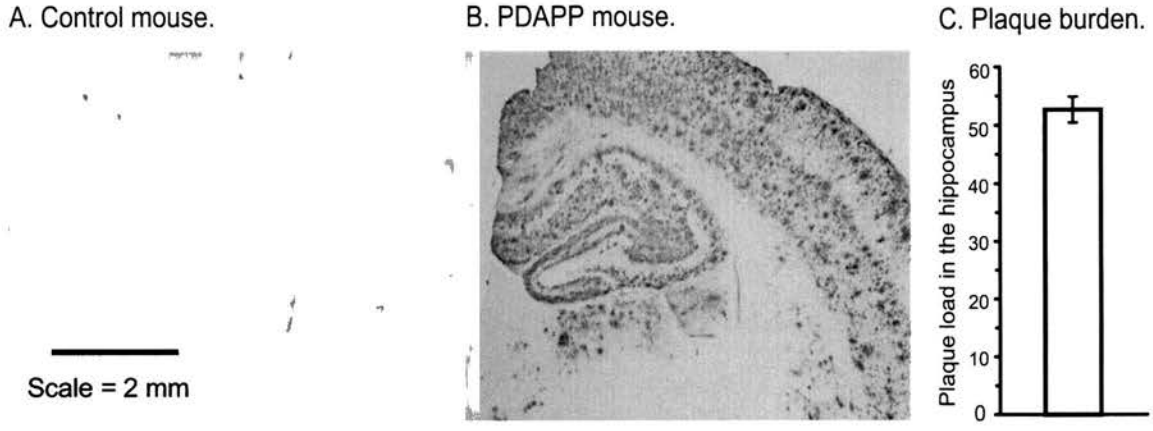

Figure 4.3.8 Amyloid Plaques in the Brain of PDAPP Mice.
A. 3D6 staining of a control mouse (age: 22 months).
B. 3D6 staining of a PDAPP mouse (age: 23 months).
C. Plaque burden in the hippocampus of 22-23 months PDAPP mice (n=10).

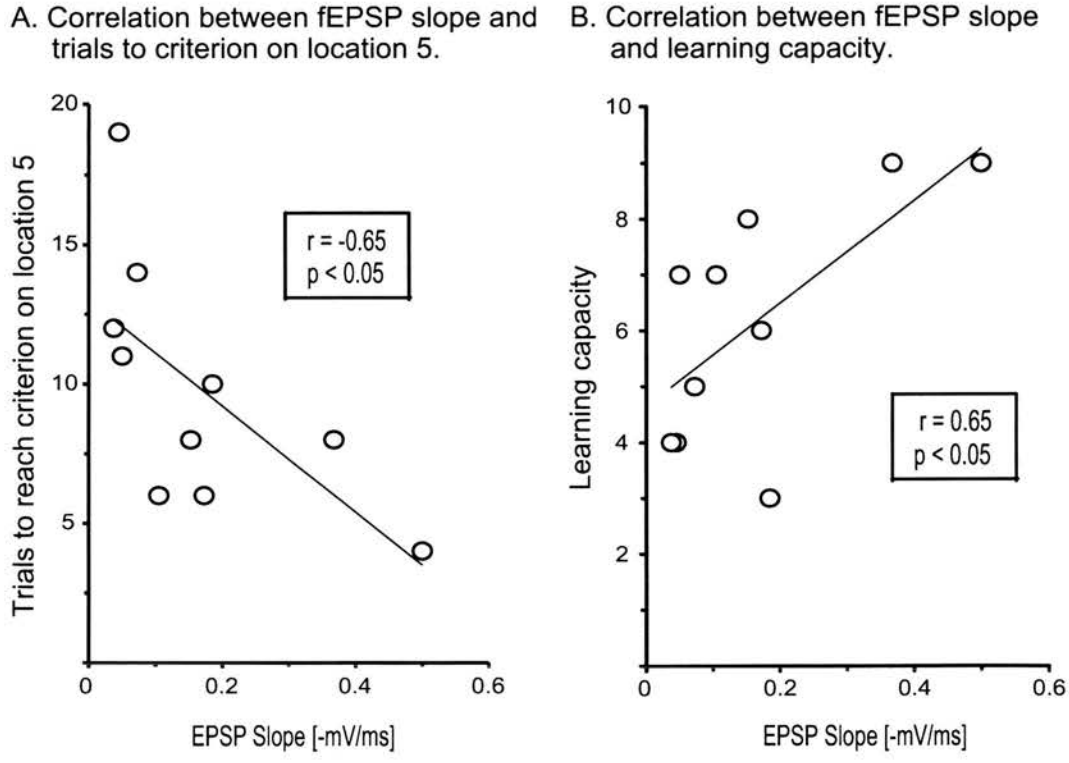

Figure 4.3.9 Significant Correlation between Basal Synaptic Transmission and Behavioural Performance. A. Significant correlation between the medium size of fEPSPs (stimulation intensity=1.0V) of the hippocampus and trials to criterion on location 5 in 22-23 months PDAPP mice. B. Significant correlation between the medium size of fEPSPs of the hippocampus and learning capacity in PDAPP mice.

4.3.5. Significant correlation between synaptic transmission and behavioural performance.

In this longitudinal study, PDAPP mice displayed deficits on both basal synaptic transmission and behavioural performance on the trials to criterion and learning capacity task. This allowed an examination of possible relationships between the reduced synaptic transmission and impaired learning in individual PDAPP mice. First, a significant negative correlation was observed between the medium size of fEPSPs and the number of trials to reach criterion on platform location 5 ($r=-0.65$, $p<0.05$; Fig. 4.3.9A). Second, a significant positive correlation of the medium size of fEPSPs to learning capacity ($r=0.65$, $p<0.05$; Fig.4.3.9B) was also observed. Analysis of plaque burden in the hippocampus of PDAPP mice by Jane Knox indicated that about 52.69% area of the hippocampus was occupied by amyloid plaques (Fig.4.3.8). However, no significant correlation between plaque burden in the hippocampus and behavioural performance was found in this longitudinal study ($ps>0.1$, for both trials to criterion and learning capacity).

4.4 Discussion.

The purpose of this longitudinal study was to use a within-subjects design to test the same mice repeatedly at different age points. One important advantage of this design over the most commonly used cross-sectional study in behavioural neuroscience is that it cuts down data noise. For example, the cross-sectional study showed that individual differences in performance on the trials to criterion and learning capacity was large, varying from 3 to 32 trials (trials to criterion) and 2 to 10 (learning capacity) in individual mice. This huge individual difference brings considerable noise into the results of between-subjects (cross-sectional) study. The main findings of this longitudinal study were that a subset of PDAPP mice also display an age-related learning deficit in the serial spatial learning task, but normal learning in the visible cuetask and unimpaired object recognition memory.

The above results essentially replicate those of my previous cross-sectional study, further validating the claim for an age-related learning deficit in PDAPP mice. These may be strong evidence to support the amyloid cascade hypothesis which suggests the central role of Aβ accumulation or deposition in the progression of AD (Hardy and

Allsop, 1991). In some way, findings from this longitudinal study are analogous to those of Barnes et al who have reported that Tg2576 mice display an age-related deficit in a forced choice T-maze alternation, using a similar longitudinal design (Barnes et al., 2001). The earliest age point in Barnes et al study was 4 months, whereas in my study, it was 6-9 months. Interestingly, these two different longitudinal studies indicated that young PDAPP mice and young Tg2576 mice can be normal in the respective tasks, suggesting that overexpression of APP may not be as important as the gradual accumulation of Aβ amyloid plaques in causing learning impairment of APP Tg mice.

One major disadvantage of the longitudinal design was that, as the same animals were tested repeatedly with the same behavioural tasks, their performance at later age points may improve, possibly through a practice effect (Winer et al., 1991). Due to the carry-over effect in the longitudinal design, the worsening in performance of the PDAPP group in the trials to criterion and learning capacity may not be a foregone conclusion, as any age-related decline of spatial learning may have been compensated by practice effects carrying over from one testing period to another. It is perhaps noteworthy that in non-Tg animals, a significant aging effect is apparent in the cross-sectional experiments when they were tested for the first time at different ages. Therefore, an aging effect in non-Tgs was less apparent in the longitudinal study (Figs. 4.3.3 and 4.3.4). This might be due to practice effect overcoming a small aging effect.

However, some differences were observed between the cross-sectional and longitudinal studies. One was that learning deficits on the trials to criterion and learning capacity were found in young PDAPP mice in the cross-sectional study, but not in the longitudinal one. More specifically, the 25 young PDAPP mice (6-9 months) in the cross-sectional study were impaired (Chapter 3: Fig. 3.3.3 and Fig. 3.3.4), but the subset of 12 PDAPP who survived a 18-month testing period did not differ from the age-matched non-Tg controls at 6-9 months. Statistical analysis showed that the initial performance of these 12 PDAPP mice was significantly better than that of the original 25 in the trials to criterion ($F=7.55$, $df1/35$, $p<0.01$), whereas the performance of 13 non-Tg mice was not different from that of the original 25 ($F<1$, $P > 0.9$). It is possible that PDAPP mice with better learning ability can live

longer, to put it another way, or demented mice with worse learning ability have shorter life span. However, the PDAPP group did not show higher mortality during the duration of this study than non-Tgs. Due to the death of several cognitively impaired PDAPP mice before the end of the study, a sampling bias may have been introduced that accounts for the entire effect.

Using *in vitro* slice electrophysiology techniques, aged PDAPP mice were found to show impaired basal synaptic transmission but normal short- and long-term synaptic plasticity (PPF and LTP) in the hippocampus. These findings are consistent with previously published reports on either PDAPP or Tg2576 mice (Hsia et al., 1999; Larson et al., 1999; Fitzjohn et al., 2001). However, Tg2576 mice were also reported by Chapman et al. (1999) to be unimpaired in basal synaptic transmission in CA1 area of the hippocampus. The reasons for the discrepancy are really unknown. One possible reason for this is that Chapman et al (1999) used kynurenate during slicing procedures. It has been suggested that hippocampal slices from APP Tg mice are more susceptible to trauma, and that using kynurenate in the dissection ACSF can improve slice viability (Fitzjohn et al., 2001). Indeed, Fitzjohn et al. (2001) have reported that kynurenate rescues impaired basal synaptic transmission in 12-month-old, but not 18-month-old TG2576 mice. As the mice used in this longitudinal study were about 23 months old, kynurenate was not used in the dissection medium. But it seems likely that the inclusion of kynurenate in the slice preparation may not be able to improve the impaired synaptic responses in very old PDAPP animals (>23 months). Nevertheless, my data here are very consistent with those by Hsia et al (1999) who used the H6 line expressing the same APPind and by Larson et al (1999) who have used the PDAPP mice. However, both Hsia et al (1999) and Larson et al (1999) have demonstrated that, like very old mice, very young (2-4 months) H6 or PDAPP mice also display significantly reduced synaptic responses. As there is no apparent plaque deposition at this age (<6 months), elevated levels of soluble Aβ may be accounted for the observed effects on basal synaptic transmission.

As behaviour, electrophysiology and histology studies were combined to examine the same PDAPP mice, this allowed further correlation analyses to explore the relationship between synaptic transmission, amyloid plaques and spatial learning. Another main finding of this longitudinal study was the significant correlation

between reduced hippocampal synaptic transmission and behavioural performance of PDAPP mice. For example, significant correlations were observed between fEPSPs and trials to criterion, and between fEPSPs and learning capacity. Although the correlation coefficients were not very high ($r=0.65$ for fEPSPs and trials to criterion; $r=-0.65$ for fEPSPs and learning capacity), they were significant. The significant correlation between reduced fEPSPs and impaired behavioural performance suggested a possible cellular mechanism to explain the impaired learning of PDAPP mice, that is, overproduction of Aβ plaques damages the circuits of several neuron systems in the hippocampus and cortex, and therefore disrupted learning of these mice.

Unlike our previous cross-sectional study, learning deficits in aged PDAPP mice were not correlated with plaques burden in this study. Plaque burden, quantified by Jane Knox, was 52.69% ± 2.20% in the hippocampus. Compared to 14.46% ± 2.28% of plaque burden for old PDAPP mice in the cross-sectional study, the difference was highly significant ($F=137.19$, $df1/15$, $p<0.001$). Very high amount of plaque burden in aged PDAPP mice for the longitudinal study may preclude any potential correlation analysis with behavioural performance. It remained unknown why these 12 PDAPP mice (22-23 months) had developed so high levels of plaque burden in the brain. Overtraining of the same PDAPP mice using a longitudinal design may accelerate the deposition of Aβ plaques. It remains unclear whether this is true or not.

The practice effects are one type of carry-overs which are potential extraneous variables to the present study. It has been suggested that the confounding carry-over effects could be reduced by counterbalancing (Kinnear and Gray, 2000). Indeed, in the trials to criterion and learning capacity task of this study, all platform locations used for the different age groups were counterbalanced as much as I could. Although the counterbalancing procedure might help to reduce the carry-over effects to a very low level, it still exists in this study. For example, in the trials to criterion, after comparing the performance for the two older age groups (middle-aged and old) from the cross-sectional and longitudinal study, a significant difference between these two designs was observed ($F=4.26$, $df1/91$, $p=0.042$), indicating that the overall performance of all old PDAPP mice in the longitudinal study was better than that in the cross-sectional one. However, analysis of learning capacity for the two old age

groups in the longitudinal and cross-sectional study revealed no such carry-over effect ($F<1$). This suggests that the trials to criterion task is more sensitive to show carry-over effects than the learning capacity.

Chapter 5: Investigation of the Effects of Aβ Vaccines on Spatial Learning and Synaptic Transmission of PDAPP Mice.

5.1 Introduction.

5.1.1. The importance of Aβ immunotherapy.

Most FDA-approved anti-AD drugs are cholinergic inhibitors that, while helpful for attention and memory show modest or no effects on the progression of AD. As Aβ abnormal accumulation and plaque deposition are believed to play a central role in neurodegeneration and dementia of AD, Aβ has become the most important molecular target for the treatment of AD. The results reported in the previous two chapters are consistent with this emphasis given the correlations with plaque deposition observed.

Novel vaccine concept for the treatment of AD first appeared in 1999 from Schenk and colleagues who reported that plaques in PDAPP mice can be completely removed when Aβ vaccines are administered at 2 months of age for 11 months; and significantly reduced when Aβ vaccines are administered at 11 months of age for 7 months (Schenk et al 1999). This groundbreaking study raised the possibility that an active Aβ vaccine might be a novel therapeutic method for AD. It also suggested that agents which can prevent Aβ production and accumulation, such as β-, γ-secretase inhibitors and Aβ blockers (antibodies), might eventually have potential clinical benefit for the treatment of AD.

Aβ immunotherapy has since received widespread attention. Using passive immunisation and PDAPP mice, two independent groups at Elan and Lilly have explored why Aβ immunotherapy works in animals. One study from Elan suggests that Aβ vaccines can stimulate the immune system to fight Aβ and remove the pre-existing plaques. For example, Bard et al examined passive immunization of PDAPP mice. They reported that Aβ antibodies can cross the BBB, enter the CNS, bind to plaques, activate microglial cells and finally clear plaques (Bard et al 2000). Another hypothesis about a possible mechanism of Aβ immunotherapy is called the peripheral Aβ sink theory (DeMattos et al 2001). Using passive immunisation, DeMattos et al have found that m266, an Aβ monoclonal antibody, induces a rapid 1000-fold

increase in plasma Aβ in PDAPP mice. This increase may be caused by a change in Aβ equilibrium between the CNS and plasma, suggesting that m266 antibodies have removed Aβ deposits from the brain by altering the equilibrium of Aβ between brain, CSF and plasma.

After the first Aβ vaccine study on PDAPP mice was published in 1999, Elan started a Phase 1 clinical trial of AN-1792 (the Aβ vaccine). Results from the Phase 1 clinical trial looked promising in a small number of participants, as AN-1792 was apparently safe and well tolerated by these people (Schenk 2002) (but see a case report (Nicoll et al 2003)). After the success of the Phase 1 trial, AN-1792 has gone to Phase IIa clinical trial, in which much more patients around the world have been involved. However, a serious side effect of meningoencephalitis has recently been observed in a very small proportion of the participants in the Phase IIa trial, so all study dosing was halted in January 2002 (Schenk 2002). It remains unknown why this side effect occurred.

5.1.2. Preclinical evidence for Aβ immunotherapy.

Early preclinical studies on the effects of Aβ vaccines on learning and memory of APP Tg mice were very positive.

In one study, TgCRND8 mice, which express a mutant human APP695 gene harbouring both the Swedish and Indiana mutations, were immunized at 6, 8, 12, 16 and 20 weeks (Janus et al 2000). A longitudinal design was employed to repeatedly test these mice at 11, 15, 19 and 23 weeks of age using the standard watermaze reference memory task. The data were analyzed using a mixed model analysis of variance, with immunogen (Aβ vs IAPP) and genotype (TgCRND8 vs non-Tg) as between-subject factors, and age as a within-subject factor. The Aβ-vaccinated Tg mice performed significantly better than IAPP-treated Tg mice in the acquisition training, although Aβ-vaccinated TgCRND8 mice were still significantly worse than non-Tg controls (Janus et al 2000). A significant reduction of Aβ deposits was also observed in Aβ-vaccinated Tg mice. Thus, an Aβ vaccine can produce a partial rescue effect in TgCRND8 mice. However, the authors did not observe any main genotype or immunisation effects in post-training probe tests, as the TgCRND8 Tg mice displayed

relatively normal reference memory. The impact of the vaccine seemed to be largely restricted to performance effects during training.

The effects of active Aβ vaccination on learning of PS1/APP double transgenic mice were investigated by a different group using a novel radial-arm watermaze (Morgan et al 2000). It is suggested that this task is very sensitive to detect plaque-related learning deficit and is more efficient in sample size requirements than the normal watermaze task. A longitudinal design was used and untreated non-Tg, Aβ-vaccinated or KLH (keyhole limpet haemocyanin, a control peptide)-vaccinated Tg mice were tested first at 11.5 months of age. All three groups displayed good learning. After five monthly inoculations of either Aβ or KLH, the same animals were re-tested at 15.5 months. Interestingly, although KLH-vaccinated Tg mice now failed to learn this task, non-Tg and Aβ-vaccinated Tg mice learned it very well, suggesting a significant Aβ vaccination effect. Unexpectedly, there were no effects of the Aβ vaccine on plaque burden in the Aβ-vaccinated Tg mice, so the improved learning of Aβ-vaccinated PS1/APP double Tg mice was explained in terms of reduced levels of soluble Aβ in the brain (Morgan et al 2000). This explanation can not be the whole story, as 11.5-month-old PS1/APP Tg mice displayed high levels of soluble Aβ and Aβ plaques, and showed normal spatial learning in the radial-arm water maze. A further puzzling feature of this study was the very small group sizes (Morgan et al 2000).

Recently, effects of passive Aβ immunisation on object recognition memory of PDAPP mice was explored (Dodart et al 2002). In this study, m266, an Aβ specific monoclonal antibody, was first administered into 24-month-old PDAPP mice for six weeks, once a week. The authors reported that the impaired object recognition memory in PDAPP mice is reversed by the administration of m266. Furthermore, m266 was also acutely injected into 11-month PDAPP mice, and the mice were then tested 24 hours later. It was observed that m266-treated PDAPP mice displayed a comparable level of object recognition memory to that of non-Tgs, although PBS-treated PDAPP mice displayed chance performance. Plaque burden was unaffected by the treatment of m266 in these two studies, however, and the level of plasma Aβ40 and Aβ42 was significantly increased as compared to PBS-treated PDAPP mice. It was suggested that the rescued object recognition memory in m266-treated animals

was associated with the cerebral clearance of Aβ40 and Aβ42, as increased plasma concentrations were observed.

5.1.3. Purpose of this Aβ vaccine study.

The preclinical studies discussed above brought a huge optimism to Aβ immunotherapy. On the other hand, the importance of amyloid plaques to dementia and cognitive impairment of AD may have been challenged by studies from Morgan et al and Dodart et al, as both of them clearly indicate that Aβ immunotherapy can significantly improve learning or memory of APP Tg mice without effect upon amyloid plaques.

Although the preclinical findings discussed above are extremely exciting, they have not answered several fundamental questions. First, in Janus et al's study, as only very young (23 weeks of age) animals were tested, it is possible that an Aβ vaccine may only partially rescue learning in APP Tg mice at early stage of life. In this study, the biggest rescue effect of Aβ vaccines can be seen as early as 11 weeks of age. As TgCRND8 mice have not developed any plaques at this age (Figure 2b of Janus et al), it clearly suggests that Aβ vaccines have effects on plaque-independent or soluble Aβ-dependent processes. It is unknown whether the same animals would display any significant rescue effects at much older age. It also remains unknown whether Aβ vaccines will show any effects on spatial learning when vaccinated at an older age, at which many plaques have developed in the brain. Second, although Morgan et al observed a rescue of the learning impairment in PS1/APP mice by active Aβ immunisation, plaque burden was unaffected at all. Paradoxically, the spatial learning deficit of PS1/APP mice has been claimed to be plaque-related by these same authors (Morgan et al 2000). If so, why should not we see any change in plaque burden in the cognitively improved Tg mice induced by Aβ vaccines?

Three fundamental questions related to potential clinical treatment of AD with active Aβ vaccination were addressed in this study: first, can Aβ vaccination rescue the plaque-related learning deficits in PDAPP mice using the trials to criterion and learning capacity task? Second, can it improve the Aβ-independent learning deficit in PDAPP mice? Third, can it have any impacts on plaque burden and soluble Aβ levels? Therefore, two separate Aβ vaccination experiments were designed. In

Experiment 1, Aβ immunisation started in PDAPP mice at 11 months and lasted for 5 months. As Aβ plaques were already seen in the brain at this age, this design is then called the 'plaque treatment' study. In Experiment 2, PDAPP mice were immunised at 7 months for 9 months. As only few plaques can be detected in the brain at 7 months, this design is called the 'plaque prevention' study. After treatments with AN-1792, spatial learning was examined using the trials to criterion and learning capacity task. At end points of these studies, electrophysiology and ELISAs of Aβ levels were conducted as well.

5.2 Methods.

5.2.1. The subjects.

All mice were non-white heterozygous males, on a Swiss Webster/DBA/C57BL6 triple strain background. In the treatment study, total 84 mice were tested (PDAPP vaccinated, n=24; PDAPP vehicle, n=19; non-Tg vaccinated, n=22; non-Tg vehicle, n=22). In the prevention study, total 73 mice were tested (PDAPP vaccinated, n=18; PDAPP vehicle, n=20; non-Tg vaccinated, n=20; non-Tg vehicle, n=15). The mice were group-housed (2-4 mice each cage). The experimenter was blind to both genotype and vaccine status.

5.2.2. The watermaze.

The watermaze and escape platform were as used previously.

5.2.3. The experimental design.

Two studies, 'treatment' and 'prevention', were designed. The mice first received Aβ vaccinations for either 5 months (treatment study) or 9 months (prevention study). Due to commercial reasons, the vaccination treatments for all mice were conducted in Elan Pharmaceuticals at San Francisco. After the treatment, all mice were shipped to Edinburgh. After one week of habituation in the lab, the mice first underwent a 5-day cuetask, followed by the concurrent trials to criterion and learning capacity task, which took 10-20 days (Fig. 5.2.1). Due to the large animal numbers in the two studies, there was insufficient time to do the object recognition task. After the serial spatial learning task was completed, all animals were subjected to *in vitro* slice electrophysiology and ELISAs for Aβ quantification.

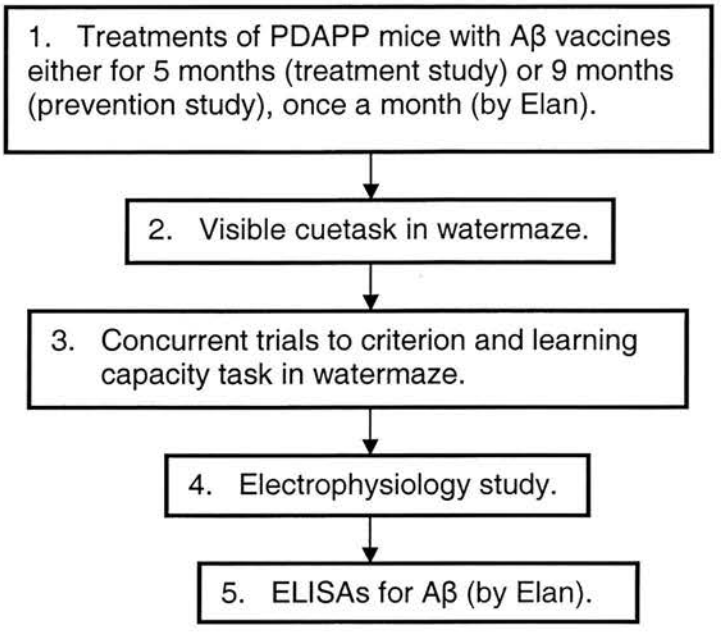

Figure 5.2.1 Experimental Design.

5.2.4. Aβ vaccination of PDAPP mice.

Although Aβ immunisation procedures were conducted in Elan Pharmaceuticals by our collaborators, they are described as follows. Aβ peptide was freshly prepared from lyophilized powder for each set of injections. For Aβ immunisations, 2mg human Aβ42 (US Peptides) was added to 0.9 ml deionized water and the mixture was vortexed to generate a relatively uniform suspension. A 100-ml aliquot of 10 × PBS (where 1 × PBS is 0.15M NaCl, 0.01M sodium phosphate, pH 7.5) was added. The suspension was vortexed again and incubated overnight at 37 °C for use the next day. The control immunogen was MPL-AF, a common mixed adjuvant to help elicit the immune response for B-cells in vaccinations. Aβ42 or MPL-AF peptides (100mg antigen per injection) were emulsified 1:1 (v/v) with complete Freund's adjuvant for the first immunisation, followed by a boost in incomplete Freund's adjuvant at 2 weeks, and monthly thereafter. Aβ42 or MPL-AF in PBS alone was injected from the fifth immunisation onward. Titres were determined by serial dilutions of sera against either aggregated Aβ42 or MPL-AF which had been coated onto microtitre wells. Detection used goat antimouse immunoglobulin conjugated to horseradish peroxidase and slow-TMB (3,30,5,59-tetramethyl benzidine; Pierce) substrate. Titres were defined as the dilution yielding 50% of the maximal signal.

5.2.5. Visible cuetask.

There were 5 days, 4 trials per day, and platform location was changed across trials.

5.2.6. Trials to criterion and learning capacity task.

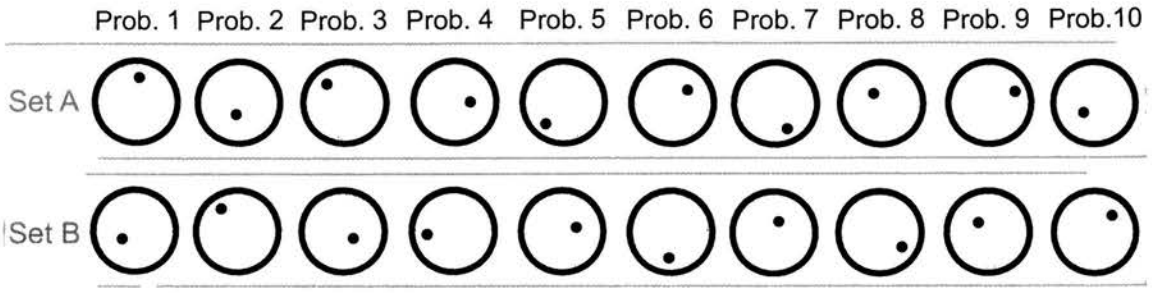

Figure 5.2.2 Platform Location Design. For counterbalancing reason, two sets of 10 platform locations were designed to test spatial learning of the mice. Half of the animals were trained by Set A, and the other half by Set B.

The trials to criterion and learning capacity tasks were concurrently conducted in both the treatment and prevention studies, whichever took longer. Figure 5.2.2 shows two sets of 10 different locations.

5.2.7. Electrophysiology.

The standard transverse slice was made using the same procedure described in Chapters 2 and 4. Input-output (I-O) curves were induced using 18 different intensities of stimulation (0.2, 0.4, 0.6, 0.8, 1, 1.2, 1.4, 1.6, 1.8, 2, 10, 20, 30, 40, 50, 60, 80 and 100 V). At any intensity of the stimuli, 2-3 fEPSPs were elicited. Due to the limited time available, only hippocampal synaptic transmission of the mice was examined, and LTP experiments for 180 mice could not be performed.

5.2.8. Tissue preparation and ELISA analysis of Aβ.

Briefly, three brain areas, including the cerebellum, hippocampus and cortex, were dissected and put into ice cold pre-weighed tubes. 5M guanidine buffer was added to each tube and the tissue was completely homogenized with a hand-held homogenizer. ELISA analysis of Aβ on all samples was conducted in Elan Pharmaceuticals and the methods for ELISA were described in Chapter 2.

5.3 Results.

1. Aβ vaccination did not affect normal cuetask learning of PDAPP mice.

Statistical analysis revealed no significant vaccination effects in either the treatment or prevention study ($F<1$; Fig.5.3.1). Interestingly, an early deficit of PDAPP mice on day 1 was observed in both the treatment and prevention studies (For the former: $F=20.48$, df 1/80, $p<0.001$; for the latter: $F=8.47$, df 1/69, $p<0.01$), indicating that PDAPP mice took much longer to approach the platform on day 1. However, after day 1, as all Aβ42- or MPL-AF-treated PDAPP mice learned this task to a comparable level to that of non-Tgs, PDAPP mice displayed no obvious deficit in sensorimotor function.

2. Aβ vaccinations did not improve learning deficits of PDAPP mice using the trials to criterion task.

Figure 5.3.2A (performance on individual platforms) and 2B (mean trials to criterion across five locations) show the performance of Aβ42- and MPL-AF-treated PDAPP and non-Tg mice in learning five different platform locations of the trials to criterion task for the treatment study. ANOVA revealed a main transgene effect ($F=28.17$, df1/80, $p<0.001$), but no vaccine effect ($F<1$).

Similarly, Figure 5.3.2C and 2D show the trials to criterion in the prevention study. Again, ANOVA revealed only a main transgene effect ($F=8.87$, df1/69, $p<0.01$) but no vaccine effect ($F<1$). These data indicated that Aβ immunisation of PDAPP mice with Aβ vaccines for either 5 months or 9 months did not improve impaired spatial learning.

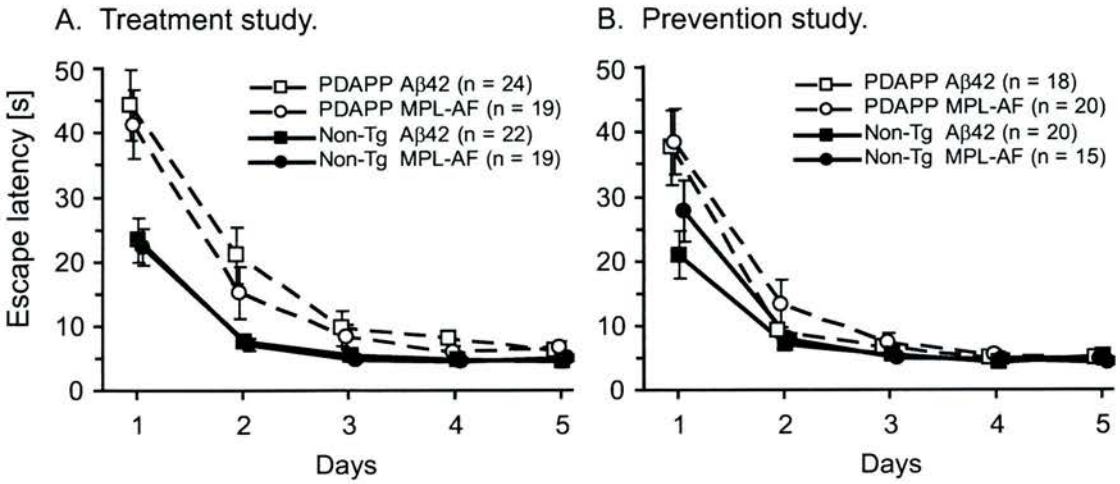

Figure 5.3.1 Effects of Aß Vaccines on Cuetask Performance of PDAPP Mice.
There was no vaccination effect on this task. A. Treatment study. B. Prevention study.

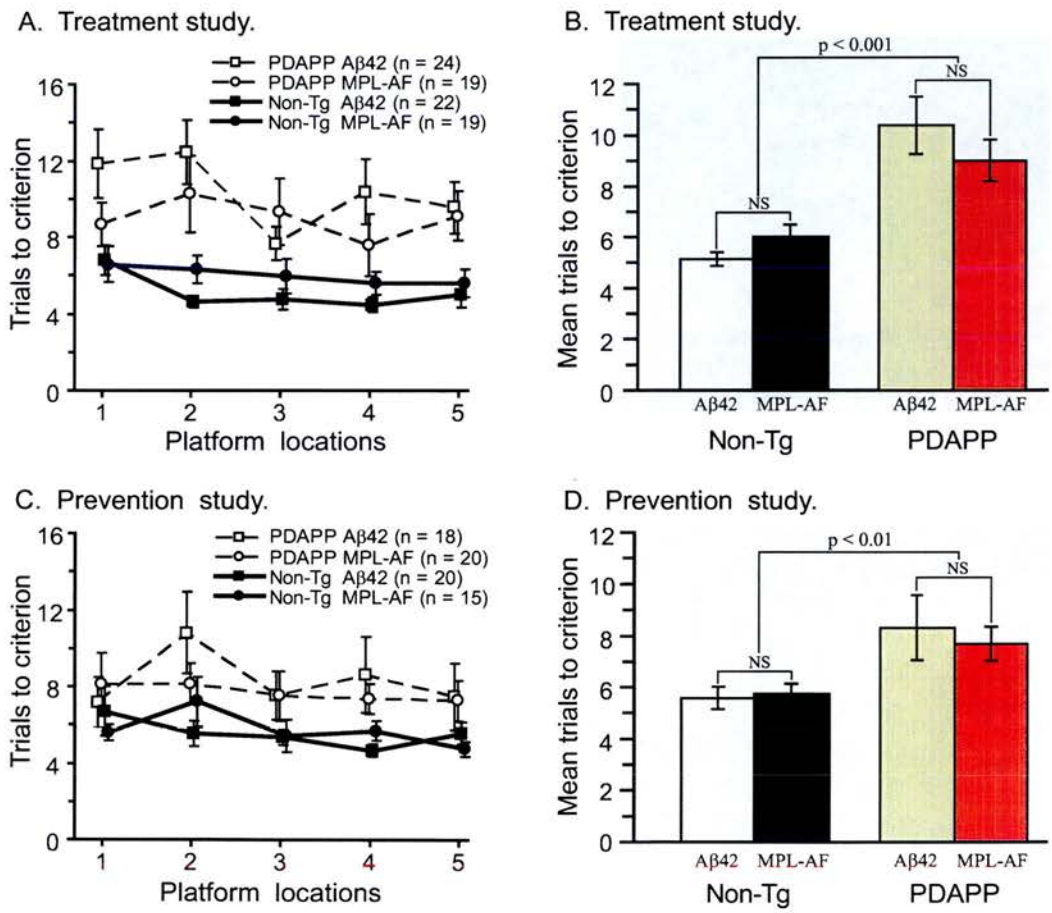

Figure 5.3.2 Effects of Aß Vaccines on Trials to Criterion of PDAPP Mice.
A. There was a significant genotype effect but no vaccination effect on trials to criterion in the treatment study. B. Mean trials to criterion in the treatment study. C. There was a significant genotype effect but no vaccination effect on trials to criterion in the prevention study. D. Mean trials to criterion in the prevention study.

3. Aβ vaccinations did not rescue learning deficit of PDAPP mice in the learning capacity task.

The effects of Aβ vaccines on spatial learning of PDAPP mice were further examined using the learning capacity task. Figure 5.3.3 shows the results for both the treatment and prevention study using Aβ vaccine or a control immunogen, MPL-AF. In terms of total number of platform locations learned in 10 days, Aβ42- and MPL-AF-treated PDAPP mice were significantly impaired as compared to non-Tg mice (Treatment study: $F=40.58$, df 1/80, $p<0.001$; Prevention study: $F=12.58$, df 1/69, $p<0.01$). However, no vaccination effects were found in two studies (Treatment study: $F<1$; Prevention study: $F<1$). These results clearly indicated that, short-term (5 months) or long-term (9 months) treatment of Aβ vaccines did not show any significant effects on impaired learning capacity of PDAPP mice.

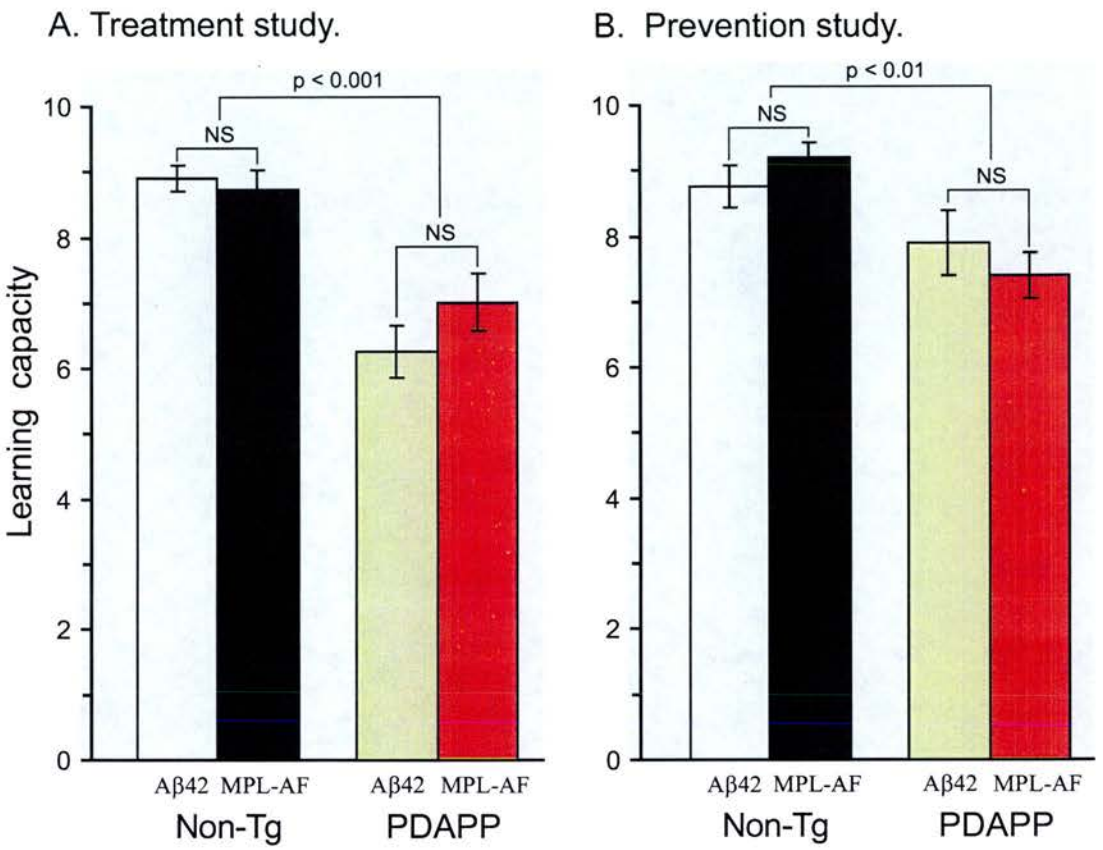

Figure 5.3.3 Effects of Aß Vaccines on Learning Capacity of PDAPP Mice.
A. There was a significant genotype effect but no vaccination effect on learning capacity in the treatment study.
B. There was a significant genotype effect but no vaccination effect on learning capacity in the prevention study.

4. Aβ vaccines did not improve deficit of synaptic transmission of PDAPP mice.

The effects of Aβ vaccination on synaptic transmission of PDAPP mice were investigated using the same animals behaviourally tested. Input-output curves were recorded from hippocampal slices of all mice. Figure 5.3.4 shows the I-O curves for the treatment and prevention study. In both studies, Aβ42- and MPL-AF-treated PDAPP mice exhibited significantly decreased fEPSP slope (Treatment study: $F=70.90$, df 1/75, $p<0.001$; Prevention study: $F=19.44$, df 1/60, $p<0.001$), but no vaccination effects were observed ($F<1$, for both the treatment and prevention studies).

Finally, as significant correlations between synaptic transmission in the hippocampus and behavioural performance have been reported in Chapter 4, a rank correlation analysis was then conducted between the sizes of fEPSPs slope of hippocampal slices and learning capacity of PDAPP mice. Significant correlations were again observed (Figure 5.3.5). Figure 5.3.5A shows the significant correlation between maximum fEPSP and learning capacity in PDAPP mice for the treatment study ($r=0.379$, $p<0.02$). Figure 5.3.5B shows the correlation between maximum fEPSP and learning capacity in PDAPP mice for the prevention study ($r=0.367$, $p<0.03$). When all PDAPP mice from these two studies were combined together, the correlation between maximum fEPSP and learning capacity was again highly significant ($r=0.411$, $p<0.001$).

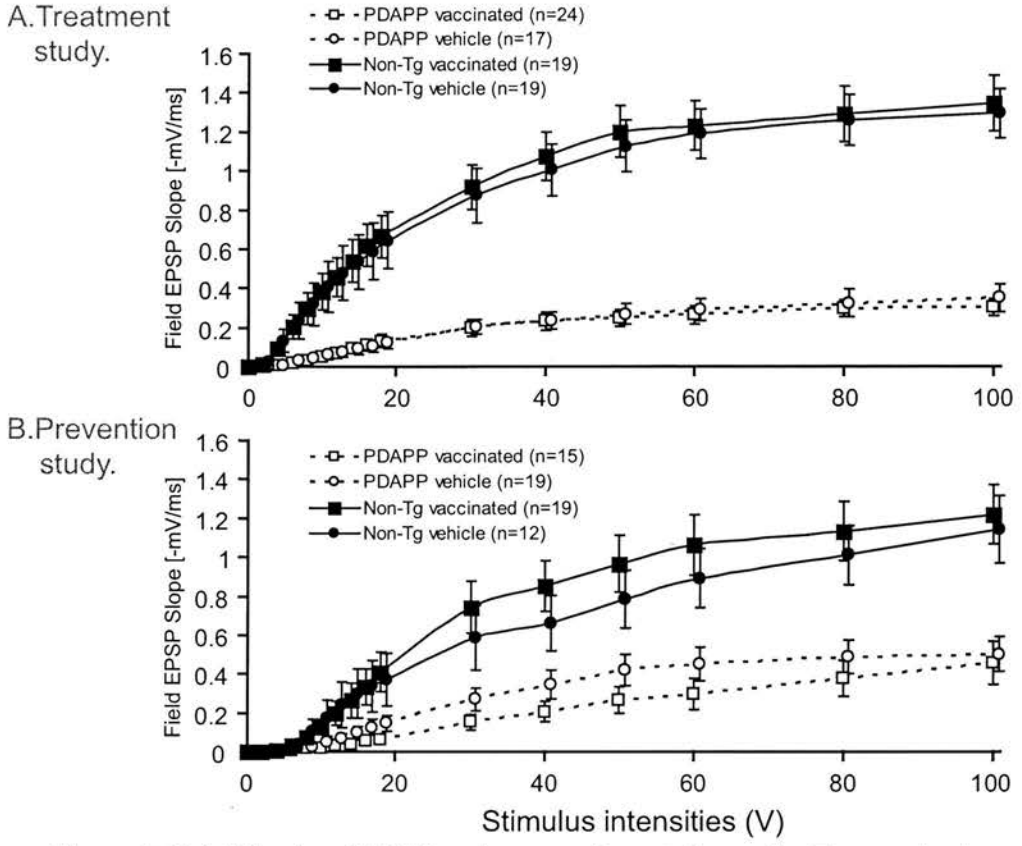

Figure 5.3.4 Effects of Aß Vaccines on Basal Synaptic Transmission of 16-17 Months PDAPP Mice. A. Input-output curves for the treatment study. There was only a significant genotype effect but no vaccination effect (F<1). B. Input-output curves for the prevention study. There was only a significant genotype effect but no vaccination effect (F<1).

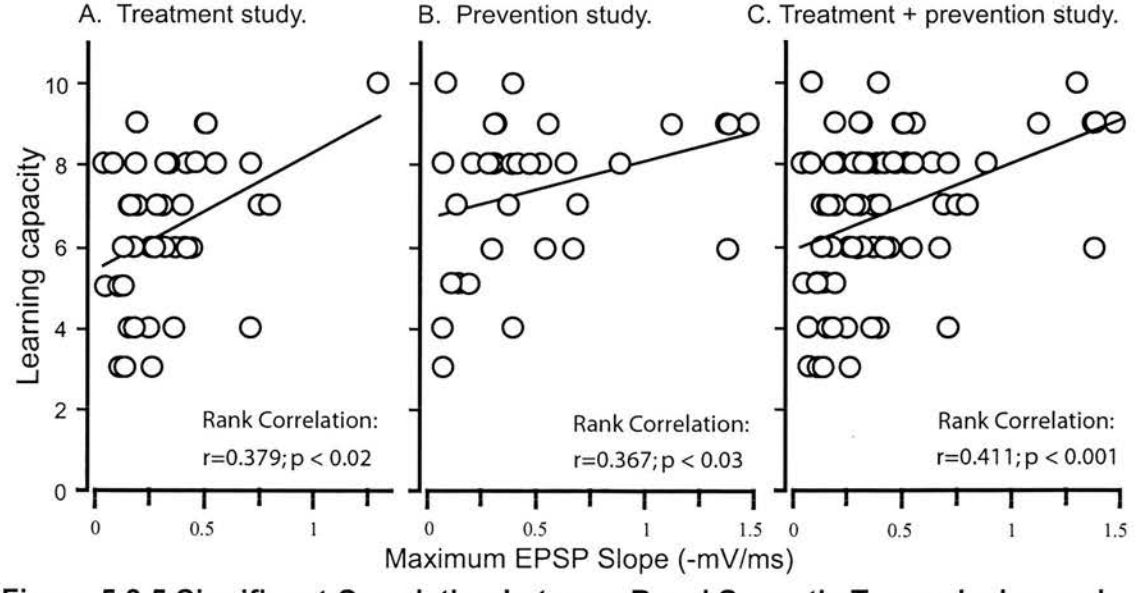

Figure 5.3.5 Significant Correlation between Basal Synaptic Transmission and Behavioural Performance. There was a significant correlation between the maximum size of fEPSP of the hippocampus and learning capacity of PDAPP mice in the treatment study (A), the prevention study (B) and the combined treatment and prevention study (C).

5.4 Discussion.

1. Aβ immunisation failed to improve cognition and synaptic transmission, but improved pathology of PDAPP mice.

Using a short-term treatment (5 months) or a long-term prevention (9 months) design, the effects of Aβ immunisations on spatial learning of PDAPP mice were examined in this study using the trials to criterion and learning capacity task. The treatment and prevention studies indicated that Aβ-vaccinated PDAPP mice did not show any improvement on learning a series of different platforms in the watermaze, no matter when the Aβ immunisation started (either at 7 or 11 months), and no matter how long the treatment lasted (either at 5 or 9 months). Furthermore, electrophysiology data also showed no rescue effects on the reduced synaptic transmission of PDAPP mice in both studies.

After behavioural and electrophysiology experiments were completed, brain tissues were processed and ELISAs was conducted by our collaborators at Elan to examine whether Aβ vaccines reduced pathology of the same mice behaviourally tested. Interestingly, Aβ vaccines seemed reasonably effective in reducing total Aβ levels in the brain. Table 1 has listed the Aβ42 levels in the brain of Aβ- or MPL-AF-treated PDAPP mice. ELISA results from Elan indicated that Aβ vaccines significantly reducd Aβ42 levels in PDAPP mice ($F=26.3$, df 1/73, $p<0.0005$). As reported previously, 9-month Aβ immunisation of PDAPP mice in the prevention study produced significantly lower levels of Aβ42 than 5-month immunisation in the treatment study ($F=8.0$, df 1/73, $p<0.01$). However, significant reductions of Aβ42 did not show any benefit to PDAPP mice in performing the trials to criterion and learning capacity task. These results thus suggest that Aβ42 vaccines might only be effective to improve AD-like pathology but not impaired cognition of APP Tg mice.

Units = ng/gm	Non-vaccinated PDAPP	Vaccinated PDAPP	% of decrease
Treatment	Aβ42 = 6902 +/- 562	Aβ42 = 3778 +/- 631	45.26%
Prevention	Aβ42 = 5219 +/- 771	Aβ42 = 1927 +/- 387	63.08%

Table 5.1 Reduction of Aβ42 in Aβ-vaccinated PDAPP Mice. 5-month treatment of Aβ vaccines produced 45.26% of Aβ42 reduction in PDAPP mice; however, 9-month treatment produced 63.08% of Aβ42 reduction.

2. Task sensitivity.

The failure of Aβ vaccines to improve the impaired learning of PDAPP mice, using a treatment and a prevention design, may also raise a question of the sensitivity of the trials to criterion and learning capacity tasks, as our findings are inconsistent with those of previously published reports (Dodart et al 2002, Janus et al 2000, Morgan et al 2000). Compared to the standard acquisition training in the watermaze used by Janus et al (2000), our serial spatial learning task is more sensitive to reveal both age-related and age-independent learning deficits in PDAPP mice, as Janus et al have not found any apparent age-related learning deficit in TgCRND8 mice using the acquisition version of reference memory task (the youngest groups (11-week-old) showed the worst performance) (Janus et al 2000). Moreover, as all TgCRND8 mice performed comparably to age-matched non-Tgs in probe trials at four different testing ages, this suggests that the reference memory task in the watermaze is not sensitive to detect memory impairment in TgCRND8 mice.

In this study, as we were trying to address whether Aβ vaccines are effective to improve plaque-related and age-independent learning deficits in PDAPP mice, we did not design any experiments using even earlier Aβ immunisation (i.e. before 2 months of age). However, as the prevention and treatment study did not show any significant Aβ vaccination effects on cognition of PDAPP mice, it remains unknown whether earlier Aβ42 immunisation can produce any significant effect on impaired learning of PDAPP mice at young and old ages. Interestingly, analysis of the performance for Aβ42-vaccinated animals in the treatment and prevention studies revealed a significant treatment effect in PDAPP mice groups (Fig. 5.3.3: $F=5.58$, df 1/77, $p<0.02$), but not in non-Tg groups ($F<1$), possibly suggesting that early treatment of Aβ vaccines might improve the performance of PDAPP mice in spatial learning. However, there was no overall vaccination effect for all PDAPP groups ($F<1$). It seems possible that earlier Aβ immunisation (before 2 months) might be effective to prevent mild functional damage of the brain caused by abnormal accumulation of Aβ or Aβ plaques in Tg animals, however, late Aβ immunisation (after 7 months) is not effective to improve the pre-existing brain lesion caused by Aβ and/or amyloid plaques, and the pre-existing memory impairment.

3. Aβ immunotherapy may be ineffective in the treatment of cognitive loss of AD.

From this study, on the one hand, an Aβ vaccine was very effective to reduce AD-like pathology in PDAPP mice. On the other hand, the vaccine did not produce any improvement in spatial learning. These findings suggest that active Aβ immunotherapy is useful for the treatment of AD-like pathology, but might not be an ideal treatment strategy for memory loss of AD. More recently, Morgan's group have re-tested active Aβ immunotherapy using 16-month-old PS1/APP Tg mice. They used 4 immunisations of Aβ42 biweekly to the Tg mice. There was no improvement in the impaired learning when tested at 18 months using the same radial-arm watermaze protocols (Austin et al 2003). Together with findings from this Aβ vaccine treatment or prevention study, it strongly suggests that active Aβ immunotherapy might not be effective in the treatment of cognitive impairment in AD.

Due to side effects of AN-1792, the clinical study dosing has been halted recently. However, clinical efficacy assessment such as MRI changes, cognitive decline and safety is still continuing. After the suspension of AN-1792 dosing, Hock et al continued to evaluate cognitive functions in a cohort of 30 patients with mild-to-moderate AD, based at Zurich. They have recently reported that 20 AN-1792-treated patients successfully produced antibodies against Aβ and showed significantly slower rates of decline in cognition and daily activities (Hock et al 2003). However, the sample size (AD subjects=20) of Hock's study is still small. Before data on a large proportion of the 376 patients on cognitive function and daily activities for the phase IIA clinical study on AN-1792 are published, it will be difficult to draw firm conclusions. Overall, much more work needs to be done to understand mechanisms of the side effects caused by Aβ vaccines before a new clinical trial is re-launched in the future.

Chapter 6: Investigations of Spatial Learning and Synaptic Transmission in PS1cKO;APP Mice.

6.1 Introduction.

1. The importance of PS1 and γ-secretase.

The significant importance of the presenilins in AD is recognized by genetic evidence showing that mutations of presenilin-1 (PS1) account for most cases of early-onset of FAD (25~50%), whereas the linkage of APP mutations to FAD is very small (~5%). Since PS1 was first identified in 1995, its structure, metabolism and other biological properties have been extensively studied (Levy-Lahad et al., 1995; Rogaev et al., 1995; Sherrington et al., 1995; Takashima et al., 1996; De Strooper et al., 1997). Recently, the importance of PS1 in early development was discovered following knockout experiments. Homozygous PS1-/- mice die prematurely, and their embryos display abnormal patterning of the axial skeleton and spinal ganglia, suggesting an important physiological role of PS1 in neuron development (Shen et al., 1997; Wong et al., 1997).

One of the most important functions of PSs is as the active site of γ-secretase, which cleaves APP and Notch to produce Aβ and NICD. Studies using overexpression and knockout techniques indicate that overexpression of mutant human form of PS leads to overproduction of Aβ in transgenic mice (Borchelt et al., 1996; Duff et al., 1996) and in stably transfected cells (Ancolio et al., 1997; Tomita et al., 1997). APP-Semliki Forest virus (SFV)-infected cultured neurons from the hippocampus of PS1 knockout mice produce significantly reduced levels of Aβ40 and Aβ42 (De Strooper et al., 1998). Recent evidence indicates that PS1 is part of the γ-secretase complex, which is generally believed to be composed of PSs, Nct, Aph1 and Pen2 (Kimberly et al., 2003).

2. Involvement of PS1 in spatial learning and memory.

Recent evidence has suggested that PS1 is involved in learning and memory. Using the newly developed conditional gene knockout techniques, two different PS1 conditional knockout mice (PS1cKO), in which PS1 inactivation is restricted to the

postnatal forebrain, were generated by two separate groups (Feng et al., 2001; Yu et al., 2001). Yu and colleagues reported that, while PS1cKO mice exhibit normal basal synaptic transmission, LTP and LTD of the hippocampus, they also display a significant long-term deficit in spatial memory (Yu et al., 2001). However, Feng et al did not find any deficit in spatial learning using a second line of PS1cKO mice (Feng et al., 2001). The discrepancy between these two groups may be due to different training protocols. Indeed, the learning deficit of PS1cKO mice observed by Yu et al (2001) is quite subtle.

3. Inhibition of PS1 or γ-secretase for intervention of AD.

As Aβ is produced as a result of sequential proteolytic cleavages of APP by the β- and γ-secretases, these two proteases have become the top targets for therapeutic intervention of AD. During the past few years, important progress has been made in searching for effective inhibitors for the β- and γ-secretases. However, as genetic inactivation of PS1 causes early perinatal lethality in homozygous PS1-/- animals, PS1 inhibition may produce severe side effects on animals and humans. This suggests that γ-secretase may not be an ideal target for therapeutic development. By contrast, BACE seems to be a more promising target than the γ-secretase, as BACE1-/- knockout animals (Cai et al., 2001; Luo et al., 2001) or BACE1/2 double knockouts display no gross phenotype (such as embryonic lethality). However, as conditional inactivation of neuronal PS1 in the forebrain reveals no gross abnormalities, partial or selective inhibition of PS1 (or γ-secretase) may still be possible for anti-AD therapy.

Modelling the amyloidosis of AD in rodents has been very successful for many years, as most different lines of APP Tg mice display age-related Aβ accumulation and amyloid plaque deposition. They also exhibit learning deficits which are either age-related or age-independent. Thus, inter-crossing of APP Tg and PS1cKO mice should allow us to examine whether inactivation of PS1 in the forebrain has any effects on both pathology and cognitive impairment of APP Tg mice.

4. The study of PS1cKO;APP mice by Shen's group.

Shortly after Shen's group published PS1cKO mice in 2001, they crossed these mice with an APP Tg line (J20) (Mucke et al., 2000), and generated PS1cKO;APP mice. The APP line J20 is similar to line J9 (described in Chapter 1). Briefly, J20 APP mice

overexpress mutant human APP with both the Indiana and Swedish mutations under the control of a β-chain PDGF promoter. J20 line mice display very high levels of Aβ production and start the formation of plaques in the brain as early as 5-6 months. However, behavioural study of this line has never been reported. In early 2002, Shen's lab did a thorough study of pathology, electrophysiology and behaviour on J20 mice while also testing PS1cKO;APP ones. What they have found on these mice is briefly reviewed as follows.

4.1. The generation of PS1cKO;APP mice by Shen's group.

J20 mice were first crossed with homozygous floxed PS1 (*fPS1/fPS1*) mice to get fPS1/+;APP mice. The latter were then bred to *fPS1/fPS1* again to obtain *fPS1/fPS1;APP* mice. Finally, *fPS1/fPS1;APP* mice were crossed to PS1cKO (*fPS1/fPS1;CaM-Cre*) to get PS1cKO;APP (*fPS1/fPS1;CaM-Cre;APP*) mice.

4.2. PS1cKO;APP mice display a significant reduction of Aβ.

Western analysis revealed that 2- and 6-month old APP and PS1cKO;APP mice display comparable levels of full-length APP (mouse and human) in the cortex which are 2-fold the endogenous level of mouse APP found in PS1cKO and control mice. The level of APP CTFs in PS1cKO;APP mice increases in an age-dependent manner. Quantitative ELISAs reveal an age-dependent accumulation of Aβ40 and Aβ42 in APP mice, but highly significantly reduced Aβ40 and Aβ42 in PS1cKO;APP mice. The levels of Aβ40 and Aβ42 are comparable between 2 and 6 months of age in PS1cKO;APP mice.

4.3. PS1cKO;APP mice display no amyloid plaques and gliosis.

At 3 months of age, both APP and PS1cKO;APP mice display no plaques in the brain. However, at 6 months, although APP mice exhibit plaques in the hippocampus and cortex, PS1cKO;APP mice display no plaques in the same brain areas. While 6-month APP mice develop much microgliosis and astrocytosis, PS1cKO;APP mice display neither of them.

4.4. PS1cKO;APP mice display a learning deficit in the watermaze.

3- and 6-month APP, PS1cKO;APP, PS1cKO and control mice were tested in a watermaze using the standard reference memory task. They were trained for 5 days (6

trials per day, 2 trials per block, interblock interval=2 hr) with a hidden platform in the watermaze. 60-s probe tests were given following the training of day 3 and day 5. APP and PS1cKO;APP mice were found to perform this task significantly more poorly than control and PS1 mice. Analysis of the two probe trials reveals that both APP and PS1cKO;APP mice did not show any preference to the training quadrant, but control and PS1 mice spent significant more time in the training quadrant. This is a disappointing result but should not be taken as the last word on the prospects of exploiting the γ-secretase.

5. Purpose of this study on PS1cKO;APP mice.

These unpublished data suggest that, although inactivation of PS1 in the forebrain effectively prevents the pathology of APP mice, it does not effectively restore the impaired reference memory. The questions to raise about this deficit in spatial learning in PS1cKO;APP mice are: can this deficit be seen in all watermaze tasks, or is it task-dependent? If it is task-dependent, could we see any rescue effect in PS1cKO;APP mice using the newly developed trials to criterion and learning capacity paradigms in watermaze? If these novel protocols can reveal rescue effects on spatial learning of PS1cKO;APP mice, will these effects be age-dependent or age-independent?

Compared to the standard reference memory task, the trials to criterion and learning capacity task is very sensitive to reveal Aβ- and/or plaque-related learning deficit in APP Tg mice, so we have tried these novel watermaze tasks to investigate spatial learning of PS1cKO;APP mice.

6.2 Methods.

6.2.1. The subjects.

48 young (3-4-month-old) and 44 old (15-17-month-old) mice including control, PS1cKO, PS1cKO;APP and APP four genotype groups were shipped from Boston, Harvard University. The genders (male and female) were balanced in each genotype group. The mice were group-housed before they arrived at Edinburgh. However, after their arrival, they were singly housed. The experimenter was blind to the genotype of all mice. The mice were given *ad libitium* access to food and water.

6.2.2. The experimental design.

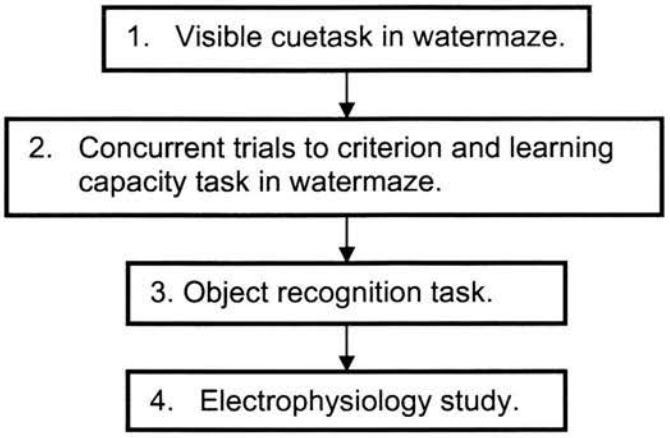

Figure 6.2.1 Experimental Design.

The watermaze was described in previous chapters. A cross-sectional design was used. There were two different age groups, one being 3-4 months and the other 15-17 months. A battery of behavioural tasks including cuetask, trials to criterion, learning capacity and object recognition task were used. After behaviour testing is completed, all mice were subjected to electrophysiology study to examine basal synaptic transmission and short-term synaptic plasticity.

6.2.3. Visible cuetask.

There were 5 days and 4 trials per day.

6.2.4. Concurrent trials to criterion and learning capacity task.

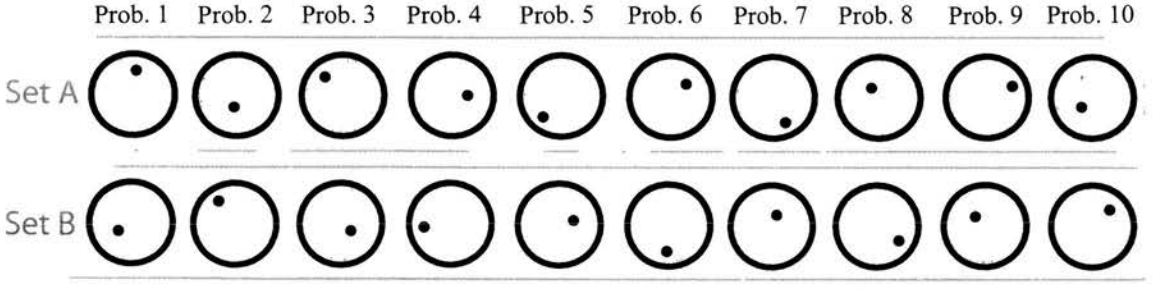

Figure 6.2.2 Platform Locations for Spatial Learning. Two sets of 10 platform locations were used. All the mice were randomly and equally assigned to two sub-groups to receive Set A or Set B training protocols.

The trials to criterion and learning capacity tasks were concurrently conducted, whichever took longer (Figure 6.2.2).

6.2.5. Object recognition task.

Several changes were made from previous studies: first, the session time for sample and choice phases was changed to 10 min, as this protocol has been reported to be more sensitive than ours (Dodart et al., 1999; Dewachter et al., 2002); second, in the sample phase, only one object, rather than two, was placed in the middle position between two side walls but 10 cm away from the back wall.

6.2.6. Electrophysiology.

Due to an upgrade of the recording system in the lab, a new automatic Hampden vibroslicer replaced our previous model for slice dissection, and fEPSPs of CA1 apical dendrites were recorded extracellularly using a steel electrode with our new recording AM system. After ~80 min incubation of slices in the recording chamber, input-output (I-O) curves were induced by 5 different intensities of stimulation (20, 40, 60, 80 and 100 μA) using a different current stimulation isolators (system upgrade: NL800, Digitimer, England). Due to time limit, LTP experiments for 92 mice were not carried out. Data were collected by the upgraded recording system based on Labview software written by Patrick Spooner, and stored into a Dell Dimension computer. The slope of field EPSP evoked by stimulation of the Schaeffer collateral-CA1 pathway was analyzed off-line.

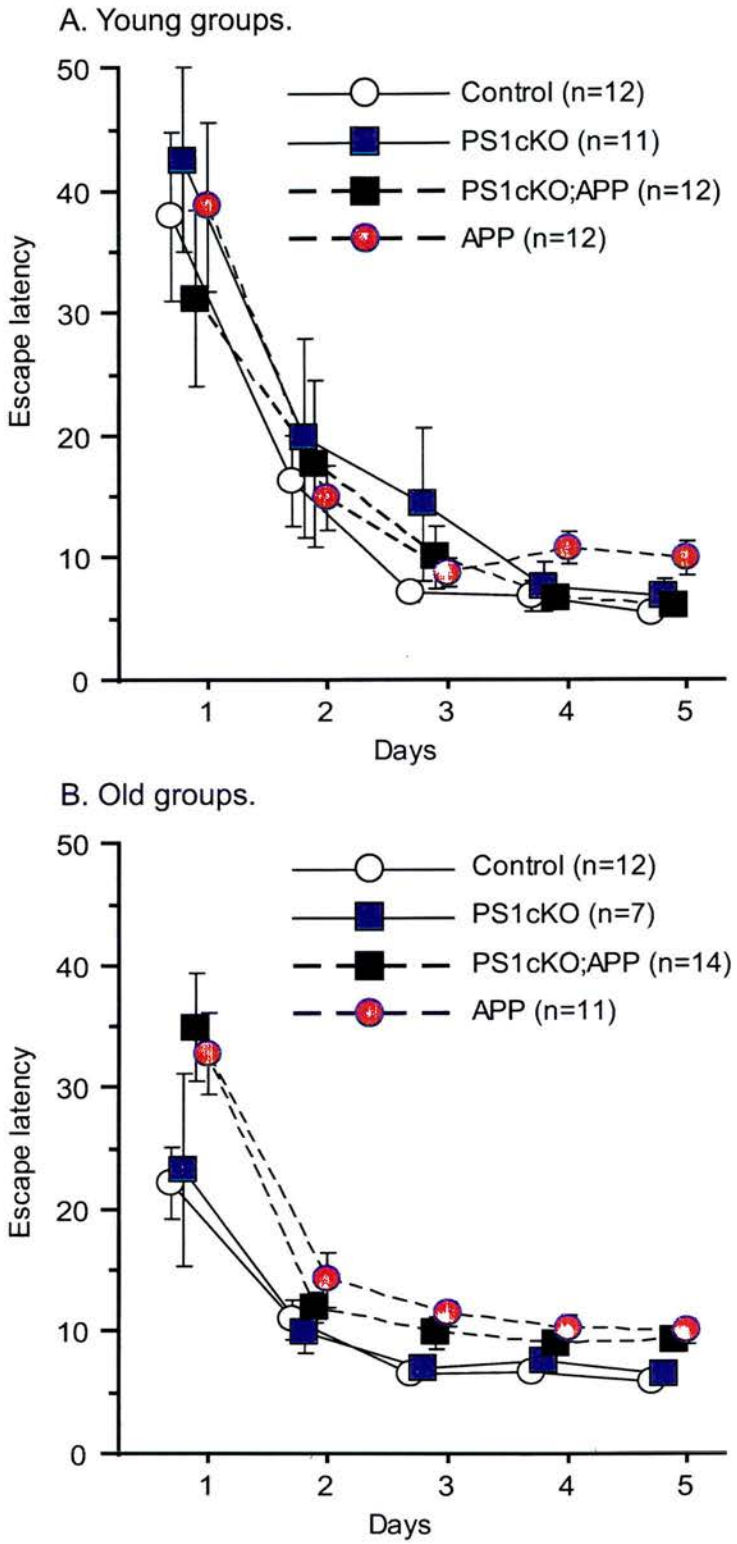

Figure 6.3.1 Cuetask Performance of the Mice.

A. Cuetask performance for mice at 3-4 months. There was no significant main genotype effect. B. Cuetask performance for mice at 15-17 months. There was a significant main genotype effect. Both APP and PS1cKO;APP mice performed worse than control and PS1cKO mice.

6.3 Results.

1. Selective age-related changes in cuetask learning.

Figure 6.3.1A shows the performance for four genotypes at 3-4 months of age in cuetask. Statistical analysis revealed that there was no significant genotype effect ($F<1$). All groups learned this task with less than 10 s of escape latency after three days of training, suggesting that, at this age, neither APP nor PS1cKO;APP mice had developed any sensorimotor problem. The overall performance of all four groups in cuetask at 15-17 months is shown in Figure 6.3.1B. Interestingly, a significant main genotype effect was observed ($F=5.84$, df3/40, $p<0.005$). Pair-wise analysis of variance showed that control mice were not different from PS1cKO group at this age ($F<1$), but were significantly different from APP ($F=12.72$, df 1/21, $p<0.005$) and PScKO;APP group ($F=10.22$, df 1/24, $p<0.005$), respectively.

It is unclear why old APP and PScKO;APP mice displayed a deficit in the cuetask. All four old genotype groups took less than 10 s to approach the visible platform on the last day of training. It seems that the basic learning ability of APP and PScKO;APP mice was indeed normal, for example, during the 5-day cuetask training, old APP group improved their performance from 32.7 s on day 1 to 9.9 s on day 5 (savings=22.7 s between day 1 and 5) and PS1cKO;APP group also showed 25.6 s improvement in escape latency from day 1 to day 5, by contrast, control and PS1cKO groups displayed 16.2 s and 16.7 s of savings between day 1 and 5, suggesting that neither APP nor PS1cKO;APP mice developed any apparent swimming or learning problem in this task. Old APP and PS1cKO;APP mice may have some subtle sensorimotor abnormalities, for example, several of them were observed to stay still in the water for a few seconds immediately after they were dropped from the start position. Perhaps these mice needed to adjust body position in order to get balanced in the water. This problem alone can explain their subtle deficit in this task. As old APP and PS1cKO;APP mice had reached an averaged escape latency of less than 20 s after 4 trials of cuetask training on day 1, they should readily reach the 20 s performance criterion on the trials to criterion and learning capacity task.

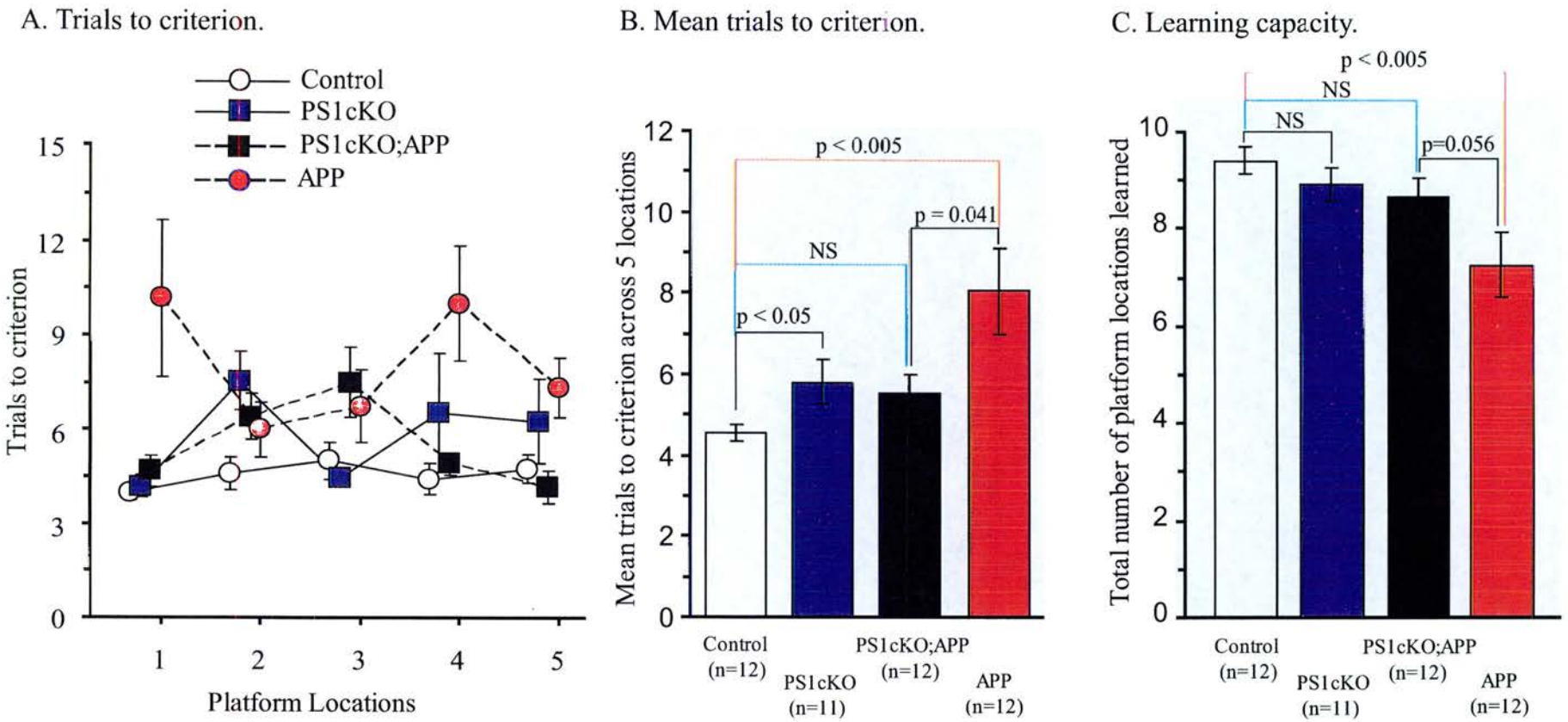

Figure 6.3.2 Performance of Young Mice in Spatial Learning. A. Trials to criterion in young mice across the five platform locations. B. Mean trials to criterion in young mice. Young APP mice were significantly impaired, but young PS1cKO;APP mice were not. C. Learning capacity in young mice. Young APP mice were again significant y impaired, but young PS1cKO;APP mice were not.

2. Young PS1cKO;APP mice show a rescue of learning.

Performance on the trials to criterion task by young animals on the 5 individual platform location is shown in Figure 6.3.2A. The mean trials to criterion across five platform locations is plotted in Figure 6.3.2B. Analysis of variance revealed a significant genotype effect (Fig. 6.3.2A and B: $F=5.12$, df3/43, $p<0.005$). Compared to control mice, separate ANOVA revealed that young PS1cKO mice displayed a subtle impairment in this task (Fig. 6.3.2A and B: $F=4.89$, df1/22, $p=0.038$), and young PS1cKO;APP mice performed this task very well and did not differ from control animals ($F=3.58$, df1/23, $p>0.05$). However, young APP mice were significantly impaired ($F=10.57$, df1/23, $p<0.005$). Very interestingly, compared to PS1cKO;APP group, young APP mice were also significantly impaired in learning the trials to criterion task ($F=4.73$, df1/23, $p<0.05$), suggesting a significant rescue effect of PS1 inactivation on spatial learning of young APP mice.

Results for the learning capacity task are quite similar to those for the trials to criterion, as statistical analysis also revealed a significant main genotype effect (Fig. 6.3.2C: $F=4.98$, df3/43, $p<0.005$). Compared to the control, separate pair-wise ANOVA showed that young PS1cKO mice were not impaired ($F=1.30$, df1/22, $p>0.05$), young PS1cKO;APP mice were not impaired ($F=2.69$, df1/23, $p>0.1$), however, young APP mice were again significantly impaired ($F=10.47$, df1/23, $p<0.005$). Interestingly, the difference between young PS1cKO;APP and APP mice was a trend towards significant in this task ($F=4.08$, df1/23, $p=0.056$). These results further suggest a rescue effect of PS1 inactivation on learning capacity of APP mice.

In summary, inactivation of PS1 successfully restored learning deficits of young (3-4 months) APP mice on both trials to criterion and learning capacity tasks. As young J20 APP mice displayed early learning deficit, this confirms that early accumulation of Aβ or other APP metabolites is sufficient to disrupt normal spatial learning of the mice. However, prevention of early accumulation of Aβ or other APP metabolites by PS1 inactivation in young APP mice improves the impaired learning.

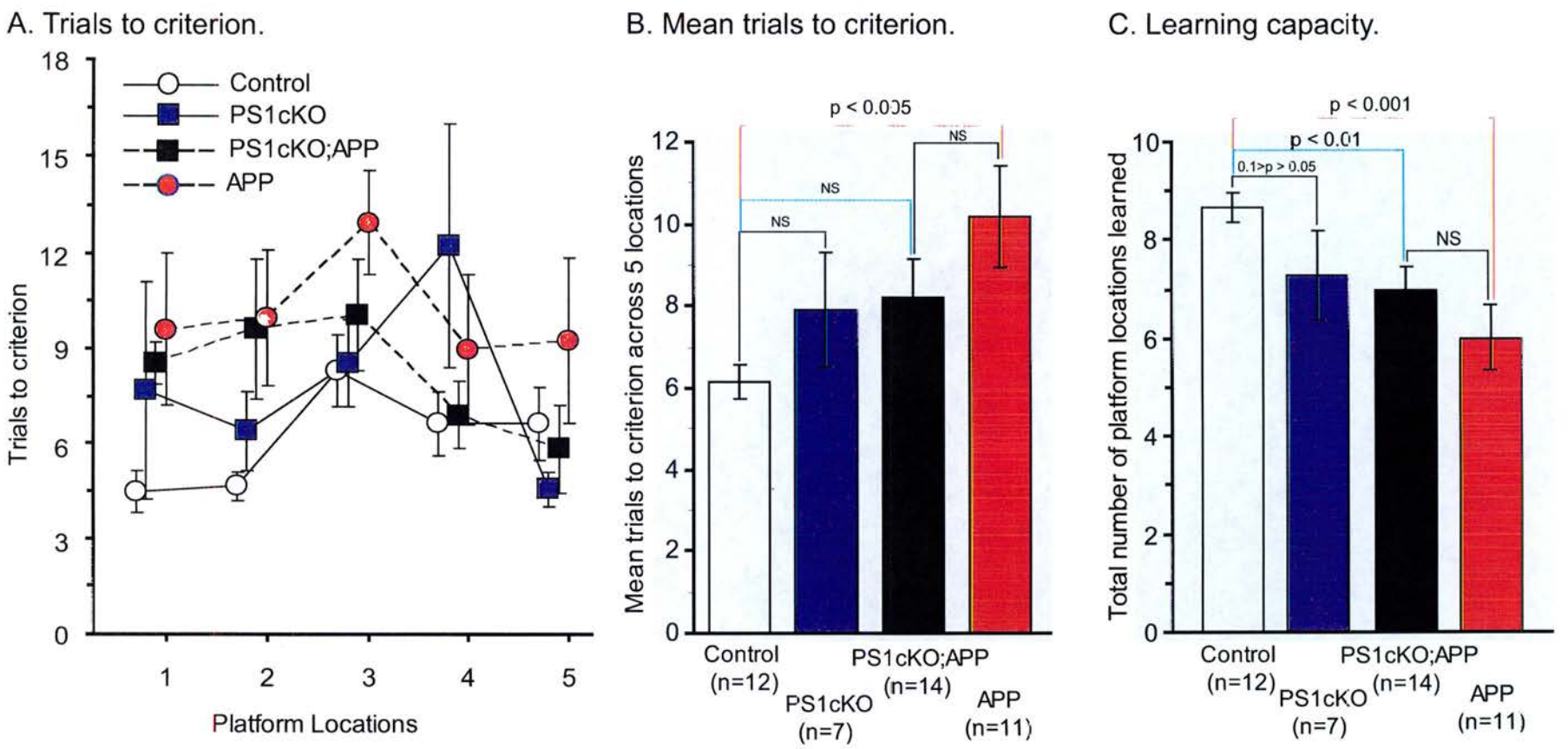

Figure 6.3.3 Performance of Old Mice in Spatial Learning. A. Trials to criterion in old mice across the five platform locations. There was no significant overall genotype effect (p>0.05). B. Mean trials to criterion in old mice. Old APP mice were significantly impaired, but old PS1cKO;APP mice were not. C. Learning capacity in old mice. Old APP mice were again significantly impaired, but old PS1cKO;APP mice were not.

3. Old PS1cKO;APP mice show only a partial rescue of learning.

Figure 6.3.3A shows the performance of old mice on the 5 individual platform location of the trials to criterion task. Figure 6.3.3B shows the mean trials to criterion across all five platform locations. Analysis of variance revealed a trend towards a significant genotype effect (Fig. 6.3.3A and B: $F=2.81$, df3/40, $p=0.051$). Compared to control mice, pair-wise comparisons showed that old PS1cKO mice were normal ($F=2.21$, df1/17, $p>0.1$), old PS1cKO;APP mice were also not abnormal ($F=3.38$, df1/24, $p>0.05$), however, old APP mice were significantly impaired ($F=10.18$, df1/21, $p<0.005$). Very interestingly, although old PS1cKO;APP mice were not significantly different from control mice, they were also not different from old APP mice (Fig. 6.3.3A and B: $F=1.63$, df1/23, $p>0.2$), suggesting only a partial rescue effects of PS1 inactivation on trials to criterion of APP mice.

The effects of conditional inactivation of PS1 were further examined using the learning capacity measure (Fig 6.3.3C). An overall ANOVA had revealed a significant main genotype effect (Fig. 6.3.3C: $F=4.19$, df3/40, $p<0.05$). Pair-wise ANOVAs revealed that the difference between old control and PS1cKO mice was a trend towards significant (Fig. 6.3.3C: $F=3.11$, df1/17, $0.05>p>0.1$). However, compared to control mice, old PS1cKO;APP mice were significantly impaired ($F=8.50$, df1/24, $p<0.01$), and old APP mice were impaired as well ($F=14.61$, df1/21, $p<0.001$). Again, old PS1cKO;APP mice were not different from APP mice (Fig. 6.3.3C: $F=1.61$, df1/23, $p>0.2$).

It seemed that old PS1cKO;APP mice displayed normal learning in trials to criterion task, but impaired learning in learning capacity task. This may suggest that PS1 inactivation partially improves the impaired learning of old APP mice. However, as old PS1cKO;APP mice were not different from APP mice in both tasks, the rescue effects of PS1 inactivation are very limited on spatial learning.

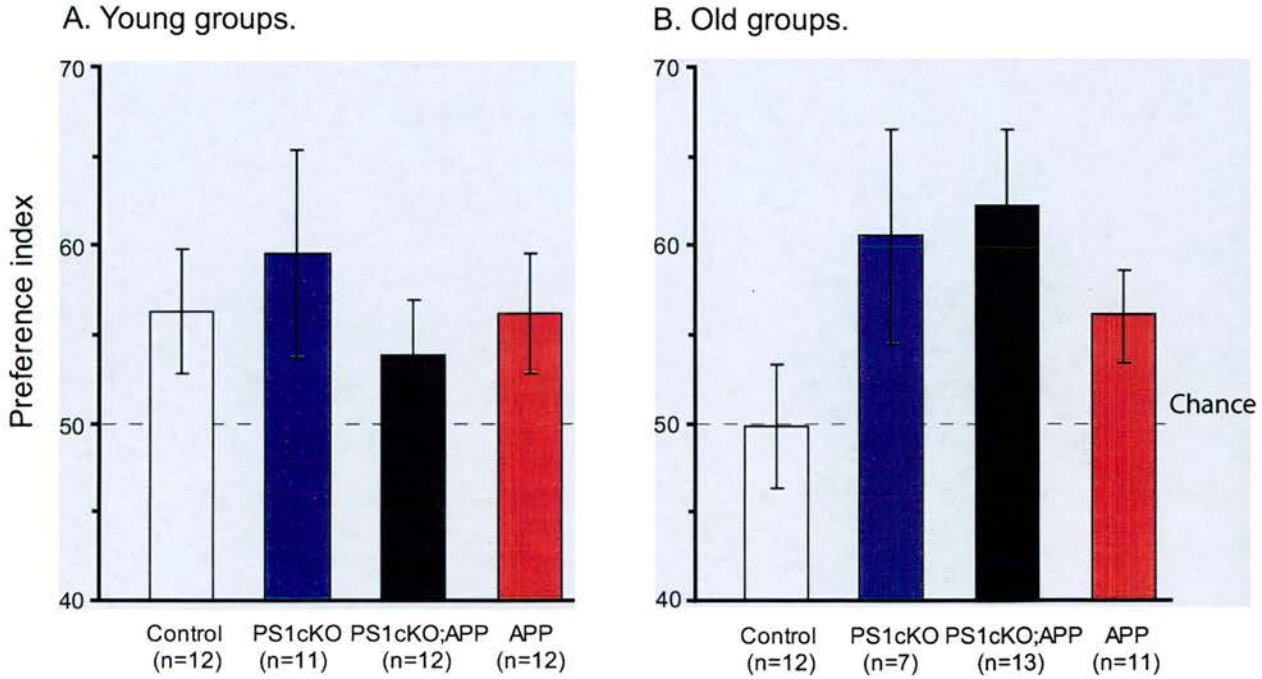

Figure 6.3.4 Object Recognition in the Mice. A. Object recognition memory for young mice. All mice showed above-chance performance. B. Object recognition memory for old mice. There was no significant genotype effect.

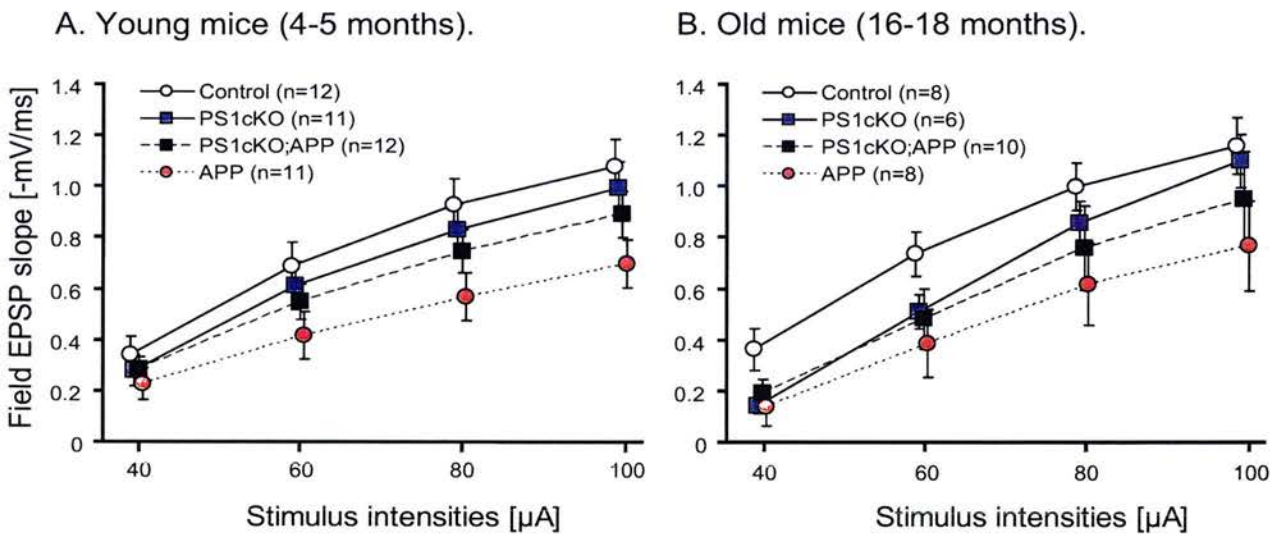

Figure 6.3.5 Impaired Basal Synaptic Transmission in APP Mice.
A. Input-output curves for young mice. There was no significant overall effect, but the difference between the control and APP groups was significant.
B. Input-output curves for old mice. There was no significant overall effect, but the difference between the control and APP groups was significant.

4. Both young and old APP and PS1cKO;APP mice displayed unimpaired object recognition memory.

In order to test whether APP and PS1cKO;APP mice displayed any impaired object recognition memory, only a 4 h retention interval was used (Dewachter et al., 2002; Dodart et al., 2002). Figure 6.3.4A shows the performance for young mice. All four groups explored the novel object preferentially ($p<0.05$, one sample t-test), and ANOVA revealed no main genotype effect ($F<1$), indicating that young APP and PS1cKO;APP mice displayed normal object recognition. The performance of old mice is shown in Figure 6.3.4B. No genotype effects were found ($F = 2.06$, df 3/39, $p>0.1$), suggesting that old APP and PS1cKO;APP mice were also not impaired in object recognition memory.

5. APP mice displayed deficit of synaptic transmission in the hippocampus.

Using similar protocols to those in my previous studies, input-output (I-O) curves were recorded in both young and old mice. Figure 6.3.5 shows basal synaptic transmission in young mice (Fig. 6.3.5A) and old mice (Fig. 6.3.5B). In Fig. 6.3.5A, ANOVA revealed a trend towards a significant genotype effect ($F=2.66$, df3/42, $p=0.06$). Compared to control animals, APP mice were impaired ($F=8.55$, df1/20, $p<0.01$) and PS1cKO;APP mice showed a trend towards significant difference ($F=3.49$, df1/21, $p=0.076$). However, APP mice were not different from PS1cKO;APP ($F=1.69$, df1/21, $p>0.2$) in hippocampal basal synaptic transmission, suggesting only a subtle rescue effect of PS1 inactivation on synaptic transmission of young APP mice.

Analysis of input-output curves for old mice (Fig. 6.3.5B) showed that there was no significant main genotype effect ($F=1.47$, df3/28, $p>0.2$). Compared to control animals, old APP mice were impaired ($F=5.0$, df1/14, $p<0.05$) and PS1cKO;APP mice were not ($F=1.74$, df1/16, $p>0.2$). However, old APP mice were not different from PS1cKO;APP ($F<1$). The data further suggested only a partial rescue effect of PS1 inactivation on synaptic transmission.

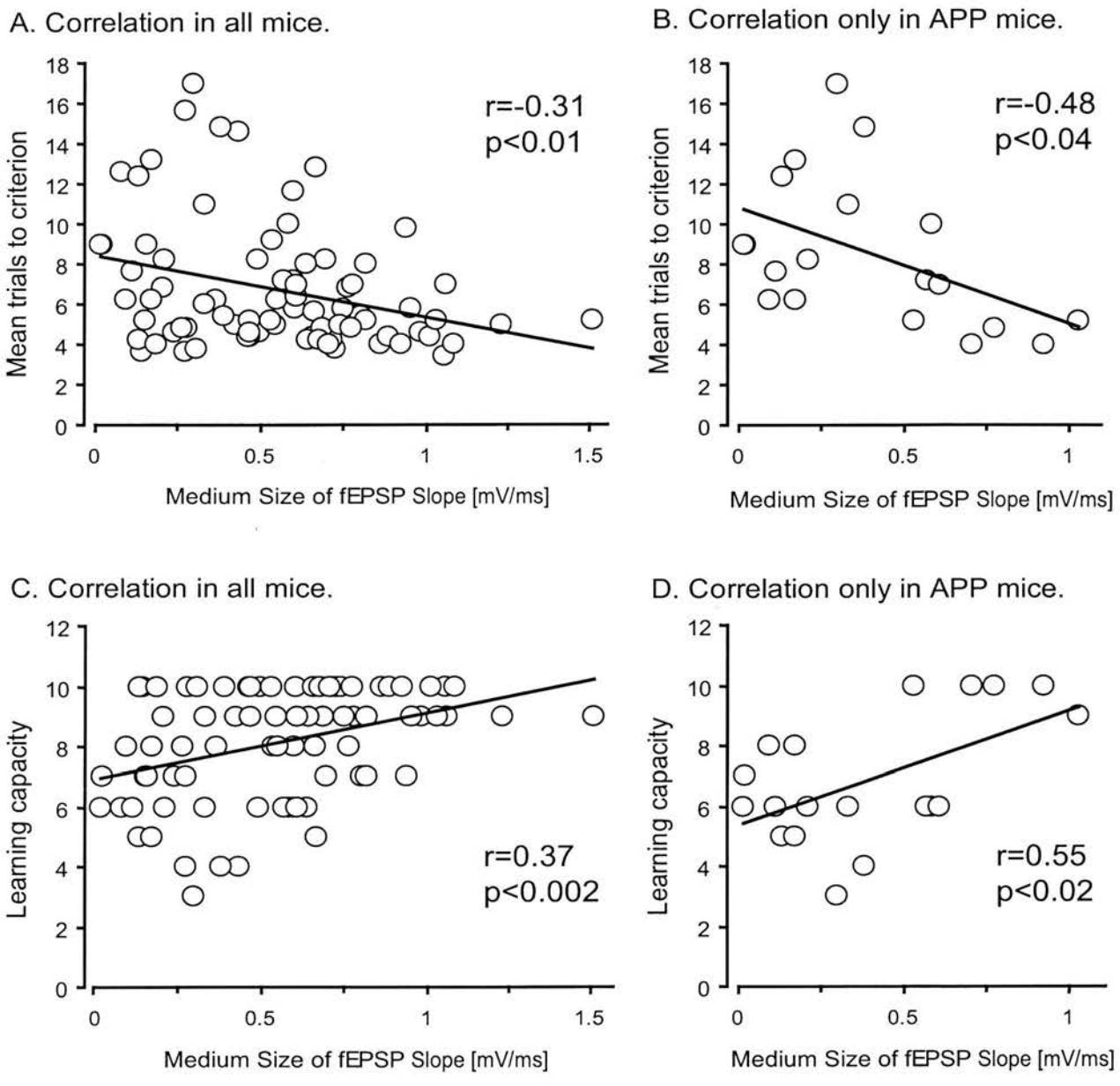

Figure 6.3.6 Significant Correlations between the Basal Synaptic Transmission and Behavioural Performance. A. Significant correlation between the medium size of fEPSP of the hippocampus and the mean trials to criterion for all mice tested in this study. B. Significant correlation between the medium size of fEPSP of the hippocampus and the mean trials to criterion only in APP mice. C. Significant correlation between the medium size of fEPSP of the hippocampus and learning capacity for all mice. D. Significant correlation between the medium size of fEPSP of the hippocampus and learning capacity only in APP mice.

6. Relationship between synaptic transmission of the hippocampus and behavioural performance in trials to criterion and learning capacity task.

Several correlation studies were conducted to analyse the relationship between synaptic transmission and behavioural performance in the same mice. First, there was a significant correlation between the size of fEPSP and the mean trials to criterion for all mice (Fig. 6.3.6A) and APP mice only (Fig. 6.3.6B). Although the correlation coefficient, r=-0.31, in Fig. 6.3.6A ($p<0.01$, all mice) was smaller than that, r=-0.48, in Fig. 6.3.6B ($p<0.05$, APP mice only), all the correlations were significant. Second, Figure 6.3.6C and 6D shows the significant positive correlations between the size of fEPSPs and learning capacity (Fig. 6.3.6C, for all mice: r=0.37, $p<0.002$; Fig. 6.3.6D, for APP mice only: r=0.55, $p<0.02$; medium size of fEPSPs). The significant correlations between behavioural performance on the trials to criterion and learning capacity task and the size of fEPSPs suggest, unsurprisingly, that basal synaptic activity is involved in spatial learning.

6.4 Discussion.

1. Conditional inactivation of PS1 in the forebrain of APP mice successfully restored impaired spatial learning at young age.

In this study, four different genotypes of mice, control, PS1cKO, PS1cKO;APP and J20 APP mice were first tested at 3-4 months of age, using a behavioural testing battery. Like PDAPP mice, the J20 APP mice displayed learning deficit in the trials to criterion and learning capacity tasks, but exhibited normal swimming ability and normal object recognition memory. These findings are consistent with previous observations on PDAPP mice. As the J20 mice do not start the formation of amyloid plaques until 5-6 months, the impairment of spatial learning at 3-4 months is plaque-independent, but presumably Aβ-dependent. When analyzed at both 2 and 6 months using ELISA, these mice displayed very high levels of Aβ40 and Aβ42 (personal communications with Dr. Carlos Saura). Due to overexpression of mutant APP in the brain, young APP mice have also developed a high amount of other APP derivatives, such as APP CTFs. However, this learning deficit in young APP mice seems not to be APP CTF-dependent, as both young PS1cKO and PS1cKO;APP mice also have high levels of APP CTFs in the brain (because Aβ production is inhibited), but they showed relatively normal spatial learning. The results from young mice strongly

suggest that learning deficit of APP mice can be fully rescued by inactivation of PS1 in the forebrain.

2. Conditional inactivation of PS1 in the forebrain of APP mice only partially improved learning deficits in old animals.

Like other APP Tg animals, as J20 APP mice aged, they progressively developed AD-like pathology, such as amyloid plaques, synaptic loss, gliosis and learning deficit. Interestingly, data from Shen's group further indicated that postnatal inactivation of PS1 in the forebrain prevented neuropathology very effectively at older ages, i.e >12 months (personal communications with Dr. Carlos Saura). In this study, four different genotypes of old mice (15-17 months) were also tested using our behavioural test battery. At this age, conditional inactivation of PS1 displayed only a subtle rescue effect on the trials to criterion measure, but not learning capacity. Furthermore, as the performance of old PS1cKO;APP mice in both tasks did not differ from that of age-matched APP mice, this suggests that inactivation of PS1 in the forebrain is less effective in old APP mice. Although the mechanisms are unknown, the findings that the rescue effect on spatial learning by conditional inactivation of PS1 in APP mice is age-related may suggest that there is an Aβ-independent component of cognitive impairment in old APP and PS1cKO;APP mice.

Unpublished data on contextual fear (CF) conditioning by Shen's group indicated that J20 APP mice displayed plaque-independent deficits at 3 and 6 months, however, PS1cKO;APP mice showed normal fear responses at 3 months but were impaired at 6 months (personal communications with Dr. Carlos Saura). So these findings are consistent with the results in this study.

3. Significant rescue effect at young age versus non-significant rescue effect at old age in PS1cKO;APP mice.

The age-dependency of the rescue effect raises the possibility that abnormal accumulation of APP CTFs in the brain may also cause disruption of learning and memory in the mice. One example is that, in this study, young PS1cKO mice showed significantly impaired spatial learning in trials to criterion task. Likewise, it has been reported that PS1cKO mice also showed subtle impairment of spatial learning and memory using the standard watermaze reference memory task (Yu et al., 2001).

Interestingly, young PS1cKO mice were found to be normal in learning capacity in this study. Do these findings suggest that inactivation of PS1 may affect several forms of spatial learning but not all in the mice? To answer this question, a factorial ANOVA (two-factor: age×genotype) was used to assess the overall effects of PS1 inactivation on spatial learning of young and old PS1cKO mice. For trials to criterion task, a significant main genotype effect was observed ($F=5.99$, $df1/38$, $p<0.05$). Similar results were also found in learning capacity task ($F=1.04$, $df1/38$, $p<0.05$). These analyses indicate that inactivation of PS1 in the forebrain of PS1cKO mice indeed has caused impairment on spatial learning. This may help to explain why a full rescue effect on learning in all PS1cKO;APP mice has not been seen. These findings further suggest a possibility that elevated levels of endogenous or mutant APP CTFs are deleterious to spatial learning of the mice.

In this study, the performance of old PS1cKO;APP mice on the trials to criterion and learning capacity did not differ from that of age-matched APP mice. Pathological differences between these two Tg lines are that, old APP mice have very high levels of human mutant Aβ/plaques and relatively low human APP CTFs in the brain, however, old PS1cKO;APP mice have no human Aβ/plaques but a huge amount of human APP CTFs in the brain. Although the pathology of old APP and PS1cKO;APP mice seems totally different, they are not different in cognition in the tests used so far. An explanation for this observation may be that either high levels of Aβ/plaques or APP CTFs in the brain damage normal cognitive functions of the mice. The mechanisms seem to be unclear. However, as there is a significant correlation between synaptic transmission and behavioural performance, it might suggest that synaptic transmission in the hippocampus may serve as a cellular mechanism for spatial learning in the mice or at least in APP animals.

Chapter 7: Investigation of the Effects of γ-Secretase Inhibitor Treatment on Spatial Learning of PDAPP Mice.

7.1 Introduction.

7.1.1. The γ- and β-secretases as therapeutic targets for the treatment of AD.

Currently, most FDA-approved drugs for AD treatment, such as tacrine, donepezil, rivastigmine and galantamine, are the AChEIs. However, these drugs only provide symptomatic treatment: they do not stop the progression of AD, but only stabilize cognitive impairment for a limited time period and eventually they become ineffective. It is very likely that a better treatment strategy would be targeting the molecules responsible for the neurodegenerative pathogenesis of AD. The primary enzymes for modulating APP processing are α-, β- and γ-secretases, with the β- and γ-secretases being directly responsible for Aβ production. Due to the central role of Aβ accumulation in the pathogenesis of AD, the β- and γ-secretases have recently become prime candidates for therapeutic development for AD. As the α-secretase is not directly involved in the production of Aβ, it seems unlikely to be a very promising therapeutic target.

The attempts to seek better agents such as the inhibitors for the β- and γ-secretases have been proven very successful during the past few years. In 1999, four groups reported the identification and characterization of the β-secretase, using either genomic-based approach or expression cloning (Hussain et al., 1999; Sinha et al., 1999; Vassar et al., 1999; Yan et al., 1999). The development of β-secretase inhibitors has been very challenging due to its pharmacological kinetics. Interestingly, since the first peptidic BACE inhibitor was reported by Elan (Sinha et al., 1999), major progress on the so-called structure-based approaches has been achieved. For examples, a group based in Oklahoma have recently reported two very powerful BACE inhibitors, OM99-2 and OM00-3, both being eight-residue transition state inhibitors (Ghosh et al., 2000; Turner et al., 2001). Very recently, Elan reported a peptidic BACE inhibitor with very small molecular weight, Compound 38, which inhibits 50% of Aβ production in cell culture at 4 μM and is also cell permeable (John et al., 2003).

Like β-secretase, pharmacological evidence indicates that γ-secretase belongs to aspartyl protease family (Li et al., 2000). However, the γ-secretase is much more complex than the β- secretase and is composed of PSs, Nct, Aph1 and Pen2 (Kimberly et al., 2003). As the active site of γ-secretase is hydrophobic, the inhibitors of γ-secretase are also hydrophobic and this property helps membrane permeability. Due to this property, searching for the cell-permeable γ-secretase inhibitors has been much less challenging than for BACE inhibitors. Much progress has been made in developing γ-secretase inhibitors since 1995 (Higaki et al., 1995). Many peptidic and nonpeptidic γ-secretase inhibitors have been reported by pharmaceutical industry and academic laboratories and are reviewed in Section 1.8.2.8 of Chapter 1. Moreover, at least one of them is currently in clinical trial (Wolfe, 2002).

7.1.2. Development of selective γ-secretase inhibitors.

The first selective γ-secretase inhibitor is called MW167, a difluoro ketone peptide analogue (Wolfe et al., 1998). This drug is highly selective, but not a very potent peptidic inhibitor for γ-secretase (IC_{50}=13 μM) and it is reported to block the production of both Aβ40 and Aβ42 in human APP-transfected CHO cells (Wolfe et al., 1998). It has also been reported that this compound inhibits γ-secretase-mediated cleavage of APP expressed in neurons using recombinant Semliki forest virus (SFV) in a concentration-dependent manner, thus leading to the accumulation of C-terminal fragment (CTF) of APP. MW167 inhibits neither the α- nor β-secretase activity, but does inhibits NICD production (IC_{50}=10-30 μM) (De Strooper et al., 1999). This latter finding thus raises the concerns that inhibition of γ-secretase activity for the treatment of AD may cause serious toxicity by blocking the Notch signalling pathway. Further, it has not been reported whether this compound can potently inhibit either Aβ production or plaque formation in APP Tg mice. Overall, MW167 and other peptidic inhibitors like MDL28170 and MG132 only display weak potency for the inhibition of γ-secretase (Higaki et al., 1995; Klafki et al., 1996).

Although there is serious concern about the impact of γ-secretase inhibitors on Notch processing, searching for an effective γ-secretase inhibitor has not been stopped. Indeed, several attempts have proven successful. One typical example is L-685458, a highly powerful transition-state analogue γ-secretase inhibitor, which was first reported by neuroscientists from Merck (Li et al., 2000; Shearman et al., 2000). L-

685458 contains a hydroxyethylene isostere and its photoreactive derivatives can specifically label PS1 and PS2 (Li, 2001). Unlike the difluoroketones γ-secretase inhibitors, L-685458 does not resemble the native peptide substrate. It was reported that L-685 458 concentration-dependently inhibits Aβ production in both Neuro2A and CHO cell lines overexpressing human APP695 and is not cytotoxic to cells. This compound seems much more potent than other published γ-secretase inhibitors, as its IC_{50} is only 14 nM for Aβ40 and 13 nM for Aβ42 using SH-SY5Y neuroblastoma cells stably transfected with SPA4CT (Shearman et al., 2000; Beher et al., 2001). It is reported that, while L-685458 inhibits the Aβ40 production in HEK293/APP695 cells and cells transfected with BACE1 or BACE2, it does not inhibit the activities of BACE1 and BACE2 (Shi et al., 2003). Scientists from Merck have disclosed several newly developed benzodiazepine-containing γ-secretase inhibitors which show even higher inhibition potency than L-685 458. For example, compound 34 displays an IC_{50}=0.06 nM (Churcher et al., 2003). It is unknown whether these highly potent nonpeptidic γ-secretase inhibitors display similar inhibition potency in vivo or are already in clinical trials for the treatment of AD.

Since scientists from Elan and Lilly published the compound 7 (DAPT, *N*-[*N*-(3,5-difluorophenacetyl)-L-alanyl]-*S*-phenglycine *t*-butyl ester) in 2001, DAPT has become the first potent γ-secretase inhibitor to be tested in vivo. Early work has shown that DAPT reduces the production of Aβ40 and Aβ42 in HEK293 cells overexpressing human APP751 and in human primary neuronal cultures. Like L-685458, the IC_{50} for DAPT is ~20nM. Very interestingly, it is reported that, after oral administration of DAPT (100 mg/kg) to PDAPP Tg mice, peak DAPT levels are found in the brain 3 hr after treatment and high levels of DAPT are maintaining throughout the first 18 hr. The reduction of Aβ reaches 40% of inhibition 3 hr after treatment. Further investigation shows that cortical total Aβ is reduced by 50% with 3 hr treatment of 100 mg/kg DAPT (Dovey et al., 2001). In a later chronic study of PDAPP mice by the same investigators, the effects of LY411575 (benzocaprolactam, or Compound 9) on Aβ accumulation and subsequent plaque pathology have been examined (May et al., 2001; Wolfe, 2002). Beginning at 6.5-7 months of age, PDAPP mice were administered with LY411575 (1 mg/kg) or corn oil vehicle twice a day for a period of 90 days. Excitingly, this chronic treatment results in 70-90% reduction of brain Aβ levels. Moreover, these researchers further display that markers of neuritic

pathology and glial inflammatory responses are also significantly attenuated (May et al., 2001). These results indicate that chronic treatment with a γ-secretase inhibitor can alter pathology in an animal model of AD and thus strongly point to the therapeutic potential of γ-secretase inhibitors for the treatment of AD.

This progress offers great hope for therapeutic intervention in AD. However, the inhibition of γ-secretase interferes with Notch processes that are pivotal to mammalian development. For example, one recent study has shown that application of γ-secretase inhibitors to fetal thymus organ cultures interferes with T cell development in a manner consistent with the loss or reduction of Notch1 function (Hadland et al., 2001). Another study also shows that treatment of zebrafish with a γ-secretase inhibitor causes a severe neurogenic phenotype (Geling et al., 2002). It seems very important that more specific inhibitors of APP relative to Notch are needed. Interestingly, novel nonpeptidic γ-secretase inhibitors such as the isocoumarin JLK inhibitors have recently been reported (Petit et al., 2001). It is shown that JLK2 and JLK6 inhibit Aβ production in a dose-dependent manner (IC50=80 μM, for both compounds) in HEK293 cells stably transfected with human wildtype or Swedish mutant APP gene. Moreover, JLK inhibitor does not affect proteolytic cleavage of endogenous PS1 (Petit et al., 2001). In vivo study of JLK inhibitors by the same group has shown that JLK compounds do not affect Notch pathways, nor to cause cell death or inhibition of BACE1, BACE2, α-secretase and other proteasome (Petit et al., 2003). Obviously, the JLK inhibitors represent a new class of highly selective and cell-permeable γ-secretase inhibitors, but their potency is much less than other transition-state based γ-secretase inhibitors (Esler et al., 2002). Due to their high selectivity for the APP pathway, the JLK compounds might be more promising than other γ-secretase inhibitors for developing the treatment of AD. But to gain this goal, several important questions related to this novel γ-secretase inhibitor need to be answered. Firstly, can the JLK agents reduce amyloid plaques or other AD-related pathology in vivo? Secondly, can the JLK agents reverse learning impairment in APP Tg mice? Thirdly, should the weak potency of the JLK agents be improved for clinical study on the treatment of AD? However, as I had no access to these compounds, I have focused on the Elan compound, ELN44989, despite its lower selectivity.

7.1.3. Purpose of this study: Evalulation of γ-secretase inhibitors on learning ability of animal models of AD.

The *in vivo* study of L-411575 seems quite exciting, as it has demonstrated that long-term treatment of a γ-secretase inhibitor could effectively reduce Aβ loads and other AD-like neuropathology in APP Tg mice (May et al., 2001). However, these researchers did not report any apparent side effect of the chronic treatment of PDAPP mice with L-411575. Perhaps, inhibition of Notch pathway with a γ-secretase inhibitor could be well tolerated in adult mice.

At the time of starting this study, no study had appeared reporting whether the treatment of a γ-secretase inhibitor can rescue cognitive deficits shown in APP Tg mice. Evaluation of the effects of γ-secretase inhibitor on learning ability of APP Tg mice is very important, as it could be a key preclinical step to establish the this novel effective treatment strategy for AD. As reported in a previous chapter of this thesis, a vaccine of Aβ has been found ineffective in improving the impaired spatial learning of PDAPP mice, despite significantly reducing the levels of Aβ and Aβ42 in the cortex and hippocampus. It would therefore be interesting to examine what effects a γ-secretase inhibitor treatment would have on both neuropathology and cognitive loss in APP Tg mice.

Recently, Elan has developed a new γ-secretase inhibitor compound, ELN44989. Confidential data by Elan show that this compound is more potent than DAPT, but with a half-life of 1.5 h (personal communication with D. Kobayashi at Elan). In a previous longitudinal study of a cohort of 25 mice (12 PDAPP and 13 non-Tg mice), as shown in Chapter 4, I have found that this cohort of PDAPP mice display normal learning at young age (6-9 months), but impaired learning at older ages (14-15 or 21-22 months). In this study, a similar longitudinal design was used, with the trials to criterion task in the watermaze.

7.2 Methods.

7.2.1. Subjects.

A total of 82 male mice (44 non-Tg and 38 PDAPP) aged at 6-7 months were shipped from Taconic (Elan Pharmaceuticals.). The mice were singly housed after they arrived

at Edinburgh. The experimenter was blind to the genotype of mice. The mice were given *ad libitium* access to food and water.

7.2.2. Watermaze.

The watermaze was used as previously.

7.2.3. Experimental design.

A within-subject (longitudinal) design was used, as shown in Fig 7.2.1. At 7-8 months of age, all mice were first examined for sensorimotor function using the standard visible cuetask. Due to previous findings showing that either PDAPP or APP J20 mice have displayed normal object recognition memory, this was excluded from the test battery. Only sensitive tasks such as trials to criterion and learning capacity over several spatial locations were utilized to test drug effects. At 7-8 months, after cuetask training was complete, all mice were subjected to the serial spatial task to test spatial learning ability.

The treatment of ELN44989 started immediately after the first phase of testing. The experiments were conducted double-blinded, that is, the experimenter who did the behavioural testing and electrophysiological study was blind to both the genotype and the drug status. A second person, who knew the genotype of the animals but not the drug identity, did the assignment of the animals into two subgroups for drug treatment according to their behavioural performance in Phase 1. To conduct this assignment, both non-Tg and PDAPP mice were divided into two sub-groups, such as Group A and Group B, which behavioural performance was equally matched each other. A third party, who knew the drug (ELN44989 or corn oil=control) but not the genotype, prepared the solution once a week. And a fourth group, the animal technicians who did the drug delivery were also blind to both the genotype and drug.

In order to get maximal effect on Aβ reduction by γ-secretase inhibitor in PDAPP mice, the total treatment period was designed as 4 months. After the chronic treatment of ELN44989, all the animals who survived for this period were first tested again with 2-day cuetask followed by the concurrent trials to criterion and leaning capacity. After the behaviour testing was done, all mice were subjected to an electrophysiology study

Phase 1: mice at 7-8 months.

1. Visible cuetask in watermaze. 5 days.
2. Concurrent trials-to-criterion and learning capacity task in watermaze, whichever took longer.

Phase 2: mice at 7-11 months.

3. Four months treatment with ELN44989.

Phase 3: mice at 11-12 months.

4. Visible cuetask in watermaze. 2 days.
5. Concurrent trials-to-criterion and learning capacity task in watermaze, whichever took longer.

Phase 4: mice at 12-13 months.

6. Electrophysiology on hippocampal synaptic transmission.
7. ELISA analysis of total Aβ.

Figure 7.2.1 Longitudinal Experiment Design.

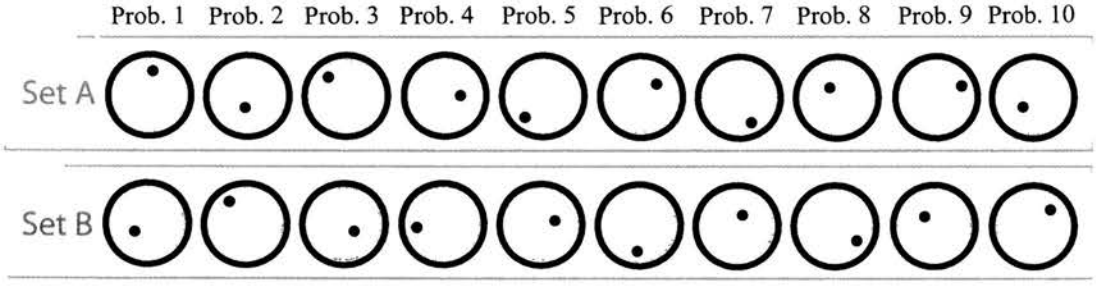

Figure 7.2.2 Design of Platform Locations for Trials to Criterion and Learning Capacity Task before ELN44989 Treatment (age: 7-8 months).
For counterbalancing reason, two sets of 10 platform locations were designed. All young mice were randomly assigned to two groups. Half of them were trained Set A, and the other half were tested by Set B.

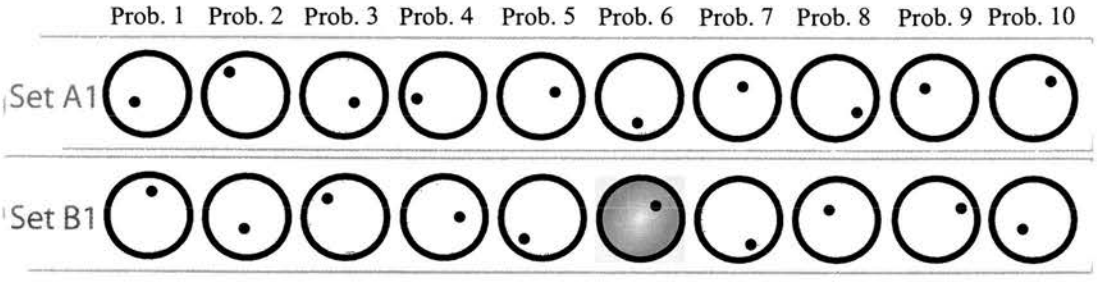

Figure 7.2.3 Design of Platform Locations for Spatial Learning after 4-month ELN44989 Treatment (age: 11-12 months). Two sets of 10 platform locations were designed as above. The mice, who were previously trained by the Set A of platform locations in Fig. 7.2.2, would now be tested with the Set A1 platform positions, and similarly, the others, who were tested with the Set B, now received the Set B1 platform locations.

to examine basal synaptic transmission. Finally, the brain tissue samples were analyzed by ELISA to evaluate the drug effects on Aβ reduction in all the animals.

7.2.4. Visible cuetask.

Before any drug treatment, there were 5 days, 4 trials/day, for cuetask training. After 4 months drug treatment, there were 2 days for cuetask training at 11-12 months.

7.2.5. Trials to criterion and learning capacity task.

Trials to criterion and learning capacity tasks were concurrently conducted again, whichever took longer. The Figures 7.2.2 (7-8 months) and 7.2.3 (11-12 months) showed two different sets of 10 consecutive platform locations for spatial testing.

7.2.6. Drug preparation and delivery.

ELN44989 was made in Elan. This compound was reported to us to be well tolerated in the mouse (up to 3mg/kg), more efficacious than DAPT, and produce >80% reduction of Aβ in plasma (personal discussion with D. Kobayashi). Due to the agreement between Elan and Prof. Richard Morris, more detailed information about the structure and efficacy of this compound was not disclosed. As the half-life is 1.5h, twice oral administrations per day were given to PDAPP mice. Dosing needles (20G × 25mm, straight) were purchased from VetTech (Cheshire, UK). For this study, the dosing concentration of the compound was 1mg/kg. Corn oil was served as the control vehicle. The drug was made up once a week by Jane Knox (who was only aware of the drug but not the genotype of the mice). Two highly experienced technicians, Richard Watson and Laraine Wells did the oral gavarage for all mice (twice a day, 8:00 AM and 17:00 PM).

7.2.7. Electrophysiology.

A new automatic Hampden vibroslicer was used for hippocampal slice dissection. The fEPSPs of CA1 apical dendrites were recorded extracellularly using a steel electrode. Input-output (I-O) curves were induced by 7 different intensities of stimulation (40, 50, 60, 70, 80, 90 and 100 μA) using current stimulation isolators (NL800, Digitimer, England). Data were collected by labview software written by Patrick Spooner and stored into a Dell computer. The slope of field EPSP evoked by stimulation of the Schaeffer collateral-CA1 pathway was analyzed off-line.

A. An ELN44989-treated mouse.

B. A corn oil-treated mouse.

Before treatment 1 month after 3 months after

C. High mortality in ELN44989-treated mice.

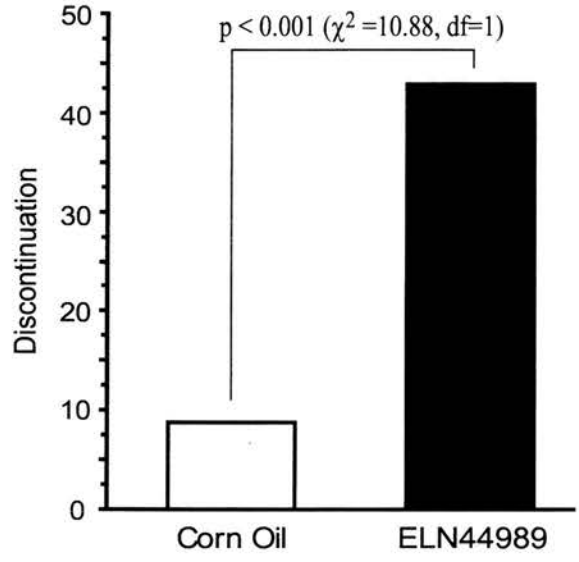

Figure 7.3.1 Side Effects Observed in the ELN44989-treated Mice.

A. Coat color change in an ELN44989-treated mouse.

B. No coat color change was found in corn oil-treated mice.

C. A significantly higher mortality was found in ELN44989-treated mice, compared to corn oil-treated animals ($p<0.001$).

7.2.8. Tissue preparation for ELISA analysis of Aβ.

The method for tissue preparation was described in Chapters 2 and 5. After preparation, all the samples were stored at -20 °C for ELISA analysis.

7.3 Results.

1. Chronic treatment with ELN44989 caused severe side effects in the mice.

In contrast to previous findings by May et al (2001), several unexpected side effects of ELN44989 on the mice were observed in this study (Fig. 7.3.1). First, a color change on the fur of ELN44989-treated mice was observed approximately 3 to 4 weeks after the start of ELN44989 treatment (Fig. 7.3.1B). Approximately 3 months after this γ-secretase inhibitor treatment, the fur of all mice became totally discolored.

The second side effect of this γ-secretase inhibitor was that it caused mortality, leading us to allow a much higher discontinuation rate (Fig. 7.3.1C). For example, nearly half the ELN44989-treated animals (42.86%) had to be discontinued in this study, as they were found dead or had displayed at least 40% weight loss (25% is the allowable severity level to maintain the study in terms of Professor Morris's Personal Project License). By contrast, the corn oil-treated groups only showed 8.82% mortality. Chi-square analysis revealed a highly significant discontinuation rate difference between the ELN44989- and corn oil-treated mice ($p < 0.001$; $\chi^2=10.88$, df=1), but no difference between genotype groups ($p > 0.5$; $\chi^2=0.19$, df=1). These findings indicate that the treatment of mice with 1mg/kg ELN44989 caused serious ''side effects'' on animals. As 1mg/kg was the only concentration used in this study, it remains unclear whether lower concentrations could minimize the side effects.

A. Cuetask before the treatment.

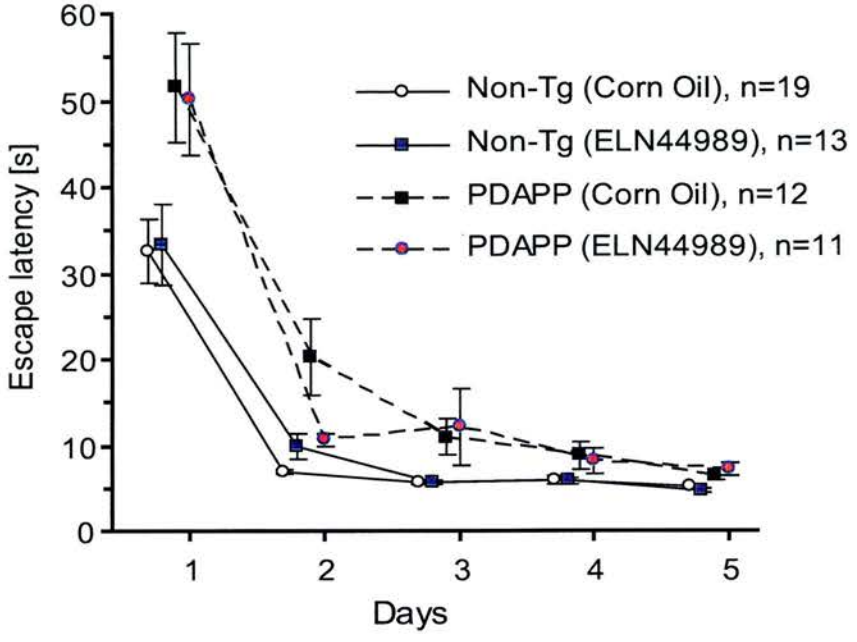

B. Cuetask after the treatment.

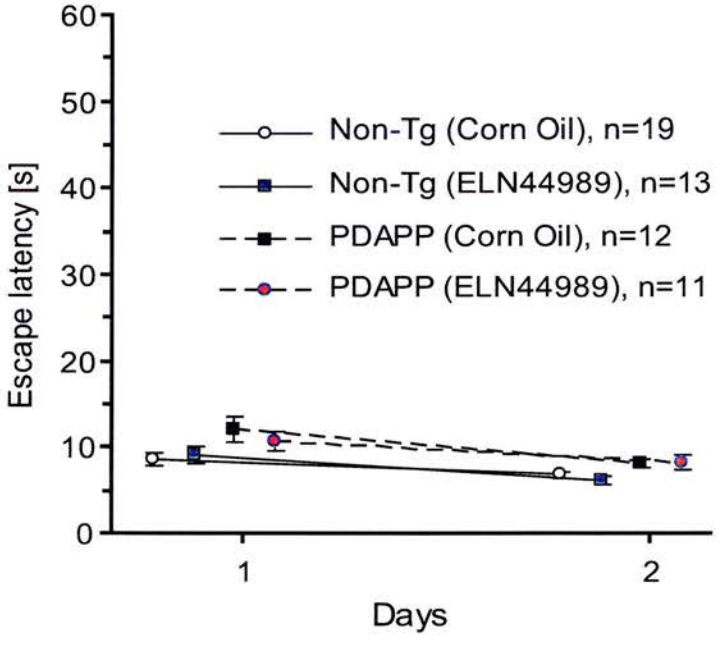

Figure 7.3.2 Cuetask Performance.

A. Cuetask performance of the mice before the treatment of ELN44989. There was a significant main genotype effect.

B. Cuetask performance of the mice 4 months after the treatment of ELN44989. There was a significant main genotype effect, but no drug effect or genotype×drug interaction.

2. APP mice displayed impaired basic learning in cuetask.

Cuetask training was conducted before and 4 months after the treatment of ELN44989. Fig. 7.3.2A shows the cuetask performance for PDAPP and non-Tg mice at 7-8 months, prior to ELN44989 treatment. Unexpectedly, statistical analysis revealed a significant main genotype effect ($F=23.26$, df1/51, $p<0.0001$) and a day × genotype interaction ($F=6.65$, df1/112.92, $p<0.01$), suggesting that this cohort of PDAPP mice were impaired in their basic learning of cuetask. Although the PDAPP mice reached 7.3 s performance on the last day of cuetask training, compared to 4.9 s by the non-Tg mice, the difference between groups was again highly significant ($F=19.29$, df1/74, $p<0.0001$). Compared with the findings reported in previous chapters of this thesis, this study indicated a clear deficit in the sensorimotor function of the newly bred PDAPP mice.

The basic learning ability of the same mice used in this study was further evaluated 4 months later after the treatment with ELN44989 (Figures 7.3.2B). Analysis of variance for 55 mice, who survived after 4 months treatment of ELN44989, again revealed a highly significant main genotype effect ($F=12.34$, df1/51, $p<0.001$) and a significant genotype × day interaction ($F=4.37$, df1/51, $p<0.05$). No treatment effect or genotype × treatment interaction was found ($Fs<1$). Although Figs. 7.3.2B shows that PDAPP mice improved their performance significantly on Day 2, compared to Day 1, the separate ANOVA for Day 2 again revealed only a significant main genotype effect ($F=5.15$, df1/51, $p<0.05$), but no significant treatment effect or genotype × treatment interaction ($Fs < 1$). Overall, in the cuetask training, 7-8 months old PDAPP mice were found to display either sensorimotor impairment or basic learning deficit and the 4-month treatment of ELN44989 did not improve the impaired performance of the same mice in this task.

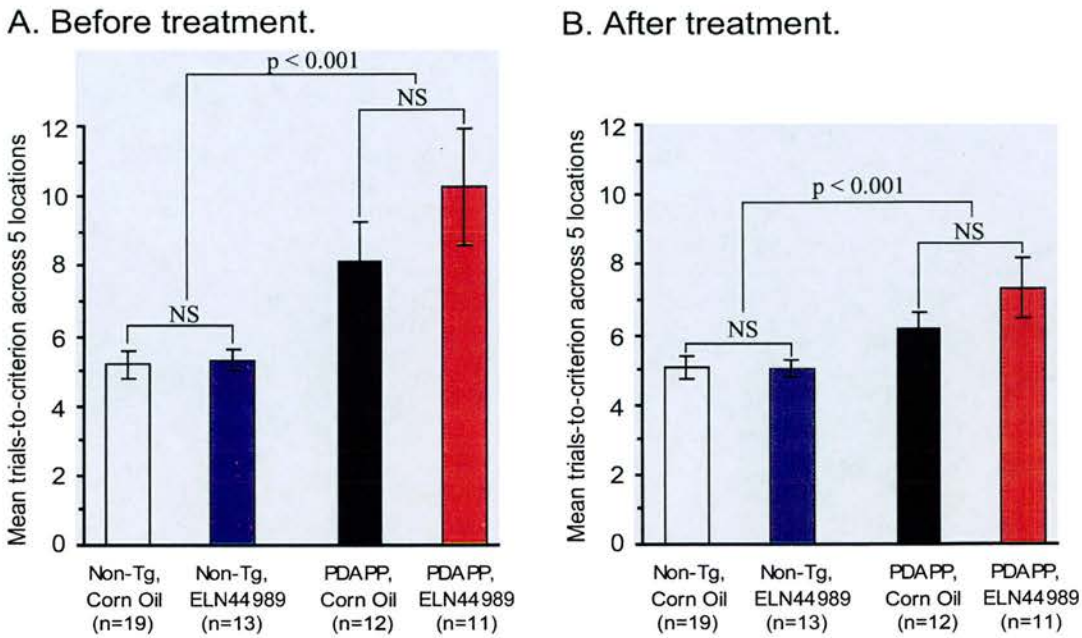

Figure 7.3.3 Performance on the Trials to Criterion Task.

A. Performance of trials to criterion in 7-8 months old mice across the five platform locations before the treatment, and "n" represents the total number of animals that survived during the study. B. After 4 months treatment of ELN44989, performance of trials to criterion in 11-12 months old mice.

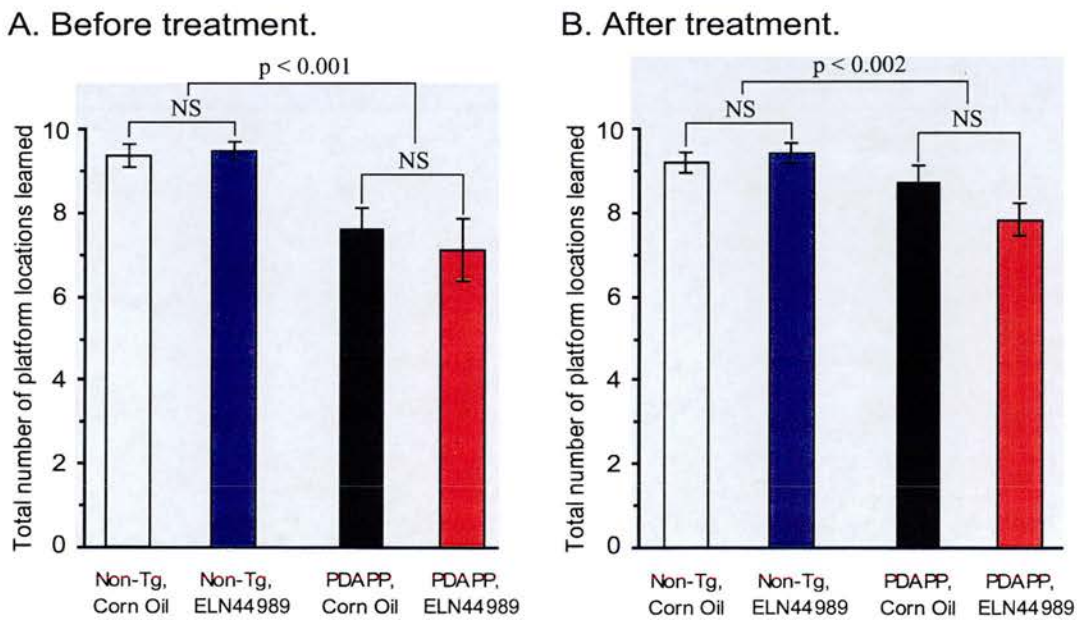

Figure 7.3.4 Performance on the Learning Capacity Task.

A. Performance of 7-8 months old mice before the treatment of ELN44989.

B. After 4 months treatment of ELN44989, performance of 11-12 months old mice.

3. PDAPP mice displayed impaired learning in serial spatial learning before and after treatment of ELN44989.

As before, trials to criterion was used as a measure to examine the learning rate of the animals on a series of 5 successive hidden platform locations in watermaze. Figure 7.3.3 shows the results for this task before and after the treatment of ELN44989. As shown in Fig. 7.3.3A, PDAPP mice displayed significant learning deficit in this task, as revealed by ANOVA ($F=19.25$, df1/51, $p<0.001$). After 4 months treatment of ELN44989, analysis of variance again revealed a significant main genotype effect (Fig. 7.3.3B: $F=13.15$, df1/51, $p<0.001$), but no significant treatment effect or genotype × treatment interaction ($Fs < 1$) (Fig. 7.3.3B). The results here indicated that the 4-month treatment of ELN44989 did not improve the performance of PDAPP mice on trials to criterion task.

4. PDAPP mice displayed impaired learning in learning capacity task before and after treatment of ELN44989.

To investigate whether there is any effect of ELN44989 on spatial learning of PDAPP mice, learning capacity task was then used to test these mice. The results were shown in Figure 7.3.4. Fig. 7.3.4A shows the performance of PDAPP mice before the treatment. Analysis of variance revealed a significant genotype effect in this task ($F=23.07$, df1/51, $p<0.001$), suggesting that PDAPP mice were impaired in learning this task at young age (7-8 months) prior to plaque deposition. After 4 months treatment of ELN44989, the same mice were tested again with a different set of 10 consecutive platform locations. Interestingly, ANOVA again revealed a significant main genotype effect (Fig. 7.3.4B: $F=11.86$, df1/51, $p<0.002$), but no significant treatment effect or genotype × treatment interaction ($Fs < 1$) (Fig. 7.3.4B). These data again indicated that the 4-month treatment of PDAPP mice with ELN44989 did not improve the performance in learning capacity task.

5. PDAPP mice displayed deficit of synaptic transmission in the hippocampus after treatment of ELN44989.

The above behavioural study showed that ELN44989 had no effect on spatial learning of PDAPP mice. As it is unknown whether the treatment of ELN44989 has any effect on synaptic transmission of PDAPP mice, the hippocampal basal synaptic transmission of the same mice, which were behaviourally tested, was further

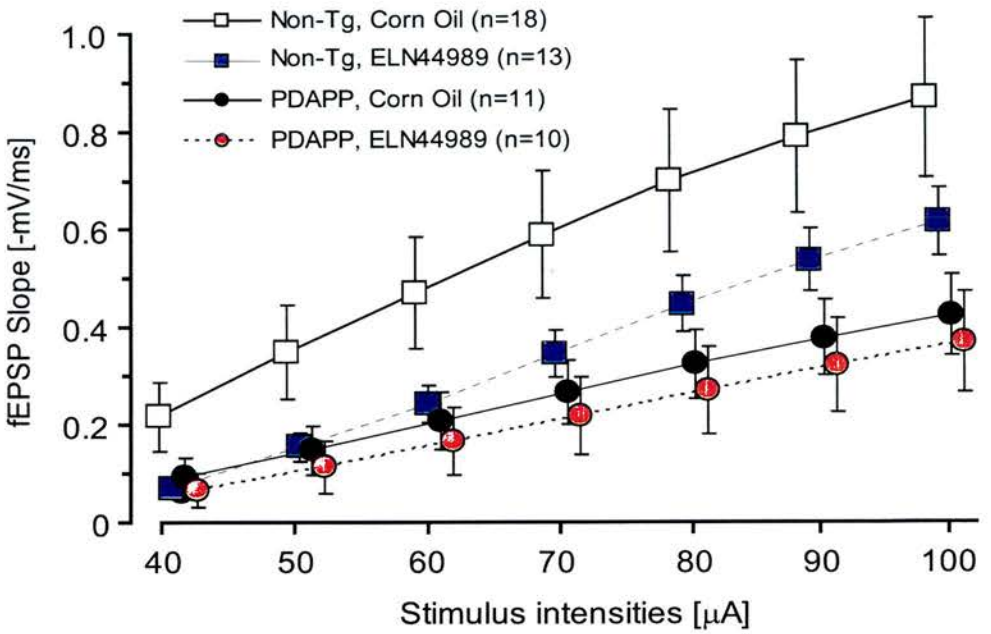

Figure 7.3.5 Impaired Basal Synaptic Transmission in PDAPP Mice.
Input-output curves for PDAPP and non-Tg mice. There was only a significant main genotype effect ($p<0.05$). The treatment of ELN44989 did not significantly affect the input-output curves of either non-Tg mice ($F=2.18$, $df1/29$, $p>0.15$) or PDAPP mice ($F<1$). N is the total number of animals used in the experiments.

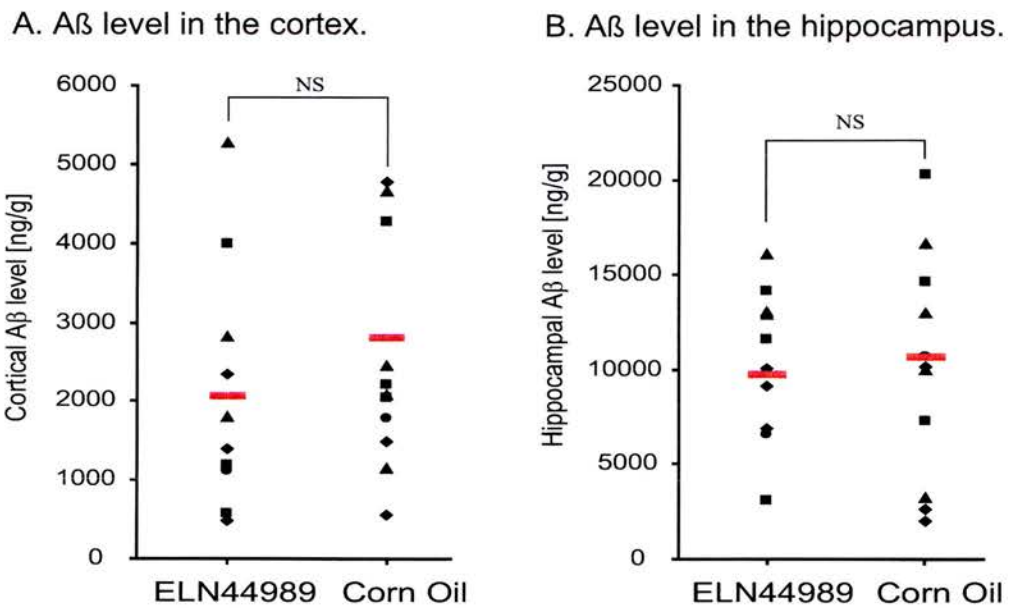

Figure 7.3.6 Total Aß Levels in the Brain.
A. Cortical total Aß level (Red bar represents the mean value). The treatment of ELN44989 did not significantly reduce Aß level in the cortex of PDAPP mice ($p>0.25$). B. Hippocampal total Aß level. The treatment of ELN44989 did not significantly reduce Aß level in the hippocampus ($p>0.6$) as well.

investigated. Using *in vitro* slice electrophysiology, the input-output curves were recorded from hippocampal slices of the mice (Figure 7.3.5). A significant main effect of genotype was found ($F=4.66$, $df1/48$, $p<0.05$), but there is no significant treatment effect ($F=1.81$, $df1/48$, $p=0.18$) or genotype × treatment interaction ($F < 1$), suggesting that the treatment of ELN44989 did not improve the reduced level of synaptic transmission in PDAPP mice.

6. Four months treatment of ELN44989 did not significantly reduce Aβ levels in PDAPP mice.

We did not observe any effects of ELN44989 on either spatial learning or synaptic transmission of PDAPP mice. There are several possible reasons. First, ELN44989 might improve AD-like pathology but not learning and memory of the same mice. Second, ELN44989 might not also affect AD-like pathology in the treated animals. To investigate the second possibility, my colleague Dione Kobayashi at Elan completed ELISAs of total Aβ levels in all PDAPP mice used in my behavioural study. Fig. 7.3.6 shows the *in vivo* effects of chronic treatment of ELN44989 on total Aβ levels in both the cortex and hippocampus of PDAPP mice. Surprisingly, the 4 months treatment of ELN44989 did not significantly reduce total Aβ levels in either the cortex (Fig. 7.3.6A: $F=1.27$, $df1/21$, $p>0.25$) or hippocampus (Fig. 7.3.6B: $F<1$), suggesting that ELN44989, a γ-secretase inhibitor did not effectively inhibit Aβ production in PDAPP mice. It is unclear why this drug did not work in this chronic *in vivo* study. As ELN44989 did not show any effect on Aβ reduction, it seems very reasonable that it failed to improve the impaired spatial learning of PDAPP mice. However, due to the failure of ELN44989 to reduce Aβ levels, it remains unknown whether more potent secretase inhibitor that did cause high levels of Aβ reduction could rescue the impaired spatial learning in APP Tg mice.

7.4 Discussion.

1. Side effects of ELN44989, a γ-secretase inhibitior.

Although previous reports do not describe side effects of acute or chronic treatment with DAPT or LY411575, such as coat colour changes or mortality (Dovey et al., 2001; May et al., 2001), side effects of ELN44989, a more potent γ-secretase inhibitor than DAPT, were observed in this study. Firstly, treatment of the mice with

ELN44989 induced a significantly higher discontinuation rate than corn oil. Initially, a total number of 42 mice (non-Tg=24, PDAPP=18) were treated with ELN44989 (1mg/kg). At the end of 4 months treatment, 18 mice had been discontinued. Among these 18 mice, 9 were found dead in their home cages, the remainder were sacrificed by named veterinary surgeons in this university due to dramatic weight loss (>40%). With such a big weight loss (>40%), they would eventually die even if they had not been sacrificed. The 42.86% discontinuation rate in the ELN44989-treated groups (8.82% in corn oil-treated groups) suggested that ELN44989 induce a very high mortality. It is unclear whether the death of animals caused by ELN44989 was through Notch pathway or other reasons. At least, one possibility is that, ELN44989 had severe toxic gastric or intestinal effects on treated animals, as bleeding in the anus in all ELN44989-treated mice was also observed. It has recently reported that doses of 10 and 20 mg/ml of Compound X (Seiffert et al., 2000), a γ-secretase inhibitor, produced severe gastrointestinal toxicities in rats after four daily doses (Searfoss et al., 2003).

Secondly, color change (discoloured fur) was observed in all ELN44989-treated mice. This side effect occurred as early as 4 weeks after ELN44989 treatment. Although not reported previously (Dovey et al., 2001; May et al., 2001; Searfoss et al., 2003), this has been seen elsewhere (personal communication with Karen Chen at Elan). The reason why this effect was not observed in a previous chronic study by May (2001) was possibly that, white PDAPP mice (Swiss Webster background) were used, so the color change of coat may not be easy to observe. It is unclear whether lower concentrations of ELN44989 can prevent these two side effects.

2. ELN44989 had no effects on Aβ levels and spatial learning of PDAPP mice.

Major findings of this study were that chronic treatment with ELN44989 showed no effects on either synaptic deficits or impaired learning of PDAPP mice, suggesting that ELN44989 might not be a good compound for the treatment of AD. The ELISA study by Dione Kobayashi further confirmed that chronic treatment of PDAPP with ELN44989 produced only a 20% reduction of total Aβ in the cortex, and this reduction was not significant. Although ELN44989 was found to be a better γ-secretase inhibitor to reduce Aβ levels (>80% reduction) *in vitro* than DAPT, its *in vivo* potency was not efficacious.

In contrast to this study on ELN44989, a group from Wyeth have since reported an acute effect of DAPT on cognition of Tg2576 mice (Comery et al., 2003). Contextual fear conditioning was used with acute treatment of Tg2576 mice 3 h before contextual fear conditioning training. 20-, 36-, 54- and 65-week old Tg2576 mice were treated with DAPT (100mg/kg) and their performance on conditioning was found to be significantly improved by this acute treatment. The efficacy of DAPT on Aβ levels in the same Tg2576 mice was not reported, but the authors showed that there was a 55% peak reduction of Aβ 4h after acute treatment with DAPT in another cohort of 12-14 weeks old Tg2576 mice (Comery et al., 2003). These results looked very interesting, as one dose of DAPT seemed enough to rescue the impaired fear contextual conditioning of Tg2576 mice. As a chronic disease, AD shows progressive memory loss and other cognitive impairment. It seems very unlikely that one dose of DAPT could cure the devastating AD, but acute as distinct from chronic effects should still be considered.

In this study, the failure of ELN44989 to significantly reduce Aβ levels and to rescue impaired spatial learning of PDAPP might not necessarily suggest that γ-secretase inhibitors are ineffective for the treatment of AD. Indeed, compared to other studies on DAPT, the concentration of ELN44989 used in this study was only 1% of the DAPT by other groups. In order to produce significant reduction of Aβ *in vivo*, a yet higher concentration of ELN44989 may be needed. However, due to severe toxic effects of this compound, it is impossible to further increase the concentration of ELN44989 for *in vivo* study as it is not tolerated by the animals. The hope of γ-secretase inhibitor for the treatment of AD is not dead because more selective JLK isocoumarin inhibitors than DAPT or ELN44989 have recently been developed (Petit et al., 2001; Petit et al., 2002; Petit et al., 2003). Although these new compounds are less potent and are reported to exert only an indirect inhibition of γ-secretase, they do act only on APP processing and not the Notch pathway (Esler et al., 2002). This raises a possibility that these JLK isocoumarin inhibitors may be free of toxicity. To validate that JLK isocoumarin inhibitors are promising candidates for the treatment of AD, more *in vivo* studies are needed to evaluate their efficacy of reducing Aβ levels in APP Tg mice or tangle/plaque mice. Furthermore, behavioural studies are also needed to assess the effects of JLK inhibitors on cognition of APP Tg mice.

On the other hand, as at least one group have started clinical studies of γ-secretase inhibitor for a couple of years (Wolfe, 2002), we may not need to wait too long to learn what the clinical trials will bring us on its potential use for the treatment of AD.

3. Sensorimotor abnormalities in young PDAPP mice.

As shown in Chapters 3 and 4, young PDAPP mice at 6-9 months of age performed as well as the non-Tg littermates (Figs. 3.3.1 and 4.3.1) on all days of testing, although old PDAPP mice (18-21 months) displayed a transient deficit in the cuetask on Day 1, their performance level matched that of old non-Tg controls in subsequent days. Unlike the mice used in the previous studies, the new cohort of PDAPP mice for this study displayed significant sensorimotor abnormalities as revealed by cuetask training. However, although statistically clear, the absolute magnitude of the impairment (differences in escape latency) of PDAPP mice was very slight on the last two days of training before the treatment of ELN44989. Similarly, only a very moderate transgene effect was again observed after 4 months of drug treatment. As all PDAPP mice could reach less than 10 s of escape latency on the last two days of the cuetak training, this indicates that young PDAPP mice may not have severe sensorimotor problem.

It is difficult to explain this difference between the present and previous studies. One possibility is related to the genetic background of these mice. The background of PDAPP mice used in my previous studies was mainly on DBA and C57/B6, whereas that for the present study was a triple background (Swiss Webster, DBA and C57/B6). We do not know why Elan changed the breeding lines of PDAPP mice to maintain these mice. Maybe the Swiss Webster is a better mouse strain to develop AD-like pathology, such as amyloid plaques and gliosis. At least, this seems to be true of the JNPL3 Tau Tg mouse line, developed by Mayo Clinics. For example, the JNPL3 mice on Swiss Webster background displayed NFTs as early as 6-9 months (Lewis et al., 2000), but the C57B/6-background JNPL3 mice did not show any NFTs by 14-15 months of age (personal communication with Dr. Karen Horsburgh).

Chapter 8: Conclusions and General Discussion.

8.1. Age-related and age-independent learning deficits in PDAPP mice: evidence for the amyloid cascade hypothesis.

Although the amyloid cascade hypothesis has become the dominant theory for the pathogenesis of AD for more than a decade (Hardy and Allsop, 1991), it is still very puzzling whether amyloid plaques play the central role in dementia and cognitive impairment in AD. For example, several clinical studies have indicated that senile plaques are correlated very well with dementia and cognitive decline in AD (Blessed et al., 1968; Cummings and Cotman, 1995; Naslund et al., 2000; Roth et al., 1966). By contrast, other clinical evidence showed that NFTs and/or neuronal loss, rather than plaques, are highly correlated with dementia and cognitive impairment in AD (Arriagada et al., 1992; Gomez-Isla et al., 1997; Guillozet et al., 2003; Hyman and Tanzi, 1992; Wilcock and Esiri, 1982).

Most of recent studies on APP rodents seemed to suggest that soluble Aβ is more important than amyloid plaques in causing learning and memory deficits. Firstly, PDAPP mice consistently display a plaque-independent learning deficit (Chen et al., 2000; Justice and Motter, 1997; Ramsay and Morris, 1998). Secondly, evidence from the studies of other known APP Tg lines has indicated that there are indeed plaque-independent synaptic deficit and learning impairment (Hsia et al., 1999; Janus et al., 2000; Moechars et al., 1999; Moran et al., 1995; Nalbantoglu et al., 1997; Van Dam et al., 2003).

In this thesis, a cross-sectional and a longitudinal design were used to investigate the relationships between learning deficits and amyloid plaques in PDAPP mice. Firstly, using three different cohorts of naïve PDAPP mice, I have indicated that PDAPP mice simultaneously display an age-independent and a plaque-related learning deficit. Very interestingly, I have found that the age-related component of cognitive impairment in old PDAPP mice is highly correlated with plaque burden in the hippocampus. Secondly, in the longitudinal study, I have found that the same PDAPP mice display significant age-related learning deficits. In other words, young PDAPP mice (6-9 months) display unimpaired spatial learning, but the same mice exhibit impaired

learning when they get older (14-15 or 21-22 months). So, the longitudinal study also suggests that amyloid plaques play a very important role in causing learning deficit. As the sample size (non-Tg=13, PDAPP=12) for the longitudinal study is relatively small, compared to that for the cross-sectional study, I did not observe any age-independent learning impairment. If the sample size for PDAPP is larger, it is very likely to observe the same age-independent learning impairment as that in the cross-sectional study. It has also been shown that Tg2576 mice display plaque-related memory deficits only (Chapman et al., 1999; Hsiao et al., 1996). Recent evidence further indicated that injection of Aβ42 and Aβ40 into rat hippocampus induces focal amyloid plaques, causes deficits in synaptic plasticity and disrupts spatial learning (Stephan et al., 2001). Therefore, these data have provided strong evidence to support the amyloid cascade hypothesis.

Although the original theory for the amyloid cascade apparently emphasizes amyloid plaques being the most important in the pathogenesis of AD (Hardy and Allsop, 1991), recently, Selkoe (2002) has systematically proposed a sequential events for this hypothesis, in which the important role of soluble Aβ in causing early synaptic function has been recognized (also see Chapter 1). Thus, the results from my longitudinal and cross-sectional studies, plus many other behavioural and electrophysiological ones support both accumulation of soluble Aβ and amyloid plaques playing the most important role in causing learning and memory deficits in APP Tg mice (Hsia et al., 1999; Janus et al., 2000; Moechars et al., 1999; Moran et al., 1995; Nalbantoglu et al., 1997; Van Dam et al., 2003). Therefore, the findings of both plaque-independent and plaque-related learning impairment in APP Tg mice are supportive to the amyloid cascade hypothesis.

8.2. Effects of active Aβ immunisation on spatial learning of PDAPP mice and potential Aβ immunotherapy in the treatment of Alzheimer's disease.

In this thesis, two active Aβ immunisation studies have been conducted. However, neither long-term prevention (prior to any apparent plaque formation in the brain of PDAPP mice) nor short-term (after plaque deposition) treatment study shows significant improvement effects on synaptic transmission and spatial learning of PDAPP mice. Interestingly, the long-term and short-term Aβ vaccination effectively reduces levels of Aβ42 to 60% and 40%, respectively. Thus, these two studies suggest

that, on the one hand, active Aβ immunotherapy seems very effective in reducing AD-like neuropathology, such as Aβ levels, microgliosis and astrocytosis, on the other hand, active Aβ immunotherapy is relatively ineffective in improving the impaired learning of PDAPP mice, possible due to the altered synaptic transmission being unimproved after active Aβ immunotherapy.

By contrast, it has been shown that active Aβ immunisation rescues impaired learning either in TgCRND8 (Janus et al., 2000) or Tg2576/PS1 Tg mice (Morgan et al., 2000). Recently, Dodart et al showed that one dose of passive Aβ immunisation improves impaired object recognition memory in PDAPP mice. The discrepancy between ours and others may be due to different behavioural paradigms and different ages of animals tested. For example, only young TgCRND8 mice (from 2- to 6-months) were tested by Janus et al (2000) in their Aβ immunisation study. It can be argued from the following two aspects for this study. First, no old Tg mice, which develop large amount of plaques, were tested. Secondly, although young TgCRND8 mice show deficit in the acquisition of the watermaze reference memory task, they display normal spatial memory in terms of the probe trials employed. It is still unclear whether old TgCRND8 mice display spatial learning deficits and whether active Aβ immunisation can produce similar rescue effects on old animals. Interestingly, although Morgan et al (2000) reported the rescue effects of Aβ immunisation on spatial learning of their Tg2576/PS1 Tg mice, the same group recently reported that short-term active Aβ immunisation does not improve performance of old Tg mice using the same task (Austin et al., 2003). One possible explanation for these two studies is that early long-term Aβ immunisation is effective in preventing impaired learning, but late Aβ immunisation is not effective in improving the impaired learning in APP Tg mice.

Another explanation for the discrepancy between ours and Janus et al (2000) and Morgan et al (2000) might be due to the sensibility of behavioural paradigms to Aβ levels. After reanalyzing my data for all vaccinated PDAPP mice from both the prevention and treatment studies, we have found that, if we divided them in two groups in terms of Aβ42 levels, one group displaying about 1000 ng/mg (low level) and the other group showing about 5000 ng/mg of Aβ42 (high level), the group with low Aβ levels showed significantly better performance than the other group with high

Aβ levels ($t=2.84$, $df=39$, $p<0.01$). More interestingly, the low-Aβ group were not different from non-Tgs in terms of behavioural performance. As Shenk et al (1999) showed that very early Aβ vaccination on PDAPP mice prior to 2 months can produce more significant effects on Aβ levels than the two paradigms used in this thesis, it might be worth doing a very early Aβ vaccination experiment using the trials to criterion and learning capacity task in the future. By contrast, the performance on the radial-arm watermaze task by PS1/APP mice seems not sensitive to both Aβ42 levels and amyloid plaques, as 15-16 months mice display normal performance compared to non-Tgs (Morgan et al., 2000).

Although active Aβ immunotherapy is very effective in improving AD-like pathology, it is ineffective in rescuing impaired spatial learning in PDAPP mice. Data presented in Chapter 5 of this thesis seem not to be very supportive to the amyloid cascade hypothesis, but they are not contradictory to it. Although Aβ levels of PDAPP mice in both the prevention and treatment studies have been significantly reduced by 9- or 5-month Aβ vaccination, the post-treatment levels of Aβ are still very high. This might be the reason why I did not observe any rescue effects on spatial learning of PDAPP mice. Indeed, as vaccinated PDAPP mice with low Aβ levels do show better performance than these with high Aβ levels, this suggests that, if the vaccination starts earlier or more vaccines are given to PDAPP mice, we may be able to find a rescue effect. Moreover, as the new version of the amyloid cascade hypothesis indeed emphasizes the important role of soluble Aβ (i.e. oligomers) in synaptic function and learning and memory in AD (Selkoe 2002), it is not surprising to observe that the vaccinated PDAPP mice with relatively high amount of Aβ levels display impaired spatial learning and memory. Very interestingly, the finding of vaccinated PDAPP mice with low Aβ levels displaying unimpaired behavioural performance might suggest that there is an Aβ Threshold Theory for AD, but more experiments need to be designed to support this idea in the future.

8.3. PS1 and γ-secretase inhibitors: potential novel treatment strategy for the treatment of Alzheimer's disease.

To investigate whether the inhibition of γ-secretase has any effects on synaptic transmission and spatial learning of APP Tg mice, two different studies (genetic and pharmacological) were conducted in this thesis.

In the genetic study, PS1cKO;APP mice, in which the PS1 gene is conditionally inactivated in the forebrain 3 weeks after birth, were tested using several cognitive tasks. Results from this study showed that, compared to age-matched non-Tg controls, young PS1cKO;APP mice (3-4 months) display normal spatial learning in the visible cuetask, trials to criterion and learning capacity task, suggesting a significant rescue effect of PS1 inactivation on spatial learning at young age. However, this study also showed that, while old PS1cKO;APP mice (15-17 months) display relatively unimpaired performance on the trials to criterion task, they show significant impairment in the cuetask and learning capacity task, suggesting only a limited partial rescue effect of PS1 inactivation in old mice. Moreover, PS1 inactivation effectively improves AD-like neuropathology such as amyloid plaques, microgliosis and astrocytosis at both young and old age. It seems very likely that massive accumulation of mutant APP CTFs causes deficits of spatial learning in old PS1cKO;APP mice. Future work should further examine the mechanisms by which the build-up of APP CTFs affects spatial learning.

Secondly, in the pharmacological study, a very potent functional γ-secretase inhibitor, ELN 44989 was administered to chronically treat PDAPP mice. I therefore have investigated whether it is effective to improve AD-like neuropathology and rescue impaired spatial learning. Firstly, this chronic *in vivo* study showed that ELN 44989 does not produce any significant effects on total Aβ levels in the cortex and hippocampus. Secondly, it also showed that ELN 44989 has no effect on rescuing the impaired learning in PDAPP mice. However, we observed that the chronic treatment of ELN 44989 causes serious side effects, including high mortality, gastric problem and color change, on the animals. By contrast, a γ-secretase inhibitor LY411575, similar to the ELN 44989, was reported to effectively inhibit Aβ accumulation (~80-90% reduction) and plaque deposition in PDAPP mice after three-month treatment (May et al., 2001). It is not clear what has caused the different observations between us and May et al. As ELN 44989 is not effective to improve either AD-like pathology or impaired learning of PDAPP mice, a more potent but less toxic γ-secretase inhibitor needs to be tested in the future.

Interestingly, the genetic study on PS1cKO;APP mice indicated that conditional inactivation of PS1 in the forebrain effectively improves both AD-like neuropathology and cognitive impairment in young animals, and effectively improves AD-like pathology but only partially rescues learning impairment in old ones. These results suggest that inactivation of PS1 is useful to prevent cognitive decline for a relatively short period, but not for the entire life. Moreover, compared to young APP mice, young PS1cKO;APP mice show no accumulation of Aβ, APP CTFs and other AD-like pathology, but they display normal spatial learning and memory. Thus, they are strong evidence to support the amyloid cascade hypothesis. On the other hand, old PS1cKO;APP mice do not show accumulation of Aβ and other AD-like pathology, but they display age-dependent accumulation of APP CTFs. Although my behavioural results on old PS1cKO;APP mice are not supportive to the amyloid cascade hypothesis, in fact, they are not the evidence to be against it. The reason is that accumulation of APP CTFs itself causes deleterious effects on learning and memory,

8.4. Sensibility of the trials to criterion and learning capacity task in determining age-related learning deficit in APP Tg mice.

In all studies of this thesis, the trials to criterion and learning capacity tasks in the water maze were developed. In the trials to criterion task, the animals are required to learn a series of 5 consecutive different platform locations to a strict performance criterion. In the learning capacity task, the animals need to learn as many platform locations as they can in a 10-day period. Both tasks require the animals not only to to encode new spatial information as quickly as they can, but also to keep forgetting the previously learned locations, or perhaps, the long-term memory traces stored in the brain. Compared with the conventional reference memory task in the water maze, these two tasks (collectively, the serial spatial learning task) are more episodic-memory-like.

It has been shown that the serial spatial learning task is sensitive to detect both plaque-independent and plaque-related learning deficits in APP Tg models of AD. Previous studies showed that the standard reference memory task and the DMP task reveal only age-independent spatial learning deficit in PDAPP mice (Justice and Motter, 1997; Ramsay and Morris, 1998). One possibility is that these two water maze tasks is less sensitive than the serial spatial learning task to detect plaque-related

learning impairment in APP Tg mice. However, recent evidence suggests a second possibility. By using two different sizes of water maze, Kelly et al (2003) observed both age-dependent and age-independent learning impairment in APP23 Tg mice, suggesting that the conventional reference memory task is still sensitive to detect age-related learning deficit in APP mice.

It seems that the trials to criterion task is not very different from the learning capacity task, as both tasks require the animal to encode new platform information (or to form new memory traces in the brain) as fast as they can and to forget old platform locations (or to erase memory traces for previously learned locations) as much as they can. The difference between them is that, the former measures the encoding rate for the individual spatial locations and the latter measures the encoding capacity of the animals. Obviously, the faster the animals learn each individual platform location (less trials to reach criterion), the more platform locations the animals will learn (bigger learning capacity). Indeed, a correlation analysis for all data available for this thesis indicated that there is a highly significant negative correlation between the trials to criterion and learning capacity ($r=-0.83$, $p<0.00001$). This strongly suggests that the two tasks are highly dependent. Overall, these two novel tasks in the water maze should be continuously serving as sensitive ones to investigate age- and plaque-related learning deficit in animal models of AD and aging brain.

References

Abbenante G, Kovacs DM, Leung DL, Craik DJ, Tanzi RE, Fairlie DP (2000) Inhibitors of beta-amyloid formation based on the beta-secretase cleavage site. Biochemical and Biophysical Research Communications 268:133-135.

Allen RD, Weiss DG, Hayden JH, Brown DT, Fujiwake H, Simpson M (1985) Gliding movement of and bidirectional transport along single native microtubules from squid axoplasm: evidence for an active role of microtubules in cytoplasmic transport. The Journal of Cell Biology 100:1736-1752.

Allsop D, Haga SI, Haga C, Ikeda SI, Mann DM, Ishii T (1989) Early senile plaques in Down's syndrome brains show a close relationship with cell bodies of neurons. Neuropathol Appl Neurobiol 15:531-542.

Alzheimer A (1907) Uber eine eigenartige Erkrankung der Hirnrinde. Allgemeine Zeitschrift fur Psychiatrie und Psychisch-Gerichtlich Medecin 64:146-148.

Alzheimer A (1911) Uber eigenartige Krankheitsfalle des spateren Alters. Zbl ges Neurol Psych 4:356-385.

Alzheimer's disease collaborative group (1995) The structure of the presenilin 1 (*S*182) gene and identification of six novel mutations in early onset AD families. Nature Genetics 11:219-222.

American Psychiatric Association (1994) Diagnostic and statistical manual of mental disorders. Fourth Edition. Washington, DC.

Ancolio K, Marambaud P, Dauch P, Checler F (1997) Alpha-secretase-derived product of beta-amyloid precursor protein is decreased by presenilin 1 mutations linked to familial Alzheimer's disease. J Neurochem 69:2494-2499.

Andreadis A, Brown WM, Kosik KS (1992) Structure and novel exons of the human tau gene. Biochemistry 31:10626-10633.

Arai H, Kosaka K, Iizuka R (1984) Changes of biogenic amines and their metabolites in postmortem brains from patients with Alzheimer-type dementia. Journal of Neurochemistry 43:388-393.

Arendash GW, King DL, Gordon MN, Morgan D, Hatcher JM, Hope CE, Diamond DM (2001) Progressive, age-related behavioral impairments in transgenic mice carrying both mutant amyloid precursor protein and presenilin-1 transgenes. Brain Research 891:42-53.

Arendt T (2001) Disturbance of neuronal plasticity is a critical pathogenetic event in Alzheimer's disease. International Journal of Developmental Neuroscience 19:231-245.

Arendt T, Holzer M, Fruth R, Bruckner MK, Gartner U (1995) Paired helical filament-like phosphorylation of tau, deposition of beta/A4-amyloid and memory impairment in rat induced by chronic inhibition of phosphatase 1 and 2A. Neuroscience 69:691-698.

Arriagada P, Growdon J, Hedley-Whyte E, Hyman B (1992) Neurofibrillary tangles but not senile plaques parallel duration and severity of Alzheimer's disease. Neurology 42:631-639.

Austin L, Arendash GW, Gordon MN, Diamond DM, DiCarlo G, Dickey C, Ugen K, Morgan D (2003) Short-term beta-amyloid vaccinations do not improve cognitive performance in cognitively impaired APP+PS1 mice. Behavioral Neuroscience 117:478-484.

Bard F, Cannon C, Barbour R, Burke RL, Games D, Grajeda H, Guido T, Hu K, Huang J, Johnson-Wood K, Khan K, Kholodenko D, Lee M, Lieberburg I, Motter R, Nguyen M, Soriano F, Vasquez N, Weiss K, Welch B, Seubert P, Schenk D, Yednock T (2000) Peripherally administered antibodies against amyloid beta-peptide enter the central nervous system and reduce pathology in a mouse model of Alzheimer disease. Nat Med 6:916-919.

Barnes PN, Zamani R, Chapman PF, Good MA (2001) Age- and task-dependent learning impairment in the Tg2576 transgenic mouse model of AD. Abstract for Society for Neuroscience:Program No. 880.886. 2001.

Bartoo GT, Nochlin D, Chang D, Kim Y, Sumi SM (1997) The mean Abeta load in the hippocampus correlates with duration and severity of dementia in subgroups of Alzheimer disease. J Neuropathol Exp Neurol 56:531-540.

Bartus RT (2000) On neurodegenerative diseases, models and treatment strategies: lessons learned and lessons forgotten a generation following the cholinergic hypothesis. Exp Neurol 163:495-529.

Bartus RT, Dean RI, Beer B, Lippa AS (1982) The cholinergic hypothesis of geriatric memory dysfunction. Science 217:408–414.

Beher D, Wrigley JDJ, Nadin A, Evin G, Masters CL, Harrison T, Castro JL, Shearman MS (2001) Pharmacological knock-down of the presenilin 1 heterodimer by a novel gamma-secretase inhibitor. Implications for presenilin biology. The Journal of Biological Chemistry 276:45394-45402.

Behl C, Davis J, Cole GM, and Schubert D (1992) Vitamin E protects nerve cells from amyloid beta protein toxicity. Biochem Biophys Res Commun 186:944-950.

Behl C, Davis JB, Lesley R, Schubert D (1994) Hydrogen peroxide mediates amyloid beta protein toxicity. Cell 77:817-827.

Bennett RG, Duckworth WC, Hamel FG (2000) Degradation of amylin by insulin-degrading enzyme. The Journal of Biological Chemistry 275:36621-36625.

Berger-Sweeney J, McPhie DL, Arters JA, Greenan J, Oster-Granite ML, Neve RL (1999) Impairments in learning and memory accompanied by neurodegeneration in mice transgenic for the carboxyl-terminus of the amyloid precursor protein. Molecular Brain Research 66:150-162.

Blanchard V, Czech C, Bonici B, Clavel N, Gohin M, Dalet K, Revah F, Pradier L, Imperato A, Moussaoui S (1997) Immunohistochemical analysis of presenilin 2 expression in the mouse brain: distribution pattern and co-localization with presenilin 1 protein. Brain Res 758:209-217.

Blessed G, Tomlinson BE, Roth M (1968) The association between quantitative measures of dementia and of senile change in the cerebral grey matter of elderly subjects. Br J Psychiatry 114:797-811.

Bliss TVP, Richards CD (1971) Some experiments with in vitro hippocampal slices. Journal of Physiology 214:7P-9P.

Borchelt DR, Thinakaran G, Eckman CB, Lee MK, Davenport F, Ratovitsky T, Prada CM, Kim G, Seekins S, Yager D, Slunt HH, Wang R, Seeger M, Levey AI, Gandy SE, Copeland NG, Jenkins NA, Price DL, Younkin SG, Sisodia SS (1996) Familial Alzheimer's disease-linked presenilin 1 variants elevate Abeta1-42/1-40 ratio in vitro and in vivo. Neuron 17:1005-1013.

Bowen DM, Smith CB, White P, Davison AN (1976) Neurotransmitter-related enzymes and indices of hypoxia in senile dementia and other abiotrophies. Brain; a Journal of Neurology 99:459-496.

Bowes MP, Masliah E, Otero DA, Zivin JA, Saitoh T (1994) Reduction of neurological damage by a peptide segment of the amyloid beta/A4 protein precursor in a rabbit spinal cord ischemia model. Exp Neurol 129:112–119.

Braak E, Braak H, Mandelkow EM (1994) A sequence of cytoskeleton changes related to the formation of neurofibrillary tangles and neuropil threads. Acta Neuropathol (Berl) 87:554-567.

Braak H, Braak E (1991) Neuropathological stageing of Alzheimer-related changes. Acta Neuropathol (Berl) 82.:239-259.

Brion JP, Tremp G, Octave JN (1999) Transgenic expression of the shortest human tau affects its compartmentalization and its phosphorylation as in the pretangle stage of Alzheimer's disease. American Journal of Pathology 154:255-270.

Brown MS, Ye J, Rawson RB, Goldstein JL (2000) Regulated intramembrane proteolysis: a control mechanism conserved from bacteria to humans. Cell 100:391-398.

Buee L, Bussiere T, Buee-Scherrer V, Delacourte A, Hof PR (2000) Tau isoforms in neurodegenerative disorders. Brain Res Rev 33:95-130.

Buxbaum JD, Liu KN, Luo Y, Slack JL, Stocking KL, Peschon JJ, Johnson RS, Castner BJ, Cerretti DP, Black RA (1998) Evidence that tumor necrosis factor alpha converting enzyme is involved in regulated alpha-secretase cleavage of the Alzheimer amyloid protein precursor. The Journal of Biological Chemistry 273:27765-27767.

Cai H, Wang Y, McCarthy D, Wen H, Borchelt DR, Price DL, Wong PC (2001) BACE1 is the major beta-secretase for generation of Abeta peptides by neurons. Nat Neurosci 4:233-234.

Cai XD, Golde TE, Younkin SG (1993) Release of excess amyloid beta protein from a mutant amyloid beta protein precursor. Science 259:514-516.

Calhoun ME, Wiederhold KH, Abramowski D, Phinney AL, Probst A, Sturchler-Pierrat C, Staufenbiel M, Sommer B, Jucker M (1998) Neuron loss in APP transgenic mice. Nature 395:755-756.

Campion D, Brice A, Dumanchin C, Puel M, Baulac M, De La Sayette V, Hannequin D, Duyckaetrs C, Michon A, Martin C, Moreau V, Penet C, Martinez M, Clerget-Darpoux F, Agid Y, Frebourg T (1996) A novel presenilin 1 mutation resulting in familial Alzheimer's disease with an onset age of 29 years. NeuroReport 7:1582-1584.

Chapman PF, White GL, Jones MW, Cooper-Blacketer D, Marshall VJ, Irizarry M, Younkin L, Good MA, Bliss TV, Hyman BT, Younkin SG, Hsiao KK (1999) Impaired synaptic plasticity and learning in aged amyloid precursor protein transgenic mice. Nat Neurosci 2:271-276.

Chartier-Harlin MC, Crawford F, Houlden H, Warren A, Hughes D, Fidani L, Goate A, Rossor M, Roques P, Hardy J, Mullan M (1991) Early-onset Alzheimer's disease caused by mutations at codon 717 of the beta-amyloid precursor protein gene. Nature 353:844–846.

Chen G, Chen KS, Knox J, Inglis J, Bernard A, Martin SJ, Justice A, McConlogue L, Games D, Freedman SB, Morris RG (2000) A learning deficit related to age and beta-amyloid plaques in a mouse model of Alzheimer's disease. Nature 408:975-979.

Chen W (1999) Medicine Literature Directory: http://www37ccomcn/literature/analecta/data/xdkf/199908/130html.

Cherny RA, Legg JT, McLean CA, Fairlie DP, Huang X, Atwood CS, Beyreuther K, Tanzi RE, Masters CL, Bush AI (1999) Aqueous dissolution of Alzheimer's disease Abeta amyloid deposits by biometal depletion. The Journal of Biological Chemistry 274:23223-23228.

Cherny RA, Atwood CS, Xilinas ME, Gray DN, Jones WD, McLean CA, Barnham KJ, Volitakis I, Fraser FW, Kim Y, Huang X, Goldstein LE, Moir RD, Lim JT, Beyreuther K, Zheng H, Tanzi RE, Masters CL, Bush AI (2001) Treatment with a copper-zinc chelator markedly and rapidly inhibits beta-amyloid accumulation in Alzheimer's disease transgenic mice. Neuron 30:665-676.

Chishti MA, Yang D-S, Janus C, Phinney AL, Horne P, Pearson J, Strome R, Zuker N, Loukides J, French J, Turner S, Lozza G, Grilli M, Kunicki S, Morissette C, Paquette J, Gervais F, Bergeron C, Fraser PE, Carlson GA, George-Hyslop PS, Westaway D (2001) Early-onset amyloid deposition and cognitive deficits in transgenic mice expressing a double mutant form of amyloid precursor protein 695. The Journal of Biological Chemistry 276:21562-21570.

Churcher I, Williams S, Kerrad S, Harrison T, Castro JL, Shearman MS, Lewis HD, Clarke EE, Wrigley JD, Beher D, Tang YS, Liu W (2003) Design and synthesis of highly potent benzodiazepine gamma-secretase inhibitors: preparation of (2S,3R)-3-(3,4-difluorophenyl)-2-(4-fluorophenyl)-4- hydroxy-N-((3S)-1-methyl-2-oxo-5- phenyl-2,3-dihydro-1H-benzo[e][1,4]-diazepin-3-yl)butyramide by use of an asymmetric Ireland-Claisen rearrangement. J Med Chem 46:2275-2278.

Citron M, Oltersdorf T HC, McConlogue L, Hung AY, Seubert P, Vigo-Pelfrey C, Lieberburg I, Selkoe DJ. (1992) Mutation of the beta-amyloid precursor protein in familial Alzheimer's disease increases beta-protein production. Nature 360:672-674.

Citron M, Diehl TS, Gordon G, Biere AL, Seubert P, Selkoe DJ (1996) Evidence that the 42- and 40-amino acid forms of amyloid beta protein are generated from the beta -amyloid precursor protein by different protease activities. Proceedings of the National Academy of Sciences of the United States of America 93:13170-13175.

Citron M, Vigo-Pelfrey C, Teplow DB, Miller C, Schenk D, Johnston J, Winblad B, Venizelos N, Lannfelt L, Selkoe DJ (1994) Excessive production of amyloid beta-protein by peripheral cells of symptomatic and presymptomatic patients carrying the

Swedish familial Alzheimer disease mutation. Proceedings of the National Academy of Sciences of the United States of America 91:11993-11997.

Citron M, Westaway D, Xia W, Carlson G, Diehl T, Levesque G, Johnson-Wood K, Lee M, Seubert P, Davis A, Kholodenko D, Motter R, Sherrington R, Perry B, Yao H, Strome R, Lieberburg I, Rommens J, Kim S, Schenk D, Fraser P, St George Hyslop P, Selkoe DJ (1997) Mutant presenilins of Alzheimer's disease increase production of 42-residue amyloid beta-protein in both transfected cells and transgenic mice. Nat Med 3:67-72.

Clark LN, Poorkaj P, Wszolek Z, Geschwind DH, Nasreddine ZS, Miller B, Li D, Payami H, Awert F, Markopoulou et a (1998) Pathogenic implications of mutations in the tau gene in pallido-ponto-nigral degeneration and related neurodegenerative disorders linked to chromosome 17. Proceedings of the National Academy of Sciences of the United States of America 95:13103-13107.

Clemens JA, Stephenson DT (1992) Implants containing beta-amyloid protein are not neurotoxic to young and old rat brain. Neurobiology of Aging 13:581-586.

Cleveland DW, Hwo SY, Kirschner MW (1977) Purification of tau, a microtubule-associated protein that induces assembly of microtubules from purified tubulin. J Mol Biol 116:207-225.

Comery TA, Aschmies S, Atchison KP, Borusovic K, Diamantidis G, Gong X, Mayer SC, Zhou H, Martone RL, Sonnenberg-Reine J, Kreft AF, Jacobsen JS, Marquis KL (2003) Acute gamma-secretase inhibition improves cognition in the Tg2576 mouse model of AD. Abstract for Society for Neuroscience:Program No. 525.521.

Cook DG, Sung JC, Golde TE, Felsenstein KM, Wojczyk BS, Tanzi RE, Trojanowski JQ, Lee VM, Doms RW (1996) Expression and analysis of presenilin 1 in a human neuronal system: localization in cell bodies and dendrites. Proceedings of the National Academy of Sciences of the United States of America 93:9223-9228.

Corder EH, Saunders AM, Strittmatter WJ, Schmechel DE, Gaskell PC, Small GW, Roses AD, Haines JL, Pericak-Vance MA (1993) Gene dose of apolipoprotein E type 4 allele and the risk of Alzheimer's disease in late onset families. Science 261:921-923.

Cork LC, Powers RE, Selkoe DJ, Davies P, Geyer JJ, Price DL (1988) Neurofibrillary tangles and senile plaques in aged bears. Journal of Neuropathology and Experimental Neurology 47:629-641.

Cowburn RF, Hardy JA, Roberts PJ (1990) Glutamatergic neurotransmission in Alzheimer's disease. Biochem Soc Trans 18:390-392.

Cross AJ, Crow TJ, Johnson JA, Joseph MH, Perry EK, Perry RH, Blessed G, Tomlinson BE (1983) Monoamine metabolism in senile dementia of Alzheimer type. Journal of the Neurological Sciences 60:383-392.

Cummings BJ, Cotman CW (1995) Image analysis of beta-amyloid load in Alzheimer's disease and relation to dementia severity. Lancet 346:1524–1528.

Cummings BJ, Pike CJ, Shankle R, Cotman CW (1996a) Beta-amyloid deposition and other measures of neuropathology predict cognitive status in Alzheimer's disease. Neurobiology of Aging 17:921-933.

Cummings BJ, Su JH, Cotman CW, White R, Russell MJ (1993) Beta-amyloid accumulation in aged canine brain: A model of early plaque formation in Alzheimer's disease. Neurobiology of Aging 14:547-560.

Cummings BJ, Head E, Afagh A, Milgram NW, Cotman CW (1996b) Beta-amyloid accumulation correlates with cognitive dysfunction in the aged canine. Neurobiol Learn Memory 66:11–23.

Davies P, Maloney AJF (1976) Selective loss of central cholinergic neurons in Alzheimer's disease. The Lancet 308:1403.

Davis JA, Naruse S, Chen H, Eckman C, Younkin S, Price DL, Borchelt DR, Sisodia SS, Wong PC (1998) An Alzheimer's disease-linked PS1 variant rescues the developmental abnormalities of PS1-deficient embryos. Neuron 20:603-609.

Davis KL, Berger PA (1978) Pharmacological investigations of the cholinergic imbalance hypotheses of movement disorders and psychosis. Biological Psychiatry 13:23-49.

Davis KL, Mohs RC, Tinklenberg JR (1979) Enhancement of memory by physostigmine. The New England Journal of Medicine 301:946.

Davis KL, Mohs RC, Tinklenberg JR, Pfefferbaum A, Hollister LE, Kopell BS (1978) Physostigmine: improvement of long-term memory processes in normal humans. Science 201:272-274.

De Strooper B, Saftig P, Craessaerts K, Vanderstichele H, Guhde G, Annaert W, von Figura K, van Leuven F (1998) Deficiency of presenilin-1 inhibits the normal cleavage of amyloid precursor protein. Nature 391:387-390.

De Strooper B, Beullens M, Contreras B, Levesque L, Craessaerts K, Cordell B, Moechars D, Bollen M, Fraser P, George-Hyslop PS, Van Leuven F (1997) Phosphorylation, subcellular localization, and membrane orientation of the Alzheimer's disease-associated presenilins. The Journal of Biological Chemistry 272:3590-3598.

De Strooper B, Annaert W, Cupers P, Saftig P, Craessaerts K, Mumm JS, Schroeter EH, Schrijvers V, Wolfe MS, Ray WJ, Goate A, Kopan R (1999) A presenilin-1-dependent gamma-secretase-like protease mediates release of Notch intracellular domain. Nature 398:466-467.

DeKosky ST, Scheff SW (1990) Synapse loss in frontal cortex biopsies in Alzheimer's disease: correlation with cognitive severity. Ann Neurol 27:457-464.

Delacourte A, Sereant N, Wattez A, Gauvreau D, Robitaille Y (1998) Vulnerable neuronal subsets in Alzheimer's and Pick's disease are distinguished by their tau isoform distribution and phosphorylation. Ann Neurol 43:193-204.

DeMattos RB, Bales KR, Cummins DJ, Dodart J-C, Paul SM, Holtzman DM (2001) Peripheral anti-Abeta antibody alters CNS and plasma Abeta clearance and decreases brain Abeta burden in a mouse model of Alzheimer's disease. Proceedings of the National Academy of Sciences of the United States of America 98:8850-8855.

DeTure M, Ko LW, Yen S, Nacharaju P, Easson C, Lewis J, van Slegtenhorst M, Hutton M, Yen SH (2000) Missense tau mutations identified in FTDP-17 have a small effect on tau-microtubule interactions. Brain Res 853:5-14.

Dewachter I, Reverse D, Caluwaerts N, Ris L, Kuiperi C, Van den Haute C, Spittaels K, Umans L, Serneels L, Thiry E, Moechars D, Mercken M, Godaux E, Van Leuven F (2002) Neuronal deficiency of presenilin 1 inhibits amyloid plaque formation and corrects hippocampal Long-term potentiation but not a cognitive defect of amyloid precursor protein (V717I) transgenic mice. The Journal of Neuroscience 22:3445-3453.

D'Hooge R, De Deyn PP (2001) Applications of the Morris water maze in the study of learning and memory. Brain Res Brain Res Rev 36:60-90.

Doan A, Thinakaran G, Borchelt DR, Slunt HH, Ratovitsky T, Podlisny M, Selkoe DJ, Seeger M, Gandy SE, Price DL, Sisodia SS (1996) Protein topology of presenilin 1. Neuron 17:1023-1030.

Dodart JC, Meziane H, Mathis C, Bales KR, Paul SM, Ungerer A (1999) Behavioral disturbances in transgenic mice overexpressing the V717F beta-amyloid precursor protein. Behav Neurosci 113:982-990.

Dodart JC, Mathis C, Saura J, Bales KR, Paul SM, Ungerer A (2000) Neuroanatomical abnormalities in behaviorally characterized APP(V717F) transgenic mice. Neurobiol Dis 7:71-85.

Dodart JC, Bales KR, Gannon KS, Greene SJ, DeMattos RB, Mathis C, DeLong CA, Wu S, Wu X, Holtzman DM, Paul SM (2002) Immunization reverses memory deficits without reducing brain Abeta burden in Alzheimer's disease model. Nat Neurosci 5:452-457.

Dong LM, Wilson C, Wardell MR, Simmons T, Mahley RW, Weisgraber KH, Agard DA (1994) Human apolipoprotein E. role of arginine 61 in mediating the lipoprotein preferences of the E3 and E4 isoforms. The Journal of Biological Chemistry 268:22358-22365.

Doody RS (2003) Current treatments for Alzheimer's disease: cholinesterase inhibitors. J Clin Psychiatry 64 Suppl 9:11-17.

Doraiswamy PM, Bieber F, Kaiser L, Krishnan KR, Reuning-Scherer J, Gulanski B (1997) The Alzheimer's Disease Assessment Scale: patterns and predictors of baseline cognitive performance in multicenter Alzheimer's disease trials. Neurology 48:1511-1517.

Dovey HF, John V, Anderson JP, Chen LZ, de Saint Andrieu P, Fang LY, Freedman SB, Folmer B, Goldbach E, Holsztynska EJ, Hu KL, Johnson-Wood KL, Kennedy SL, Kholodenko D, Knops JE, Latimer LH, Lee M, Liao Z, Lieberburg IM, Motter RN, Mutter LC, Nietz J, Quinn KP, Sacchi KL, Seubert PA, Shopp GM, Thorsett ED, Tung JS, Wu J, Yang S, Yin CT, Schenk DB, May PC, Altstiel LD, Bender MH, Boggs LN, Britton TC, Clemens JC, Czilli DL, Dieckman-McGinty DK, Droste JJ, Fuson KS, Gitter BD, Hyslop PA, Johnstone EM, Li W-Y, Little SP, Mabry TE, Miller FD, Ni B, Nissen JS, Porter WJ, Potts BD, Reel JK, Stephenson D, Su Y, Shipley LA, Whitesitt CA, Yin T, Audia JE (2001) Functional gamma-secretase inhibitors reduce beta-amyloid peptide levels in brain. J Neurochem 76:173-181.

Duff K, Hardy J (1995) Mouse model made. Nature 373:476-477.

Duff K, Eckman C, Zehr C, Yu X, Prada CM, Perez-tur J, Hutton M, Buee L, Harigaya Y, Yager D, Morgan D, Gordon MN, Holcomb L, Refolo L, Zenk B, Hardy J, Younkin S (1996) Increased amyloid-beta42(43) in brains of mice expressing mutant presenilin 1. Nature 383:710-713.

Dugu M, Neugroschl J, Sewell M, Marin D (2003) Review of dementia. Mt Sinai J Med 70:45-53.

Edbauer D, Winkler E, Haass C, Steiner H (2002) Presenilin and nicastrin regulate each other and determine amyloid beta-peptide production via complex formation. Proceedings of the National Academy of Sciences of the United States of America 99:8666-8671.

Elder GA, Tezapsidis N, Carter J, Shioi J, Bouras C, Li HC, Johnston JM, Efthimiopoulos S, Friedrich VL, Jr., Robakis NK (1996) Identification and neuron specific expression of the S182/presenilin I protein in human and rodent brains. The Journal of Neuroscience Res 45:308-320.

Ennaceur A, Delacour J (1988) A new one-trial test for neurobiological studies of memory in rats. 1: Behavioral data. Behavioural Brain Research 31:47-59.

Ennaceur A, Cavoy A, Costa JC, Delacour J (1989) A new one-trial test for neurobiological studies of memory in rats. II: Effects of piracetam and pramiracetam. Behav Brain Res 33:197-207.

Ernst R, Hay J (1994) The US economic and social costs of Alzheimer's disease revisited. Am J Public Health 84:1261-1264.

Esch FS, Keim PS, Beattie EC, Blacher RW, Culwell AR, Oltersdorf T, McClure D, Ward PJ (1990) Cleavage of amyloid beta peptide during constitutive processing of its precursor. Science 248:1122-1124.

Esler WP, Kimberly WT, Ostaszewski BL, Ye W, Diehl TS, Selkoe DJ, Wolfe MS (2002a) Activity-dependent isolation of the presenilin-gamma-secretase complex reveals nicastrin and a gamma substrate. Proceedings of the National Academy of Sciences of the United States of America 99:2720-2725.

Esler WP, Kimberly WT, Ostaszewski BL, Diehl TS, Moore CL, Tsai JY, Rahmati T, Xia W, Selkoe DJ, Wolfe MS (2000) Transition-state analogue inhibitors of gamma-secretase bind directly to presenilin-1. Nat Cell Biol 2:428-434.

Esler WP, Das C, Campbell WA, Kimberly WT, Kornilova AY, Diehl TS, Ye W, Ostaszewski BL, Xia W, Selkoe DJ, Wolfe MS (2002b) Amyloid-lowering isocoumarins are not direct inhibitors of gamma-secretase. Nat Cell Biol 4:E110-111; author reply E111-112.

Evans DA, Funkenstein HH, Albert MS, Scherr PA, Cook NR, Chown MJ, Hebert LE, Hennekens CH, Taylor JO (1989) Prevalence of Alzheimer's disease in a community population of older persons. Higher than previously reported. JAMA 262:2551-2556.

Feng R, Rampon C, Tang Y-P, Shrom D, Jin J, Kyin M, Sopher B, Martin GM, Kim S-H, Langdon RB (2001) Deficient neurogenesis in forebrain-specific presenilin-1 knockout mice Is associated with reduced clearance of hippocampal memory traces. Neuron 32:911-926.

Ferrer I, Pastor P, Rey MJ, Munoz E, Puig B, Pastor E, Oliva R, Tolosa E (2003) Tau phosphorylation and kinase activation in familial tauopathy linked to deln296 mutation. Neuropathol Appl Neurobiol 29:23-34.

Fibiger HC (1991) Cholinergic mechanisms in learning, memory and dementia: a review of recent evidence. Trends in Neurosciences 14:220-223.

Figueiredo-Pereira ME, Efthimiopoulos S, Tezapsidis N, Buku A, Ghiso J, Mehta P, Robakis NK (1999) Distinct secretases, a cysteine protease and a serine protease, generate the C-termini of amyloid-beta proteins Abeta1-40 and Abeta1-42, respectively. Journal of Neurochemistry 72:1417-1422.

Fitzjohn SM, Morton RA, Kuenzi F, Rosahl TW, Shearman M, Lewis H, Smith D, Reynolds DS, Davies CH, Collingridge GL, Seabrook GR (2001) Age-related impairment of synaptic transmission but normal long-term potentiation in transgenic mice that overexpress the human APP695SWE mutant form of amyloid precursor protein. The Journal of Neuroscience 21:4691-4698.

Flanagan LA, Cunningham CC, Chen J, Prestwich GD, Kosik KS, Janmey PA (1997) The structure of divalent cation-induced aggregates of PIP2 and their alteration by gelsolin and tau. Biophys J 73:1440-1447.

Flood JF, E. Morley J (1997) Learning and memory in the SAMP8 mouse. Neuroscience & Biobehavioral Reviews 22:1-20.

Folstein MF, Folstein SE, McHugh PR (1975) "Mini-mental state". A practical method for grading the cognitive state of patients for the clinician. J Psychiatr Res 12:189-198.

Foy MR, Xu J, Xie X, Brinton RD, Thompson RF, Berger TW (1999) 17-beta-estradiol enhances NMDA receptor-mediated EPSPs and long-term potentiation. J Neurophysiol 81:925-929.

Francis R, McGrath G, Zhang J, Ruddy DA, Sym M, Apfeld J, Nicoll M, Maxwell M, Hai B, Ellis MC, Parks AL, Xu W, Li J, Gurney M, Myers RL, Himes CS, Hiebsch R, Ruble C, Nye JS, Curtis D (2002) aph-1 and pen-2 are required for Notch pathway signaling, gamma-secretase cleavage of betaAPP, and presenilin protein accumulation. Dev Cell 3:85-97.

Frautschy SA, Baird A, Cole GM (1991) Effects of injected Alzheimer beta-amyloid cores in rat brain. Proceedings of the National Academy of Sciences of the United States of America 88:8362-8366.

Fukuchi K-i, Kunkel DD, Schwartzkroin PA, Kamino K, Ogburn CE, Furlong CE, Martin GM (1994) Overexpression of a C-terminal portion of the beta-amyloid precursor protein in mouse brains by transplantation of transformed neuronal cells. Experimental Neurology 127:253-264.

Fukuchi K-I, Ogburn CE, Smith AC, Kunkel DD, Furlong CE, Deeb SS, Nochlin D, Sumi SM, Martin GM (1993) Transgenic animal models for Alzheimer's disease. Annals of the New York Academy of Sciences 695:217-223.

Games D, Khan KM, Soriano FG, Keim PS, Davis DL, Bryant K, Lieberburg I (1992) Lack of Alzheimer pathology after beta-amyloid protein injections in rat brain. Neurobiology of Aging 13:569-576.

Games D, Adams D, Alessandrini R, Barbour R, Berthelette P, Blackwell C, Carr T, Clemens J, Donaldson T, Gillespie F, et al. (1995) Alzheimer-type neuropathology in transgenic mice overexpressing V717F beta-amyloid precursor protein. Nature 373:523-527.

Geling A, Steiner H, Willem M, Bally-Cuif L, Haass C (2002) A gamma-secretase inhibitor blocks Notch signaling in vivo and causes a severe neurogenic phenotype in zebrafish. EMBO Reports 3:688-694.

Ghosh A, Shin D, Downs D, Koelsch G, Lin X, Ermolieff J, Tang J (2000) Design of potent inhibitors for human brain memapsin 2 (beta-secretase). J Am Chem Soc 122:3522-3523.

Glenner GG, Wong CW (1984) Alzheimer's disease: Initial report of the purification and characterisation of a novel cerebrovascular amyloid protein. Biophysical and Biochemical Research Communications 120:885-890.

Goate A, Chartier-Harlin MC, Mullan M, Brown J, Crawford F, Fidani L, Giuffra L, Haynes A, Irving N, James L, et al. (1991) Segregation of a missense mutation in the amyloid precursor protein gene with familial Alzheimer's disease. Nature 349:704-706.

Goedert M, Jakes R (1990) Expression of separate isoforms of human tau protein: correlation with the tau pattern in brain and effects on tubulin polymerization. The EMBO Journal 9:4225-4230.

Goedert M, Jakes R, Vanmechelen E (1995) Monoclonal antibody AT8 recognises tau protein phosphorylated at both serine 202 and threonine 205. Neuroscience Letters 189:167-169.

Goedert M, Spillantini MG, Crowther RA, Chen SG, Parchi P, Tabaton M, Lanska DJ, Markesbery WR, Wilhelmsen KC, Dickson et a (1999) Tau gene mutation in familial progressive subcortical gliosis. Nature Medicine 5:454-457.

Goldgaber D, Lerman MI, McBride OW, Saffiotti U, Gajdusek DC (1987) Characterization and chromosomal localization of a cDNA encoding brain amyloid of Alzheimer's disease. Science 235:877–880.

Goldman-Rakic PS, Brown RM (1981) Regional changes of monoamines in cerebral cortex and subcortical structures of aging rhesus monkeys. Neuroscience 6:177-187.

Gomez-Isla T, Hollister R, West H, Mui S, Growdon JH, Petersen RC, Parisi JE, Hyman BT (1997) Neuronal loss correlates with but exceeds neurofibrillary tangles in Alzheimer's disease. Ann Neurol 41:17-24.

Gotz J, Chen F, van Dorpe J, Nitsch RM (2001a) Formation of neurofibrillary tangles in P301L tau transgenic mice induced by Abeta42 fibrils. Science 293:1491-1495.

Gotz J, Chen F, Barmettler R, Nitsch RM (2001b) Tau filament formation in transgenic mice expressing P301L tau. The Journal of Biological Chemistry 276:529-534.

Gotz J, Probst A, Spillantini MG, Schafer T, Jakes R, Burki K, Goedert M (1995) Somatodendritic localization and hyperphosphorylation of tau protein in transgenic mice expressing the longest human brain tau isoform. The EMBO Journal 14:1304-1313.

Graeber MB, Kosel S, Egensperger R, Banati RB, Muller U, Bise K, Hoff P, Moller HJ, Fujisawa K, Mehraein P (1997) Rediscovery of the case described by Alois Alzheimer in 1911: historical, histological and molecular genetic analysis. Neurogenetics 1:73-80.

Greenberg BD, Savage MJ, Howland DS, Ali SM, Siedlak SL, Perry G, Siman R, Scott RW (1996) APP transgenesis: Approaches toward the development of animal models for Alzheimer disease neuropathology. Neurobiology of Aging 17:153-171.

Greenberg SM, Rebeck GW, Vonsattel JP, Gomez-Isla T, Hyman BT (1995) Apolipoprotein E epsilon 4 and cerebral hemorrhage associated with amyloid angiopathy. Ann Neurol 38:254-259.

Grundke-Iqbal I, Iqbal K, Quinlan M, Tung YC, Zaidi MS, Wisniewski HM (1986) Microtubule-associated protein tau. A component of Alzheimer paired helical filaments. The Journal of Biological Chemistry 261:6084-6089.

Guillozet AL, Weintraub S, Mash DC, Mesulam MM (2003) Neurofibrillary tangles, amyloid, and memory in aging and mild cognitive impairment. Arch Neurol 60:729-736.

Gutzmann H, Hadler D (1998) Sustained efficacy and safety of idebenone in the treatment of Alzheimer's disease: update on a 2-year double-blind multicentre study. J Neural Transm Suppl 54:301-310.

Gutzmann H, Kuhl KP, Hadler D, Rapp MA (2002) Safety and efficacy of idebenone versus tacrine in patients with Alzheimer's disease: results of a randomized, double-blind, parallel-group multicenter study. Pharmacopsychiatry 35:12-18.

Haass C, Hung AY, Selkoe DJ, Teplow DB (1994) Mutations associated with a locus for familial Alzheimer's disease result in alternative processing of amyloid beta-protein precursor. The Journal of Biological Chemistry 269:17741-17748.

Haass C, Hung AY, Schlossmacher MG, Oltersdorf T, Teplow DB, Selkoe DJ (1993) Normal cellular processing of the beta-amyloid precursor protein results in the secretion of the amyloid beta peptide and related molecules. Ann N Y Acad Sci 695:109-116.

Hadland BK, Manley NR, Su D-m, Longmore GD, Moore CL, Wolfe MS, Schroeter EH, Kopan R (2001) Gamma-secretase inhibitors repress thymocyte development. Proceedings of the National Academy of Sciences of the United States of America 98:7487-7491.

Harada A, Oguchi K, Okabe S, Kuno J, Terada S, Ohshima T, Sato-Yoshitake R, Takei Y, Noda T, Hirokawa et a (1994) Altered microtubule organization in small-calibre axons of mice lacking tau protein. Nature 369:488-491.

Hardegg W, Heilbronn E (1961) Oxidation of serotonin and tyramine by rat liver mitochondria. Biochim Biophys Acta 51:553-560.

Hardy J (1997) Amyloid, the presenilins and Alzheimer's disease. Trends in Neurosciences 20:154-159.

Hardy J, Allsop D (1991) Amyloid deposition as the central event in the aetiology of Alzheimer's disease. Trends Pharmacol Sci 12:383-388.

Hardy J, Gwinn-Hardy K (1998) Genetic classification of primary neurodegenerative disease. Science 282:1075-1079.

Hardy JA, Higgins GA (1992) Alzheimer's disease: the amyloid cascade hypothesis. Science 256:184-185.

Harman D (2002) Alzheimer's disease: Role of aging in pathogenesis. Ann NY Acad Sci 959:384-395.

Harper AJ, Harrison SM, Morrison AD, Austin AA, Dingwall C (2003) BACE 1 and 2 double knockout mice are indistinguishable from wild type littermate controls. Abstract for Society for Neuroscience:Program No. 842.812.

Hebert LE, Scherr PA, Bienias JL, Bennett DA, Evans DA (2003) Alzheimer disease in the US population: Prevalence estimates using the 2000 census. Arch Neurol 60:1119-1122.

Helmuth L (2003) Detangling Alzheimer's disease. Sci Aging Knowledge Environ 2003:oa2.

Hendriks L, van Duijn CM, Cras P, Cruts M, Van Hul W, van Harskamp F, Warren A, McInnis MG, Antonarakis SE, Martin JJ, al. e (1992) Presenile dementia and cerebral haemorrhage linked to a mutation at codon 692 of the beta-amyloid precursor protein gene. Nature Genetics 1:218–221.

Higaki J, Quon D, Zhong Z, Cordell B (1995) Inhibition of beta-amyloid formation identifies proteolytic precursors and subcellular site of catabolism. Neuron 14:651-659.

Higaki JN, Chakravarty S, Bryant CM, Cowart LR, Harden P, Scardina JM, Mavunkel B, Luedtke GR, Cordell B (1999) A combinatorial approach to the identification of dipeptide aldehyde inhibitors of beta-amyloid production. J Med Chem 42:3889-3898.

Higgins LS, Cordell B (1995) Genetically engineered animal models of human neurodegenerative diseases. Neurodegeneration 4:117-129.

Higgins LS, Holtzman DM, Rabin J, Mobley WC, Cordell B (1994) Transgenic mouse brain histopathology resembles early Alzheimer's disease. Annals of Neurology 35:598-607.

Higgins LS, Rodems JM, Catalano R, Quon D, Cordell B (1995) Early Alzheimer disease-like histopathology increases in frequency with age in mice transgenic for beta-APP751. Proceedings of the National Academy of Sciences of the United States of America 92:4402-4406.

Higuchi M, Ishihara T, Zhang B, Hong M, Andreadis A, Trojanowski J, Lee VM-Y (2002) Transgenic mouse model of tauopathies with glial pathology and nervous system degeneration. Neuron 35:433-446.

Himmler A, Drechsel D, Kirschner MW, Martin DWJ (1989) Tau consists of a set of proteins with repeated C-terminal microtubule-binding domains and variable N-terminal domains. Mol Cell Biol 9:1381-1388.

Hock C, Konietzko U, Streffer JR, Tracy J, Signorell A, Muller-Tillmanns B, Lemke U, Henke K, Moritz E, Garcia E (2003) Antibodies against beta-amyloid slow cognitive decline in Alzheimer's disease. Neuron 38:547-554.

Holcomb L, Gordon MN, McGowan E, Yu X, Benkovic S, Jantzen P, Wright K, Saad I, Mueller R, Morgan D, Sanders S, Zehr C, O'Campo K, Hardy J, Prada CM, Eckman C, Younkin S, Hsiao K, Duff K (1998) Accelerated Alzheimer-type phenotype in transgenic mice carrying both mutant amyloid precursor protein and presenilin 1 transgenes. Nat Med 4:97-100.

Holcomb LA, Gordon MN, Jantzen P, Hsiao K, Duff K, Morgan D (1999) Behavioral changes in transgenic mice expressing both amyloid precursor protein and presenilin-1 mutations: lack of association with amyloid deposits. Behav Genet 29:177-185.

Hom RK, Gailunas AF, Mamo S, Fang LY, Tung JS, Walker DE, Davis D, Thorsett ED, Jewett NE, Moon JB, John V (2004) Design and synthesis of hydroxyethylene-based peptidomimetic inhibitors of human beta-secretase. J Med Chem 47:158-164.

Hong L, Turner RT, Koelsch G, Ghosh AK, Tang J (2002) Memapsin 2 (beta-secretase) as a therapeutic target. Biochem Soc Trans 30:530-534.

Hong L, Koelsch G, Lin X, Wu S, Terzyan S, Ghosh AK, Zhang XC, Tang J (2000) Structure of the protease domain of memapsin 2 (beta -secretase) complexed with inhibitor. Science 290:150-153.

Horsburgh K, Fitzpatrick M, Nilsen M, Nicoll JAR (1997) Marked alterations in the cellular localisation and levels of apolipoprotein E following acute subdural haematoma in rat. Brain Research 763:103-110.

Horsburgh K, McCarron MO, White F, Nicoll JAR (2000) The role of apolipoprotein E in Alzheimer's disease, acute brain injury and cerebrovascular disease: evidence of common mechanisms and utility of animal models. Neurobiology of Aging 21:245-255.

Hotoda N, Koike H, Sasagawa N, Ishiura S (2002) A secreted form of human ADAM9 has an alpha-secretase activity for APP. Biochemical and Biophysical Research Communications 293:800-805.

Hsia AY, Masliah E, McConlogue L, Yu GQ, Tatsuno G, Hu K, Kholodenko D, Malenka RC, Nicoll RA, Mucke L (1999) Plaque-independent disruption of neural circuits in Alzheimer's disease mouse models. Proceedings of the National Academy of Sciences of the United States of America 96:3228-3233.

Hsiao K (1996) Understanding the biology of β-amyloid precursor proteins in transgenic mice. Neurobiology of Aging 16:705-706.

Hsiao K, Chapman P, Nilsen S, Eckman C, Harigaya Y, Younkin S, Yang F, Cole G (1996) Correlative memory deficits, Abeta elevation, and amyloid plaques in transgenic mice. Science 274:99-103.

Hsiao KK, Borchelt DR, Olson K, Johannsdottir R, Kitt C, Yunis W, Xu S, Eckman C, Younkin S, Price D (1995) Age-related CNS disorder and early death in transgenic FVB/N mice overexpressing Alzheimer amyloid precursor proteins. Neuron 15:1203-1218.

Hussain I, Powell D, Howlett DR, Tew DG, Meek TD, Chapman C, Gloger IS, Murphy KE, Southan CD, Ryan DM (1999) Identification of a novel aspartic protease (Asp 2) as beta-secretase. Molecular and Cellular Neuroscience 14:419-427.

Hutton M, Lendon CL, Rizzu P, Baker M, Froelich S, Houlden H, Pickering-Brown S, Chakraverty S, Isaacs A, Grover A, Hackett J, Adamson J, Lincoln S, Dickson D, Davies P, Petersen RC, Stevens M, de Graaff E, Wauters E, van Baren J, Hillebrand M, Joosse M, Kwon JM, Nowotny P, Heutink P, al. e (1998) Association of missense and 59-splice-site mutations in tau with the inherited dementia FTDP-17. Nature 393:702-705.

Hyman BT, Tanzi RE (1992) Amyloid, dementia and Alzheimer's disease. Curr Opin Neurol Neurosurg 5:88-93.

Hyman BT, Irizarry MC, Soriano F, McNamara M, Page KJ, Schenk D, Games D (1997) Aβ deposition is associated with neuritic changes and gliosis but not with overt neuronal loss in the PDAPP transgenic mouse. Society for Neuroscience Abstracts 23, Part 2:1115.

Ikeda S, Allsop D, Glenner GG (1989a) A study of the morphology and distribution of amyloid beta protein immunoreactive plaque and related lesions in the brains of Alzheimer's disease and adult Down's syndrome. Prog Clin Biol Res 317:313-323.

Ikeda S, Yanagisawa N, Allsop D, Glenner GG (1989b) Evidence of amyloid beta-protein immunoreactive early plaque lesions in Down's syndrome brains. Lab Invest 61:133-137.

in 't Veld BA, Ruitenberg A, Hofman A, Launer LJ, van Duijn CM, Stijnen T, Breteler MMB, Stricker BHC (2001) Nonsteroidal antiinflammatory drugs and the risk of Alzheimer's disease. N Engl J Med 345:1515-1521.

Irizarry MC, Soriano F, McNamara M, Page KJ, Schenk D, Games D, Hyman BT (1997) Abeta deposition is associated with neuropil changes, but not with overt neuronal loss in the human amyloid precursor protein V717F (PDAPP) transgenic mouse. The Journal of Neuroscience 17:7053-7059.

Ishihara T, Zhang B, Higuchi M, Yoshiyama Y, Trojanowski JQ, Lee VM (2001) Age-dependent induction of congophilic neurofibrillary tau inclusions in tau transgenic mice. American Journal of Pathology 158:555-562.

Ishihara T, Hong M, Zhang B, Nakagawa Y, Lee MK, Trojanowski JQ, Lee VM (1999) Age-dependent emergence and progression of a tauopathy in transgenic mice overexpressing the shortest human tau isoform. Neuron 24:751-762.

Itoh A, Akaike T, Sokabe M, Nitta A, Iida R, Olariu A, Yamada K, Nabeshima T (1999) Impairments of long-term potentiation in hippocampal slices of beta-amyloid-infused rats. European Journal of Pharmacology 382:167-175.

Jaffe A, Toran-Allerand C, Greengard P, Gandy S (1994) Estrogen regulates metabolism of Alzheimer amyloid beta precursor protein. The Journal of Biological Chemistry 269:13065-13068.

Janus C, Pearson J, McLaurin J, Mathews PM, Jiang Y, Schmidt SD, Chishti MA, Horne P, Heslin D, French J, Mount HT, Nixon RA, Mercken M, Bergeron C, Fraser PE, St George-Hyslop P, Westaway D (2000) A beta peptide immunization reduces behavioural impairment and plaques in a model of Alzheimer's disease. Nature 408:979-982.

Jarrett JT, Berger EP, Lansbury PTJ (1993) The carboxy terminus of the beta amyloid protein is critical for the seeding of amyloid formation: implications for the pathogenesis of Alzheimer's disease. Biochemistry 32:4693-4697.

Jicha GA, Rockwood JM, Berenfeld B, Hutton M, Davies P (1999) Altered conformation of recombinant frontotemporal dementia-17 mutant tau proteins. Neurosci Lett 260:153-156.

John V, Beck JP, Bienkowski MJ, Sinha S, Heinrikson RL (2003) Human beta-secretase (BACE) and BACE inhibitors. J Med Chem 46:4625-4630.

Johnson-Wood K, Lee M, Motter R, Hu K, Gordon G, Barbour R, Khan K, Gordon M, Tan H, Games D, Lieberburg I, Schenk D, Seubert P, McConlogue L (1997) Amyloid precursor protein processing and Abeta 42 deposition in a transgenic mouse model of Alzheimer disease. Proceedings of the National Academy of Sciences of the United States of America 94:1550-1555.

Jorgensen OS, Brooksbank BWL, Balazs R (1990) Neuronal plasticity ans astrocytic reaction in Down syndrome and Alzheimer disease. J Neurol Sci 98:63-79.

Justice A, Motter R (1997) Behavioral characterization of PDAPP transgenic Alzheimer mice. Soceity for Neuroscience Abstracts 23:636.636.

Kammesheidt A, Boyce F, Spanoyannis A, Cummings B, Ortegon M, Cotman C, Vaught J, Neve R (1992) Deposition of beta/A4 immunoreactivity and neuronal pathology in transgenic mice expressing the carboxyl-terminal fragment of the Alzheimer amyloid precursor in the brain. Proceedings of the National Academy of Sciences of the United States of America 89:10857-10861.

Kang J, Lemaire H, Unterbeck A, al. e (1987) The precursor of Alzheimer's disease amyloid A4 protein resembles a cell surface receptor. Nature 325:733-736.

Kawabata S, Higgins GA, Gordon JW (1991) Amyloid plaques, neurofibrillary tangles and neuronal loss in brains of transgenic mice overexpressing a C-terminal fragment of human amyloid precursor protein. Nature 354:476-478.

Kawabata S, Higgins GA, Gordon JW (1992) Alzheimer's retraction. Nature 356:23.

Kelly PH, Bondolfi L, Hunziker D, Schlecht H-P, Carver K, Maguire E, Abramowski D, Wiederhold K-H, Sturchler-Pierrat C, Jucker M (2003) Progressive age-related impairment of cognitive behavior in APP23 transgenic mice. Neurobiology of Aging 24:365-378.

Kidd M (1963) Paired helical filaments in electron microscopy of Alzheimer's disease. Nature 197:192-193.

Kimberly WT, LaVoie MJ, Ostaszewski BL, Ye W, Wolfe MS, Selkoe DJ (2003) Gamma-secretase is a membrane protein complex comprised of presenilin, nicastrin, Aph-1, and Pen-2. Proceedings of the National Academy of Sciences of the United States of America 100:6382-6387.

King DL, Arendash GW (2002) Behavioral characterization of the Tg2576 transgenic model of Alzheimer's disease through 19 months. Physiology & Behavior 75:627-642.

King DL, Arendash GW, Crawford F, Sterk T, Menendez J, Mullan MJ (1999) Progressive and gender-dependent cognitive impairment in the APPSW transgenic mouse model for Alzheimer's disease. Behavioural Brain Research 103:145-162.

Kinnear PR, Gray CD (2000) SPSS for windows made simple. Psychology Press.

Klafki H-W, Abramowski D, Swoboda R, Paganetti PA, Staufenbiel M (1996) The carboxyl termini of beta-amyloid peptides 1-40 and 1-42 are generated by distinct gamma - secretase activities. The Journal of Biological Chemistry 271:28655-28659.

Knapp MJ, Knopman DS, Solomon PR, Pendlebury WW, Davis CS, Gracon SI (1994) A 30-week randomized controlled trial of high-dose tacrine in patients with Alzheimer's disease. The Tacrine Study Group. JAMA 271:985-991.

Kobayashi DT, Zeller M, Soriano F, McConlogue L, Sinha S, Freedman S, Chen KS (2003) Learning and memory deficits in BACE1 KO X PDAPP mice. Abstract for Society for Neuroscience:Program No. 524.524.

Koike H, Tomioka S, Sorimachi H, Saido TC, Maruyama K, Okuyama A, Fujisawa-Sehara A, Ohno S, Suzuki K, Ishiura S (1999) Membrane-anchored metalloprotease MDC9 has an alpha-secretase activity responsible for processing the amyloid precursor protein. Biochem J 343 Pt 2:371-375.

Koudinov AR, Koudinova NV (2001) Brain cholesterol pathology is the cause of Alzheimer's disease. Clin Med:2001100005.

Kovacs DM, Fausett HJ, Page KJ, Kim TW, Moir RD, Merriam DE, Hollister RD, Hallmark OG, Mancini R, Felsenstein KM, Hyman BT, Tanzi RE, Wasco W (1996) Alzheimer-associated presenilins 1 and 2: neuronal expression in brain and localization to intracellular membranes in mammalian cells. Nat Med 2:224-229.

Kowall NW, McKee AC, Yankner BA, Beal MF (1992) In vivo neurotoxicity of beta-amyloid beta(1-40) and the beta(25-35) fragment. Neurobiology of Aging 13:537-542.

Kowall NW, Beal MF, Busciglio J, Duffy LK, Yankner BA (1991) An in vivo model for the neurodegenerative effects of beta amyloid and protection by substance P. Proceedings of the National Academy of Sciences of the United States of America 88:7247-7251.

Kuentzel SL, Ali SM, Altman RA, Greenberg BD, Raub TJ (1993) The Alzheimer beta-amyloid protein precursor/protease nexin-II is cleaved by secretase in a trans-Golgi secretory compartment in human neuroglioma cells. Biochem J 295 (Pt 2):367-378.

Lamb BT, Sisodia SS, Lawler AM, Slunt HH, Kitt CA, Kearns WG, Pearson PL, Price DL, Gearhart JD (1993) Introduction and expression of the 400 kilobase amyloid precursor protein gene in transgenic mice. Nature Genetics 5:22-30.

Lammich S, Kojro E, Postina R, Gilbert S, Pfeiffer R, Jasionowski M, Haass C, Fahrenholz F (1999) Constitutive and regulated alpha-secretase cleavage of Alzheimer's amyloid precursor protein by a disintegrin metalloprotease. Proceedings of the National Academy of Sciences of the United States of America 96:3922-3927.

Landi F, Cesari M, Onder G, Russo A, Torre S, Bernabei R (2003) Non-steroidal anti-inflammatory drug (NSAID) use and Alzheimer disease in community-dwelling elderly patients. Am J Geriatr Psychiatry 11:179-185.

Larson J, Lynch G, Games D, Seubert P (1999) Alterations in synaptic transmission and long-term potentiation in hippocampal slices from young and aged PDAPP mice. Brain Res 840:23-35.

Le Bars PL, Katz MM, Berman N, Itil TM, Freedman AM, Schatzberg AF (1997) A placebo-controlled, double-blind, randomized trial of an extract of Ginkgo biloba for dementia. North American EGb Study Group. JAMA 278:1327-1332.

Lee G, Rook SL (1992) Expression of tau protein in non-neuronal cells: microtubule binding and stabilization. Journal of Cell Science 102 (Pt 2):227-237.

Lee G, Neve RL, Kosik KS (1989) The microtubule binding domain of tau protein. Neuron 2:1615-1624.

Lee MK, Slunt HH, Martin LJ, Thinakaran G, Kim G, Gandy SE, Seeger M, Koo E, Price DL, Sisodia SS (1996) Expression of presenilin 1 and 2 (PS1 and PS2) in human and murine tissues. The Journal of Neuroscience 16:7513-7525.

Lee VM, Goedert M, Trojanowski JQ (2001) Neurodegenerative tauopathies. Annual Review of Neuroscience 24:1121-1159.

Lemere CA, Blusztajn JK, Yamaguchi H, Wisniewski T, Saido TC, al. e (1996) Sequence of deposition of heterogeneous amyloid-beta peptides and APO E in Down syndrome: implications for initial events in amyloid plaque formation. Neurobiol Dis 3:16–32.

Levitan D, Yu G, St George Hyslop P, Goutte C (2001) APH-2/nicastrin functions in LIN-12/Notch signaling in the Caenorhabditis elegans somatic gonad. Dev Biol 240:654-661.

Levy E, Carman MD, Fernandez-Madrid IJ, Power MD, Lieberburg I, al. e (1990) Mutation of the Alzheimer's disease amyloid gene in hereditary cerebral hemorrage, Dutch type. Science 248:1124–1126.

Levy-Lahad E, Poorkaj P, Wang K, Fu YH, Oshima J, Mulligan J, Schellenberg GD (1996) Genomic structure and expression of STM2, the chromosome 1 familial Alzheimer disease gene. Genomics 34:198-204.

Levy-Lahad E, Wijsman EM, Nemens E, Anderson L, Goddard KAB, Weber JL, Bird TD, Schellenberg GD (1995a) A familial Alzheimer's disease locus on chromosome I. Science 269:970-973.

Levy-Lahad E, Wasco W, Poorkaj P, Romano DM, Oshima J, Pettingell WH, Yu CE, Jondro PD, Schmidt SD, Wang K, al. e (1995b) Candidate gene for the chromosome 1 familial Alzheimer's disease locus. Science 269:973-977.

Lewis J, McGowan E, Rockwood J, Melrose H, Nacharaju P, Van Slegtenhorst M, Gwinn-Hardy K, Paul Murphy M, Baker M, et a (2000) Neurofibrillary tangles, amyotrophy and progressive motor disturbance in mice expressing mutant (P301L) tau protein. Nature Genetics 25:402-405.

Lewis J, Dickson DW, Lin WL, Chisholm L, Corral A, Jones G, Yen SH, Sahara N, Skipper L, Yager D, Eckman C, Hardy J, Hutton M, McGowan E (2001) Enhanced neurofibrillary degeneration in transgenic mice expressing mutant tau and APP. Science 293:1487-1491.

Li J, Xu M, Zhou H, Ma J, Potter H (1997) Alzheimer presenilins in the nuclear membrane, interphase kinetochores, and centrosomes suggest a role in chromosome segregation. Cell 90:917-927.

Li YM (2001) Gamma-secretase: A catalyst of Alzheimer disease and signal transduction. Mol Interv 1:198-207.

Li YM, Xu M, Lai MT, Huang Q, Castro JL, DiMuzio-Mower J, Harrison T, Lellis C, Nadin A, Neduvelil JG, Register RB, Sardana MK, Shearman MS, Smith AL, Shi XP, Yin KC, Shafer JA, Gardell SJ (2000) Photoactivated gamma-secretase inhibitors directed to the active site covalently label presenilin 1. Nature 405:689 - 694.

Lim GP, Yang F, Chu T, Chen P, Beech W, Teter B, Tran T, Ubeda O, Ashe KH, Frautschy SA, Cole GM (2000) Ibuprofen suppresses plaque pathology and inflammation in a mouse model for Alzheimer's disease. The Journal of Neuroscience 20:5709-5714.

Lin X, Koelsch G, Wu S, Downs D, Dashti A, Tang J (2000) Human aspartic protease memapsin 2 cleaves the beta -secretase site of beta -amyloid precursor protein. Proceedings of the National Academy of Sciences of the United States of America 97:1456-1460.

Lobo A, Launer LJ, Fratiglioni L, Andersen K, Di Carlo A, Breteler MM, Copeland JR, Dartigues JF, Jagger C, Martinez-Lage J, Soininen H, Hofman A (2000) Prevalence of dementia and major subtypes in Europe: A collaborative study of population-based cohorts. Neurologic Diseases in the Elderly Research Group. Neurology 54:S4-9.

Lopez-Perez E, Seidah NG, Checler F (1999) Proprotein convertase activity contributes to the processing of the Alzheimer's beta-amyloid precursor protein in human cells: evidence for a role of the prohormone convertase PC7 in the constitutive alpha-secretase pathway. J Neurochem 73:2056-2062.

Luo Y, Bolon B, Kahn S, Bennett BD, Babu-Khan S, Denis P, Fan W, Kha H, Zhang J, Gong Y, Martin L, Louis JC, Yan Q, Richards WG, Citron M, Vassar R (2001) Mice deficient in BACE1, the Alzheimer's beta-secretase, have normal phenotype and abolished beta-amyloid generation. Nat Neurosci 4:231-232.

Malleret G, Haditsch U, Genoux D, Jones MW, Bliss TV, Vanhoose AM, Weitlauf C, Kandel ER, Winder DG, Mansuy IM (2001) Inducible and reversible enhancement of learning, memory, and long-term potentiation by genetic inhibition of calcineurin. Cell 104:675-686.

Mann DM, Brown A, Prinja D, Davies CA, Landon M, Masters CL, Beyreuthers K (1989) An analysis of the morphology of senile plaques in Down's syndrome patients of different ages using immunocytochemical and lectin histochemical techniques. Neuropathology And Applied Neurobiology 15:317-329.

Masliah E, Terry RD, DeTeresa RM, Hansen LA (1989) Immunohistochemical quantification of the synapse-related protein synaptophysin in Alzheimer disease. Neuroscience Letters 103:234-239.

Masliah E, Sisk A, Mallory M, Mucke L, Schenk D, Games D (1996) Comparison of neurodegenerative pathology in transgenic mice overexpressing V717F abeta-amyloid precursor protein and Alzheimer's disease. The Journal of Neuroscience 16:5795-5811.

Masters CL, Simmons G, Weimann NA, Multhaup G, McDonald BL, Beyreuther K (1985) Amyloid plaque core protein in Alzheimer disease and Down syndrome. Proceedings of the National Academy of the Sciences USA 82:4245-4249.

Matsumoto A, Itoh K, Matsumoto R (2000) A novel carboxypeptidase B that processes native beta-amyloid precursor protein is present in human hippocampus. The European Journal Of Neuroscience 12:227-238.

Mattson MP, Cheng B, Culwell AR, Esch FS, Lieberburg I, and Rydel RE (1993) Evidence for excitoprotective and intraneuronal calcium-regulating roles for secreted forms of the beta-amyloid precursor protein. Neuron 10:243-254.

May PC, Altstiel LD, Bender MH, Boggs LN, Calligaro DO, Fuson KS, Gitter B, Hyslop PA, Jordan WH, Li WY, Marbry TE, al. e (2001) Marked reduction of Abeta accumulation and beta-amyloid plaque pathology in mice upon chronic treatment with a functional gamma-secretase inhibitor. Society for Neuroscience, 2001 Program No. 687.1.

Mayeux R, Saunders AM, Shea S, Mirra S, Evans D, al. e (1998) Utility of the apolipoprotein-E genotype in the diagnosis of AD. N Engl J Med 338:506-511.

Mayeux R, Stern Y, Ottman R, Tatemichi TK, Tang MX, Maestre G, Ngai C, Tycko B, Ginsberg H (1993) The apolipoprotein epsilon 4 allele in patients with Alzheimer's disease. Annals Of Neurology 34:752-754.

McGeer PL, McGeer E, Rogers J, Sibley J (1990) Anti-inflammatory drugs and Alzheimer disease. Lancet 335:1037.

McGowan E, Sanders S, Iwatsubo T, Takeuchi A, Saido T, Zehr C, Yu X, Uljon S, Wang R, Mann D (1999) Amyloid phenotype characterization of transgenic mice overexpressing both mutant amyloid precursor protein and mutant presenilin 1 transgenes. Neurobiology of Disease 6:231-244.

Miyamoto M, Kiyota Y, Yamazaki N, Nagaoka A, Matsuo T, Nagawa Y, Takeda T (1986) Age-related changes in learning and memory in the senescence-accelerated mouse (SAM). Physiology & Behavior 38:399-406.

Moechars D, Dewachter I, Lorent K, Reverse D, Baekelandt V, Naidu A, Tesseur I, Spittaels K, Haute CV, Checler F, Godaux E, Cordell B, Van Leuven F (1999) Early phenotypic changes in transgenic mice that overexpress different mutants of amyloid precursor protein in brain. The Journal of Biological Chemistry 274:6483-6492.

Moller HJ, Graeber MB (1998) The case described by Alois Alzheimer in 1911. Historical and conceptual perspectives based on the clinical record and neurohistological sections. Eur Arch Psychiatry Clin Neurosci 248:111-122.

Moran PM, Higgins LS, Cordell B, Moser PC (1995) Age-related learning deficits in transgenic mice expressing the 751-amino acid isoform of human beta-amyloid precursor protein. Proceedings of the National Academy of Sciences of the United States of America 92:5341-5345.

Morgan D, Diamond DM, Gottschall PE, Ugen KE, Dickey C, Hardy J, Duff K, Jantzen P, DiCarlo G, Wilcock D, Connor K, Hatcher J, Hope C, Gordon M, Arendash GW (2000) A beta peptide vaccination prevents memory loss in an animal model of Alzheimer's disease. Nature 408:982-985.

Morley JE, Kumar VB, Bernardo AE, Farr SA, Uezu K, Tumosa N, Flood JF (2000) Beta-amyloid precursor polypeptide in SAMP8 mice affects learning and memory. Peptides 21:1761-1767.

Morris JC, Mohs RC, Rogers H, Fillenbaum G, Heyman A (1988) Consortium to establish a registry for Alzheimer's disease (CERAD) clinical and neuropsychological assessment of Alzheimer's disease. Psychopharmacol Bull 24:641-652.

Morris JC, Heyman A, Mohs RC, Hughes JP, van Belle G, Fillenbaum G, Mellits ED, Clark C (1989) The consortium to establish a registry for Alzheimer's disease (CERAD). Part I. Clinical and neuropsychological assessment of Alzheimer's disease. Neurology 39:1159-1165.

Morris RGM (1981) Spatial localization does not require the presence of local cues. Learning and Motivation 12:239-249.

Morris RGM, Garrud P, Rawlins JN, O' Keefe J (1982) Place navigation is impaired in rats with hippocampal lesions. Nature 297:681-683.

Morris RGM, Anderson E, Lynch GS, Baudry M (1986) Selective impairment of learning and blockade of long-term potentiation by an N-methyl-D-aspartate receptor antagonist, AP5. Nature 319:774-776.

Mucke L, Masliah E, Johnson WB, Ruppe MD, Alford M, Rockenstein EM, Forss-Petter S, Pietropaolo M, Mallroy M, Abraham CR (1994) Synaptotrophic effects of human amyloid beta-protein precursors in the cotex of transgenic mice. Brain Research 666:151-176.

Mucke L, Masliah E, Yu G-Q, Mallory M, Rockenstein EM, Tatsuno G, Hu K, Kholodenko D, Johnson-Wood K, McConlogue L (2000) High-level neuronal expression of Abeta 1-42 in wild-type human amyloid protein precursor transgenic mice: Synaptotoxicity without plaque formation. The Journal of Neuroscience 20:4050-4058.

Mullan M, Crawford F, Axelman K, Houlden H, Lilius L, Winblad B, Lannfelt L (1992) A pathogenic mutation for probable Alzheimer's disease in the APP gene at the N-terminus of beta-amyloid. Nature Genetics 1:345-347.

Murphy MP, Uljon SN, Fraser PE, Fauq A, Lookingbill HA, Findlay KA, Smith TE, Lewis PA, McLendon DC, Wang R, Golde TE (2000) Presenilin 1 regulates pharmacologically distinct gamma-secretase activities. The Journal of Biological Chemistry 275:26277-26284.

Murrell J, Farlow M, Ghetti B, Benson MD (1991) A mutation in the amyloid precursor protein associated with hereditary Alzheimer's disease. Science 254:97-99.

Nalbantoglu J, Tirado-Santiago G, Lahsaini A, Poirier J, Goncalves O, Verge G, Momoli F, Welner SA, Massicotte G, Julien JP, Shapiro ML (1997) Impaired learning and LTP in mice expressing the carboxy terminus of the Alzheimer amyloid precursor protein. Nature 387:500-505.

Nangaku M, Sato-Yoshitake R, Okada Y, Noda Y, Takemura R, Yamazaki H, Hirokawa N (1994) KIF1B, a novel microtubule plus end-directed monomeric motor protein for transport of mitochondria. Cell 79:1209-1220.

Naslund J, Haroutunian V, Mohs R, Davis KL, Davies P, Greengard P, Buxbaum JD (2000) Correlation between elevated levels of amyloid-beta peptide in the brain and cognitive decline. JAMA 283:1571-1577.

Ni CY, Murphy MP, Golde TE, Carpenter G (2001) Gamma-secretase cleavage and nuclear localization of ErbB-4 receptor tyrosine kinase. Science 294:2179-2181.

Nicoll JAR, Wilkinson D, Holmes C, Steart P, Markham H, Weller RO (2003) Neuropathology of human Alzheimer disease after immunization with amyloid-beta peptide: a case report. Nature Medicine 9:448-452.

Nishiyama K, Murayama S, Suzuki T, Mitsui Y, Sakaki Y, Kanazawa I (1996) Presenilin 1 mRNA expression in hippocampi of sporadic Alzheimer's disease patients. Neurosci Res 26:75-78.

Nordberg A, Hellstrom-Lindahl E, Lee M, Johnson M, Mousavi M, Hall R, Perry E, Bednar I, Court J (2002) Chronic nicotine treatment reduces beta-amyloidosis in the brain of a mouse model of Alzheimer's disease (APPsw). J Neurochem 81:655-658.

Nukina N, Ihara Y (1985) Proteolytic fragments of Alzheimer's paired helical filaments. J Biochem (Tokyo) 98:1715-1718.

Nukina N, Ihara Y (1986) One of the antigenic determinants of paired helical filaments is related to tau protein. J Biochem (Tokyo) 99:1541-1544.

Nunan J, Small DH (2000) Regulation of APP cleavage by alpha-, beta- and gamma-secretases. FEBS Lett 483:6-10.

O'Brien C (1996) Auguste D. and Alzheimer's disease. Science 273:28.

Oddo S, Caccamo A, Shepherd JD, Murphy MP, Golde TE, Kayed R, Metherate R, Mattson MP, Akbari Y, La Ferla FM (2003) Triple-transgenic model of Alzheimer's disease with plaques and tangles: intracellular Abeta and synaptic dysfunction. Neuron 39:409-421.

Oh M, Kim SY, Oh YS, Choi D-Y, Sin HJ, Jung IM, Park WJ (2003) Cell-based assay for beta-secretase activity. Analytical Biochemistry 323:7-11.

Ohno M, Sametsky EA, Younkin LH, Oakley H, Younkin SG, Citron M, Vassar R, Disterhoft JF (2004) BACE1 deficiency rescues memory deficits and cholinergic dysfunction in a mouse model of Alzheimer's disease. Neuron 41:27-33.

Ohta A, Akiguchi I, Seriu N, Ohnishi K, Yagi H, Higuchi K, Hosokawa M (2001) Deterioration in learning and memory of fear conditioning in response to context in aged SAMP8 mice1. Neurobiology of Aging 22:479-484.

O'Keefe J, Nadel L (1978) The hippocampus as a cognitive map, Oxford Univ. Press, Oxford.

Oyama Y, Chikahisa L, Ueha T, Kanemaru K, Noda K (1996) Ginkgo biloba extract protects brain neurons against oxidative stress induced by hydrogen peroxide. Brain Res 712:349-352.

Pastor P, Pastor E, Carnero C, Vela R, Garcia T, Amer G, Tolosa E, Oliva R (2001) Familial atypical progressive supranuclear palsy associated with homozigosity for the delN296 mutation in the tau gene. Annals Of Neurology 49:263-267.

Pearl GS (1997) Diagnosis of Alzheimer's disease in a community hospital-based brain bank program. South Med J 90:720-722.

Perry E, Walker M, Grace J, Perry R (1999) Acetylcholine in mind: a neurotransmitter correlate of consciousness? Trends in Neurosciences 22:273-280.

Perry EK, Perry RH (1995) Acetylcholine and hallucinations: disease-related compared to drug-induced alterations in human consciousness. Brain Cogn 28:240–258.

Petit A, Dumanchin-Njock D, Andrau D, Alves da Costa C, Checler F (2002) Amyloid-lowering isocoumarins are not direct inhibitors of gamma-secretase-Reponse. Nature Cell Biology 4:E111 - E112.

Petit A, Bihel F, da Costa CA, Pourquie O, Checler F, Kraus J-L (2001) New protease inhibitors prevent gamma-secretase-mediated production of Abeta40/42 without affecting Notch cleavage. Nature Cell Biology 3:507-511.

Petit A, Pasini A, Alves Da Costa C, Ayral E, Hernandez JF, Dumanchin-Njock C, Phiel CJ, Marambaud P, Wilk S, Farzan M, Fulcrand P, Martinez J, Andrau D, Checler F (2003) JLK isocoumarin inhibitors: selective gamma-secretase inhibitors that do not interfere with notch pathway in vitro or in vivo. J Neurosci Res 74:370-377.

Pike CJ, Walencewicz AJ, Glabe CG, Cotman CW (1991) In vitro aging of beta-amyloid protein causes peptide aggregation and neurotoxicity. Brain Research 563:311-314.

Pike CJ, Burdick D, Walencewicz AJ, Glabe CG, Cotman CW (1993) Neurodegeneration induced by beta-amyloid peptides in vitro: the role of peptide assembly state. The Journal of Neuroscience 13:1676-1687.

Poirier J, Bertrand P, Poirier J, Kogan S, Gauthier S, Poirier J, Gauthier S, Davignon J, Bouthillier D, Davignon J (1993) Apolipoprotein E polymorphism and Alzheimer's disease. The Lancet 342:697-699.

Poorkaj P, Bird TD, Wijsman E, Nemens E, Garruto RM, Anderson L, Andreadis A, Wiederholt WC, Raskind M, Schellenberg GD (1998) Tau is a candidate gene for chromosome 17 frontotemporal dementia. Ann Neurol 43:815-825.

Potter A, Corwin J, Lang J, Piasecki M, Lenox R, Newhouse PA (1999) Acute effects of the selective cholinergic channel activator (nicotinic agonist) ABT-418 in Alzheimer's disease. Psychopharmacology (Berl) 142:334-342.

Powen DM, Sims NR, Benton JS, Curzon G, Davison AN, Neary D, Thomas DJ (1981) Treatment of Alzheimer's disease: a cautionary note. N Engl J Med 305:1016.

Price DL, Sisodia SS (1998) Mutant genes in familial Alzheimer's disease and transgenic models. Annual Review of Neuroscience 21:479-505.

Price DL, Tanzi RE, Borchelt DR, Sisodia SS (1998) Alzheimer's disease: genetic studies and transgenic models. Annual Review of Genetics 32:461-493.

Probst A, Gotz J, Wiederhold KH, Tolnay M, Mistl C, Jaton AL, Hong M, Ishihara T, Lee VM, Trojanowski et a (2000) Axonopathy and amyotrophy in mice transgenic for human four-repeat tau protein. Acta Neuropathologica 99:469-481.

Qian S, Jiang P, Guan XM, Singh G, Trumbauer ME, Yu H, Chen HY, Van de Ploeg LH, Zheng H (1998) Mutant human presenilin 1 protects presenilin 1 null mouse against embryonic lethality and elevates Abeta1-42/43 expression. Neuron 20:611-617.

Querfurth HW, Wijsman EM, St George-Hyslop PH, Selkoe DJ (1995) Beta APP mRNA transcription is increased in cultured fibroblasts from the familial Alzheimer's disease-1 family. Brain Res Mol Brain Res 28:319-337.

Quon D, Wang Y, Catalano R, Scardina JM, Murakami K, Cordell B (1991) Formation of beta-amyloid protein deposits in brains of transgenic mice. Nature 18:239-241.

Ramsay M, Morris RGM (1998) A longitudinal study of spatial learning in PDAPP mice. Eur J Neurosci 10 (Suppl.):32.

Rasmusson DX, Brandt J, Steele C, al. e (1996) Accuracy of clinical diagnosis of Alzheimer disease and clinical features of patients with non-Alzheimer neuropathology. Alzheimer Dis Assoc Disord 10:180–188.

Reisberg B, Borenstein J, Salob SP, Ferris SH, Franssen E, Georgotas A (1987) Behavioral symptoms in Alzheimer's disease: phenomenology and treatment. J Clin Psychiatry 48:9-15.

Reisberg B, Doody R, Stoffler A, Schmitt F, Ferris S, Mobius HJ (2003) Memantine in moderate-to-severe Alzheimer's disease. N Engl J Med 348:1333-1341.

Rich JB, Rasmusson DX, Folstein MF, Carson KA, Kawas C, Brandt J (1995) Nonsteroidal anti-inflammatory drugs in Alzheimer's disease. Neurology 45:51-55.

Ritchie CW, Bush AI, Mackinnon A, Macfarlane S, Mastwyk M, MacGregor L, Kiers L, Cherny R, Li Q-X, Tammer A, Carrington D, Mavros C, Volitakis I, Xilinas M, Ames D, Davis S, Beyreuther K, Tanzi RE, Masters CL (2003) Metal-protein attenuation with iodochlorhydroxyquin (Clioquinol) targeting Abeta amyloid deposition and toxicity in Alzheimer disease: A pilot phase 2 clinical trial. Arch Neurol 60:1685-1691.

Robakis NK, Ramakrishna N, Wolfe G, Wisniewski HM (1987) Molecular cloning and characterization of a cDNA encoding the cerebrovascular and the neuritic plaque amyloid peptides. Proceedings of the National Academy of Sciences of the United States of America 84:4190–4194.

Robbins TW, James M, Owen AM, Sahakian BJ, McInnes L, Rabbitt P (1994) Cambridge Neuropsychological Test Automated Battery (CANTAB): a factor analytic study of a large sample of normal elderly volunteers. Dementia 5:266-281.

Roberds SL, Anderson J, Basi G, Bienkowski MJ, Branstetter DG, Chen KS, Freedman SB, Frigon NL, Games D, Hu K, Johnson-Wood K, Kappenman KE, Kawabe TT, Kola I, Kuehn R, Lee M, Liu W, Motter R, Nichols NF, Power M, Robertson DW, Schenk D, Schoor M, Shopp GM, Shuck ME, Sinha S, Svensson KA, Tatsuno G, Tintrup H, Wijsman J, Wright S, McConlogue L (2001) BACE knockout mice are healthy despite lacking the primary beta-secretase activity in brain: implications for Alzheimer's disease therapeutics. Hum Mol Genet 10:1317-1324.

Rockenstein EM, McConlogue L, Tan H, Power M, Masliah E, Mucke L (1995) Levels and alternative splicing of amyloid beta protein precursor (APP) transcripts in brains of APP transgenic mice and humans with Alzheimer's disease. The Journal of Biological Chemistry 270:28257-28267.

Rogaev EI, Sherrington R, Rogaeva EA, Levesque G, Ikeda M, Liang Y, Chi H, Lin C, Holman K, Tsuda T, al. e (1995) Familial Alzheimer's disease in kindreds with missense mutations in a gene on chromosome 1 related to the Alzheimer's disease type 3 gene. Nature 376:775-778.

Rogers SL, Farlow MR, Doody RS, Mohs R, Friedhoff LT (1998) A 24-week, double-blind, placebo-controlled trial of donepezil in patients with Alzheimer's disease. Donepezil Study Group. Neurology 50:136-145.

Rosen W, Mohs R, Davis K (1984) A new rating scale for Alzheimer's disease. Am J Psychiatry 141:1356-1364.

Rosler M, Anand R, Cicin-Sain A, Gauthier S, Agid Y, Dal-Bianco P, Stahelin HB, Hartman R, Gharabawi M (1999) Efficacy and safety of rivastigmine in patients with Alzheimer's disease: international randomised controlled trial. Bmj 318:633-638.

Roth M, Tomlinson BE, Blessed G (1966) Correlation between scores for dementia and counts of "senile plaques" in cerebral grey matter of elderly patients. Nature 209:109–110.

Routtenberg A, Hsiao K, Chapman P, Nilsen S, Eckman C, Harigaya Y, Younkin S, Yang F, Cole; G (1997) Measuring memory in a mouse model of Alzheimer's disease. Science 277:839-841.

Sato M, Kawarabayashi T, Shoji M, Kobayashi T, Tada N, Matsubara E, Hirai S (1997) Neurodegeneration and gliosis in transgenic mice overexpressing a carboxy-terminal fragment of Alzheimer amyloid-beta protein precursor. Dementia and Geriatric Cognitive Disorders 8:296-307.

Saunders AJ, Kim TW, Tanzi RE, Fan W, Bennett BD, Babu-Kahn S, Luo Y, Louis J-C, McCaleb M, Citron M, Vassar R, Richards; WG (1999) BACE maps to chromosome 11 and a BACE homolog, BACE2, reside in the obligate Down syndrome region of chromosome 21. Science 286:1255.

Saunders AM, Strittmatter WJ, Schmechel D, George-Hyslop PH, Pericak-Vance MA, Joo SH, Rosi BL, Gusella JF, Crapper-MacLachlan DR, Alberts et a (1993) Association of apolipoprotein E allele epsilon 4 with late-onset familial and sporadic Alzheimer's disease. Neurology 43:1467-1472.

Schellenberg GD (1995) Genetic dissection of AD, a heterogeneous disorder. Proceedings of the National Academy of Sciences of the United States of America 92:8552-8559.

Schenk D (2002) Amyloid-beta immunotherapy for Alzheimer's disease: the end of the beginning. Nature Reviews Neuroscience 3:824-828.

Schenk D, Barbour R, Dunn W, Gordon G, Grajeda H, Guido T, Hu K, Huang J, Johnson-Wood K, Khan K, Kholodenko D, Lee M, Liao Z, Lieberburg I, Motter R, Mutter L, Soriano F, Shopp G, Vasquez N, Vandevert C, Walker S, Wogulis M, Yednock T, Games D, Seubert P (1999) Immunization with amyloid-beta attenuates Alzheimer-disease-like pathology in the PDAPP mouse. Nature 400:173-177.

Scheuner D, Eckman C, Jensen M, Song X, Citron M, Suzuki N, Bird TD, Hardy J, Hutton M, Kukull W, Larson E, Levy-Lahad E, Viitanen M, Peskind E, Poorkaj P, Schellenberg G, Tanzi R, Wasco W, Lannfelt L, Selkoe D, Youkin S (1996) Secreted amyloid beta-protein similar to that in the senile plaques of Alzheimer's disease is increased *in vivo* by the presenilin 1 and 2 and *APP* mutations linked to familial Alzheimer's disease. Nature Medicine 2:864-870.

Schmechel DE, Saunders AM, Strittmatter WJ, Crain BJ, Hulette CM, Joo SH, Pericak-Vance MA, Goldgaber D, Roses AD (1993) Increased amyloid beta-peptide deposition in cerebral cortex as a consequence of apolipoprotein E genotype in late-onset Alzheimer disease. Proceedings of the National Academy of Sciences of the United States of America 90:9649-9653.

Searfoss GH, Jordan WH, Calligaro DO, Galbreath EJ, Schirtzinger LM, Berridge BR, Gao H, Higgins MA, May PC, Ryan TP (2003) Adipsin, a biomarker of gastrointestinal

toxicity mediated by a functional gamma-secretase inhibitor. The Journal of Biological Chemistry 278:46107-46116.

Seiffert D, Bradley JD, Rominger CM, Rominger DH, Yang F, Meredith JE, Jr., Wang Q, Roach AH, Thompson LA, Spitz SM, Higaki JN, Prakash SR, Combs AP, Copeland RA, Arneric SP, Hartig PR, Robertson DW, Cordell B, Stern AM, Olson RE, Zaczek R (2000) Presenilin-1 and -2 are molecular targets for gamma-secretase inhibitors. The Journal of Biological Chemistry 275:34086-34091.

Selkoe DJ (1994) Alzheimer's disease: a central role for amyloid. J Neuropathol Exp Neurol 53:438-447.

Selkoe DJ (2001) Alzheimer's disease: genes, proteins, and therapy. Physiol Rev 81:741-766.

Selkoe DJ (2002) Alzheimer's disease is a synaptic failure. Science 298:789-791.

Shearman MS, Beher D, Clarke EE, Lewis HD, Harrison T, Hunt P, Nadin A, Smith AL, Stevenson G, Castro JL (2000) L-685,458, an aspartyl protease transition state mimic, is a potent inhibitor of amyloid beta-protein precursor gamma-secretase activity. Biochemistry 39:8698-8704.

Shen J, Bronson RT, Chen DF, Xia W, Selkoe DJ, Tonegawa S (1997) Skeletal and CNS defects in Presenilin-1-deficient mice. Cell 89:629-639.

Sherrington R, Rogaev EI, Liang Y, Rogaeva EA, Levesque G, Ikeda M, Chi H, Lin C, Li G, Holman K, al. e (1995) Cloning of a gene bearing missense mutations in early-onset familial Alzheimer's disease. Nature 375:754-760.

Sherrington R, Froelich S, Sorbi S, Campion D, Chi H, Rogaeva E, Levesque G, Rogaev E, Lin C, Liang Y, Ikeda M, Mar L, Brice A, Agid Y, Percy M, Clerget- Darpoux F, Piacentini S, Marcon G, Nacmias B, Amaducci L, Frebourg T, Lannfelt L, Rommens J, St George-Hyslop P (1996) Alzheimer's disease associated with mutations in presenilin 2 is rare and variably penetrant. Hum Mol Genet 5:985-988.

Shi XP, Tugusheva K, Bruce JE, Lucka A, Wu GX, Chen-Dodson E, Price E, Li Y, Xu M, Huang Q, Sardana MK, Hazuda DJ (2003) Beta-secretase cleavage at amino acid residue 34 in the amyloid-beta peptide is dependent upon gamma-secretase activity. The Journal of Biological Chemistry 278:21286-21294.

Sigurdsson EM, Scholtzova H, Mehta PD, Frangione B, Wisniewski T (2001) Immunization with a nontoxic/nonfibrillar amyloid-beta homologous peptide reduces Alzheimer's disease-associated pathology in transgenic mice. Am J Pathol 159:439-447.

Sinha S, Lieberburg I (1999) Cellular mechanisms of beta-amyloid production and secretion. Proceedings of the National Academy of Sciences of the United States of America 96:11049-11053.

Sinha S, Anderson JP, Barbour R, Basi GS, Caccavello R, Davis D, Doan M, Dovey HF, Frigon N, Hong J, Jacobson-Croak K, Jewett N, Keim P, Knops J, Lieberburg I, Power M, Tan H, Tatsuno G, Tung J, Schenk D, Seubert P, Suomensaari SM, Wang S, Walker D, John V, et al. (1999) Purification and cloning of amyloid precursor protein beta-secretase from human brain. Nature 402:537-540.

Sisodia SS, Koo EH, Hoffman PN, Perry G, Price DL (1993) Identification and transport of full-length amyloid precursor proteins in rat peripheral nervous system. The Journal of Neuroscience 13:3136-3142.

Skovronsky DM, Lee VM (2000) Beta-secretase revealed: starting gate for race to novel therapies for Alzheimer's disease. Trends Pharmacol Sci 21:161-163.

Small GW, Rabins PV, Barry PP, Buckholtz NS, DeKosky ST, Ferris SH, Finkel SI, Gwyther LP, Khachaturian ZS, Lebowitz BD, McRae TD, Morris JC, Oakley F, Schneider LS, Streim JE, Sunderland T, Teri LA, Tune LE (1997) Diagnosis and treatment of Alzheimer disease and related disorders: consensus statement of the American Association for Geriatric Psychiatry, the Alzheimer's Association, and the American Geriatrics Society. JAMA 278:1363–1371.

Snape MF, Misra A, Murray TK, De Souza RJ, Williams JL, Cross AJ, Green AR (1999) A comparative study in rats of the in vitro and in vivo pharmacology of the acetylcholinesterase inhibitors tacrine, donepezil and NXX-066. Neuropharmacology 38:181-193.

Spencer CM, Noble S (1998) Rivastigmine. A review of its use in Alzheimer's disease. Drugs Aging 13:391-411.

Spencer HJ, Gribkoff VK, Cotman CW, Lynth GS (1976) GDEE antagonism of iontophoretic amino acid excitations in the intact hippocampus and in the hippocampal slice preparation. Brain Res Rev 105:471-481.

Spillantini MG, Murrell JR, Goedert M, Farlow MR, Klug A, Ghetti B (1998) Mutation in the tau gene in familial multiple system tauopathy with presenile dementia. Proceedings of the National Academy of Sciences of the United States of America 95:7737–7741.

Spittaels K, Van den Haute C, Van Dorpe J, Bruynseels K, Vandezande K, Laenen I, Geerts H, Mercken M, Sciot R, Van Lommel A, Loos R, Van Leuven F (1999) Prominent axonopathy in the brain and spinal cord of transgenic mice overexpressing four-repeat human tau protein. Am J Pathol 155:2153-2165.

Squire LR (1992) Memory and the hippocampuss: A synthesis from findings with rats, monkeys, and humans. Psychological Review 99:195-231.

St George-Hyslop, Tanzi RE, Polinsky RJ, Haines JL, Nee L, Watkins PC, Myers RH, Feldman RG, Pollen D, Drachman D, Growdon J, Bruni A, Foncin J-F, Salmon D, Frommelt P, Amaducci L, Sorbi S, Piacentini S, Stewart GD, Hobbs WJ, Conneally PM, Gusella JF (1987) The genetic defect causing familial Alzheimer's disease maps on chromosome 21. Science 235:885–890.

St George-Hyslop P, Haines J, Rogaev E, Mortilla M, Vaula G, Pericak-Vance M, Foncin JF, Montesi M, Bruni A, Sorbi S, al. e (1992) Genetic evidence for a novel familial Alzheimer's disease locus on chromosome 14. Nature Genetics 2:330-334.

Steele RJ, Morris RGM (1999) Delay-dependent impairment of a matching-to-place task with chronic and intrahippocampal infusion of the NMDA-antagonist D-AP5. Hippocampus 9:118-136.

Stephan A, Laroche S, Davis S (2001) Generation of aggregated beta-amyloid in the rat hippocampus impairs synaptic transmission and plasticity and causes memory deficits. The Journal of Neuroscience 21:5703-5714.

Stern Y, Sano M, Mayeux R (1988) Long-term administration of oral physostigmine in Alzheimer's disease. Neurology 38:1837-1841.

Stewart WF, Kawas C, Corrada M, Metter EJ (1997) Risk of Alzheimer's disease and duration of NSAID use. Neurology 48:626-632.

Strittmatter WJ, Saunders AM, Schmechel D, Pericak-Vance M, Enghild J, Salvesen GS, al. e (1993a) Apolipoprotein E: high-avidity binding to beta-amyloid and increased frequency of type 4 allele in late-onset familial Alzheimer disease. Proceedings of the National Academy of Sciences of the United States of America 90:1977-1981.

Strittmatter WJ, Weisgraber KH, Huang DY, Dong LM, Salvesen GS, Pericak-Vance M, Schmechel D, Saunders AM, Goldgaber D, Roses AD (1993b) Binding of human apolipoprotein E to synthetic amyloid beta peptide: isoform-specific effects and implications for late-onset Alzheimer disease. Proceedings of the National Academy of Sciences of the United States of America 90:8098-8102.

Strittmatter WJ, Saunders AM, Goedert M, Weisgraber KH, Dong LM, Jakes R, Huang DY, Pericak-Vance M, Schmechel D, Roses AD (1994) Isoform-specific interactions of apolipoprotein E with microtubule-associated protein tau: Implications for Alzheimer disease. Proceedings of the National Academy of Sciences of the United States of America 91:11183-11186.

Struble RG, Hedreen JC, Cork LC, Price DL (1984) Acetylcholinesterase activity in senile plaques of aged macaques. Neurobiology of Aging 5:191-198.

Struble RG, Price DLJ, Cork LC, Price DL (1985) Senile plaques in cortex of aged normal monkeys. Brain Research 361:267-275.

Sturchler-Pierrat C, Abramowski D, Duke M, Wiederhold K-H, Mistl C, Rothacher S, Ledermann B, Burki K, Frey P, Paganetti PA, Waridel C, Calhoun ME, Jucker M, Probst A, Staufenbiel M, Sommer B (1997) Two amyloid precursor protein transgenic mouse models with Alzheimer disease-like pathology. Proceedings of the National Academy of Sciences of the United States of America 94:13287-13292.

Suh Y-H, Checler F (2002) Amyloid precursor protein, presenilins, and alpha-synuclein: Molecular pathogenesis and pharmacological applications in Alzheimer's disease. Pharmacol Rev 54:469-525.

Sun L, Liu SY, Zhou XW, Wang XC, Liu R, Wang Q, Wang JZ (2003) Inhibition of protein phosphatase 2A- and protein phosphatase 1-induced tau hyperphosphorylation and impairment of spatial memory retention in rats. Neuroscience 118:1175-1182.

Sunderland T, Hill JL, Mellow AM, Lawlor BA, Gundersheimer J, Newhouse PA, Grafman JH (1989) Clock drawing in Alzheimer's disease. A novel measure of dementia severity. J Am Geriatr Soc 37:725-729.

Suzuki N, Cheung TT, Cai X, Odaka A, Otvos LJ, Eckman C, Golde TE, Younkin SG (1994) An increased percentage of long amyloid beta protein secreted by familial amyloid beta protein precursor (beta APP717) mutants. Science 264:1336-1340.

Tabira T, Bush AI, Masters CL (2001) Clioquinol's return: Cautions from Japan. Science 292:2251-2252.

Takashima A, Sato M, Mercken M, Tanaka S, Kondo S, Honda T, Sato K, Murayama M, Noguchi K, Nakazato Y, Takahashi H (1996) Localization of Alzheimer-associated presenilin 1 in transfected COS-7 cells. Biochem Biophys Res Commun 227:423-426.

Takeda T, Hosokawa M, Takeshita S, Irino M, Higuchi K, Matsushita T, Tomita Y, Yasuhira K, Hamamoto H, Shimizu K (1981) A new murine model of accelerated senescence. Mechanisms of Ageing and Development 17:183-194.

Tanemura K, Akagi T, Murayama M, Kikuchi N, Murayama O, Hashikawa T, Yoshiike Y, Park JM, Matsuda K, Nakao S, Sun X, Sato S, Yamaguchi H, Takashima A (2001) Formation of filamentous tau aggregations in transgenic mice expressing V337M human tau. Neurobiol Dis 8:1036-1045.

Tang M-X, Diane Jacobs YS, Karen Marder, Peter Schofield, Barry Gurland, Howard Andrews,, Mayeux R (1996) Effect of oestrogen during menopause on risk and age at onset of Alzheimer's disease. Lancet 348:429–432.

Tang YP, Shimizu E, Dube GR, Rampon C, Kerchner GA, Zhuo M, Liu G, Tsien JZ (1999) Genetic enhancement of learning and memory in mice [see comments]. Nature 401:63-69.

Tanzi RE, McClatchey AI, Lamperti ED, Villa-Komaroff L, Gusella JF, Neve RL (1988) Protease inhibitor domain encoded by an amyloid precursor mRNA associated with Alzheimer's disease. Nature 331:528-532.

Tanzi RE, Vaula G, Romano DM, Mortilla M, Huang TL, Tupler RG, Wasco W, Hyman BT, Haines JL, Jenkins BJ, et al. (1992) Assessment of amyloid beta-protein precursor gene mutations in a large set of familial and sporadic Alzheimer disease cases. Am J Hum Genet 51:273-282.

Tariot PN, Solomon PR, Morris JC, Kershaw P, Lilienfeld S, Ding C (2000) A 5-month, randomized, placebo-controlled trial of galantamine in AD. Neurology 54:2269-2276.

Tatebayashi Y, Miyasaka T, Chui D-H, Akagi T, Mishima K-I, Iwasaki K, Fujiwara M, Tanemura K, Murayama M, et a (2002) Tau filament formation and associative memory deficit in aged mice expressing mutant (R406W) human tau. Proceedings of the National Academy of Sciences of the United States of America 99:13896-13901.

Terry R, Hansen L, DeTeresa R, Davies P, Tobias H, R. K (1987) Senile dementia of the Alzheimer type without neocortical neurofibrillary tangles. J Neuropathol Exp Neurol 46:262-268.

Terry RD (1963) The fine structure of neurofibrillary tangles in Alzheimer's disease. J Neuropathol Exp Neurol 22:629-642.

Terry RD, Masliah E, Salmon DP, Butters N, DeTeresa R, Hill R, Hansen LA, Katzman R (1991) Physical basis of cognitive alterations in Alzheimer's disease: synapse loss is the major correlate of cognitive impairment. Ann Neurol 30:572-580.

Thal LJ, Masur DM, Sharpless NS, Fuld PA, Davies P (1986) Acute and chronic effects of oral physostigmine and lecithin in Alzheimer's disease. Progress in Neuro-Psychopharmacology and Biological Psychiatry 10:627-636.

Thal LJ, Grundman M, Berg J, Ernstrom K, Margolin R, Pfeiffer E, Weiner MF, Zamrini E, Thomas RG (2003) Idebenone treatment fails to slow cognitive decline in Alzheimer's disease. Neurology 61:1498-1502.

The National Institute on Aging and Reagan Institute Working Group on Diagnostic Criteria for the Neuropathological Assessment of Alzheimer's D (1997) Consensus recommendations for the postmortem diagnosis of Alzheimer's disease. Neurobiology of Aging 18:S1-S2.

Thinakaran G, Harris CL, Ratovitski T, Davenport F, Slunt HH, Price DL, Borchelt DR, Sisodia SS (1997) Evidence that levels of presenilins (PS1 and PS2) are coordinately regulated by competition for limiting cellular factors. The Journal of Biological Chemistry 272:28415-28422.

Thinakaran G, Borchelt DR, Lee MK, Slunt HH, Spitzer L, Kim G, Ratovitsky T, Davenport F, Nordstedt C, Seeger M, Hardy J, Levey AI, Gandy SE, Jenkins NA, Copeland NG, Price DL, Sisodia SS (1996) Endoproteolysis of presenilin 1 and accumulation of processed derivatives in vivo. Neuron 17:181-190.

Tomita T, Maruyama K, Saido TC, Kume H, Shinozaki K, Tokuhiro S, Capell A, Walter J, Grunberg J, Haass C, Iwatsubo T, Obata K (1997) The presenilin 2 mutation (N141I) linked to familial Alzheimer disease (Volga German families) increases the secretion of amyloid beta protein ending at the 42nd (or 43rd) residue. Proceedings of the National Academy of Sciences of the United States of America 94:2025-2030.

Trinczek B, Ebneth A, Mandelkow EM, Mandelkow E (1999) Tau regulates the attachment/detachment but not the speed of motors in microtubule-dependent transport of single vesicles and organelles. Journal Of Cell Science 112 (Pt 14):2355-2367.

Turner RT, Koelsch G, Hong L, Castanheira P, Ermolieff J, Ghosh AK, Tang J, Castenheira P, Ghosh A (2001) Subsite specificity of memapsin 2 (beta-secretase): implications for inhibitor design. Biochemistry 40:10001-10006.

Van Broeckhoven C, Backhovens H, Cruts M, De Winter G, Bruyland M, Cras P, Martin JJ (1992) Mapping of a gene predisposing to early-onset Alzheimer's disease to chromosome 14q24.3. Nature Genetics 2:335-339.

Van Dam D, D'Hooge R, Staufenbiel M, Van Ginneken C, Van Meir F, De Deyn PP (2003) Age-dependent cognitive decline in the APP23 model precedes amyloid deposition. Eur J Neurosci 17:388-396.

Vassar R, Bennett BD, Babu-Khan S, Kahn S, Mendiaz EA, Denis P, Teplow DB, Ross S, Amarante P, Loeloff R, Luo Y, Fisher S, Fuller J, Edenson S, Lile J, Jarosinski MA, Biere AL, Curran E, Burgess T, Louis JC, Collins F, Treanor J, Rogers G, Citron M (1999) Beta-secretase cleavage of Alzheimer's amyloid precursor protein by the transmembrane aspartic protease BACE. Science 286:735-741.

von Koch CS, Lahiri DK, Mammen AL, Copeland NG, Gilbert DJ, Jenkins NA, Sisodia S (1995) The mouse APLP2 gene. Chromosomal localization and promoter characterization. The Journal of Biological Chemistry 270:25475-25480.

Wasco W, Bupp K, Magendantz M, Gusella JF, Tanzi RE, Solomon F (1992) Identification of a mouse brain cDNA that encodes a protein related to the Alzheimer disease-associated amyloid beta protein precursor. Proceedings of the National Academy of Sciences of the United States of America 89:10758 –10762.

Weiner HL, Lemere CA, Maron R, Spooner ET, Grenfell TJ, Mori C, Issazadeh S, Hancock WW, Selkoe DJ (2000) Nasal administration of amyloid-beta peptide decreases cerebral amyloid burden in a mouse model of Alzheimer's disease. Ann Neurol 48:567-579.

Weisgraber KH, Rall SCJ, Mahley RW (1981) Human E apoprotein heterogeneity. Cysteine-arginine interchanges in the amino acid sequence of the apoE isoforms. The Journal of Biological Chemistry 256:9077-9083.

West HJ, Gundersen HJ (1990) Unbiased stereological estimation of the number of neurons in the human hippocampus. J Comp Neurol 296:1-22.

Westerman MA, Cooper-Blacketer D, Mariash A, Kotilinek L, Kawarabayashi T, Younkin LH, Carlson GA, Younkin SG, Ashe KH (2002) The relationship between Abeta and memory in the Tg2576 mouse model of Alzheimer's disease. The Journal of Neuroscience 22:1858-1867.

Whishaw IQ, Tomie JA (1997) Perseveration on place reversals in spatial swimming pool tasks: further evidence for place learning in hippocampal rats. Hippocampus 7:361-370.

White F, Nicoll JAR, Roses AD, Horsburgh K (2001) Impaired neuronal plasticity in transgenic mice expressing human apolipoprotein E4 compared to E3 in a model of entorhinal cortex lesion. Neurobiology of Disease 8:611-625.

Whitehouse PJ, Price DL, Clark AW, Coyle JT, DeLong MR (1981) Alzheimer disease: evidence for selective loss of cholinergic neurons in the nucleus basalis. Annals Of Neurology 10:122-126.

Whitson JS, Selkoe DJ, Cotman CW (1989) Amyloid beta protein enhances the survival of hippocampal neurons in vitro. Science 243:1488-1490.

Whitson JS, Glabe CG, Shintani E, Abcar A, Cotman CW (1990) Beta-amyloid protein promotes neuritic branching in hippocampal cultures. Neuroscience Letters 110:319-324.

Wilcock GK, Esiri MM (1982) Plaques, tangles and dementia: A quantitative study. Journal of the Neurological Sciences 56:343-356.

Wilkins RH, Brody IA (1969) Alzheimer's disease. Arch Neurol 21:109-110.

Winer BJ, Brown DR, Michels KM (1991) Statistical principles in experimental design. (3rd ed.). New York: McGraw-Hill.

Wisniewski HM, Wegiel J (1994) Beta-protein fibrillogenesis and neuritic plaques. In: Neurodegenerative Diseases, 1 Edition (Calne DB, ed), pp 83-95: W.B. Saunders Company.

Wisniewski HM, Ghetti B, Terry RD (1973) Neuritic (senile) plaques and filamentous changes in aged rhesus monkeys. J Neuropath Exp Neurol 32:566-584.

Wisniewski HM, Sturman JA, Shek JW (1980) Aluminum chloride induced neurofibrillary changes in the developing rabbit:a chronic animal model. Ann Neur 8:479-490.

Wisniewski T, Lalowski M, Golabek A, Vogel T, Frangione B (1995) Is AD an apolipoprotein E amyloidosis? Lancet 345:956-958.

Wolfe MS (2002) Secretase as a target for Alzheimer's disease. Curr Top Med Chem 2:371-383.

Wolfe MS, Citron M, Diehl TS, Xia W, Donkor IO, Selkoe DJ (1998) A substrate-based difluoro ketone selectively inhibits Alzheimer's gamma-secretase activity. J Med Chem 41:6-9.

Wolozin B, Kellman W, Ruosseau P, Celesia GG, Siegel G (2000) Decreased prevalence of Alzheimer disease associated with 3-hydroxy-3-methyglutaryl coenzyme A reductase inhibitors. Arch Neurol 57:1439-1443.

Wong PC, Zheng H, Chen H, Becher MW, Sirinathsinghji DJ, Trumbauer ME, Chen HY, Price DL, Van der Ploeg LH, Sisodia SS (1997) Presenilin 1 is required for Notch1 and DII1 expression in the paraxial mesoderm. Nature 387:288-292.

Wyss-Coray T, Masliah E, Mallory M, McConlogue L, Johnson-Wood K, Lin C, Mucke L (1997) Amyloidogenic role of cytokine TGF-beta1 in transgenic mice and in Alzheimer's disease. Nature 389:603-606.

Yamada K, Tanaka T, Han D, Senzaki K, Kameyama T, Nabeshima T (1999) Protective effects of idebenone and alpha-tocopherol on beta-amyloid-(1-42)-induced learning and memory deficits in rats: implication of oxidative stress in -amyloid-induced neurotoxicity in vivo. Eur J Neurosci 11:83-90.

Yamaguchi F, Richards SJ, Beyreuther K, Salbaum M, Carlson GA, Dunnett SB (1991) Transgenic mice for the amyloid precursor protein 695 isoform have impaired spatial memory. Neuroreport 2:781-784.

Yamamoto C, McIlwain H (1966) Electrical activities in thin sections from the mammalian brain maintained in chemically defined media in vitro. Journal of Neurochemistry 13:1333-1343.

Yamamoto C, Kawai N (1967) Presynaptic action of acetylcholine in thin sections from the guinea pig dentate gyrus in vitro. Experimental Neurology 19:176-187.

Yan Q, Zhang J, Liu H, Babu-Khan S, Vassar R, Biere AL, Citron M, Landreth G (2003) Anti-inflammatory drug therapy alters beta-amyloid processing and deposition in an animal model of Alzheimer's disease. J Neurosci 23:7504-7509.

Yan R, Bienkowski MJ, Shuck ME, Miao H, Tory MC, Pauley AM, Brashier JR, Stratman NC, Mathews WR, Buhl AE, Carter DB, Tomasselli AG, Parodi LA, Heinrikson RL, Gurney ME (1999) Membrane-anchored aspartyl protease with Alzheimer's disease beta-secretase activity. Nature 402:533-537.

Yankner BA, Benowitz LI, Villa-Komaroff L, Neve RL (1990) Transfection of PC12 cells with the human GAP-43 gene: effects on neurite outgrowth and regeneration. Brain Res Mol Brain Res 7:39–44.

Yu H, Saura CA, Choi S-Y, Sun LD, Yang X, Handler M, Kawarabayashi T, Younkin L, Fedeles B, Wilson MA, Younkin S, Kandel ER, Kirkwood A, Shen J (2001) APP processing and synaptic plasticity in presenilin-1 conditional knockout mice. Neuron 31:713-726.

Zhang ZX (2003) Health Directory: http://www37ccomcn/health/200307/2003073291xml?tmp=388302.

APPENDIX

Published Work

APPENDIX: PAPER I

The Journal of Neuroscience, September 15, 1999, 19(18):7983–7990

Relative Contribution of Endogenous Neurotrophins in Hippocampal Long-Term Potentiation

Guiquan Chen, Roland Kolbeck, Yves-Alain Barde, Tobias Bonhoeffer, and Albrecht Kossel

Max-Planck-Institut für Neurobiologie, D-82152 München-Martinsried, Germany

Recent evidence has shown that brain-derived neurotrophic factor (BDNF) is involved in hippocampal long-term potentiation (LTP). Because the reagents used in acute experiments react not only with BDNF but also with neurotrophin-4/5 (NT4/5) and neurotrophin-3 (NT3), we examined the involvement of these neurotrophins in LTP using two highly specific, function-blocking monoclonal antibodies against BDNF and NT3, as well as a TrkB-IgG fusion protein. Our results show that NT3 antibodies did not have any effects on LTP. However, both TrkB-IgG fusion proteins and BDNF antibody similarly reduced LTP, suggesting that only BDNF but no other ligands of the TrkB-receptor are likely to be involved in LTP induction. The reduction in LTP depended on the inducing stimuli and was only observed with theta-burst stimulation (TBS) but not with tetanic stimulation. We further observed that LTP was only reduced if BDNF was blocked before and during TBS stimulation, and BDNF antibodies did not affect early or late stages of LTP if they were applied 10, 30, or 60 min after TBS stimulation. These results point toward a specific and unique role of endogenous BDNF but not of other neurotrophins in the process of TBS-induced hippocampal LTP. Additionally, they suggest that endogenous BDNF is required for a limited time period only shortly before or around LTP induction but not during the whole process of LTP.

Key words: BDNF; NT3; NT4/5; monoclonal antibodies; TrkB-IgG fusion protein; LTP

Neurotrophins are proteins that control the survival and differentiation of many types of neurons during development (Davies, 1994; Lewin and Barde, 1996). In addition, there is increasing evidence indicating that neurotrophins are also involved in activity-dependent neuronal plasticity in the developing CNS (for review, see Lo, 1995; Thoenen, 1995; Berninger and Poo, 1996; Bonhoeffer, 1996). Compared with NGF, brain-derived neurotrophic factor (BDNF), and neurotrophin-3 (NT3), mRNAs are highly expressed in the hippocampus and neocortex (Wetmore et al., 1989; Ernfors et al., 1990; Hofer et al., 1990; Maisonpierre et al., 1990), and the expression of BDNF is tightly regulated by neuronal activity (Zafra et al., 1990, 1991; Castrén et al., 1992; Knipper et al., 1994; for review, see Lindholm et al., 1994). Interestingly, tetanization, a stimulation paradigm used to induce long-term potentiation (LTP) in the hippocampus, can induce both BDNF and NT3 mRNA expression in different hippocampal areas (Patterson et al., 1992; Dragunow et al., 1993). Also, the release of neurotrophins is dependent on neuronal activity (Blöchl et al., 1995; Blöchl and Thoenen, 1995; Griesbeck et al., 1995). Using BDNF and NT3, Lohof et al. (1993) were the first to show a direct influence of exogenous neurotrophins on synaptic transmission in neuromuscular synapses in developing *Xenopus*. Later, several reports demonstrated that acute application of exogenous BDNF, neurotrophin-4/5 (NT4/5), or NT3 can alter or potentiate synaptic transmission in rat hippocampal cultures and slices (Lessmann et al., 1994; Kang and Schuman, 1995; Levine et al., 1995). Although these experiments indirectly suggested that neurotrophins can participate in synaptic plasticity, work with mice carrying a null mutation in the BDNF gene showed that the lack of endogenous BDNF leads to drastically impaired LTP (Korte et al., 1995; Patterson et al., 1996) and to a limited capability of these animals to perform certain learning tasks (Linnarsson et al., 1997). Importantly, it was also shown that reexpression of the BDNF gene (Korte et al., 1996) or treatment of slices with recombinant BDNF (Patterson et al., 1996) were both able to restore LTP in slices of these mutant mice within <14 hr, making unspecific developmental deficits unlikely as an explanation for impaired LTP.

An additional approach to determine the involvement of endogenous neurotrophins in LTP is to block their function acutely in slices from wild-type animals. Two recent studies used a TrkB-IgG fusion protein (FP) and antibodies (Abs) against the TrkB receptor to block the ligands or the function of the TrkB receptor. This led to impaired LTP in slices from rat hippocampus (Figurov et al., 1996; Kang et al., 1997). Because both BDNF and NT4/5 can interact with the TrkB receptor, these experiments still leave the issue unresolved as to which of the two particular ligands actually contribute to LTP. The situation is further complicated by the fact that TrkB FPs are not selective for BDNF and NT4/5 but also bind NT3 (Shelton et al., 1995). The availability of specific, function-blocking monoclonal antibodies against BDNF and NT3 allowed us to acutely and selectively interfere with these neurotrophins and to determine their function in hippocampal LTP. We compared their effects on LTP with those of TrkB-IgG FPs and assessed the time period relative to the induction of LTP during which neurotrophins need to be available.

Received May 5, 1999; revised June 28, 1999; accepted June 30, 1999.

This work was supported in part by the Deutsche Forschungsgemeinschaft (SFB391) and the European Community Biotech Program (T.B.). We thank Volker Staiger for excellent technical assistance, Martin Korte for critical comments on this manuscript, and Ilse Bartke at Roche Diagnostics (Penzberg, Germany) for providing us with the monoclonal neurotrophin antibodies.

G. C.'s present address: Center for Neuroscience, The University of Edinburgh, Edinburgh EH8 9LE, UK.

Correspondence should be addressed to Dr. Tobias Bonhoeffer, Max-Planck-Institut für Neurobiologie, Am Klopferspitz 18 A, 82152 München-Martinsried, Germany.

MATERIALS AND METHODS

Slice preparation. Hippocampal transversal slices (400-μm-thick) were prepared from male wild-type mice of SV129 strain (4–8 weeks old) using conventional techniques (Korte et al., 1995) and maintained under standard conditions [medium contained (in mM): 124 NaCl, 3 KCl, 1.25 KH_2PO_4, 2 Mg_2SO_4, 26 $NaHCO_3$, 2.5 $CaCl_2$, and 10 glucose; at room temperature) and gassed with 95% O_2 and 5% CO_2. Slices were allowed to recover in an incubation chamber for at least 1.5 hr at room temperature before they were transferred to the perfusion chamber and used for the electrophysiological experiments.

Perfusion of slices with antibodies. The following antibodies were used for LTP experiments: (1) a TrkB receptor body, which is a fusion protein between the extracellular domain of the chick TrkB receptor and the Fc part of a human IgG antibody (Dechant et al., 1993); (2) a mouse monoclonal antibody (MAB) (clone #21, IgG_{2B}) raised against BDNF, characterized by its function blocking action with the same specificity as MAB clone #9 described by Kolbeck et al. (1999); and (3) a mouse monoclonal function-blocking NT3 antibody (IgG_1) (Gaese et al., 1994). Antibody solutions were freshly prepared in perfusate artificial CSF (ACSF) from frozen antibody aliquots. The final concentration used for TrkB-IgG fusion protein, anti-BDNF, or anti-NT3 antibody was 4 μg/ml. In the course of this study, we realized that it is of paramount importance to counteract adhesion of the antibodies to surfaces of beakers, tubing, etc. Therefore, tubing and beakers were siliconized for 1 hr and dried afterward. Before the actual experiments, siliconized tubing was washed extensively with fresh ACSF for 30 min. Additionally, BSA (0.1 mg/ml) was added to the antibody, as well as to the control solutions. To test for the presence and stability of the antibodies in the perfusion solution, the level of antibodies was determined from probes taken at different time points during perfusion using a specific enzyme immunoassay (ELISA). All experiments were performed in a blind way; the experimenter performing the electrophysiological recordings did not know what type of solution was added to the perfusion medium. A closed-loop perfusion system was used for all experiments with a total volume of 30 ml of perfusion medium. During preincubation of slices with either antibody or control solution, perfusion rates were alternated between fast rate at 40 ml/min, which potentially facilitates diffusion of exogenously applied substances into slices (Kang et al., 1996), and slow rate at 1 ml/min to prevent possible damage to the slices. For electrophysiological recordings, perfusion rate was kept constant at 1 ml/min during all experiments. After each recording, tubings and the recording chamber were extensively washed with fresh ACSF for 5–10 min.

Electrophysiology. Recordings were performed at 32°C. Slices were transferred from the incubation chamber to the recording chamber. In the pretreatment LTP experiments, they were perfused for 1 hr in either control or antibody-containing medium before electrophysiological recordings were started. In the other experiments in which antibody or control aliquots were added at different time points after theta-burst stimulation (TBS), the control or anti-BDNF antibody solutions were washed into the recording chamber at 10, 30, or 60 min after TBS, respectively. Control and antibody experiments were performed at the same experimental day. Field EPSPs (fEPSPs) of CA1 apical dendrites were recorded extracellularly with a glass electrode filled with 3 M NaCl solution (resistance of 4–10 MΩ) at a depth of ~120 μm below the slice surface. Two stimulating electrodes (monopolar, coated tungsten) were placed on either side of the recording electrode (within 200–400 μm). Stimuli were delivered alternating between these two independent Schaffer collateral–CA1 pathways, one serving as test and the other as control pathway, at a frequency of 0.1 Hz to each pathway. Stimulation in each pathway was set to elicit a fEPSP with an amplitude of ~40–50% of maximum. LTP was induced in the testing pathway by either tetanus consisting of 3 × 30 pulses (100 Hz, 5 sec intertrain interval) or theta-burst stimulation of three trains (10 sec intertrain interval), each consisting of 15 [200 msec interstimulus interval (ISI)] × 4 pulses (100 Hz).

Data analysis. Data were collected with a program written in LABVIEW (National Instruments, Austin, TX) and stored onto computer. The initial slope and amplitude of fEPSPs evoked by stimulation of the Schaffer collateral afferents was observed online but later reanalyzed off-line. Responses in each experiment were normalized to baseline, which was defined as the mean value obtained in 100 responses before tetanus or TBS, and shown as mean ± SEM. Experiments were excluded from the experimental data set if (1) the baseline of testing pathway was unstable (variability more than ±20%), or (2) the control pathway or the testing pathway were unstable or showed an apparent drift (variability more than ±20%). The "identity" of all slices was not revealed to the experimenter performing the electrophysiological recordings before the analysis was completed. As statistical test, the unpaired one-tailed Student's *t* test was used. A one-tailed test was chosen because the effect of the antibody and fusion protein treatments, if any, should be directional i.e., with smaller LTP in the experimental group than the respective controls. Significance levels are indicated in text. $p > 0.05$ were considered as not significant.

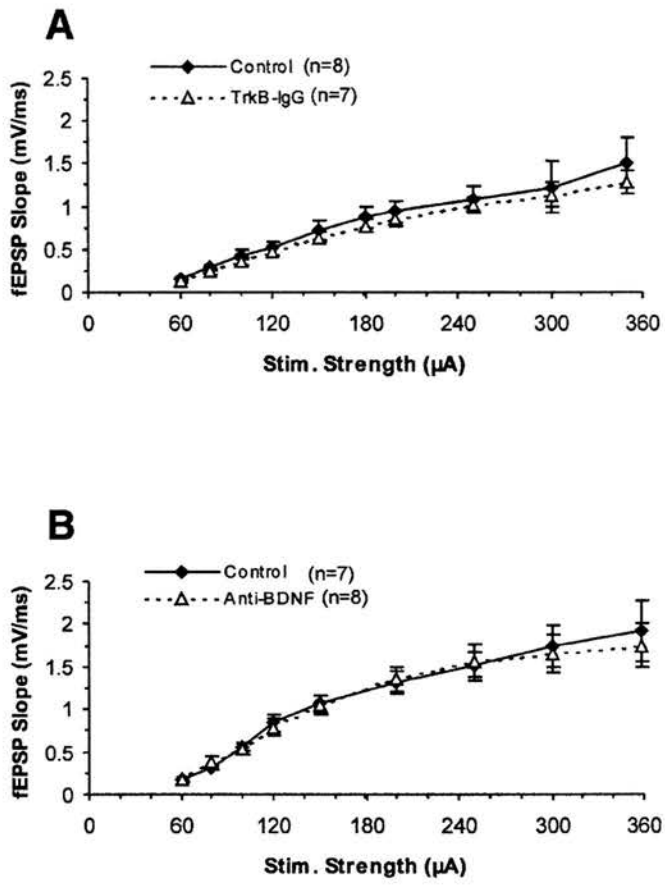

Figure 1. Basal synaptic transmission at the Schaffer collateral–CA1 pathway of hippocampal slices is not affected by treatment with TrkB-IgG fusion protein or BDNF antibody. The slope of field EPSPs was plotted against stimulus strength (in microamperes). *A*, TrkB-IgG fusion protein (*triangles*, *dotted line*; $n = 7$ slices, 4 mice) and controls (*diamonds*, *solid line*; $n = 8$ slices, 4 mice) ($p > 0.2$). *B*, BDNF antibody (*triangles*, *dotted line*; $n = 8$ slices, 4 mice) and controls (*diamonds*, *solid line*; $n = 7$ slices, 4 mice) ($p > 0.3$).

RESULTS

Effects of TrkB-IgG fusion protein and BDNF antibodies on basal synaptic transmission

We first tested whether the basal synaptic transmission at the Schaffer collateral–CA1 synapses was affected by pretreatment of the slices with TrkB-IgG FP or anti-BDNF antibody. Basal synaptic transmission was assessed in two ways. First, we measured the input–output curves of synaptic strength by plotting the slope of the fEPSPs versus the stimulus strength in control and antibody–fusion protein-treated slices. As shown in Figure 1*A*, the size of field EPSP slope in TrkB-IgG FP-treated slices was not significantly lower than in the controls for all the stimuli used. Also, incubation of slices with anti-BDNF monoclonal antibody for 1 hr did not show any effect on the input–output curves (Fig.

1*B*). We also compared the maximal response that we could elicit in control and antibody treated slices. The maximal slope of field EPSPs under treatments with both antibodies was also not significantly reduced from control slices (data not shown). The data above suggest that there is no deficit in basal synaptic transmission after acutely blocking endogenous BDNF with BDNF antibodies or other TrkB ligands with a TrkB-IgG fusion protein in hippocampal slices.

Effects of TrkB-IgG fusion proteins and BDNF antibodies on short-term plasticity

We next examined the presynaptic function in antibody-treated slices checking two forms of short-term synaptic plasticity in the Schaffer collateral–CA1 pathway of hippocampal slices: paired-pulse facilitation (PPF) and post-tetanic potentiation (PTP). First, we measured PPF in control and antibody-treated slices. PPF is a form of presynaptic short-term plasticity in which the response of a neuron to the second of two consecutive stimuli with a given ISI to the first one is increased (Katz and Miledi, 1968; Zucker, 1989). One hour after perfusion of the slices with control or antibody solutions, we tested PPF by using ISIs of 30, 40, 60, and 100 msec in control and antibody-treated slices. We found that PPF was reduced in neither TrkB-IgG fusion protein-treated slices compared with control slices ($p > 0.2$ for all ISIs; one-tailed t test) (Fig. 2*A*) nor in BDNF antibody-treated slices ($p > 0.2$ for all ISIs; one-tailed t test) (Fig. 2*B*). No deficits in PPF suggest that presynaptic forms of short-term plasticity stay normal after blocking endogenous BDNF or other TrkB ligands in antibody-treated slices. These results are consistent with our earlier findings in BDNF mutant mice (Korte et al., 1995). We also measured PTP, another form of short-term plasticity induced by tetanic stimulation, by averaging the EPSPs during the first minute after tetanic stimulation (average of six EPSPs) and calculating the ratio between this and the baseline value. We found that the size of PTP immediately after tetanic stimulation was not significantly reduced in TrkB receptor body-treated slices (TrkB-IgG, 301 ± 43%; $n = 6$; control, 281 ± 20%; $n = 6$; $p > 0.3$; one-tailed t test) (Fig. 3*A*), as well as BDNF antibody-treated slices compared with their controls (BDNF Ab, 324 ± 27%; $n = 7$; control, 264 ± 25%; $n = 7$; $p > 0.08$; one-tailed t test) (Fig. 4*A*). Together, the above results indicate that neither TrkB-IgG FP nor BDNF antibody alter short-term plasticity in hippocampal slices, thus suggesting that presynaptic neurotransmitter release is not disturbed by blocking ligands of TrkB receptor.

TrkB-IgG fusion protein attenuates LTP induced by TBS but not by tetanus

At present, two kinds of LTP-inducing stimuli, tetanus and TBS, are widely used to induce LTP in hippocampal slices. Both protocols were applied in our experiments in combination with the blockade of neurotrophins. First, we checked the effect of TrkB-IgG FP on LTP induced by tetanus. After the slice was superfused by medium containing either 4 μg/ml FP or the control solution for 1 hr, three trains of 100 Hz tetani were delivered to the Schaffer collateral–CA1 synapses to induce LTP. We found that LTP measured 1 hr after tetanus was not reduced by the TrkB-IgG FP compared with control slices (average slope of fEPSPs to baseline 55–60 min after tetanus: TrkB-IgG, 157 ± 24%; $n = 6$; control, 135 ± 10%; $n = 6$; $p > 0.2$; one-tailed t test) (Fig. 3*A*). TBS constitutes another important stimulus protocol to induce LTP. Compared with tetanus, TBS is a weak stimulus, and it is designed to mimic the theta rhythm in the hippocampus. We therefore also used this stimulus paradigm to induce LTP. In contrast to the tetanus-induced LTP, we found a significant reduction in LTP 1 hr after TBS in TrkB-IgG fusion protein-treated slices compared with their controls (average slope of fEPSPs to baseline 55–60 min after TBS: TrkB-IgG, 132 ± 14%; $n = 7$; control, 167 ± 12%; $n = 5$; $p < 0.04$; one-tailed t test) (Fig. 3*B*). Interestingly, PTP was also significantly lower in the treatment group, similar to the results of Figurov et al. (1996), who used a similar stimulation paradigm to test the effects of TrkB-IgG fusion proteins. Synaptic transmission in the control pathway remained unaffected (average slope of fEPSPs to baseline in the nontetanized pathway 1 hr after TBS: TrkB-IgG, 93 ± 5%; $n = 7$; control, 93 ± 3.0%; $n = 5$; $p > 0.45$; one-tailed t test). This confirms previous reports (Figurov et al., 1996; Kang et al., 1997)

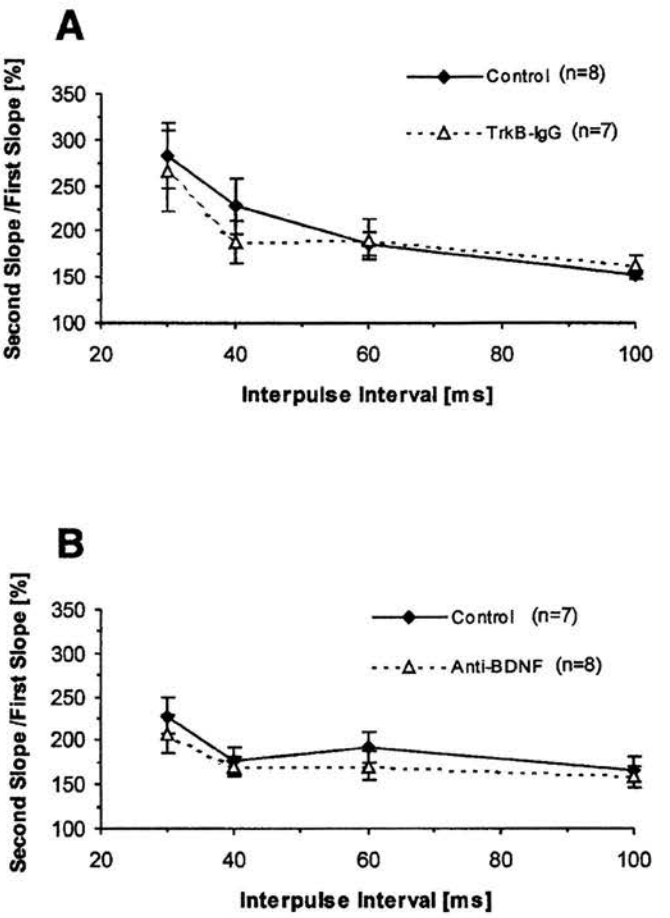

Figure 2. Short-term plasticity measured by PPF remains normal and unaffected at the Schaffer collateral–CA1 pathway of hippocampal slices after treatment with TrkB-IgG fusion protein or BDNF antibody. Plot depicting the percent ratio of responses to the second pulse relative to the first one. Pairs of pulses were delivered at interpulse intervals of 30, 40, 60, and 100 msec. *A*, TrkB-IgG fusion protein-treated slices (*triangles, dotted line*; $n = 7$ slices, 4 mice) versus control slices (*diamonds, solid line*; $n = 8$ slices, 4 mice). *B*, BDNF antibody-treated slices (*triangles, dotted line*; $n = 8$ slices, 4 mice) versus control slices (*diamonds, solid line*; $n = 7$ slices, 4 mice).

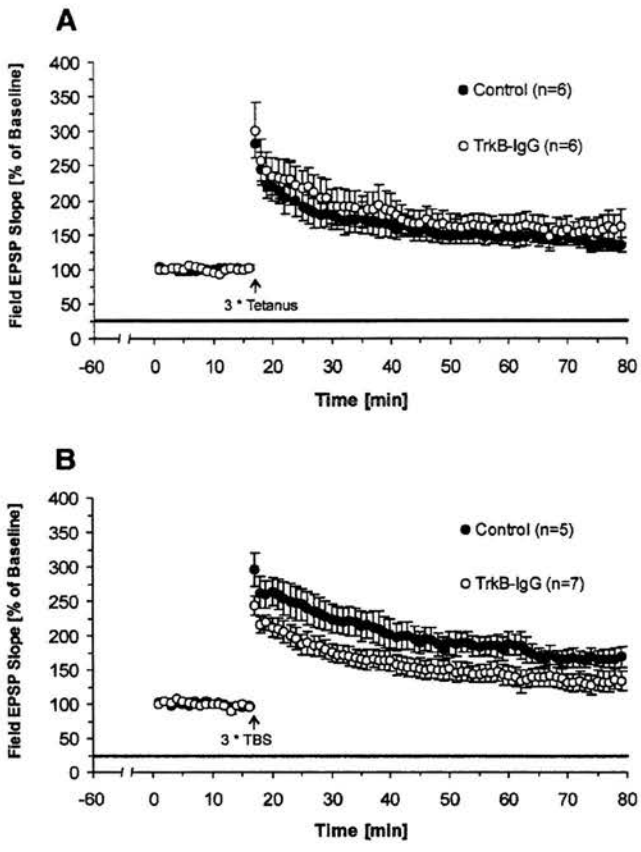

Figure 3. Effects of blocking all endogenous TrkB ligands on LTP. Pretreatment with TrkB-IgG fusion protein for 1 hr reduces LTP in a stimulus-dependent manner; only LTP induced by TBS at the Schaffer collateral–CA1 synapses of hippocampal slices is affected but not LTP induced by tetanic stimulation. Field EPSP slopes were plotted as percent of baseline (mean ± SEM). *Straight black line* represents the presence of TrkB-IgG fusion protein. *First data point* after LTP induction represents PTP. *A*, Tetanus-induced LTP and the effects of TrkB-IgG fusion protein (TrkB-IgG, $n = 6$ slices, 4 mice; control, $n = 6$ slices, 4 mice). *B*, TBS-induced LTP and the effects of TrkB-IgG fusion protein (TrkB-IgG, $n = 7$ slices, 4 mice; control, $n = 5$ slices, 4 mice).

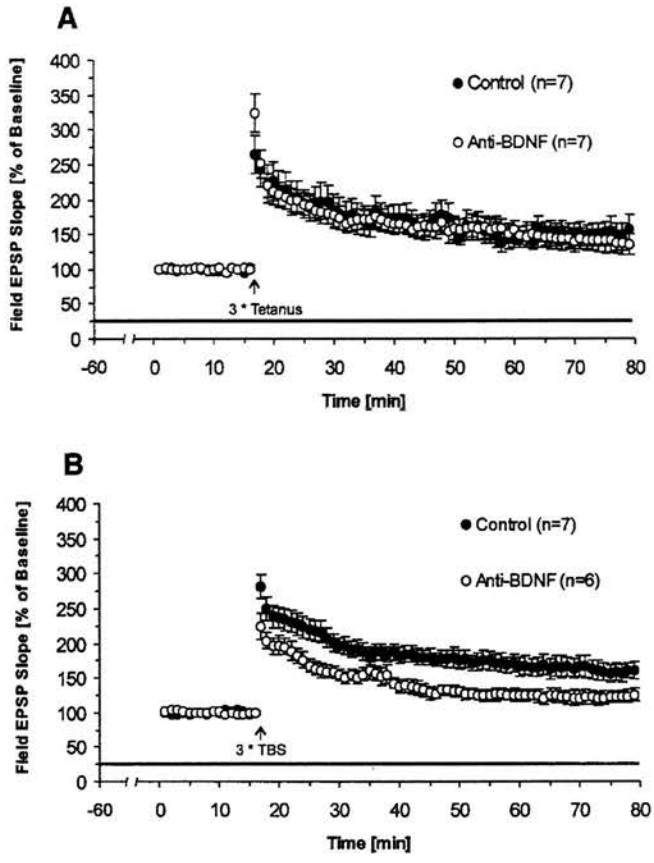

Figure 4. Effect of selectively blocking endogenous BDNF on LTP. Pretreatment with BDNF antibody for 1 hr significantly reduces LTP induced by TBS but not by tetanic stimulation. *A*, Effects of BDNF antibody on tetanus-induced LTP (BDNF Ab, $n = 7$ slices, 4 mice; control, $n = 7$ slices, 4 mice). *B*, Effects of BDNF antibody on TBS-induced LTP (BDNF Ab, $n = 6$ slices, 4 mice; control, $n = 7$ slices, 4 mice).

suggesting that ligands of TrkB receptor might have direct effects on TBS-induced LTP.

BDNF antibody reduces LTP induced by TBS but not by tetanus

The experiments above showed that blocking ligands of TrkB receptor reduced TBS-induced LTP. However, it still remains unclear which of the endogenous ligands of the TrkB receptor (BDNF, NT4/5, or both) participate in the process of LTP. Therefore, in the following experiments, we also used a specific monoclonal antibody against BDNF to determine whether blocking endogenous BDNF alone will affect hippocampal LTP in the same way. As before, we first checked the effect of BDNF antibody on tetanus-induced LTP and found that, in the presence of 4 μg/ml BDNF antibody, LTP was again not significantly reduced (average slope of fEPSPs to baseline 55–60 min after tetanus: BDNF Ab, 138 ± 16%; $n = 7$; control, 151 ± 18%; $n = 7$; $p > 0.3$; one-tailed t test) (Fig. 4*A*). Slices pretreated with 4 μg/ml BDNF antibody for 1 hr and stimulated with TBS, however, showed significant reduction in LTP (average slope of fEPSPs to baseline 55–60 min after TBS: BDNF Ab, 122 ± 7%; $n = 6$; control, 157 ± 12%; $n = 7$; $p < 0.018$; one-tailed t test) (Fig. 4*B*), whereas basal synaptic transmission in the control pathway remained unaffected (average slope of fEPSPs to baseline in the nontetanized pathway 55–60 min after TBS: BDNF Ab, 85 ± 1%; $n = 4$; control, 90 ± 4%; $n = 4$; $p > 0.2$; one-tailed t test). The difference between the two groups became apparent immediately after TBS. Thus, PTP after TBS stimulation was reduced by application of BDNF antibodies in contrast to PTP after tetanic stimulation. Together, these results show that hippocampal LTP is significantly reduced by the BDNF-antibody and to a comparable degree as seen with TrkB-IgG FP.

Anti-NT3 antibody does not block LTP induced by either tetanus or TBS

Previous studies that applied neurotrophins exogenously to the medium have suggested a direct role for NT3 in the process of LTP. We therefore asked the question whether blocking of endogenous NT3 by a specific function-blocking monoclonal antibody alters the induction or expression of hippocampal LTP. First, we checked the antibody effect on basal synaptic transmission and short-term plasticity. We found that neither basal synaptic transmission nor short-term synaptic plasticity in hippocampal slices were affected (data not shown). Second, we pretreated slices with antibodies for 1 hr and recorded LTP in control and

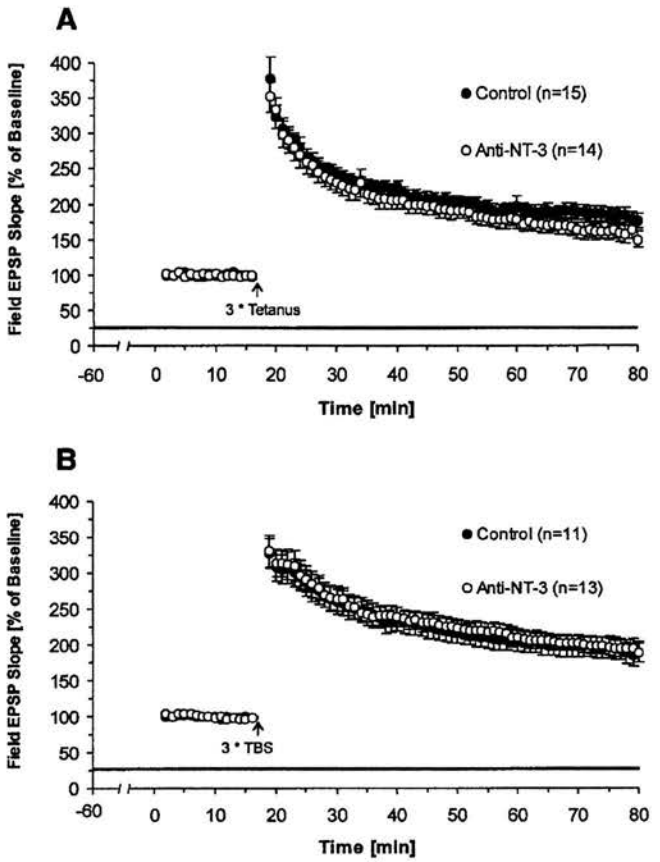

Figure 5. Effect of blocking endogenous NT3 on LTP. NT3 antibody does not affect LTP induced by either tetanus or TBS. Pretreatment time for slices was again 1 hr before recordings were started. *A*, Effects of NT3 antibody on tetanus-induced LTP (NT3 Ab, $n = 14$ slices, 10 mice; control, $n = 15$ slices, 9 mice). *B*, Effects of NT3 antibody on TBS-induced LTP (NT3 Ab, $n = 13$ slices, 10 mice; control, $n = 11$ slices, 8 mice).

NT3 antibody-treated slices. We also did not find any significant reduction effect in NT3 antibody-treated slices on either tetanus-induced LTP (average slope of fEPSPs to baseline 55–60 min after tetanus: NT3 Ab, 160 ± 12%; $n = 14$; control, 182 ± 10%; $n = 15$; $p > 0.09$; one-tailed t test) (Fig. 5*A*) or TBS-induced LTP (average slope of fEPSPs to baseline 55–60 min after TBS: NT3 Ab, 190 ± 11%; $n = 13$; control, 194 ± 16%; $n = 11$; $p > 0.2$; one-tailed t test) (Fig. 5*B*). These results indicate that endogenous NT3 seems not to be directly involved in hippocampal LTP.

BDNF antibody does not significantly reduce LTP when applied after TBS

Because the data thus far indicate that endogenous BDNF but not NT-4/5 or NT3 directly participates in TBS-induced LTP, we were then interested in determining the time during which BDNF needs to be present. Is endogenous BDNF required during a longer time period before and after LTP induction, arguing for a more permissive role, or might it be only required during the time period of LTP induction, in line with an instructive role of the protein? To address this question, we washed the BDNF antibody into the recording chamber at different time points (10, 30, and 60 min after delivery of TBS), and LTP was recorded for at least 1 hr after antibody infusion. In these experiments, we only used slices with a strong initial PPF (>200% at 30 msec ISI), because these slices expressed reliably more stable and higher levels of

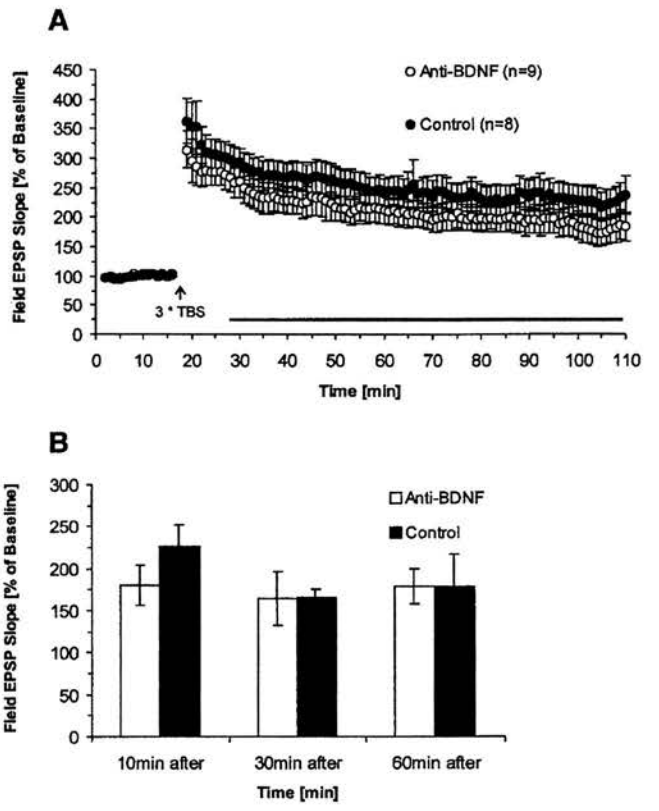

Figure 6. Effect on LTP is dependent on the time when endogenous BDNF is blocked by the antibodies. *A*, BDNF antibodies do not reduce LTP significantly when applied 10 min after TBS. *B*, Applications 30 or 60 min after TBS also do not affect LTP and its maintenance. Field EPSP slopes were plotted as percent of baseline. *Bars* indicate level of LTP at the end of each recording averaged over a 5 min period. Late phase LTP (3 hr after TBS) was measured for 30 and 60 min treatment groups (10 min group: BDNF Ab, $n = 9$ slices, 7 mice; control, $n = 8$ slices, 7 mice; 30 min group: BDNF Ab, $n = 6$ slices, 6 mice; control, $n = 4$ slices, 4 mice; 60 min group: BDNF Ab, $n = 5$ slices, 5 mice; control, $n = 5$ slices, 5 mice).

LTP, important for long-term recordings. When the BDNF antibody was applied 10 min after TBS, we found that early phase LTP in BDNF antibody-treated slices was reduced; however, this reduction was not significant (average slope of fEPSPs to baseline 90 min after TBS: BDNF Ab, 177 ± 23%; $n = 9$; control, 223 ± 24%; $n = 8$; $p > 0.1$; one-tailed t test; control pathway: BDNF Ab, 84 ± 5% $n = 6$; control, 97 ± 8%; $n = 5$; $p > 0.1$) (Fig. 6*A*). Although the greater variability of the data in this experiment require a cautious interpretation and conclusion about the absence of a significant reduction effect, it is important to note that wash-in of the antibodies does not cause any increase in the difference between the two groups. Second, the smaller LTP present in the antibody group already exists from the very beginning after TBS, that is, at a time before the antibodies were washed in. Together, this experiment suggest that, after induction, endogenous BDNF does not seem to be required anymore for the maintenance of early phase LTP. We also tested whether blocking of BDNF had effects on the later periods of LTP. For this, antibodies were also applied 30 or 60 min after TBS, and long-term recordings (>3 hr) were made. There was no significant reduction of long-lasting LTP in antibody-treated slices (30 min after treatment–average slope of fEPSPs to baseline 180 min

after TBS: BDNF Ab, 164 ± 32%; $n = 6$; control, 167 ± 9%; $n = 4$; $p > 0.5$; one-tailed t test; 60 min after treatment–average slope of fEPSPs to baseline 180 min after TBS: BDNF Ab, 179 ± 21%; $n = 5$; control, 180 ± 38%; $n = 5$; $p > 0.5$; one-tailed t test) (Fig. 6*B*). These results strongly suggest that, after the delivery of TBS, endogenous BDNF is not required, for neither early nor medium-to-late phase LTP.

DISCUSSION

Although several recent studies have focused on the role of BDNF in neurotransmission and LTP within the hippocampus, data on the potential involvement of other neurotrophins are sparse and mainly based on experiments using application of exogenous neurotrophins. With regard to potentiation of synaptic strength in CA1 (the area investigated in our study), BDNF and NT3 seem to be equally effective (Kang and Schuman, 1995). In this study, we specifically addressed the question as to what role the endogenous neurotrophins BDNF, NT4/5, and NT3 play in the process of LTP.

Specificity of neurotrophic action on LTP

Direct evidence for the involvement of endogenous BDNF on LTP has been obtained by experiments using BDNF knock-out mice that show greatly reduced enhancement (Korte et al., 1995). Unlike NT3 −/− animals, BDNF null mutants survive long enough for the kind of experiments to be performed in the postnatal hippocampus. LTP can be "rescued" in BDNF −/− and +/− animals by incubating these slices either in recombinant BDNF (Patterson et al., 1996) or by reintroducing the BDNF gene (Korte et al., 1996). Additionally, two recent studies demonstrate that blocking the endogenous ligands of the TrkB receptor in slices by TrkB-IgG FP also affects LTP (Figurov et al., 1996; Kang et al., 1997). These studies left the question unresolved as to whether the effect was obtained by blockade of endogenous BDNF, by blockade of NT4/5, or both. Although the relative abundance of BDNF could be taken as evidence for a significant physiological role (Ernfors et al., 1990; Hofer et al., 1990; Martinez et al., 1998), it is clear that NT4/5 is also expressed in the hippocampus during all stages of development (Klein et al., 1992; Timmusk et al., 1993). Experiments using a TrkB-IgG FP and a BDNF-specific antibody enabled us to distinguish between the roles of NT4/5 and BDNF in hippocampal LTP. Although TrkB fusion protein bind equally to NT4/5 and BDNF and with slightly lower affinity, even to NT3 (Shelton et al., 1995), the similar reduction in LTP seen in response to the fusion protein and the BDNF-specific antibody argues against a direct and necessary involvement of NT-4/5 in hippocampal LTP.

So far, no clear evidence is available on the role of endogenous NT3 in the process of hippocampal CA1 LTP. Although NT3 and TrkC are strongly expressed early in development, the expression of both is weaker but still present within the adult hippocampus (Ernfors et al., 1990; Maisonpierre et al., 1990; Lamballe et al., 1994; Martinez et al., 1998). Previous studies have shown that exogenous NT3 added to the perfusion medium of slices leads to a fast potentiation of synaptic strength in the CA1 region of hippocampus, similar to the effects obtained with BDNF (Kang and Schuman, 1995), suggesting that NT3 could be potentially as important as BDNF for LTP. The experiments presented here tested the role of endogenous NT3 in LTP by blocking its function through a specific antibody. They show that blocking of NT3 affects neither TBS- nor tetanus-induced LTP. Given that both the NT3 and the BDNF antibodies are IgG molecules, their diffusion properties should be very similar, and both should reach the same sites. Therefore, our results strongly argue against a direct role of endogenous NT3 in the induction of hippocampal CA1 LTP. A similar conclusion was recently drawn by Kokaia et al. (1998) for LTP in the lateral perforant path–granular cell pathway. However, it was based on results using heterozygous +/− NT3 knock-out mice, because of the nonviability of the homozygous −/− mice. Several reports document the fact that the presence of one NT3 allele has readily measurable functional consequences, for example, on the number of sensory neurons or on muscles spindles (Ernfors et al., 1994; Airaksinen and Meyer, 1996; Airaksinen et al., 1996).

Previous findings about NT3 and synaptic transmission may then have been caused by fast, short-term effects of NT3 through increase in evoked EPSC amplitude or increase in miniature EPSC frequency akin to the effects observed for BDNF of minis, not directly related to LTP (Lohof et al., 1993; Lessman et al., 1994; Levine et al., 1995; Li et al., 1998). Moreover, the increase of synaptic transmission by exogenous NT3 may also have been brought about by the secondary release of BDNF. Neurotrophins can trigger the release of other neurotrophins in dissociated cultures of hippocampal neurons (Canossa et al., 1997) and PC12 cells (Kruttgen et al., 1998). Neurotrophin-induced neurotrophin release could therefore not only be an explanation of the NT3 results, but it could also constitute an important factor during normal LTP induction. Still, the lack of any effects of NT3 blockade on LTP makes it highly unlikely that this neurotrophin is directly involved in LTP or that BDNF-induced release of other members of the neurotrophin family is involved in LTP induction.

Stimulus dependency

Interestingly, blocking of BDNF by antibodies only impaired LTP induced by theta-burst stimulation but not by tetanic stimulation, whereas in BDNF knock-out mice, tetanic stimulation-induced LTP was strongly impaired (Korte et al., 1995, 1996; Patterson et al., 1996). One possible explanation for the failure of BDNF antibodies to block tetanus-induced LTP is that BDNF levels after a tetanus might exceed the buffering capacities of the antibody in the tissue at the critical time point. In fact, a number of reports showing that BDNF is released in an activity-dependent manner (Blöchl and Thoenen 1995; Blöchl et al., 1995; Thoenen, 1995) would predict that BDNF concentrations are considerably higher after a tetanus than after TBS, thereby providing a straightforward explanation for this observation.

A second explanation is that tetanus and TBS activate different signaling pathways that are necessary for LTP induction (Kang et al., 1997). Small differences in stimulation paradigms are known to trigger different signaling pathways leading to potentiation, depotentiation, or depression of synapses (Stäubli and Chun, 1996; Xu et al., 1998). Thus, unlike tetanic stimulation, TBS could act through a pathway that involves immediate BDNF effects. In particular, application of exogenous BDNF can occlude subsequent potentiation induced by TBS but not by tetanus (Kang et al., 1997). However, because tetanic stimulation-induced LTP was so strongly diminished in BDNF knock-out mice, these additional signaling pathway(s) would have to depend on the constitutive presence of BDNF. BDNF could activate gene expression through cAMP-response element binding protein, an important component of LTP in hippocampus (Bourtchuladze et al., 1994; Finkbeiner et al., 1997). Thus, these additional pathways in LTP may be impaired and not be activated by tetanic stimulation in

BDNF knock-out mice while they were active when endogenous BNDF was blocked by antibodies only for a short period of time.

Time dependency of BDNF requirement

A major question concerning the role of BDNF in LTP is the time period during which BDNF has to be present to exert its effects. One hypothesis is that BDNF acts as a retrograde messenger that is released during LTP induction from the dendrites of pyramidal neurons and subsequently induces the potentiation of synaptic transmission. Direct evidence proving this hypothesis is still missing. Using the BDNF antibody, we could acutely block endogenous BDNF during different time periods relative to the induction of LTP to determine when endogenous BDNF is needed for induction or expression of LTP. Our results show that the presence of BDNF antibodies in the superfusion solution for 80 min before LTP induction significantly reduced LTP induced by TBS from the beginning, which suggests that BDNF is needed during the induction process or before. Figurov et al. (1996) have recently described for young animals that BDNF may influence LTP by changing the effectiveness of tetanic stimulation or TBS via facilitation of synaptic transmission. This effect also led to enhanced paired-pulse facilitation at short interpulse intervals. In our experiments, blockade of BDNF had no measurable effects on basic synaptic transmission (Figs. 1, 2) or on synaptic depression measured during TBS or tetanus stimulation. BDNF therefore seems to affect LTP induction directly rather than by changing the effectiveness of the LTP-inducing stimulus.

Infusion of the antibody starting at different time points after TBS did not significantly reduce early (90 min after TBS) or late (up to 3 hr after TBS) LTP. Although in the 10 min postapplication experiment the larger variability of the data may have obscured a potential significant reduction in LTP by the antibodies, later stages of LTP (up to 3 hr after TBS) clearly remained unaffected when the antibodies were applied 30 or 60 min after TBS. Endogenous BDNF therefore seems to be only required within a short time period before (80 min) or around the time of induction of TBS-induced LTP. Assuming similar short penetration times of the BDNF antibody, these results seem to be in contrast to the results obtained by Kang et al. (1997). Using TrkB-IgG fusion proteins, they found that the application 30–60 min after LTP could still block late phase of LTP, whereas later application had no effect. Because in these experiments a different tetanic stimulation protocol (1 sec at 100 Hz, three times, 5 min apart) was used to induce late phase LTP, this could indicate that the pattern of stimulation might have relevant consequences on the effect of BDNF on later stages of LTP. Another explanation for the different findings may be differences between the onset of blocking in the two sets of experiments. A delayed onset of blocking in the postapplication experiments with the antibody could exceed a potential critical time window during which BDNF is needed. Unfortunately, the question of when the onset of the critical blocking concentration of the antibodies within tissue is reached cannot conclusively be answered. Thus, postapplication experiments in which the antibodies were applied after LTP induction can only give a rough estimate of the temporal requirements of BDNF for LTP.

In summary, our results provide clear evidence that endogenous BDNF plays a unique and specific role in LTP. We could show that, under the same stimulus conditions and similar blocking antibody concentrations, other neurotrophins are not involved in CA1 LTP. Our study demonstrates that BDNF affects LTP directly and not via secondary effects through induced release of other neurotrophins. Although the exact mechanism of the BDNF action still remains unclear, our results further show that the lack of BDNF for a relatively short period of time, before but not after LTP-induction, is sufficient to block LTP. This seems to point toward the possibility that BDNF is important during LTP induction. However, the need for a constitutive activation of TrkB receptors before LTP induction cannot be excluded and may be very important for the activation of other LTP relevant pathways.

REFERENCES

Airaksinen MS, Meyer M (1996) Most classes of dorsal root ganglion neurons are severely depleted but not absent in mice lacking neurotrophin-3. Neuroscience 73:907–911.

Airaksinen MS, Koltzenburg M, Lewin GR, Masu Y, Helbig C, Wolf E, Brem G, Toyka KV, Thoenen H, Meyer M (1996) Specific subtypes of cutaneous mechanoreceptors require neurotrophin-3 following peripheral target innervation. Neuron 16:287–295.

Berninger B, Poo M-M (1996) Fast action of neurotrophic factors. Curr Opin Neurobiol 6:324–330.

Blöchl A, Thoenen H (1995) Characterization of nerve growth factor (NGF) release from hippocampal neurons: evidence for a constitutive and an unconventional sodium-dependent regulated pathway. Eur J Neurosci 7:1220–1228.

Blöchl A, Berninger B, Berzaghi M, Castrén E, Lindholm D, Thoenen H (1995) Neurotrophins as mediators of neuronal plasticity. In: Life and death in the nervous system (Ibanez CF, ed), pp 260–272. Oxford: Elsevier.

Bonhoeffer T (1996) Neurotrophins and activity-dependent development of the neocortex. Curr Opin Neurobiol 6:119–126.

Bourtchuladze R, Frenguelli B, Blendy J, Cioffi D, Schutz G, Silva AJ (1994) Deficient long-term memory in mice with a targeted mutation of the cAMP-responsive element-binding protein. Cell 79:59–68.

Canossa M, Griesbeck O, Berninger B, Campana G, Kolbeck R, Thoenen, H (1997) Neurotrophin release by neurotrophins; implications for activity dependent neuronal plasticity. Proc Natl Acad Sci USA 94:13279–13286.

Castrén E, Zafra F, Thoenen H, Lindholm D (1992) Light regulates expression of brain-derived neurotrophic factor mRNA in the visual cortex. Proc Natl Acad Sci USA 89:9444–9448.

Davies AM (1994) The role of neurotrophins in the developing nervous system. J Neurobiol 25:1334–1349.

Dechant G, Biffo S, Okazawa H, Kolbeck R, Pottgiesser J, Barde Y-A (1993) Expression and binding characteristics of the BDNF receptor chick trkB. Development 119:545–558.

Dragunow M, Beilharz E, Mason B, Lawlor P, Abraham W, Gluckman P (1993) Brain-derived neurotrophic factor expression after long-term potentiation. Neurosci Lett 160:232–236.

Ernfors P, Wetmore C, Olsom L, Persson H (1990) Identification of cells in rat brain and peripheral tissues expressing mRNA for members of the NGF family. Neuron 5:511–526.

Ernfors P, Lee KF, Kucera J, Jaenisch R (1994) Lack of neurotrophin-3 leads to deficiencies in the peripheral nervous system and loss of limb proprioceptive afferents. Cell 77:503–512.

Figurov A, Pozzo-Miller LD, Olafsson P, Wang T, Lu, B (1996) Regulation of synaptic responses to high-frequency stimulation and LTP by neurotrophins in the hippocampus. Nature 381:706–709.

Finkbeiner S, Tavazoie SF, Maloratsky A, Jacobs KM, Harris KM, Greenberg ME (1997) CREB: a major mediator of neuronal neurotrophin responses. Neuron 19:1031–1047.

Gaese F, Kolbeck R, Barde Y-A (1994) Sensory ganglia require neurotrophin-3 early in development. Development 120:1613–1619.

Griesbeck O, Blöchl A, Carnahan JF, Nawa H, Thoenen H (1995) Characterization of brain-derived neurotrophic factor (BDNF) secretion from hippocampal neurons. Soc Neurosci Abstr 21:417.

Hofer M, Pagliusi SR, Hohn A, Leibrock J, Barde YA (1990) Regional distribution of brain-derived neurotrophic factor mRNA in the adult mouse brain. EMBO J 9:2459–2464.

Kang H, Schuman EM (1995) Long-lasting neurotrophin-induced enhancement of synaptic transmission in the adult hippocampus. Science 267:1658–1662.

Kang H, Jia LZ, Suh K-Y, Tang L, Schuman EM (1996) Determinants of BDNF-induced hippocampal plasticity: role of the trkB receptor and the kinetics of neurotrophin delivery. Learn Mem 3:188–196.

Kang H, Welcher AA, Shelton D, Schuman EM (1997) Neurotrophins and time: different roles for trkB signaling in hippocampal long-term potentiation. Neuron 19:653–664.

Katz B, Miledi, R (1968) The role of calcium in neuromuscular facilitation. J Physiol (Lond) 195:481–492.

Klein R, Lamballe F, Bryant S, Barbacid M (1992) The trkB tyrosine protein kinase is a receptor for neurotrophin-4. Neuron 8:947–956.

Knipper M, Berzaghi M, Blöchl A, Breer H, Thoenen H, Lindholm D (1994) Positive feedback between acetylcholine and the neurotrophins nerve growth factor and brain-derived neurotrophic factor in the rat hippocampus. Eur J Neurosci 6:668–671.

Kokaia M, Asztely F, Olofsdotter K, Balet Sindreu C, Kullmann DM, Olle Lindvall (1998) Endogenous neurotrophin-3 regulates short-term plasticity at lateral perforant path–granule cell synapses. J Neurosci 1998 18:8730–8739.

Kolbeck R, Bartke I, Eberle W, Barde YA (1999) Brain-derived neurotrophic factor (BDNF) levels in the nervous system of wild-type and neurotrophin gene mutant micc. J Neurochem 72:1930–1938.

Korte M, Carroll P, Wolff E, Brem G, Thoenen H, Bonhoeffer, T (1995) Hippocampal long-term potentiation is impaired in mice lacking brain-derived neurotrophic factor. Proc Natl Acad Sci USA 92:8856–8860.

Korte M, Griesbeck O, Gravel C, Carroll P, Staiger V, Thoenen H, Bonhoeffer T (1996) Virus-mediated gene transfer into hippocampal CA1 region restores long-term potentiation in brain-derived neurotrophic factor mutant mice. Proc Natl Acad Sci USA 93:12547–12552.

Kruttgen A, Moller JC, Heymach JV, Shooter EM (1998) Neurotrophins induce release of neurotrophins by the secretory pathway. Proc Natl Acad Sci USA 95:9614–9619.

Lamballe F, Smeyne RJ, Barbacid M (1994) Developmental expression of trkC, the neurotrophin-3 receptor, in the mammalian nervous system. J Neurosci 14:14–28.

Lessmann V, Gottman K, Heumann R (1994) BDNF and NT-4/5 enhance glutamatergic synaptic transmission in cultured hippocampal neurons. NeuroReport 6:21–25.

Levine ES, Dreyfus CF, Black IB, Plummer MR (1995) Brain-derived neurotrophic factor rapidly enhances synaptic transmission in hippocampal neurons via postsynaptic tyrosine kinase receptors. Proc Natl Acad Sci USA 92:8074–8077.

Lewin G, Barde YA (1996) Physiology of the neurotrophins. Annu Rev Neurosci 19:289–317.

Li Y-X, Xu Y, Ju D, Lester HA, Davidson N, Schuman EM (1998) Expression of a dominant negative TrkB receptor, T1, reveals a requirement for presynaptic signaling in BDNF-induced synaptic potentiation in cultured hippocampal neurons. Proc Natl Acad Sci USA 95:10884–10889.

Lindholm D, Castren E, Berzaghi M, Blöchl A, Thoenen H (1994) Activity-dependent and hormonal regulation of neurotrophin mRNA levels in the brain- implications for neuronal plasticity. J Neurobiol 25:1362–1372.

Linnarsson S, Bjorklund A, Ernfors P (1997) Learning deficit in BDNF mutant mice. Eur J Neurosci 9:2581–2587.

Lo DC (1995) Neurotrophic factors and synaptic plasticity. Neuron 15: 979–981.

Lohof AM, Ip NY, Poo M-M (1993) Potentiation of developing neuromuscular synapses by neurotrophins NT-3 and BDNF. Nature 363:350–353.

Maisonpierre PC, Belluscio L, Friedman B, Alderson RF, Wiegand SJ, Furth ME, Lindsay RM, Yancopoulos GD (1990) NT-3, BDNF, and NGF in the developing rat nervous system: parallel as well as reciprocal patterns of expression. Neuron 5:501–509.

Martinez A, Alcantara S, Borrell V, Delrio JA, Blasi J, Otal R, Campos N, Boronat A, Barbacid M, Silossantiago I, Soriano E (1998) TrkB and TrkC signaling are required for maturation and synaptogenesis of hippocampal connection. J Neurosci 18:7336–7350.

Patterson SL, Grover, LM, Schwartzkroin PA, Bothwell M (1992) Neurotrophin expression in rat hippocampal slices: a stimulus paradigm inducing LTP in CA1 evokes increases in BDNF and NT-3 mRNAs. Neuron 9:1080–1088.

Patterson SL, Abel T, Deuel TAA, Martin KC, Rose JC, Kandel ER (1996) Recombinant BDNF rescues deficits in basal synaptic transmission and hippocampal LTP in BDNF knockout mice. Neuron 16:1137–1145.

Shelton DL, Sutherland J, Gripp J, Camerato T, Armanini MP, Phillips HS, Carroll K, Spencer SD, Levinson AD (1995) Human trks: molecular cloning, tissue distribution, and expression of extracellular domain immunoadhesins. J Neurosci 15:477–491.

Stäubli U, Chun D (1996) Factors regulating the reversibility of long-term potentiation. J Neurosci 16:853–860.

Thoenen H (1995) Neurotrophins and neuronal plasticity. Science 270:593–598.

Timmusk T, Belluardo N, Metsis M, Persson H (1993) Widespread and developmentally regulated expression of neurotrophin-4 mRNA in rat brain and peripheral tissues. Eur J Neurosci 5:605–613.

Wetmore C, Ernfors P, Persson H, Olson L (1989) Localization of BDNF mRNA to neurons in the brain by *in situ* hybridization. Exp Neurol 109:141–152.

Xu L, Anwyl R, Rowan MJ (1998) Spatial exploration induces a persistent reversal of long-term potentiation in rat hippocampus. Nature 394:891–894.

Zafra F, Hengerer B, Leibrock J, Thoenen H, Lindholm D (1990) Activity dependent regulation of BDNF and NGF mRNAs in the rat hippocampus is mediated by non-NMDA glutamate receptors. EMBO J 9:3545–3550.

Zafra F, Castrén E, Thoenen H, Lindholm D (1991) Interplay between glutamate and γ-aminobutyric acid transmitter systems in the physiological regulation of brain-derived neurotrophic factor and nerve growth factor synthesis in hippocampal neurons. Proc Natl Acad Sci USA 88:10037–10041.

Zucker RS (1989) Short-term synaptic plasticity. Annu Rev Neurosci 12:13–31.

15. Chafee, M. V. & Goldman-Rakic, P. S. Matching patterns of activity in primate prefrontal area 8a and parietal area 7ip neurons during a spatial working memory task. *J. Neurophysiol.* **79,** 2919–2940 (1998).
16. Duhamel, J. R., Colby, C. L. & Goldberg, M. E. The updating of the representation of visual space in parietal cortex by intended eye movements. *Science* **255,** 90–92 (1992).
17. Andersen, R. A. in *Handbook of Physiology, Section 1: The Nervous System* (eds Mountcastle, V. B., Plum, F. & Geiger, S. R.) 483–518 (Am. Physiol. Soc., Bethesda, 1987).
18. Everling, S., Spantekow, A., Krappmann, P. & Flohr, H. Event-related potentials associated with correct and incorrect responses in a cued antisaccade task. *Exp. Brain Res.* **118,** 27–34 (1998).
19. Horwitz, G. D. & Newsome, W. T. Separate signals for target selection and movement specification in the superior colliculus. *Science* **284,** 1158–1161 (1999).
20. Grunewald, A., Linden, J. F. & Andersen, R. A. Responses to auditory stimuli in macaque lateral intraparietal area. I. Effects of training. *J. Neurophysiol.* **82,** 330–342 (1999).
21. Thier, P. & Andersen, R. A. Electrical microstimulation distinguishes distinct saccade-related areas in the posterior parietal cortex. *J. Neurophysiol.* **80,** 1713–1735 (1998).
22. Colby, C. L., Gattass, R., Olson, C. R. & Gross, C. G. Topographical organization of cortical afferents to extrastriate visual area PO in the macaque: a dual tracer study. *J. Comp. Neurol.* **269,** 392–413 (1988).
23. Barash, S., Melikyan, A., Sivakov, A. & Tauber, M. Shift of visual fixation dependent on background illumination. *J. Neurophysiol.* **79,** 2766–2781 (1998).
24. Newsome, W. T., Britten, K. H. & Movshon, J. A. Neuronal correlates of a perceptual decision. *Nature* **341,** 52–54 (1989).

Acknowledgements

We thank E. Ahissar for his involvement, and A. Melikyan and X. Wang for participation in some experiments. We thank M. Glickstein, P. Thier, E. Seidemann, Y. Ritov and M. Tsodyks for discussions and for reading the manuscript. This work was supported by the Israel Science Foundation, and by the Murray H. and Meyer Grodetsky Center for Research of Higher Brain Functions and the Einhorn-Dominic Institute of Brain Research at the Weizmann Institute, and by the Paul Godfrey Research Foundation.

Correspondence and requests for materials should be addressed to S.B. (e-mail: shabtai.barash@weizmann.ac.il).

A learning deficit related to age and β-amyloid plaques in a mouse model of Alzheimer's disease

Guiquan Chen*, Karen S. Chen†, Jane Knox*, Jennifer Inglis*, Andrew Bernard*, Stephen J. Martin*, Alan Justice†, Lisa McConlogue†, Dora Games†, Stephen B. Freedman† & Richard G. M. Morris*

** Department of Neuroscience, University of Edinburgh, 1 George Square, Edinburgh, EH8 9JZ, UK*
† Elan Pharmaceuticals, 800 Gateway Boulevard, South San Francisco, California 94080, USA

Mice that overexpress the human mutant amyloid precursor protein (hAPP) show learning deficits, but the apparent lack of a relationship between these deficits and the progressive β-amyloid plaque formation that the hAPP mice display is puzzling. In the water maze[1], hAPP mice are impaired before and after amyloid plaque deposition[2–7]. Here we show, using a new water-maze training protocol, that PDAPP mice[8] also exhibit a separate age-related deficit in learning a series of spatial locations. This impairment correlates with β-amyloid plaque burden and is shown in both cross-sectional and longitudinal experimental designs. Cued navigation and object-recognition memory are normal. These findings indicate that Aβ overexpression and/or Aβ plaques are associated with disturbed cognitive function and, importantly, suggest that some but not all forms of learning and memory are suitable behavioural assays of the progressive cognitive deficits associated with Alzheimer's-disease-type pathologies.

We have developed a new water-maze protocol for mice in which, after they learn to escape quickly and reliably onto the hidden platform at one location, we move the platform to a new location. Numerous locations are used successively, one at a time. In such a procedure, earlier locations of the platform will be encoded in long-term memory, potentially causing interference. Memory retrieval must therefore be selective for the most recently encoded location, an 'episodic-like' component of the task. The idea behind using such a procedure, embedded within a larger test battery, derives from lesion and single-unit recording studies in rodents that implicate the hippocampal formation in only certain aspects of spatial, working- or episodic-like memory[9–13]. Such a protocol is worth exploring as, in the PDAPP mouse, the highest density of β-amyloid plaques is first seen in the outer molecular layer of the dentate gyrus and other regions of the hippocampus.

PDAPP and non-transgenic (non-Tg) littermate control mice ($n = 99$) swam normally and climbed successfully onto the escape

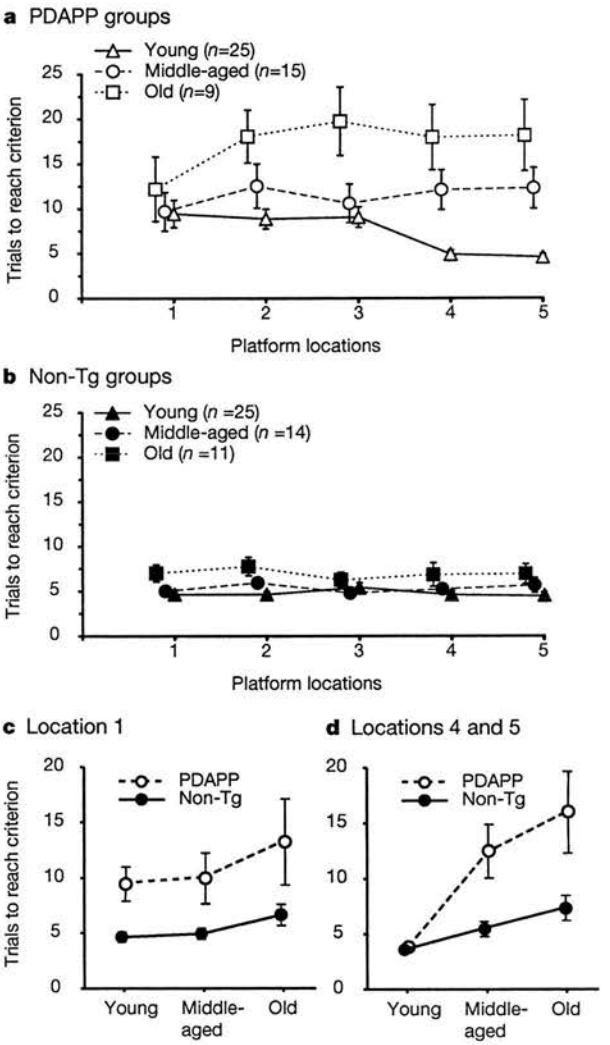

Figure 1 Age-related and age-independent deficits in spatial learning in PDAPP mice. Analysis of variance of 'trials to criterion' (3 successive trials with mean escape latency < 20 s) for each platform location of the first place navigation task revealed a significant groups × age effect ($F = 5.27$, d.f. 2/93, $P < 0.01$). This interaction justified separate analyses of the two groups. **a**, PDAPP mice. Trials to criterion (inclusive) for each successive platform location in the main series of five locations revealed a significant age-related worsening of performance ($F = 8.32$, d.f. 2/46, $P = 0.001$) and a locations × age interaction ($F = 2.17$, d.f. 6.59/151.7, $P < 0.05$; Greenhouse–Geisser correction). **b**, Non-Tg mice also showed a modest decline with age ($F = 7.24$, d.f. 2/47, $P < 0.005$) but no interaction. **c**, Platform location 1. A separate analysis of platform location 1 revealed poorer performance by the PDAPP mice which learned more slowly than non-Tgs ($F = 15.2$, d.f. 1/93, $P < 0.001$) but there was no age-related effect or interaction. **d**, Platform locations 4 and 5. There were significant main effects of group and age and, critically, a group × age interaction ($F = 8.30$, d.f. 2/93, $P < 0.001$). This was because the PDAPP mice got worse with age ($F = 12.56$, d.f. 2/46, $P < 0.0005$) at a much faster rate than non-Tgs ($F = 4.45$, d.f. 2/47, $P < 0.05$). Results shown are mean ± 1 s.e.m.

platform in the pool. Performance in the initial cued-navigation task (see Methods) revealed no persistent sensorimotor or motivational abnormalities. Escape latencies averaged less than 10 s in all groups by the end of this pretraining.

Two key findings emerged in the new 'training-to-criterion' task, which requires the learning of five successive platform locations. The first of these (cross-sectional study) is a striking age-related deficit in the number of trials required to reach the performance criterion as the mice learned the series of individual platform locations (Fig. 1a). Young PDAPP mice (6–9 months) improved such that criterion was reached in fewer trials for later platform locations, whereas middle-aged (13–15 months) and old PDAPP animals (18–21 months) took longer to learn each new location. The non-Tg control groups did not show this pattern (Fig. 1b). Second, the PDAPP groups of all ages took longer to learn the first platform location of the series than the non-Tg groups (Fig. 1c). This second deficit was age-independent, in contrast to the age-related learning deficit apparent for spatial locations 4 and 5 in the PDAPP groups (Fig. 1d).

Measured over the first three trials of training, swim speeds of PDAPP and non-Tg mice declined in parallel as a function of age, with PDAPP mice swimming only slightly more slowly (0.024 m s^{-1}) than non-Tgs (Fig. 2a, b). Fig 2c shows the swim-paths of representative animals for all trials of location 5 at each age. The young PDAPP mouse reached the performance criterion (trials labelled C1 to C3) as quickly as its non-Tg control (top two rows). In contrast, the middle-aged and old PDAPP mice displayed persistent deficits (taking 13 and 19 trials, respectively, to learn, compared with 4 and 6 trials by non-Tgs). The paths taken by the older PDAPP animals were noteworthy in two respects. First, path length showed great variability from trial to trial until the criterion was reached, suggestive of a retrieval deficit. Second, there was little indication of thigmotaxis (that is, staying near the side walls) which is a pattern of behaviour frequently displayed in the standard reference memory task by mice that fail to learn well.

The test of 'learning capacity' provided a point of comparison between the cross-sectional and longitudinal components of the study. Both revealed a greater age-related decline in the PDAPP groups (Fig. 3). This deficit was remarkably similar in both the cross-sectional (Fig. 3a) and longitudinal (Fig. 3b) data.

The brains of a subset of PDAPP mice in the cross-sectional study were analysed using the anti-Aβ monoclonal antibody 3D6 which shows diffuse plaques. Very few plaques were visible in scattered regions of the hippocampal formation at 9 months (Fig. 4a, young mutant animal). By 16–17 months, plaque density was higher, particularly in the termination zones of the axons of layers II and

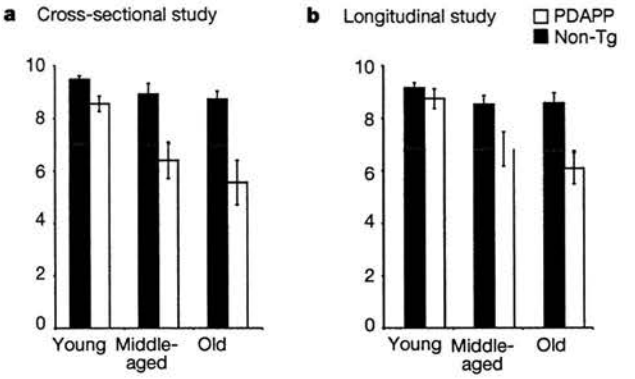

Figure 3 An age-related decline in learning capacity in PDAPP mice. The *y* axes show the number of successive spatial locations of a single hidden platform learned to criterion in 10 d of training ('learning capacity'). Older PDAPP mice performed significantly more poorly than older non-Tgs (interaction effect for cross-sectional: $F = 4.05$, d.f. 2/93, $P < 0.05$; longitudinal: $F = 6.83$, d.f. 2/46, $P < 0.005$). **a**, Cross-sectional study. There was a trend towards an age-related decline in learning capacity in non-Tgs ($F = 2.94$, d.f. 2/47, $0.10 > P > 0.05$), but the decline was highly significant in the PDAPP mice ($F = 8.84$, d.f. 2/46, $P < 0.005$). **b**, Longitudinal study. Learning capacity declines in the same age-related way in individual PDAPP mice retested throughout the lifespan. Non-Tgs again showed no change in learning capacity as a function of age ($F = 1.66$, d.f. 2/24, $P > 0.2$), whereas the PDAPP mice learned steadily fewer platform locations ($F = 18.30$, d.f. 2/22, $P < 0.001$). Results shown are mean ± 1 s.e.m.

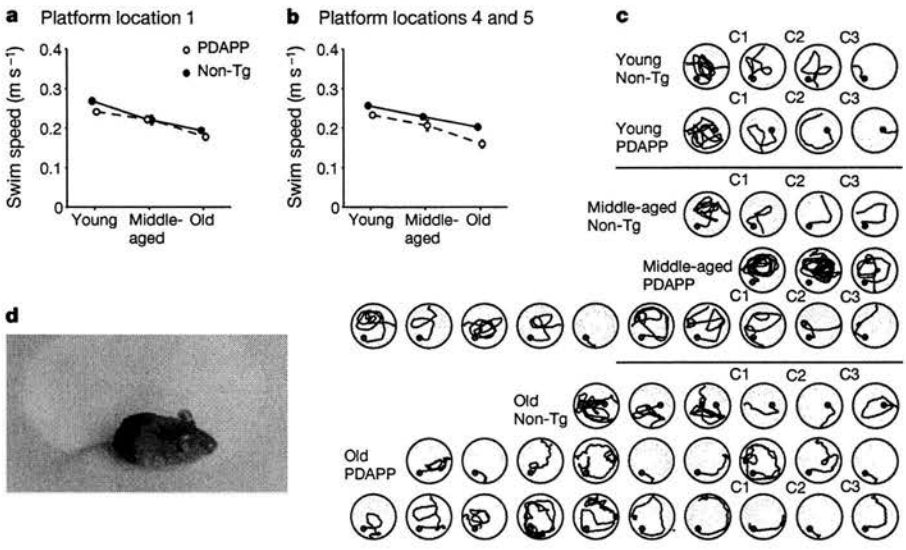

Figure 2 Swim speeds and swim paths. **a**, **b**, Mean (± s.e.m.) swim speeds over the first three trials of training to the first, and the 4th and 5th platform locations. These trials were chosen because, with the performance criterion being three trials with an escape latency less than 20 s, the first three trials of training are only ones for which we have data from all animals. Swim-speed declines with age (location 1: $F = 27.46$, d.f. 2/93, $P < 0.001$; locations 4 and 5: $F = 26.67$, d.f. 2/93, $P < 0.001$). The small but significant difference between PDAPPs and non-Tgs (overall: 0.024 m s^{-1}; location 1: $0.10 > P > 0.05$; locations 4 and 5: $F = 18.91$, d.f. 1/93, $P < 0.001$) did not change as a function of age ($F < 1$). **c**, Paths taken by representative animals (that is, close to the group mean in terms of trials to criterion) in learning the 5th location at each of the three ages. Note similar patterns in PDAPP and non-Tg mice at 6–9 months, but circuitous paths taken by the PDAPP mice on some but not all trials at 13–15 and 18–21 months. **d**, A PDAPP mouse on the hidden escape platform in the water maze.

III entorhinal cells in the outer blade of the molecular layer of the dentate gyrus and stratum moleculare lacunosum of area CA1 (Fig. 4b, middle-aged animal). Occasional plaques were seen in cortex, particularly the cingulate cortex. By 21–22 months, amyloid plaques were apparent through many regions of the hippocampal formation, the cingulate cortex, insular cortex dorsal to the rhinal fissure and entorhinal cortex (Fig. 4c, old animal). A zone of cortex between these areas showed a lower density of amyloid plaques but a light background of diffuse staining. No amyloid plaques were observed in control mice. β-Amyloid plaque burden in the hippocampus increased as a function of age as described previously (Fig. 4d)[8,14]. Behavioural performance declined as a function of plaque burden (Fig. 4e). A scatter plot of middle-aged and old mice only revealed a significant negative correlation between learning capacity and plaque burden (Fig. 4f).

In contrast to the learning of several spatial locations, object-recognition memory was normal in PDAPP animals across their lifespan. This was tested using a task requiring the spontaneous recognition of a series of new and familiar objects[15,16]. We observed (cross-sectional study) that both PDAPP and non-Tg mice preferentially explored each of five separate new objects to the same extent (Fig. 5). The memory retention interval was varied to examine forgetting rates. Forgetting occurred at the same rate in PDAPP and non-Tg mice.

These findings indicate that the spatial learning impairment displayed by PDAPP mice can be dissociated into age-related and age-independent components. The age-related component became apparent through the use of a new task in which mice are required to learn a series of successive spatial locations. This task is sensitive to age in non-transgenic controls but, in PDAPP mice, the age-related

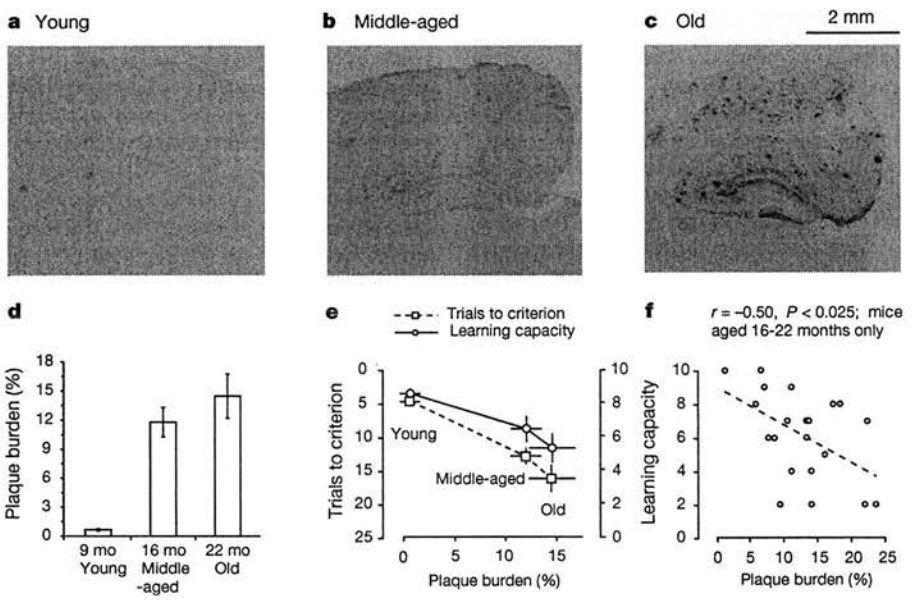

Figure 4 The relationship between performance and β-amyloid plaque deposition. **a–c**, Diffuse amyloid plaque deposition revealed using the 3D6 antibody in PDAPP mice of different ages. These sections are taken from the three mice whose paths are shown in Fig. 2. Note prominent deposition of plaques in the outer molecular layer of the dentate gyrus by age 16 months. **d**, Plot of plaque burden as a function of age measured in a subset of mice. Quantitative analysis of plaque burden in the hippocampus confirmed an age-related increase ($F = 13.4$, d.f. 2/24, $P < 0.001$). **e**, Two measures of performance in learning a series of spatial locations as a function of plaque burden. Left-hand *y* axis, trials to criterion on locations 4 and 5 (note axis is inverted); right-hand *y* axis, learning capacity (number of platform locations learned to criterion in 10 d). The behavioural scores are the means ± s.e.m. of all animals tested at each age. **f**, Scatter plot of learning capacity scores in the subset of middle-aged and old animals for which plaque burden measures are available. An overall analysis of all 27 PDAPP mice revealed significant correlations between hippocampal plaque burden and both the number of trials to reach criterion for platform locations 4 and 5, and the separate measure of learning capacity ($r = 0.57$ and $r = -0.59$, respectively; $P < 0.01$). However, these correlations may be artificially inflated by the inclusion of young mice displaying few plaques. We also examined the middle-aged and old animals as a single group (age range 16–22 months; $n = 21$; these age groups did not differ significantly with respect to either plaque burden or behavioural performance, $P > 0.5$ in all cases, Bonferroni post-hoc comparisons). The correlation coefficients for these 21 animals were lower but were significant in both cases ($r = 0.43$ (trials to criterion) and $r = -0.50$ (learning capacity); $P < 0.05$).

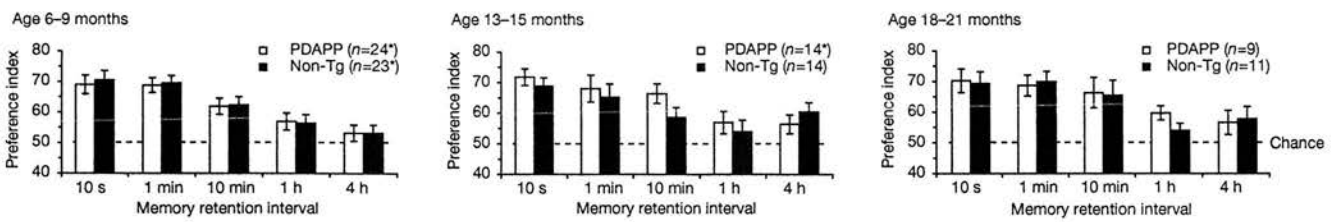

Figure 5 Normal object-recognition memory. Preference index for recognition of a familiar object as a function of memory delay interval, group and age (mean ± s.e.m.). Chance performance is 50% (dotted line). PDAPP and non-Tgs show equivalent above chance performance reflecting their greater exploration of the new object. The memory delay was varied across objects and familiarity observed to decay over time ($F = 20.8$, d.f. 4/352, $P < 0.001$) at the same rate in PDAPP and non-Tg mice ($F < 1$). The mean performance of both groups was significantly above chance at all time intervals ($P < 0.05$ or better; one-sample *t*-tests). Comparable results were obtained in the longitudinal study (data not shown). Three young mice (1 PDAPP, 2 non-Tg) and one middle-aged PDAPP mouse failed to explore the objects in the groups marked with an asterisk and these were excluded from the data analysis Results shown are mean ± s.e.m.

decline is substantially greater. The deficit in learning and recalling separate platform locations learned successively was apparent both when the PDAPP mice received their first training at the different ages tested, and when initially young PDAPP mice were re-tested through their lifespan. The use of a longitudinal design in the behavioural testing of hAPP mice is new, and reveals that individual PDAPP mice have, relative to age-matched controls, a declining capacity to learn and/or recall as they get older. This deficit in working- or episodic-like memory in the PDAPP mouse is consistent with the age-related deficit in T-maze alternation exhibited by $APP_{695}SWE$ mice[17].

The age-independent learning deficit in PDAPP mice was restricted to learning the first platform location, an impairment analogous to that seen in previous water-maze reference memory experiments[2–7]. In the single report claiming an age-related impairment in reference memory in $APP_{695}SWE$ mice[18], there is reasonable concern that an age-related change occurred in the control rather than the transgenic animals. This age-independent deficit is unrelated to progressive changes in β-amyloid levels and plaque deposition[19], but may be associated with the smaller size of hippocampus and glucose hypometabolism that occurs in V717F mice at a young age[20,21].

A general implication is that dissociations between age-related and age-independent components of representational memory need to be taken into account in animal models of progressive neurodegenerative diseases if valid tests of the differential effects of Aβ overexpression, β-amyloid plaques and other neurodegenerative changes on cognitive function are to be made. We propose that as β-amyloid plaques are deposited, β-amyloid levels rise and fast synaptic transmission in the hippocampus and other brain areas becomes less effective[19,22], PDAPP mice are gradually less able to rapidly encode changes in their memory representation of an environment and/or to retrieve information selectively—a deficit in 'episodic-like' memory[12,23]. These mice also show an early and age-independent deficit in spatial learning[24] but not in object-recognition memory (but see ref. 25).

The decline in performance in this new water-maze task correlates with the age-related increase in β-amyloid plaque deposition, even when young animals with minimal deposits are excluded. However, we do not yet know if this relationship to plaque deposition is causal for our findings are also consistent with the primary pathological trigger being elevated Aβ levels rather than frank plaque deposition[26]. It will be valuable to use this new test to examine hAPP mice that have received exogenous treatments limiting the deposition of β-amyloid plaques[27]. □

Methods

Animals

In the cross-sectional study, there were 99 PDAPP and non-transgenic littermate control mice (non-Tg) aged 6–9 months (young), 13–15 months (middle-aged) and 18–21 months (old). A subset of the young animals formed the longitudinal study, with repeat testing at the two later ages, and a total of 25 mice completing the study at age 22 months (PDAPP = 12, non-Tg = 13). All animals were male, of common parentage, on a Swiss Webster/DBA/C57BL6 background and fed freely on food and water.

Experimental protocol

Behavioural testing took place in a water maze and an exploratory arena. For cued navigation, testing began with 5 d of cued training to a visible platform. For training to criterion, place navigation to a single hidden platform was then tested, followed by training to four successive new locations. Each animal was trained, for up to eight trials per day, to a rigorous performance criterion of three successive trials with an escape latency of less than 20 s before being transferred to the next location on the next day. For object-recognition memory, testing took place in the arena over 5 d to examine rapidly acquired memory for object familiarity. For learning capacity, place navigation consisting of training to criterion of as many successive spatial locations as could be learned in a fixed 10-day training period. The only difference between the training-to-criterion and learning-capacity tests was that the former measured the extent of training required to learn five locations, and the latter measured the total number of platform locations that could be acquired over a set number of days. The animals were killed when all behavioural training was completed to measure the extent of β-amyloid plaque burden in the hippocampus. The longitudinal component of the study involved only minor procedural modifications. On re-testing the mice when they became middle-aged and old, they were given 2 d of cued training, 3 d of object-recognition memory, and either 10 d or 5 successive platform locations (whichever took longer) of place-navigation training.

Water maze

Mice were trained in a 2-m diameter open-field water maze (opaque water at 25 ± 1 °C, 20-cm diameter platform, top surface 1.5 cm below water level, maximum trial duration = 90 s, 30 s on platform at end of trials). They were placed into the water at and facing the side walls, being transported there by hand from a holding cage in an adjacent room. Swim paths were monitored using an automated tracking system (Watermaze). The mice were run in squads of six at a time by two experimenters who were 'blind' with respect to their group assignment (three animals per squad were in each group). For cued training (four trials per day over 5 d), the pool was surrounded by white curtains to occlude sight of extra-maze cues. The platform was cued by means of a 15-cm high dark cylinder placed onto it and placed pseudo-randomly in different locations across trials. For the training-to-criterion and learning-capacity tests (eight trials per day), the curtains were pulled to the side to reveal extra-maze cues and the platform was unmarked by any local cues within the pool. For each mouse, the platform was moved between different locations, drawn from a set of 20 possible locations. The performance criterion for both tests was three trials in a row with an average escape latency of less than 20 s (maximum trials = 40 for location 1, and 32 trials thereafter).

Object recognition

The animals were tested in an arena with sloping side-walls to prevent shadows from overhead illumination (50 cm × 50 cm, 1 cm sawdust on floor). Habituation consisted of daily 5-min periods in the empty arena over 5 d. The mice were then allowed to explore two identical objects placed into the arena at fixed locations until they had accumulated 30 s of total inspection time (where this is defined as active exploration, sniffing, and so on, of the objects) or for a maximum of 20 min. Five different sets of identical objects were used on different days. After the initial period of inspection, the mice and the objects were removed from the arena for the prescribed memory delay interval (10 s, 1 min, 10 min, 1 h or 4 h spent in a transport cage in the laboratory). A third copy of the earlier identical objects was then placed into the arena at one location and a new object at the other. The mice were returned to the arena and allowed to explore until 30 s of inspection time had again accumulated. The toy objects (for example, a model duck) measured about 10–15 cm in height and were washed in alcohol between successive tests. Memory of the familiar object is associated with increased exploration of the new object and a performance index (PI) is calculated using the formula PI = 100 × (new object inspection time)/30.

Immunocytochemistry

The brains of a subset of mice ($n = 27$; young, $n = 6$; middle-aged, $n = 14$; old, $n = 7$) were removed and one hemisphere was drop-fixed in formalin. The tissue was mounted coronally and 30-μm sections collected using a cryostat. Every eighth section throughout the extent of the brain was stored in antifreeze solution (30% glycerol/30% ethylene glycol in 40 mM $NaPO_4$) at −20 °C before immunostaining. The sections were incubated with 3D6-biotinylated antibody overnight at 4 °C and then reacted with the horseradish peroxidase–avidin–biotin complex (Vector Laboratories) and developed using 3,3′-diaminobenzidine as the chromagen[28]. Amyloid deposition was quantified automatically using a Leica Q-Win image analysis system. Video images of the brain were captured, the area of the hippocampus outlined and a threshold optical density was obtained that discriminated staining from background. The amyloid 'plaque burden' was defined as the average percentage of hippocampal area covered by amyloid depositions over six sections.

Received 5 October; accepted 22 November 2000.

1. Morris, R. G. M., Garrud, P., Rawlins, J. N. P. & O'Keefe, J. Place navigation impaired in rats with hippocampal lesions. *Nature* **297,** 681–683 (1982).
2. Yamaguchi, F. *et al.* Transgenic mice for the amyloid precursor protein 695 isoform have impaired spatial memory. *NeuroReport* **2,** 781–784 (1991).
3. D'Hooge, R., Nagels, G., Westland, C. E., Muck, L. & De Deyn, P. P. Spatial learning deficit in mice expressing human 751-amino acid beta-amyloid precursor protein. *NeuroReport* **7,** 2807–2811 (1996).
4. Nalbantoglu, J. *et al.* Impaired learning and LTP in mice expressing the carboxy terminus of the Alzheimer amyloid precursor protein. *Nature* **387,** 500–505 (1997).
5. Justice, A. & Motter, R. Behavioral characterization of PDAPP transgenic Alzheimer mice. *Soc. Neurosci. Abstracts* **23,** 1637 (1997).
6. Moechars, D. *et al.* Early phenotypic changes in transgenic mice that overexpress different mutants of amyloid precursor protein in brain. *J. Biol. Chem.* **274,** 6483–6492 (1999).
7. Raber, J. *et al.* Apolipoprotein E and cognitive performance. *Nature* **404,** 352–354 (2000).
8. Games, D. *et al.* Alzheimer-type neuropathology in transgenic mice overexpressing V717F β-amyloid precursor protein. *Nature* **373,** 523–527 (1995).
9. Rawlins, J. N. P. Associations across time: The hippocampus as a temporary memory store. *Behav. Brain Sci.* **8,** 479–497 (1985).
10. Whishaw, I. Q. & Tomie, J. A. Perseveration on place reversals in spatial swimming pool tasks: further evidence for place learning in hippocampal rats. *Hippocampus* **7,** 361–370 (1997).
11. Steele, R. J. & Morris, R. G. M. Delay-dependent impairment of a matching to place task with chronic and intrahippocampal infusion of the NMDA antagonist D-AP5. *Hippocampus* **9,** 118–136 (1999).
12. Wood, E. R., Dudchenko, P. A. & Eichenbaum, H. The global record of memory in hippocampal neuronal activity. *Nature* **397,** 613–616 (1999).
13. Aggleton, J. P. & Brown, M. W. Episodic memory, amnesia, and the hippocampal-anterior thalamic axis. *Behav. Brain Sci.* **22,** 425–489 (1999).

14. Chen, K. S. *et al.* Neurodegenerative Alzheimer-like pathology in PDAPP 717V→F transgenic mice. *Prog. Brain Res.* **117,** 327–334 (1998).
15. Ennaceur, A. & Delacour, J. A new one-trial test for neurobiological studies of memory in rats. 1: Behavioral data. *Behav. Brain Res.* **31,** 47–59 (1988).
16. Tang, Y. P. *et al.* Genetic enhancement of learning and memory in mice. *Nature* **401,** 63–69 (1999).
17. Chapman, P. F. *et al.* Impaired synaptic plasticity and learning in aged amyloid precursor protein transgenic mice. *Nature Neurosci.* **2,** 271–276 (1999).
18. Hsiao, K. *et al.* Correlative memory deficits, Aβ elevation, and amyloid plaques in transgenic mice. *Science* **274,** 99–102 (1996).
19. Johnson-Wood, K. *et al.* Amyloid precursor protein processing and Aβ42 deposition in a transgenic mouse model of Alzheimer disease. *Proc. Natl Acad. Sci. USA* **94,** 1550–1555 (1997).
20. Dodart, J.-C., Mathis, C., Bales, K. R., Paul, S. M. & Ungerer, A. Early regional cerebral glucose hypometabolism in transgenic mice overexpressing the V717F β-amyloid precursor protein. *Neurosci. Lett.* **277,** 49–52 (1999).
21. Dodart, J.-C. *et al.* Neuroanatomical abnormalities in behaviorally characterised APPV717F Transgenic Mice. *Neurobiol. Dis.* **7,** 71–85 (2000).
22. Larson, J., Lynch, G., Games, D. & Seubert, P. Alterations in synaptic transmission from young and aged PDAPP mice. *Brain Res.* **840,** 23–35 (1999).
23. Clayton, N. S. & Dickinson, A. What, where and when: Episodic-like memory during cache recovery by scrub jays. *Nature* **395,** 272–274 (1998).
24. O'Keefe, J. & Nadel, L. *The Hippocampus as a Cognitive Map* (Clarendon, Oxford, 1978).
25. Dodart, J. C. *et al.* Behavioral disturbances in transgenic mice overexpressing the V717F β-amyloid precursor protein. *Behav. Neurosci.* **113,** 982–990 (1999).
26. Naslund, J. *et al.* Correlation between elevated levels of amyloid β-peptide in the brain and cognitive decline. *J. Am. Med. Assoc.* **283,** 1571–1577 (2000).
27. Schenk, D. *et al.* Immunization with amyloid-β attenuates Alzheimer-disease-like pathology in the PDAPP mouse. *Nature* **400,** 173–177 (1999).
28. Masliah, E. *et al.* Comparison of neurodegenerative pathology in transgenic mice overexpressing V717F β-amyloid precursor protein and Alzheimer's disease. *J. Neurosci.* **16,** 5795–5811 (1996).

Acknowledgements

This work was supported by grants from the MRC and the Cunningham Trust. We are indebted to Bill Nailon (CJD Surveillance Unit, Edinburgh) and Karen Khan (Elan Pharmaceuticals) for assistance with immunocytochemistry and image analysis.

Correspondence and requests for materials should be addressed to R.G.M.M. (e-mail: R.G.M.Morris@ed.ac.uk).

Aβ peptide immunization reduces behavioural impairment and plaques in a model of Alzheimer's disease

Christopher Janus*, Jacqueline Pearson*, JoAnne McLaurin*, Paul M. Mathews†, Ying Jiang†, Stephen D. Schmidt†, M. Azhar Chishti*, Patrick Horne*, Donna Heslin*, Janet French*, Howard T.J. Mount*, Ralph A. Nixon†, Marc Mercken‡, Catherine Bergeron*§, Paul E. Fraser*, Peter St George-Hyslop*§ & David Westaway*

** Centre for Research in Neurodegenerative Diseases, Departments of Medicine, Laboratory Medicine and Pathobiology, and Medical Biophysics, University of Toronto, Tanz Neuroscience Building, 6 Queen's Park Crescent West, Toronto, Ontario M5S 3H2, Canada*

† Nathan Kline Institute Center for Dementia Research, and New York University School of Medicine, 140 Old Orangeburg Road, Orangeburg, New York 10962, USA

‡ Janssen Research Foundation, Turnhoutseweg, 30, B-2340 Beerse, Belgium

§ Departments of Medicine (Division of Neurology) and Pathology, Toronto Western Hospital, University Health Network, Toronto, Ontario M5S 1A8, Canada

Much evidence indicates that abnormal processing and extracellular deposition of amyloid-β peptide (Aβ), a proteolytic derivative of the β-amyloid precursor protein (βAPP), is central to the pathogenesis of Alzheimer's disease (reviewed in ref. 1). In the PDAPP transgenic mouse model of Alzheimer's disease, immunization with Aβ causes a marked reduction in burden of the brain amyloid[2,3]. Evidence that Aβ immunization also reduces cognitive dysfunction in murine models of Alzheimer's disease would support the hypothesis that abnormal Aβ processing is essential to the pathogenesis of Alzheimer's disease, and would encourage the development of other strategies directed at the 'amyloid cascade'. Here we show that Aβ immunization reduces both deposition of cerebral fibrillar Aβ and cognitive dysfunction in the TgCRND8 murine model of Alzheimer's disease without, however, altering total levels of Aβ in the brain. This implies that either a ~50% reduction in dense-cored Aβ plaques is sufficient to affect cognition, or that vaccination may modulate the activity/abundance of a small subpopulation of especially toxic Aβ species.

To explore the behavioural consequences of Aβ immunization, we used the TgCRND8 murine model of Alzheimer's disease that expresses a mutant (K670N/M671L and V717F) human βAPP_{695} transgene under the regulation of the Syrian hamster prion promoter on a C3H/B6 strain background (M.A.C. *et al.*, manuscript in preparation). TgCRND8 mice have spatial learning deficits at 3 months of age that are accompanied by both increasing levels of SDS-soluble Aβ and increasing numbers of Aβ-containing amyloid plaques in the brain. Age- and sex-matched TgCRND8 mice and non-Tg littermates in three cohorts were vaccinated at 6, 8, 12, 16 and 20 weeks with either $A\beta_{42}$ or islet-associated polypeptide (IAPP), which has similar biophysical properties to Aβ but is associated with a non-central nervous system (CNS) amyloidosis. Both immunogens were in β-pleated-sheet conformation at the

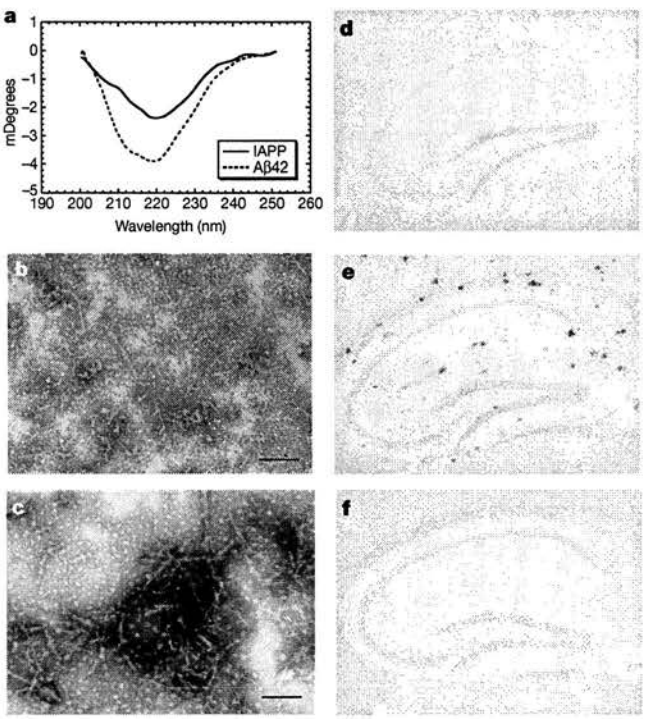

Figure 1 Aβ and IAPP peptide immunogens were predominantly β-structured and induced antibodies recognizing fibrillar Aβ deposits. **a**, Circular dichroism spectra of $A\beta_{42}$ (dotted line) and IAPP (solid line) before immunization are predominantly β-structured. *m*Degrees, millidegrees. **b**, Negative-stain electron microscopy (scale 150 nm) of $A\beta_{42}$ peptide immunogen showed varying length fibres; **c**, IAPP peptide immunogen showed short laterally aggregated fibres. **d**, **f**, Serum (1:1,000 dilution) from non-immunized TgCRND8 mice (**d**) and from 23-week old IAPP-immunized mice (**f**) did not recognize the Aβ plaques in adjacent, non-formic-acid treated sections from a non-immunized TgCRND8 mouse with abundant Aβ-positive plaques. **e**, Sera from $A\beta_{42}$-immunized mice strongly labelled dense-cored amyloid plaques but not diffuse Aβ deposits (which are profusely present in these animals and were labelled with other anti-Aβ antibodies such as 4G8; ref. 28).

APPENDIX: PAPER III

Original Paper

NEURO-SIGNALS

Neurosignals 2003;12:78–88
DOI: 10.1159/000071817

Received: December 9, 2002
Accepted after revisions: February 6, 2003

GDNF Acutely Potentiates Ca^{2+} Channels and Excitatory Synaptic Transmission in Midbrain Dopaminergic Neurons

Jun Wang[a] Guiquan Chen[a] Bai Lu[b] Chien-ping Wu[a]

[a]Institute of Neuroscience, Chinese Academy of Sciences, Shanghai, China; [b]Unit on Synapse Development and Plasticity, NICHD, NIH, Bethesda, Md., USA

Key Words

Neurotrophic factors · Voltage-gated calcium channels · Calcium imaging · Neuronal culture · Substantia nigra

Abstract

Glial cell line-derived neurotrophic factor (GDNF) is best known for its long-term survival effect on dopaminergic neurons in the ventral midbrain. A recent study showed that acute application of GDNF to these neurons suppresses A-type potassium channels and potentiates neuronal excitability. Here we have characterized the acute effects of GDNF on Ca^{2+} channels and synaptic transmission. GDNF rapidly and reversibly potentiated the high voltage-activated (HVA) Ca^{2+} channel currents in cultured dopaminergic neurons. Analyses of channel kinetics indicate that GDNF decreased the activation time constant, increased the inactivation and deactivation time constants of HVA Ca^{2+} channel currents. Ca^{2+} imaging experiments demonstrate that GDNF facilitated Ca^{2+} influx induced by membrane depolarization. To investigate the physiological consequences of the Ca^{2+} channel modulation, we examined the acute effects of GDNF on excitatory synaptic transmission at synapses made by these dopaminergic neurons, which co-release the transmitter glutamate. Within 3 min of application, GDNF increased the amplitude of spontaneous and evoked excitatory autaptic- or multiple-postsynaptic currents. The frequency as well as the amplitude of miniature excitatory postsynaptic currents was also increased. These results reveal, for the first time, an acute effect of GDNF on synaptic transmission and its potential mechanisms, and suggest that an important function of GDNF for midbrain dopaminergic neurons is the acute modulation of transmission and ion channels.

Introduction

GDNF is a potent neurotrophic factor capable of eliciting diverse biological functions not only in the nervous system but also in kidney and gastrointestinal system [1, 2]. It was originally identified as a potent survival factor for cultured midbrain dopaminergic neurons [3]. Subsequent studies demonstrated that administration of GDNF into the brain in vivo protects midbrain dopaminergic neurons from death induced by mechanical lesion of medial forebrain bundle [4]. GDNF also prevents and reverses the degeneration of midbrain dopaminergic neurons induced by chemical insults [5–7]. Therefore, GDNF is considered as a potential therapeutic agent for Parkinson's disease [8]. However, the physiological role of GDNF in normal, healthy dopaminergic neurons is un-

KARGER

Fax + 41 61 306 12 34
E-Mail karger@karger.ch
www.karger.com

1424–862X/03/0122–0078$19.50/0

Accessible online at:
www.karger.com/nsg

Dr. Jun Wang
Molecular and Cell Biology Department
115 Life Sciences Addition, University of California
Berkeley, CA 94720-3200 (USA)
Tel. +1 510 642 5297, Fax +1 510 643 6971, E-Mail junwong@uclink.berkeley.edu

clear. Homozygous mice lacking GDNF gene do not exhibit any loss in the number of midbrain dopaminergic neurons [9–11, but see 12]. Injection of GDNF into the nigra or striatum of normal rats does not increase the number of nigra dopaminergic neurons [13, 14]. While both could be attributed to compensation by or redundancy with the GDNF homologs (e.g. neuturin), it is also possible that the major function of GDNF in normal midbrain is not (or is in addition to) to regulate the long-term survival of dopaminergic neurons.

Indeed, GDNF has been shown to elicit long-term changes in the structure and function of synapses in a number of systems. Transgenic mice overexpressing GDNF in skeletal muscle cells exhibit hyperinnervation of the neuromuscular junction (NMJ) [15]. In the *Xenopus* nerve-muscle co-culture, the probability of transmitter release is potentiated in the neuromuscular synapses exposed to GDNF for 1–2 days [16]. This effect appears to be mediated by an increase in the levels of frequenin, a neuron-specific Ca^{2+}-binding protein expressed in motoneurons. GDNF/frequenin facilitates the activation of N-type Ca^{2+} channels, leading to an enhancement of Ca^{2+} influx at the nerve terminals. Long-term treatment with GDNF also elicits a marked increase in the number and the size of synaptic vesicle clustering, as demonstrated by synaptobrevin-GFP fluorescent imaging, and FM dye staining [17]. Unlike neurotrophins, however, acute application of GDNF to the NMJ does not elicit any effects on the neuromuscular synapses [16, but see 18].

Long-term treatment with GDNF also modulates synapses made by the midbrain dopaminergic neurons. Amperometric recording demonstrates that treatment with GDNF enhanced quantal synaptic transmission in cultured dopaminergic neurons [19]. The quantal size recorded from GDNF-treated varicosities is dramatically increased. These dopaminergic neurons also co-release glutamate [20]. Both the frequency of spontaneous and the amplitude of evoked synaptic currents are increased in autapses of isolated dopaminergic neurons in GDNF-treated cultures [21]. In addition to these long-term effects, we have recently reported an unexpected acute modulation of ion channels by GDNF [22]. Application of GDNF to dopaminergic neurons in culture or slices elicits a rapid and reversible enhancement of neuronal excitability. This effect appears to be mediated by a suppression of A-type K^+ channels through a mechanism that involves activation of MAP kinase. GDNF also elicits a potentiating effect on Ca^{2+} channels. Changes in neuronal excitability and ion channels are expected to result in functional consequences on synaptic transmission. The present study is designed to investigate whether synaptic transmission is indeed regulated by acute application of GDNF. We characterized in detail the acute modulation of Ca^{2+} channels by GDNF in the dopaminergic neurons. We also investigated the effect of GDNF on excitatory transmission at synapses made by the midbrain dopaminergic neurons. These experiments demonstrated GDNF not only rapidly potentiates presynaptic transmitter release, but also enhances postsynaptic responses. Our study has revealed, for the first time, an acute modulation of synaptic transmission by GDNF. These results may help understand the normal function of GDNF in the midbrain dopaminergic neurons in vivo.

Materials and Methods

Cell Culture

Neuronal cultures were prepared from ventral midbrain as described [22]. Briefly, embryos at gestation day 14 (E14) were removed from anaesthetized pregnant rats. Ventral midbrains were dissected, cut into pieces, and digested with 0.125% trypsin in D-Hanks' solution at 37°C for 30–45 min. The pieces then were triturated gently in DMEM/F12 (1:1, plus 100 U/ml penicillin, 0.1 mg/ml streptomycin), and were centrifuged for 3 min at 1,200 rpm. The pellets were resuspended by gentle trituration in DMEM/F12 containing 10% fetal bovine serum (FBS), and plated at 0.3 million cells per 35 mm culture dish coated with poly-*D*-lysine (0.1 mg/ml). Cultures were maintained at 37°C, 5% CO_2 and 95% humidity, first in 10% FBS/DMEM, and switched 8 h later to the serum-free medium (DMEM/F12 plus Neurobasal B27, 1:50 and glutamine, 0.5 m*M*). All culture media and reagents were obtained from Life Technologies. GDNF was purchased from Promega. Unless indicated otherwise, all chemicals were from Sigma or RBI. The cultures were grown for 10–14 days and media were changed twice a week.

Calcium Imaging

Neurons were loaded with the membrane-permeable fluorescence dye fluo-3/AM (10 μ*M*, Molecular Probes) in darkness at 37°C for 45 min [23]. After dye loading, cells were washed with DMEM to remove any remaining dye, and kept in darkness for 0.5–1 h [24]. A coverslip of cells was transferred to a glass-bottomed chamber on the stage of a confocal microscope, and continuously superfused with standard extracellular solution (SES, in m*M*, NaCl 158, KCl 3, $CaCl_2$ 2, *D*-glucose 10, Na pyruvate 1, HEPES 10, pH 7.3) at a rate of 1 ml/min. Depolarization was evoked by high potassium solution (HKS, same as SES except 50 m*M* Na^+ was replaced by 50 m*M* K^+). Fluorescence measurements were performed at room temperature using a Bio-Rad MRC 1000 scanning confocal microscope coupled to an imaging system. Optical excitation was accomplished using the 488-nm line of a krypton/argon laser. The emitted fluorescence passed through a 515-nm primary barrier filter before it reached a CCD camera. The laser intensity was minimized to prevent dye bleaching. The fluorescence images were acquired in real-time mode (1 frame/2 s), and the data were stored for off-line analysis.

Electrophysiological Recording

The cultured midbrain dopaminergic neurons were perfused with SES, using an MSC-200 fast solution changer system. Spontaneous and evoked synaptic currents were recorded using whole-cell, voltage-clamp recording techniques as described [22]. The recording electrodes were filled with intracellular pipette solution (in m*M*, KCl 140, $MgCl_2$ 1, $CaCl_2$ 0.5, EGTA 5, ATP 3, HEPES 10, GTP 0.2, pH 7.3), with a typical resistance of 2–4 MΩ when measured in SES. For recording of HVA Ca^{2+} channel currents, extracellular solution contained (in m*M*): NaCl 102, $BaCl_2$, *D*-glucose 10, Na pyruvate 1, TEA 30, 4-AP 5, CsCl 5, TTX 0.001 and HEPES 10, pH 7.3. Ionic current or voltage was measured using Axopatch 200A amplifier, digitized at 20 kHz using pClamp 6.04 or Axotape 2.1 software, and stored on a computer and monitored on storage oscilloscope. Miniature synaptic currents were identified automatically by the SCAN software (gift from Dr. J. Dempster, University of Strathclyde, Glasgow). All events were included if their peak amplitudes were greater than 15 pA. All data are shown as mean ± SEM. Capacitance was compensated and leak currents were subtracted by P/4 protocol. All recordings were made at room temperature (20–24°C). Series resistance was measured and partially compensated (typically 60–75%). A small percentage of cells with any one of the following criteria were considered as unhealthy and not included for analysis: a resting membrane potential less than –50 mV; action potential overshoot less than 15 mV; gradual changes in membrane potential, input resistance, or action potential amplitudes.

Results

Modulation of Voltage-Gated Calcium Channels by GDNF

Whole-cell, current- or voltage-clamp recordings were performed on ventral midbrain neurons cultured for 10–14 days. In general, the GDNF-responsive dopaminergic neurons were large, multipolar neurons that extend two to five thick and rather straight primary processes, with relatively large varicosities found mainly in the distal segment of the processes. In contrast, nondopaminergic neurons possessed highly branched thick and thin primary processes with intensive arborization and numerous varicosities [20, 25]. The dopaminergic neurons were tyrosine hydroxylase (TH) immunoreactive [22]. The identity of dopaminergic neurons was further confirmed by their distinctive electrophysiological properties [26–29]. When step depolarization currents were applied to the cell body under the current-clamp mode, these neurons fired an action potential with much broader duration (fig. 1A). They also exhibited a typical 'anomalous rectification', or 'sag' potential when stimulated with a strong hyperpolarizing current injection (fig. 1B). Only cells with apparent sag potential or action potential half duration (APD_{50}) greater than 2.0 ms were chosen for further investigation.

Previous studies showed that GDNF acutely regulates high voltage-activated (HVA), but not low voltage-activated Ca^{2+} channels in midbrain dopaminergic neurons [22]. To determine the mechanisms as well as the potential physiological significance of such regulation, we recorded HVA Ca^{2+} currents in cultured midbrain dopaminergic neurons. SES was modified to include tetrodotoxin (TTX, 1 μ*M*) to block Na^+ channels, 4-aminopyridine (4-AP, 5 m*M*), CsCl (5 m*M*), and tetraethylammonium (TEA, 30 m*M*) to block K^+ channels. Extracellular Ba^{2+} (5 m*M*) was used as the charge carrier to avoid Ca^{2+}-induced inactivation of Ca^{2+} channels. A step depolarization (from –60 to 0 mV, 200 ms) activated HVA Ca^{2+} channels, which slowly inactivated and exhibited a typical tail current when membrane potential was repolarized to 0 mV (fig. 1C). It was reported that GDNF induced the maximal responses on Ret autophosphorylation [30] and the inhibition of K^+ channels [22] at a concentration of 20–50 ng/ml. To elicit the maximal effect, we used 25 ng/ml GDNF in this and all other experiments unless indicated otherwise. It markedly increased the Ba^{2+} currents (fig. 1C). The GDNF-induced potentiation of Ba^{2+} current was rapid; within 40 s after GDNF was perfused into the cultures, the peak Ba^{2+} currents began to increase, reaching maximal levels in less than 200 s (fig. 1D). The effect of GDNF was also transient and reversible. Within 4 min after GDNF withdrawal, the peak current returned to control levels (fig. 1D).

The voltage-clamp result was supported by calcium imaging experiments. Cells were loaded with the membrane-permeable indicator fluo-3/AM (10 μ*M*), and changes in intracellular calcium concentration ($[Ca^{2+}]_i$) were monitored using a confocal microscope. As shown in figure 1E, application of GDNF alone did not change the basal levels of $[Ca^{2+}]_i$. Perfusion of the depolarizing agent high potassium solution (HKS, 50 m*M* KCl) rapidly increased $[Ca^{2+}]_i$. This increase was blocked when HKS was perfused in the presence of a general Ca^{2+} channel blocker Cd^{2+} (200 μ*M*), suggesting Ca^{2+} influx via voltage-gated calcium channels. Application of HKS together with GDNF increased HKS-induced Ca^{2+} fluorescence (fig. 1E). On average, treatment with GDNF increased Ca^{2+} influx by 32.9 ± 18.3% ($p < 0.01$, $n = 7$, t test).

Effects of GDNF on the Kinetics of HVA Channels

To understand how GDNF modulates HVA channels, we analyzed the kinetics of channel activation. HVA current was evoked by a step depolarization from –60 to 0 mV for 200 ms before and after GDNF application. The rise phase of the HVA Ba^{2+} currents was fitted with single

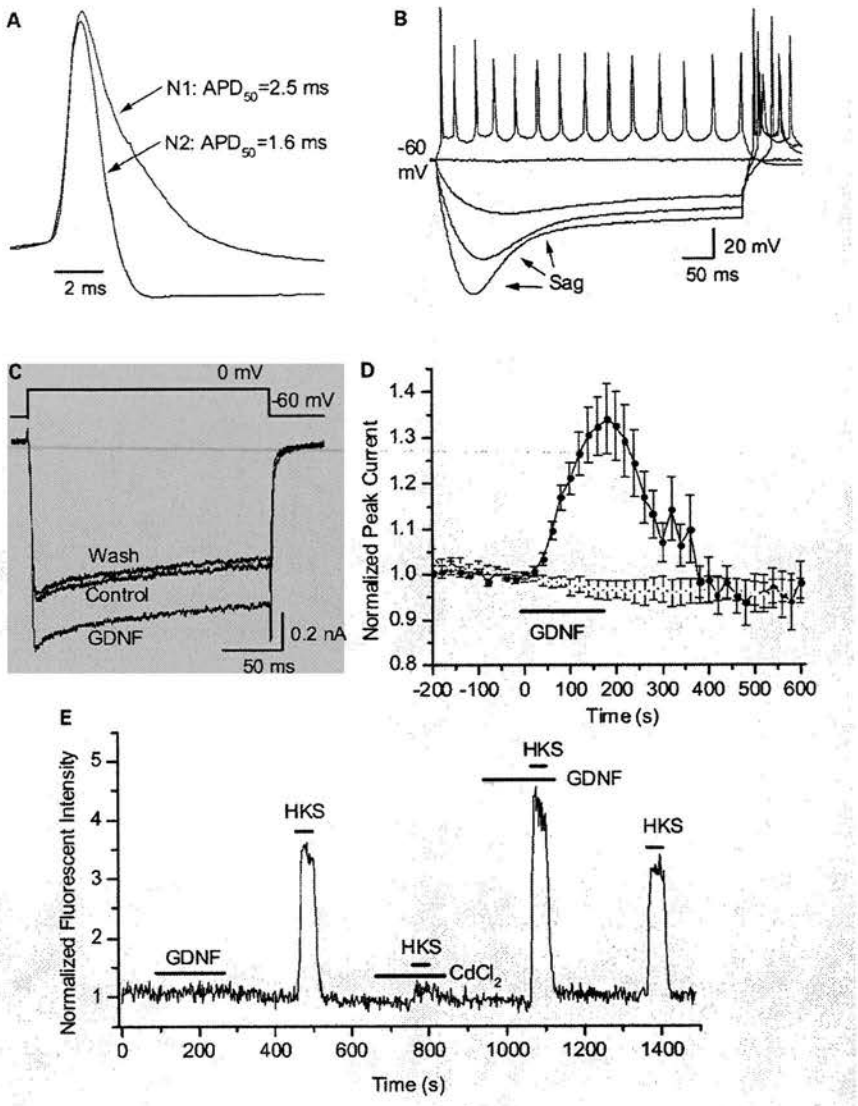

Fig. 1. Acute effect of GDNF on HVA Ca^{2+} channels. **A** Superimposed waveforms of action potentials recorded from dopaminergic and non-dopaminergic neurons. The half-width of the action potential (APD_{50}) of the dopaminergic neuron (N1) was greater than that of non-dopaminergic neuron (N2). **B** Characteristic response of a dopaminergic neuron to a strong hyperpolarization. Currents were injected into a dopaminergic neurons with various amplitudes (–0.09 to 0.03 nA, in 0.03-nA increments). At membrane potentials below –90 mV there was a typical delayed relaxation of the voltage response to hyperpolarizing current known as 'sag' potential. **C** Enhancement of HVA Ca^{2+} channels by GDNF. HVA Ba^{2+} currents, induced by step depolarization from –60 to 0 mV (protocol shown on top), were compared before, 3 min after GDNF application, and 10 min after washout of GDNF. **D** Time course of GDNF regulation of HVA Ba^{2+} currents. GDNF (n = 21), 25 ng/ml for 3 min, control (n = 12). **E** Effect of GDNF on high K^+ solution (HKS)-evoked Ca^{2+} influx. GDNF itself did not induce any change in Ca^{2+} influx. HKS evoked Ca^{2+} influx via voltage-gated Ca^{2+} channels since the influx could be blocked by $CdCl_2$ (200 μM). GDNF reversibly potentiated the response induced by HKS. This experiment was repeated 7 times and similar results were obtained.

exponential curve, and the time constant of HVA channel activation (τ_{act}) was obtained (fig. 2A). Application of GDNF elicited a small but significant decrease in τ_{act} (control: 2.97 ± 0.10 ms; GDNF-treated: 2.17 ± 0.10 ms; $p < 0.01$, n = 14, t test). The decay phase of the HVA Ba^{2+} currents was fitted by a single exponential function (fig. 2B). The amplitude of the peak current in control was scaled up to match that after GDNF application (fig. 2B). On average, treatment with GDNF increased the inactivation time constant (τ_{inact}) from 41.6 ± 3.5 ms to 54.0 ± 2.2 ($p < 0.05$, n = 5, t test).

We next analyzed deactivation kinetics. After a 50-ms depolarization to 0 mV, the dopaminergic neurons were repolarized to –40 mV to activate the tail current. The decay phase of tail current, which can be fitted with single exponential curve, reflects the channel deactivation time course during closing. The decay time constant (τ_{deact}) increased from 5.7 ± 0.2 to 8.0 ± 0.3 ms ($p < 0.01$, n = 14, t test) after GDNF application (fig. 2C). These results suggest that GDNF attenuates the deactivation of HVA Ca^{2+} channel and increases the ratio of opened channels.

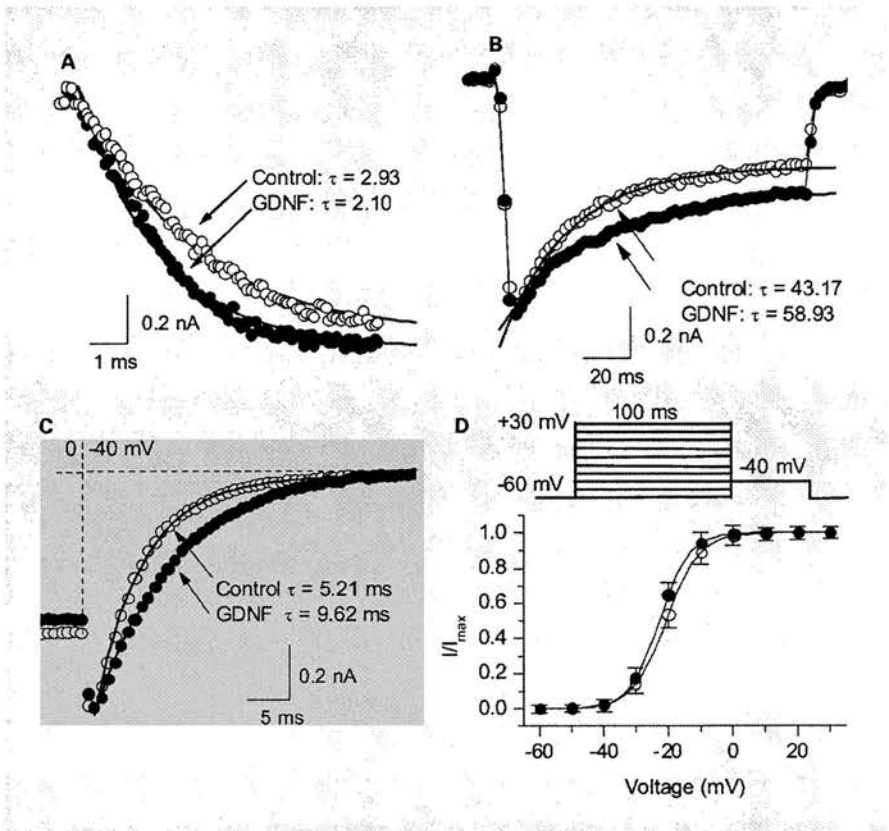

Fig. 2. Kinetic analyses of HVA Ca^{2+} channel currents. **A** Effect of GDNF on activation of HVA Ba^{2+} currents. HVA Ba^{2+} current was evoked by a step depolarization from −60 to 0 mV for 200 ms before and after GDNF application. The rising phase of the currents were fitted by a single exponential function. **B** Effect of GDNF on inactivation of HVA currents. The amplitude of the peak current in control was scaled up to match that after GDNF application. The decay phase of the currents was fitted by a single exponential function. Note that the inactivation was much slower after GDNF application. **C** Effect of GDNF on deactivation of HVA currents. The neurons were held at −60 mV and then depolarized to 0 mV for 50 ms. Tail currents were induced by stepping membrane potential from 0 to −40 mV, before and after GDNF application. The amplitude of peak currents after GDNF application was scaled to that before GDNF application. The current traces were fitted with a single exponential. Note that application of GDNF resulted in a slower deactivation during the repolarization phase. **D** Effect of GDNF on steady-state activation of HVA Ca^{2+} channel current. The depolarization protocol is shown on top. Steady-state activation curves were derived from tail current amplitudes, which were measured at 0.5 ms after repolarization to −40 mV from voltage steps ranging from −60 to +30 mV for 100 ms. Holding potentials were −60 mV. Normalized tail current amplitude (I/I_{max}) was plotted as a function of membrane potentials, and the data were fitted with a single Boltzmann function $I/I_{max} = 1/\{1 + \exp[-(V - V_{1/2})/K]\}$, where $V_{1/2}$ is half-activation potential. K is the slope factor. GDNF had no significant effect on the steady-state activation ($p > 0.05$, $n = 14$, covariance test).

We also constructed steady-state activation curves based on tail currents [31]. Cells were repolarized to −40 mV, after a depolarization from −60 mV to a series of test potentials (from −60 to +30 mV). Tail currents were measured at 0.5 ms after the repolarization. The maximal currents (I_{max}) were obtained when cells were repolarized from +30 mV. The steady-state activation of tail currents was obtained by plotting normalized peak tail current I/I_{max} against various depolarizing potentials. The data were fitted with a Boltzmann function: $I/I_{max} = 1/\{1 + \exp[-(V - V_{1/2})/K]\}$, where V is membrane potential, $V_{1/2}$ is the membrane potential at which the current amplitude is half-maximum, and K is slope factor. As shown in figure 2D, treatment with GDNF did not produce a significant effect on the steady-state activation curve ($V_{1/2}$ is −22.8 ± 1.3 mV for GDNF and −20.7 ± 0.9 mV for control, $p > 0.05\%$, covariance analysis).

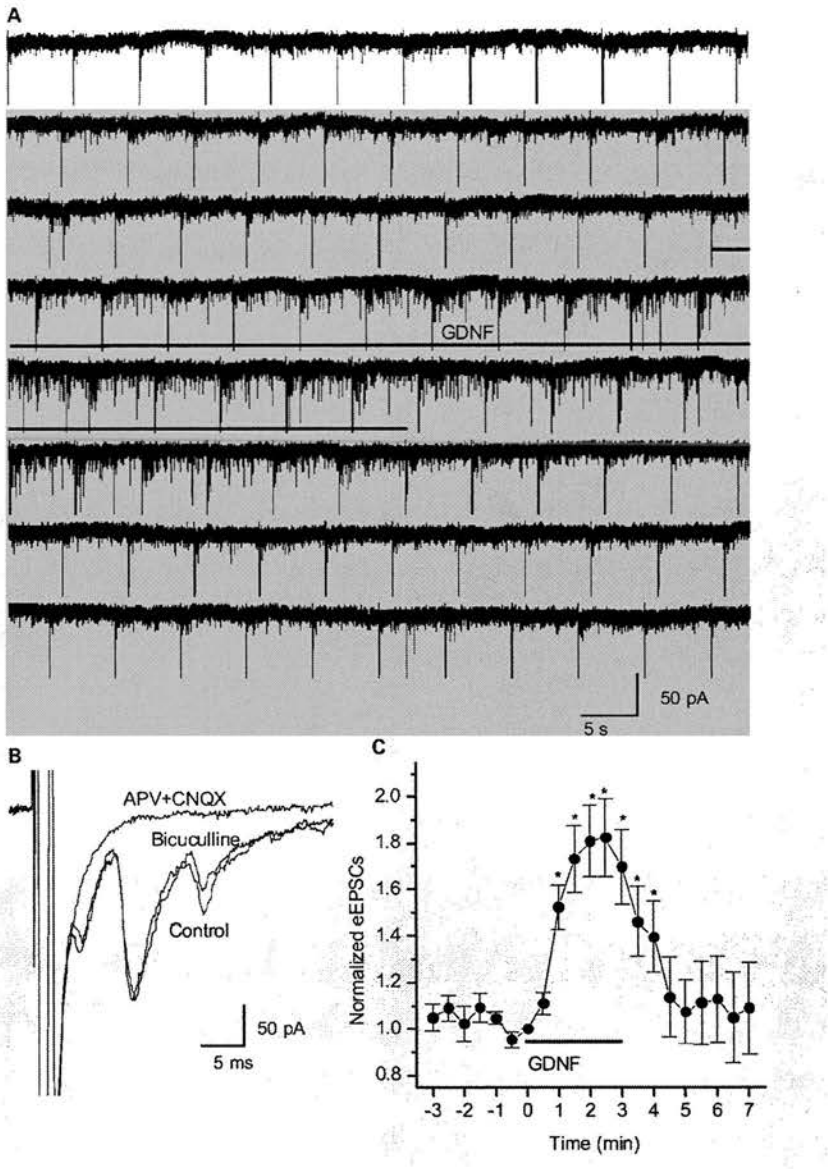

Fig. 3. GDNF potentiates glutamate-mediated sEPSCs and eEPSCs. **A** GDNF-induced increase in the amplitude and frequency of sEPSCs. A neuron was voltage clamped at −70 mV and was stimulated by depolarizing steps (0 mV, 2 ms) at every 6 s. The large downward currents are evoked EPSCs (eEPSCs) induced by inward Na^+ spikes. The currents in between eEPSCs are sEPSCs, which can be blocked by TTX. Perfusion of GDNF (50 ng/ml) dramatically and reversibly increased the frequency and the average amplitude of sEPSCs. This experiment was repeated 8 times and similar results were obtained. **B** Inhibition of eEPSCs by glutamate receptor antagonists. Depolarization step (2 ms to 0 mV from holding potential of −70 mV) elicited three EPSCs at the latencies of 3.5, 8.5 and 17.0 ms. All the currents were blocked by APV (100 μM) + CNQX (10 μM) and not by bicuculline (10 μM), suggesting that they were all glutamatergic. **C** Time course of the change in the peak amplitude of eEPSCs. Peak amplitude of eEPSCs was normalized to the control response right before GDNF application. * $p < 0.01$ ($n = 8$, Q test).

Potentiation of Synaptic Transmission by GDNF

An increase in the neuronal excitability induced by GDNF, as a consequence of the enhancement of I_A and HVA Ca^{2+} currents, could lead to a potentiation of synaptic transmission. To test this possibility, we recorded evoked synaptic currents under the whole-cell voltage-clamp mode. It has been shown that these midbrain dopaminergic neurons also secrete the excitatory neurotransmitter glutamate [20]. To avoid the interference of inhibitory transmission, we blocked $GABA_A$ receptor mediated currents by including bicuculline (10 μM) in the perfusion. Under the voltage-clamp conditions, a single depolarizing step (from the holding potential of −70 to 0 mV, 2 ms) initiated an action potential in the unclamped axonal processes, leading to autaptic or feedback polysynaptic currents that can be recorded at the soma (fig. 3B). Figure 3A shows an example of evoked excitatory postsynaptic currents (eEPSCs, the regularly spaced

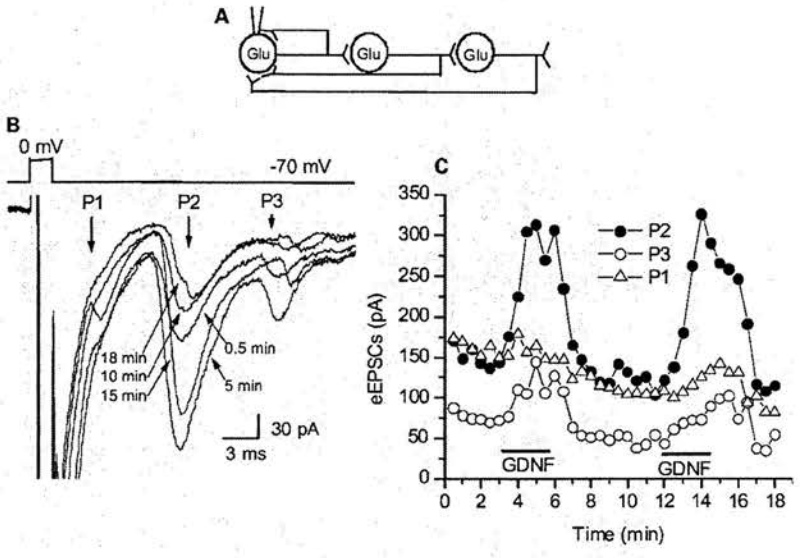

Fig. 4. Effect of GDNF on eEPSCs of autaptic and polysynaptic feedback connections. **A** Schematic diagram of possible neuronal network. **B** Changes in eEPSCs amplitudes after twice GDNF applications with a corresponding time course shown in **C**. A step depolarization applied to the cell under recording induced three eEPSCs (P1, P2, P3) with fixed latencies, possibly due to autaptic (from neuron 1) and polysynaptic feedback connections (from neurons 2 and 3). The eEPSCs before, during, after the first GDNF application, and during and after the second GDNF application were indicated by 0.5, 5, 10, 15 and 18 min, respectively. Application of GDNF resulted in a gradual increase of all three peaks (P1, P2, P3). **C** Time course of GDNF-induced increase in eEPSC amplitudes. GDNF repeatedly and reversibly increased the amplitudes of all three eEPSCs.

large downward currents), which are superimposed with inward Na^+ currents, and spontaneous synaptic currents (sEPSCs, smaller downward currents randomly occurring between eEPSCs). We observed eEPSCs in 34 of 78 neurons recorded. Both eEPSCs and sEPSCs were mediated by glutamate receptors because they could be completely blocked by the NMDA receptor antagonist *DL*-2-amino-5-phosphonovaleric acid (APV, 100 μM) plus the non-NMDA receptor antagonist cyano-7-nitroquinoxaline-2,3-dione (CNQX, 10 μM) (fig. 3B). Application of GDNF reliably increased the frequency of sEPSCs as well as the amplitude of eEPSCs (fig. 3A). The peak amplitude of eEPSCs increased shortly after GDNF was perfused into the culture medium, reaching the maximum in less than 3 min (fig. 3C). No desensitization was observed during 3-min application of GDNF. The eEPSCs returned to control values 3–5 min after GDNF washing out (fig. 3C).

In these cultures, the axons of midbrain neurons could innervate themselves through monosynaptic (autaptic) as well as polysynaptic feedback connections (fig. 4A). Occasionally, multiple peaks of eEPSCs were observed, with relatively constant intervals (fig. 4B), suggesting a polysynaptic feedback connection as outlined in figure 4A (diagram). Interestingly, GDNF appeared to increase the amplitudes of eEPSPs in at least some, if not all, of the connections (fig. 4C). Moreover, repeated applications of GDNF seemed to elicit comparable effects on eEPSC amplitudes.

To determine whether GDNF acts presynaptically or postsynaptically, we investigated the effect of GDNF on miniature EPSCs (mEPSCs). TTX (1 μM) was included in the perfusion solution to block all Na^+ channels mediated action potentials. Bicuculline (10 μM) was also included in the medium to block $GABA_A$ receptors. Application of APV (100 μM) plus CNQX (10 μM) completely blocked the currents (data not shown), indicating that the mEPSCs were mediated by excitatory synaptic currents. An example recording is shown in figure 5A. We observed that application of GDNF elicited a rapid increase in the frequency of mEPSCs ($p < 0.01$, $n = 14$, Q test). On average, mEPSCs frequencies increased 2.3-fold, and reached maximum 2 min after application of GDNF (fig. 5B). In 14 of 32 neurons recorded, we observed an acute effect of GDNF on mEPSCs. Interestingly, GDNF increased not only the frequency but also the amplitude of mEPSCs. There was a significant right shift of the cumulative frequency plot of mEPSCs amplitude (fig. 5C, $p < 0.01$, $n = 14$, Kolmogorov-Smirnov test). These results suggest that GDNF could modulate postsynaptic glutamate receptors, in addition to potentiate presynaptic transmitter release.

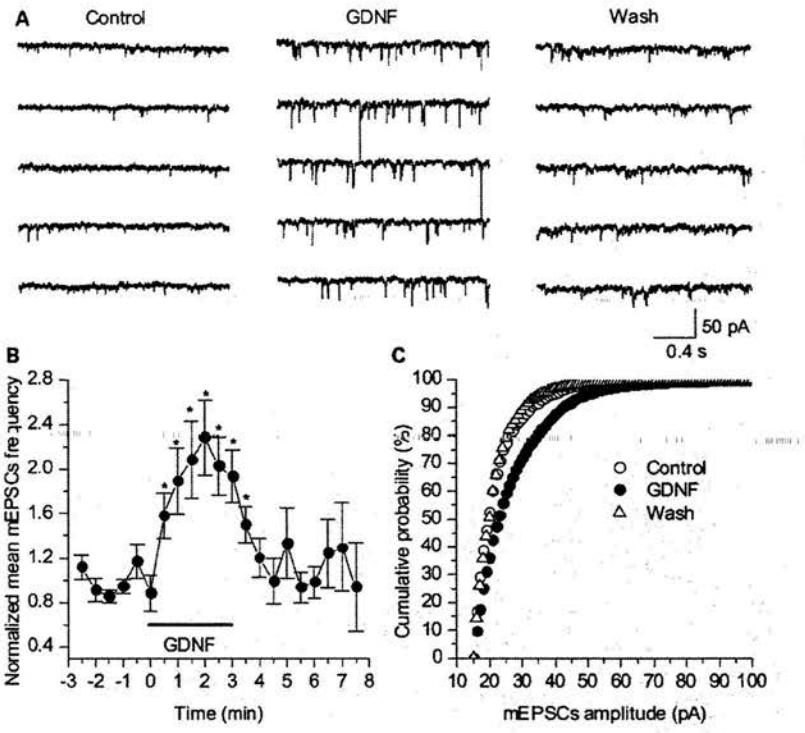

Fig. 5. Increase in the frequency and amplitude of mEPSCs by GDNF. **A** Consecutive recording traces of miniature EPSCs obtained before (control), during, and after (wash) GDNF (50 ng/ml) application under voltage-clamp (V_h = −70 mV). Note that GDNF increased the frequency and amplitude of mEPSCs. **B** Time course of GDNF-induced increase in mean mEPSCs frequency (over 30-second intervals). GDNF was perfused (indicated by the bar) at time 0. Data were normalized to the mean mEPSCs frequency of the same cell prior to the addition of GDNF. * Significantly different from control values (n = 14, $p < 0.05$, Q test). **C** Cumulative plot of mEPSCs amplitude distribution. The difference between GDNF and control groups, and that between GDNF and wash groups, are significant ($p < 0.001$, Kolmogorov-Smirnov test). The distribution curve for GDNF-treated synapses was shifted to the right, indicating that GDNF increases the amplitude of mEPSCs.

Discussion

Ever since the discovery of GDNF, a dogmatic view holds that GDNF is a long-term survival factor for the midbrain dopaminergic neurons. Careful examination of the literature, however, indicates that most, if not all, of the studies of survival promoting effects of GDNF were done on damaged dopaminergic neurons. In these studies, an elevation of GDNF levels in the brain, either by infusion of the protein or by transplantation of GDNF-expressing cells, protects and even reverses the death of the midbrain dopaminergic neurons induced by mechanical or chemical insults [4–7, 32–34]. In the adult ventral midbrain, the receptors for GDNF, c-Ret and GFR-α1, are highly expressed in adult dopaminergic neurons [35–37]. Moderate levels of GDNF have also been detected in striatum, the target of the midbrain dopaminergic neurons [37]. A critical question is then: What is the function of GDNF in the normal, undamaged dopaminergic neurons in adult midbrain? It has been shown that injection of GDNF into the nigra or striatum of normal adult rats does not increase the number of nigra dopaminergic neurons [13, 14]. Interestingly, a single injection of GDNF to nigra of normal rats elicits a dose-dependent increase in dopamine release in the striatum, as well as an enhancement of locomotor activity [38, 39]. Thus, GDNF may regulate the function, rather than survival, of the dopaminergic neurons in normal midbrain. Recently, we showed that GDNF acutely suppresses the A-type potassium channels and potentiates the excitability of the dopaminergic neurons in culture and in brain slices [22]. The present study further demonstrates that GDNF acutely potentiates high-voltage activated Ca^{2+} channels, and enhances excitatory synaptic transmission in these dopaminergic neurons. Taken together, these data reinforce the notion that the main function of GDNF in the dopaminergic neurons in normal midbrain is the acute modulation of synaptic transmission and ion channels, rather than (or in addition to) the long-term regulation of survival. The new results also imply that GDNF may acutely potentiate the release of dopamine at the terminals of the midbrain neurons. Direct recording with am-

perometric method will be necessary to demonstrate whether GDNF acutely potentiates dopamine release.

A number of recent studies have demonstrated the long-term, nonsurvival effects of GDNF on the midbrain dopaminergic neurons. For example, in the cultured dopaminergic neurons treated with GDNF for a number of days, glutamatergic transmission at autapses is significantly enhanced [21]. Long-term treatment with GDNF has been shown to increase the quantal size recorded from nerve terminals of dopaminergic neurons [19]. Using *Xenopus* nerve-muscle co-culture, the mechanisms underlying the long-term synaptic effects of GDNF have been studied in some detail [16]. Electrophysiological recording and FM dye imaging demonstrate that GDNF facilitates synaptic transmission at the neuromuscular synapses. These effects are very similar to the synaptic potentiation elicited by presynaptic expression of frequenin, a neuron-specific Ca^{2+}-binding protein. GDNF enhances the expression of frequenin in *Xenopus* motoneurons. Inhibition of frequenin expression or activity prevents the synaptic action of GDNF. Ca^{2+} imaging experiments show that GDNF also facilitates Ca^{2+} influx at the nerve terminals during evoked synaptic transmission by enhancing Ca^{2+} currents. The effect of GDNF on Ca^{2+} currents is blocked by inhibition of frequenin expression, occluded by overexpression of frequenin, and is selective to N-type Ca^{2+} channels. Thus, the long-term effects of GDNF on transmission and Ca^{2+} channels at the neuromuscular synapses are mediated by the Ca^{2+}-binding protein frequenin. In the present study, we show that GDNF acutely potentiates synaptic transmission and non-L-type HVA calcium channels in cultured midbrain dopaminergic neurons. This effect also appears to be mediated, at least in part, by potentiating Ca^{2+} channels. Through accelerating activation and inhibiting inactivation during depolarization, GDNF may keep Ca^{2+} channels open for a longer time resulting in a larger amount of Ca^{2+} influx. This is supported by the finding that GDNF enhances HKS-induced Ca^{2+} influx through voltage-gated Ca^{2+} channels. Also, the fast deactivation of the presynaptic Ca^{2+} channels during repolarization may be important for the termination of exocytosis. The rapid Ca^{2+} signaling will be a critical determinant of the precise timing of transmitter release [40]. In addition to presynaptic Ca^{2+} channels, GDNF might regulate postsynaptic glutamate receptors to potentiate synaptic transmission, suggested by GDNF increasing the amplitude of mEPSCs. This is unlike its acute effect on isolated nerve-muscle preparations [18], which shows that GDNF increased the frequency, but not the amplitude of mEPSCs. GDNF lack of effect on acetylcholine receptor at neuromuscular synapse might be the reason. In either presynaptic or postsynaptic mechanism, modulation occurs within a few minutes after GDNF application, and it seems unlikely that these acute effects are mediated by an upregulation of frequenin expression. While the precise molecular mechanisms remain to be established, it is plausible that the acute effects of GDNF are mediated by a cascade of phosphorylation events triggered by c-Ret tyrosine kinase.

To reveal the acute effects of GDNF on synaptic transmission, we studied autapses and feedback synapses on the midbrain dopaminergic neurons in culture. These neurons have been shown to release glutamate as a co-transmitter in response to electric stimulation [20]. Dopamine is known to be packaged in large dense-core vesicles (LDCV). It is unclear whether glutamate is packaged in the same LDCV or classic small clear vesicles in these dopaminergic neurons. In situ hybridization and immunocytochemistry experiments demonstrate that the midbrain dopaminergic neurons express AMPA and NMDA receptors [41, 42]. Iontophoretic application of specific ligands for glutamate receptors reveal that functional AMPA and NMDA receptors are present on the surface of the dopaminergic neurons [43]. In the case of polysynaptic feedback connections, the secondary and tertiary neurons do not have to be dopaminergic. The increase in the amplitudes of all three eEPSCs after GDNF application (fig. 4) could be achieved by either a global enhancement of AMPA/NMDA responses in the primary neurons, or an enhancement of glutamate release at the synapses made by the secondary and tertiary neurons.

Another interesting question is why regulation of both Ca^{2+} channels (14 of 32, 43.75%) and synaptic transmission (34 of 78, 43.58%) occurred only on a subgroup of dopaminergic neurons? Recent morphological studies demonstrated that not all midbrain dopaminergic neurons express GFRα1, GDNF preferred receptor [44]. Different sub-regions, i.e. substantia nigra compacta, reticulate, lateralis and ventral tegmental area, have different percentages of dopaminergic neurons expressing GFRα-1, ranging from 36 to 90%. It is unlikely that GDNF would act through GFRαs other than GFRα1 in the midbrain. While GFRα1, 2 and 4 mRNAs are expressed there [35, 45, 46], GDNF only binds GFRα2 at low affinity, but not GFRα4 [46].

In summary, our study has provided the first demonstration that GDNF rapidly potentiates synaptic transmission in midbrain dopaminergic neurons. Our results also suggest that such potentiation is mediated, at least in part, by modulating the activation and inactivation kinet-

ics of the high voltage-activated Ca^{2+} channels. These results may have help understand the normal function of GDNF in the midbrain dopaminergic neurons in vivo, and therefore may have implications in the use of GDNF to treat Parkinson's disease.

Acknowledgments

We thank Drs. Feng Yang and Linyin Feng for valuable advice on preparation of midbrain neuronal cultures and experiments on ion channels, Mr. Chuan Wang for helps in data analysis, and Mr. Jin-Gen Lu for technical assistance.

References

1 Airaksinen MS, Titievsky A, Saarma M: GDNF family neurotrophic factor signaling: Four masters, one servant? Mol Cell Neurosci 1999;13:313–325.

2 Baloh RH, Enomoto H, Johnson EM Jr, Milbrandt J: The GDNF family ligands and receptors: Implications for neural development. Curr Opin Neurobiol 2000;10:103–110.

3 Lin LF, Doherty DH, Lile JD, Bektesh S, Collins F: GDNF: A glial cell line-derived neurotrophic factor for midbrain dopaminergic neurons. Science 1993;260:1130–1132.

4 Beck KD, Valverde J, Alexi T, Poulsen K, Moffat B, Vandlen RA, Rosenthal A, Hefti F: Mesencephalic dopaminergic neurons protected by GDNF from axotomy-induced degeneration in the adult brain. Nature 1995;373:339–341.

5 Sauer H, Rosenblad C, Bjorklund A: Glial cell line-derived neurotrophic factor but not transforming growth factor β3 prevents delayed degeneration of nigral dopaminergic neurons following striatal 6-hydroxydopamine lesion. Proc Natl Acad Sci USA 1995;92:8935–8939.

6 Gash DM, Zhang Z, Ovadia A, Cass WA, Yi A, Simmerman L, Russell D, Martin D, Lapchak PA, Collins F, Hoffer BJ, Gerhardt GA: Functional recovery in parkinsonian monkeys treated with GDNF. Nature 1996;380:252–255.

7 Cass WA: GDNF selectively protects dopamine neurons over serotonin neurons against the neurotoxic effects of methamphetamine. J Neurosci 1996;16:8132–8139.

8 Gao W, Dugich-Djordjevic MM, Weil RJ, Lu B: Therapeutical usage of neurotrophic factors: Patent analysis. Expert Opinion on Therapeutic Patents 1997;7:325–338.

9 Moore MW, Klein RD, Farinas I, Sauer H, Armanini M, Phillips H, Reichardt LF, Ryan AM, Carver-Moore K, Rosenthal A: Renal and neuronal abnormalities in mice lacking GDNF. Nature 1996;382:76–79.

10 Sanchez MP, Silos-Santiago I, Frisen J, He B, Lira SA, Barbacid M: Renal agenesis and the absence of enteric neurons in mice lacking GDNF. Nature 1996;382:70–73.

11 Cacalano G, Farinas I, Wang LC, Hagler K, Forgie A, Moore M, Armanini M, Phillips H, Ryan AM, Reichardt LF, Hynes M, Davies A, Rosenthal A: GFRα1 is an essential receptor component for GDNF in the developing nervous system and kidney. Neuron 1998;21:53–62.

12 Granholm AC, Reyland M, Albeck D, Sanders L, Gerhardt G, Hoernig G, Shen L, Westphal H, Hoffer B: Glial cell line-derived neurotrophic factor is essential for postnatal survival of midbrain dopamine neurons. J Neurosci 2000; 20:3182–3190.

13 Bowenkamp KE, Hoffman AF, Gerhardt GA, Henry MA, Biddle PT, Hoffer BJ, Granholm AC: Glial cell line-derived neurotrophic factor supports survival of injured midbrain dopaminergic neurons. J Comp Neurol 1995;355: 479–489.

14 Beck KD, Irwin I, Valverde J, Brennan TJ, Langston JW, Hefti F: GDNF induces a dystonia-like state in neonatal rats and stimulates dopamine and serotonin synthesis. Neuron 1996;16:665–673.

15 Nguyen QT, Parsadanian AS, Snider WD, Lichtman JW: Hyperinnervation of neuromuscular junctions caused by GDNF overexpression in muscle. Science 1998;279:1725–1729.

16 Wang CY, Yang F, He X, Chow A, Du J, Russell JT, Lu B: Ca^{2+} binding protein frequenin mediates GDNF-induced potentiation of Ca^{2+} channels and transmitter release. Neuron 2001; 32:99–112.

17 Wang CY, Yang F, He XP, Je HS, Zhou JZ, Eckermann K, Kawamura D, Feng L, Shen L, Lu B: Regulation of neuromuscular synapse development by glial cell line-derived neurotrophic factor and neurturin. J Biol Chem 2002;277:10614–10625.

18 Ribchester RR, Thomson D, Haddow LJ, Ushkaryov YA: Enhancement of spontaneous transmitter release at neonatal mouse neuromuscular junctions by the glial cell line-derived neurotrophic factor (GDNF). J Physiol 1998; 512:635–641.

19 Pothos EN, Davila V, Sulzer D: Presynaptic recording of quanta from midbrain dopamine neurons and modulation of the quantal size. J Neurosci 1998;18:4106–4118.

20 Sulzer D, Joyce MP, Lin L, Geldwert D, Haber SN, Hattori T, Rayport S: Dopamine neurons make glutamatergic synapses in vitro. J Neurosci 1998;18:4588–4602.

21 Bourque MJ, Trudeau LE: GDNF enhances the synaptic efficacy of dopaminergic neurons in culture. Eur J Neurosci 2000;12:3172–3180.

22 Yang F, He X, Feng L, Mizuno K, Liu XW, Russell J, Xiong WC, Lu B: PI-3 kinase and IP3 are both necessary and sufficient to mediate NT3-induced synaptic potentiation. Nat Neurosci 2001;4:19–28.

23 Andjus PR, Khiroug L, Yakel JL, Cherubini E, Nistri A: Changes in intracellular calcium induced by NMDA in cultured rat hippocampal neurons require exogenous glycine. Neurosci Lett 1996;210:25–28.

24 Pan ZH, Lipton SA: Multiple GABA receptor subtypes mediate inhibition of calcium influx at rat retinal bipolar cell terminals. J Neurosci 1995;15:2668–2679.

25 Grace AA, Onn SP: Morphology and electrophysiological properties of immunocytochemically identified rat dopamine neurons recorded in vitro. J Neurosci 1989;9:3463–3481.

26 Silva NL, Mariani AP, Harrison NL, Barker JL: 5,7-Dihydroxytryptamine identifies living dopaminergic neurons in mesencephalic cultures. Proc Natl Acad Sci USA 1988;85:7346–7350.

27 Yung WH, Hausser MA, Jack JJ: Electrophysiology of dopaminergic and non-dopaminergic neurones of the guinea-pig substantia nigra pars compacta in vitro. J Physiol 1991;436: 643–667.

28 Cardozo DL: Midbrain dopaminergic neurons from postnatal rat in long-term primary culture. Neuroscience 1993;56:409–421.

29 Steensen BH, Nedergaard S, Ostergaard K, Lambert JD: Electrophysiological characterization of dopaminergic and non-dopaminergic neurones in organotypic slice cultures of the rat ventral mesencephalon. Exp Brain Res 1995; 106:205–214.

30 Jing S, Wen D, Yu Y, Holst PL, Luo Y, Fang M, Tamir R, Antonio L, Hu Z, Cupples R, Louis JC, Hu S, Altrock BW, Fox GM: GDNF-induced activation of the ret protein tyrosine kinase is mediated by GDNFR-α, a novel receptor for GDNF. Cell 1996;85:1113–1124.

31 Lorenzon NM, Foehring RC: Characterization of pharmacologically identified voltage-gated calcium channel currents in acutely isolated rat neocortical neurons. I. Adult neurons. J Neurophysiol 1995;73:1430–1442.

32 Hoffer BJ, Hoffman A, Bowenkamp K, Huettl P, Hudson J, Martin D, Lin LF, Gerhardt GA: Glial cell line-derived neurotrophic factor reverses toxin-induced injury to midbrain dopaminergic neurons in vivo. Neurosci Lett 1994; 182:107–111.

33 Tomac A, Lindqvist E, Lin LF, Ogren SO, Young D, Hoffer BJ, Olson L: Protection and repair of the nigrostriatal dopaminergic system by GDNF in vivo. Nature 1995;373:335–339.

34 Choi-Lundberg DL, Lin Q, Chang YN, Chiang YL, Hay CM, Mohajeri H, Davidson BL, Bohn MC: Dopaminergic neurons protected from degeneration by GDNF gene therapy. Science 1997;275:838–841.
35 Trupp M, Belluardo N, Funakoshi H, Ibanez CF: Complementary and overlapping expression of glial cell line-derived neurotrophic factor (GDNF), c-ret proto-oncogene, and GDNF receptor-α indicates multiple mechanisms of trophic actions in the adult rat CNS. J Neurosci 1997;17:3554–3567.
36 Widenfalk J, Nosrat C, Tomac A, Westphal H, Hoffer B, Olson L: Neurturin and glial cell line-derived neurotrophic factor receptor-β (GDNFR-β), novel proteins related to GDNF and GDNFR-α with specific cellular patterns of expression suggesting roles in the developing and adult nervous system and in peripheral organs. J Neurosci 1997;17:8506–8519.
37 Golden JP, Baloh RH, Kotzbauer PT, Lampe PA, Osborne PA, Milbrandt J, Johnson EM Jr: Expression of neurturin, GDNF, and their receptors in the adult mouse CNS. J Comp Neurol 1998;398:139–150.
38 Hudson J, Granholm AC, Gerhardt GA, Henry MA, Hoffman A, Biddle P, Leela NS, Mackerlova L, Lile JD, Collins F, et al: Glial cell line-derived neurotrophic factor augments midbrain dopaminergic circuits in vivo. Brain Res Bull 1995;36:425–432.
39 Hebert MA, Van Horne CG, Hoffer BJ, Gerhardt GA: Functional effects of GDNF in normal rat striatum: Presynaptic studies using in vivo electrochemistry and microdialysis. J Pharmacol Exp Ther 1996;279:1181–1190.
40 Bischofberger J, Geiger JR, Jonas P: Timing and efficacy of Ca^{2+} channel activation in hippocampal mossy fiber boutons. J Neurosci 2002;22:10593–10602.
41 Paquet M, Tremblay M, Soghomonian JJ, Smith Y: AMPA and NMDA glutamate receptor subunits in midbrain dopaminergic neurons in the squirrel monkey: An immunohistochemical and in situ hybridization study. J Neurosci 1997;17:1377–1396.
42 Albers DS, Weiss SW, Iadarola MJ, Standaert DG: Immunohistochemical localization of N-methyl-*D*-aspartate and alpha-amino-3-hydroxy-5-methyl-4-isoxazolepropionate receptor subunits in the substantia nigra pars compacta of the rat. Neuroscience 1999;89:209–220.
43 Gotz T, Kraushaar U, Geiger J, Lubke J, Berger T, Jonas P: Functional properties of AMPA and NMDA receptors expressed in identified types of basal ganglia neurons. J Neurosci 1997;17:204–215.
44 Sarabi A, Hoffer BJ, Olson L, Morales M: GFRα-1 mRNA in dopaminergic and nondopaminergic neurons in the substantia nigra and ventral tegmental area. J Comp Neurol 2001; 441:106–117.
45 Nosrat CA, Tomac A, Hoffer BJ, Olson L: Cellular and developmental patterns of expression of Ret and glial cell line-derived neurotrophic factor receptor alpha mRNAs. Exp Brain Res 1997;115:410–422.
46 Lindahl M, Timmusk T, Rossi J, Saarma M, Airaksinen MS: Expression and alternative splicing of mouse GFRα4 suggest roles in endocrine cell development. Mol Cell Neurosci 2000;15:522–533.